

Analysis of breath allows for non-invasive identification and quantification of diseases and metabolic dysfunction



Im Fachbereich Physik
der Freien Universität Berlin
eingereichte Dissertation

vorgelegt von
Suha Adel Al-Ani

Berlin
2015

Erster Gutachter: Prof. Dr. Karsten Heyne
Zweiter Gutachter: Prof. Dr. Ulrike Alexiev
Date of Defense: 14.09.2015

Abstract

In the last decade breath gas analysis (BGA) became more and more important in industry and sciences. This trend is caused by the development of new and stable semiconductor lasers, e.g. quantum cascade lasers, in the mid-infrared region ranging from 3 μm to 15 μm . Moreover, specific mass spectrometers were developed for detection of volatile organic compounds (VOCs) in a volume sensitivity range of parts per trillion. Companies like Ionicon and B&S Analytic GmbH specialized on detection of VOCs in breath, food and exhaust air.

A new measurement device FLIP (Fast Liver Investigation Packet) based on breath gas analysis of CO_2 was developed in the AG Heyne to assess the liver power or liver function capacity of humans. This device together with the LiMAX-test (Liver Maximal capacity) developed by Priv.-Doz. Martin Stockmann (Charité-Universitätsmedizin) enables a personalized and quantitative determination of the liver function capacity by detecting the increase of $^{13}\text{CO}_2$ in the exhaled air after ^{13}C -methacetin administration.

Functionally, ^{13}C -methacetin is metabolized in all hepatic cells by the enzyme Cytochrome P450 1A2 to paracetamol and $^{13}\text{CO}_2$. Thus, the speed of metabolism measured by the $^{13}\text{CO}_2$ to $^{12}\text{CO}_2$ ratio in the breath is directly proportional to the liver function capacity. No other test can provide this information. The value measured is called the LiMAX value and calculated from the maximum of the $^{13}\text{CO}_2$ to $^{12}\text{CO}_2$ ratio. However, the kinetics of this ratio during 60 minutes also contains information for the physicians treating the liver disease. The combination of FLIP device and LiMAX-test is already in clinical use.

My work is divided into two parts. After a general introduction, in the first part, I analyzed data taken at the Charité to investigate the influence of dosage and sports on the outcome of the LiMAX-test. Furthermore, I compare the reproducibility of the breath test measurements with blood levels of paracetamol and methacetin. I will show that the $^{13}\text{CO}_2$ detection enables a direct tracking of methacetin metabolization in the liver cells.

In the second part of my work, I studied the occurrence of VOCs in the exhaled air with mass spectrometry. The sensitivity and speed of analysis of these detection devices have increased greatly in the last decade. The knowledge on metabolic processes in the human body has a lot of advantages in early diagnosis of diseases and metabolic malfunctions. Since non-invasive breath tests experiences a high acceptance from patients, an assessment of the possible uses of breath gas analysis is of high importance. Diagnosing a disease with BGA is a safe, non-invasive and fast technique.

The breath gas contains both non-volatile (e.g. CO_2) and volatile substances. The observation of volatile substances in human breath (e.g. acetone) has been made by medical professionals for a long time (Hippocrates). The detection of bad smell/odor in the breath was used to identify specific diseases. Each VOC can be considered as a partial indicator for a specific metabolization or disease such as respiratory disease, liver disease and etc.

In my study, two different spectrometry methods, the Proton Transfer Reaction Mass Spectrometry (PTR-MS) and Ion Mass Spectrometry (IMS) were used to study the occurrence of VOCs in breath and to investigate the effect of different health statuses on the production of VOCs. Since, these methods were new in the AG Heyne, we started with measurements to verify the reproducibility of the measurements and the independence of other parameters,

such as how we collected the breath. Here, we studied the behaviour of the VOCs concentrations in time by collecting breath samples from volunteers and analysing them over one week. This part of study was performed with the PTR-MS and the IMS device.

With PTR-MS, two types of studies were done: The first study is considered as a comparative study between three different types of groups, who had different health statuses. We investigated a group of vegans (denoted as super healthy), a group of healthy volunteers and patients with liver diseases in cooperation with the Charité. Each VOC has a specific signature that is affected by the health status, so it increases or decreases more in one case than in others. In the second study we investigated the LiMAX-value of the patients to correlate the VOC concentration with the liver status.

Another study was done using the IMS to identify factors that have an influence on the VOCs intensities such as the effect of diet statuses, the differences between direct and indirect breath and smoking. Since we found that the reproducibility of the IMS measurements are not reliable enough, and the identification of VOC peaks is largely missing, these results are presented in the appendix of this work.

Zusammenfassung

Im letzten Jahrzehnt ist die Atemgasanalyse immer wichtiger für die Industrie und die Wissenschaften geworden. Dieser Vorgang wird durch die Entwicklung von neuen und stabilen Halbleiterlasern im mittleren Infrarot von 3 μm bis 15 μm getrieben. Zusätzlich werden Massenspektrometer zum Nachweis von flüchtigen organischen Verbindungen (VOCs) mit einer Empfindlichkeit (bezüglich des Volumens) von einigen Billionstel entwickelt. Firmen wie Ionicon und B&S Analytic GmbH spezialisieren sich auf den Nachweis von VOCs im Atem, in der Nahrung und in Abgasen.

Ein neues Meßgerät FLIP (Fast Liver Investigation Packet), basierend auf der Analyse des CO_2 in der Atemluft, wurde von der AG Heyne entwickelt, um die Leberleistung und die Leberfunktionskapazitäten beim Menschen zu bewerten. Dieses Gerät unter Hinzunahme des LiMAX-tests (Liver MAXimal capacity) von Priv.-Doz. Martin Stockmann (Charité - Universitätsmedizin) entwickelt, erlaubt eine personalisierte und quantitative Bestimmung der Leberfunktionskapazität durch Messung des erhöhten $^{13}\text{CO}_2$ in der ausgeatmeten Luft nach ^{13}C -Methacetin IV-Injektion.

Von der Funktion her wird ^{13}C -Methacetin in allen hepatischen Zellen durch das Enzym P450 1A2 zu Paracetamol und $^{13}\text{CO}_2$ metabolisiert. Das heißt, die Schnelligkeit des Metabolismus gemessen durch das $^{13}\text{CO}_2$ zu $^{12}\text{CO}_2$ Verhältnis im Atem ist direkt proportional zu der Leberfunktionskapazität. Kein anderes Prüfverfahren kann diese Information liefern. Der gemessene Wert wird LiMAX-Wert genannt und errechnet sich aus dem Maximum des $^{13}\text{CO}_2$ zu $^{12}\text{CO}_2$ Verhältnisses. Jedoch liefert die Kinetik dieses Verhältnisses in der sechzigminütigen Meßzeit auch Informationen für den die Leberkrankheit behandelnden Arzt. Die Verbindung vom FLIP-Gerät und LiMAX-Tests wird schon in Kliniken verwendet.

Meine Arbeit kann in zwei Hauptteile geteilt werden. Nach einer allgemeinen Einleitung, untersuchte ich im ersten Hauptteil Daten, welche an der Charité erhoben wurden, um den Einfluß der Dosierung und Sport auf das Ergebnis der LiMAX-tests zu untersuchen. Weiterhin verglich ich die Reproduzierbarkeit des Atem-Tests mit den Blutwerten für Paracetamol und Methacetin. Ich werde zeigen, daß der $^{13}\text{CO}_2$ Nachweis ein direktes Verfolgen des Methacetin-Metabolismus in Leberzellen erlaubt.

Im zweiten Hauptteil meiner Arbeit untersuchte ich das Vorkommen von VOCs in der Atemluft mit Massenspektroskopie. Die Empfindlichkeit und Schnelligkeit der Analyse dieser Geräte sind im letzten Jahrzehnt sehr gestiegen. Das Wissen um metabolische Prozesse des menschlichen Körpers ist von Vorteil für die Frühdiagnose von Krankheit und metabolischen Fehlfunktionen. Da nicht-invasive Atemuntersuchungen von Patienten gut akzeptiert werden, ist eine Bewertung möglicher Anwendungen von Atemuntersuchungen sehr wichtig. Die Diagnose einer Krankheit mit BGA ist sicher, nicht-invasiv und schnell.

Die Atemluft enthält sowohl „nicht-flüchtige“ (z.B. CO_2) wie auch flüchtige (leicht verdampfbare) Stoffe. Die Feststellung von flüchtigen Stoffen in der menschlichen Atemluft (z.B. Aceton) ist von Medizinern seit langem (Hippokrates) gemacht worden. Das Vorhandensein eines schlechten Geruches des Atems wurde benutzt, um gewisse Krankheiten zu erkennen. Jede VOC ist ein Teilindikator eines spezifischen Metabolismus oder einer spezifischen Krankheit, wie Atemwegkrankungen, Leberkrankheit, usw.

In meinen Untersuchungen fanden zwei unterschiedliche Spektroskopische Verfahren Anwendung: Protonentransfer-Reaktion-Massenspektrometrie (PTR-MS) und Ionenmobilitätsspektrometrie (IMS). Das Vorhandensein von VOCs im Atem, und der Einfluß von unterschiedlichen Gesundheitszuständen auf die Produktion von VOCs wurden untersucht. Da diese Verfahren in der AG Heyne noch nicht angewendet worden waren, begannen wir mit Messungen, die die Reproduzierbarkeit der Messungen und die Abhängigkeit von anderen Parametern, wie das Verfahren zum Einsammeln der Atemluft, untersuchten. Hier betrachteten wir das zeitliche Verhalten der Konzentration der VOCs. Atemproben von Freiwilligen wurden eingesammelt und über die Dauer einer Woche untersucht. Dieser Teil der Studie wurde sowohl mit PTR-MS und IMS durchgeführt.

Mit der PTR-MS erfolgten zwei Untersuchungen. Die erste war ein Vergleich von drei unterschiedlichen Gruppen von Probanden, die in unterschiedliche Gesundheitszustände eingestuft waren. Die erste Gruppe waren Veganer, die als sehr gesund eingestuft waren. Die zweite waren gesunde Freiwillige. Die dritte waren Patienten der Charité. Jede VOC hat eine eigene Signatur, die von dem „Gesundheitszustand“ bestimmt wird, und größer oder kleiner ist in Vergleich zu anderen. In der zweiten Untersuchung wurde die Korrelation zwischen LiMAX-Wert (bei Patienten), VOC-Konzentration und Leberzustand gesucht.

Eine weitere Studie wurde mit der IMS durchgeführt zur Bestimmung der Faktoren, die die VOC-Intensitäten - wie Diät, direktes Atmen gegenüber gesammelter Atem, und Rauchen -beeinflussen. Da wir feststellten, daß die Reproduzierbarkeit der IMS-Messung nicht zuverlässig war, und die Identifizierung von VOC-Linien weitgehend fehlten, wurden diese Resultate im Anhang angeführt.

List of Abbreviations

VOCs	: Volatile Organic Compounds
BGA	: Breath Gas Analysis
Ppbv	: Parts per Billion Volume
EBV	: Exhaled Breath Vapour
EBC	: Exhaled Breath Condensate
CO ₂	: Carbon Dioxide
¹³ C-MBT	: C-13 methacetin breath test
DOB value	: Delta over Baseline
LiMAX test	: Liver Maximum Capacity
FANci2	: Fischer ANalysen Instrument
FLIP	: Flow-through Fast Liver Investigation Packet
BMI	: Body Mass Index
BSA	: Body Surface Area
NDIR	: Non-Dispersive Infra-Red
IV	: Intravenously
PTFE	: Polytetrafluoroethylene
PTR-MS	: Proton-Transfer Reaction Mass Spectrometry
IMS	: Ion Mobility Spectrometry
QMS	: Quadrupole Mass system
SEM	: Secondary Electron Multiplier
CI	: chemical ionization
DC	: Direct Current
ISAS	: Institute for Analytical Sciences
MCC	: Multi-Capillary Column
PA	: Binding Affinity
CPS	: Count per Second
k ₀	: Ion Mobility
1/k ₀	: Inverse Ion Mobility
DT	: Drift Time
RT	: Retention Time
RIP	: Reactant Ion Peak
MCL	: Maximum Contaminant Level

List of Figures

Figure No.	Subjects	Page No.
Chapter 1		
Figure 1.1:	The three ways that the VOCs can enter the body: i) ingestion, ii) inhalation and iii) topical contact.	1
Figure 1.2:	The sources of the VOCs in the breath.	2
Figure 1.3:	The VOCs pathways through different compartments of the body.	3
Figure 1.4:	(A) A schematic view of the respiratory tract, (B) Anatomical view of the lungs that shows the position of the alveoli, (C) An enlarged view of the alveoli (gas sac) and pulmonary capillaries (blood vessels) and (D) A close-up view of the O ₂ and CO ₂ exchange between the alveoli and pulmonary capillaries.	5
Chapter 2		
Figure 2.1:	The physiological bicarbonate model that consists of three pools: i) the vascular pool, ii) the heart-brain-“other” pool and iii) the muscle pool.	11
Figure 2.2:	Some possible ¹³ C-Breath Tests.	13
Chapter 3		
Figure 3.1:	(A) A schematic view shows the location of the liver, (B) Anatomical view of the liver that shows the lobes, (C) An enlarged view of the functional unit of the liver and (D) A close-up view of the hepatocytes plate.	15
Figure 3.2:	The hepatic portal circulation.	16
Figure 3.3:	The types and the effects of liver diseases on the liver cells.	16
Figure 3.4:	The conversion process of ¹³ C-methacetin to paracetamol and CO ₂ in the liver. Formaldehyde is fast metabolized by formaldehyde dehydrogenase.	18
Figure 3.5:	The schematic of the 3-compartment model uses to describe the observed kinetics of ¹³ C-methacetin (M), paracetamol (P) and ¹³ CO ₂ (C) (quantified in the breath as DOB): (1) Injection of M into the blood, (2) reversible exchange of (M) between blood and liver, (3) hepatic metabolism of (M) to (P) and (C), (4) reversible exchange of (P) between blood and other body compartments, (5) reversible exchange of CO ₂ between blood and other body compartments, (6) respiratory removal of (M) and (7) injection of H ¹³ CO ₃ (in the proposed novel 2DOB-method). Ω _B , Ω _L and Ω _X denote the volume of the three compartments.	19
Figure 3.6:	The influence of oxygen on the DOB measurement by using FANci2: The increase corresponds to 20 (1) DOB after replacing 100% N ₂ with 100% O ₂ as a residual gas.	25
Figure 3.7:	Scheme of ¹³ C-methacetin breath test / LiMAx test: Iv administration of ¹³ C-methacetin and NaCl induces the metabolism (upper left) to paracetamol and ¹³ CO ₂ ; ¹³ CO ₂ is dissolved in the blood, transported to	26

the lungs and exhaled; exhaled air is analyzed by a gas analyzer detecting the additional exhaled $^{13}\text{CO}_2$ plotted in ‰ as a function of time (**upper right**). The maximal DOB value indicates the liver status (healthy liver, bad liver and liver failure).

- Figure 3.8: : Measurement schemes for 5 days as a function of time in minutes with different dosages and different cycling times; bed: resting time; syringe: ^{13}C -methacetin iv bolus application; bicycle: cycling period. 26
- Figure 3.9: The typical DOB kinetics, **x**: the day of the measurement, **d**: the max. of the graph, **I**: the max. of the fitting, **i**: the integration of DOB, **t**: the time and **a**: the area (i/t). 28
- Figure 3.10: The effect of different doses of ^{13}C -methacetin: **(A)** doing sports from min(50) to min(60) and **(B)** doing sports from min(-10) to min(20). 29
- Figure 3.11: DOB kinetics, methacetin blood level and paracetamol blood level of the same person as a function of time after methacetin administration: Day 1: DOB kinetics (black dots) and simulation (black curve), methacetin blood level (dark yellow diamonds), and paracetamol blood level (red triangles); day 2: DOB kinetics (grey dots) and simulation (grey curve), methacetin blood level (green diamonds), and paracetamol blood level (magenta triangles). Left: Units for the DOB kinetics; right: Units for the blood levels. 31
- Figure 3.12: Analysis of the reproducibility of DOB_{max} , and maximal paracetamol blood level at two different days for the all subjects: DOB_{max} with correlation coefficient of $R_D=0.78$ (**upper left**), maximal paracetamol blood level with correlation coefficient of $R_p=0.83$ (**upper right**), correlation of DOB_{max} with maximal paracetamol blood level of $R_{DP}=0.5$ (**lower left**) and maximal methacetin blood level with correlation coefficient of $R_p=-0.06$ (**lower right**). 32
- Figure 3.13: Example DOB kinetics and simulations with single dosage without sports (day 1: black dots and black curve) and with sports (day 4: blue dots and blue curve). Kinetics without sports have a single exponential rise and decay; kinetics with sports have a single rise time, followed by a slower rise time upon resting at about 20 min, followed by an exponential decay. The long decay constant is fixed to 180 minutes; time constants are given. 35

Chapter 4

- Figure 4.1: **(A)** two Tedlar bags one of them is inflated with breath and the other is not and **(B)** the Teflon tube. 37
- Figure 4.2: Schematic view shows the steps of measurement with PTR-MS. 39
- Figure 4.3: The process of the measurement with PTR-MS. 40
- Figure 4.4: Schematic view shows the steps of the measurement with IMS. 44
- Figure 4.5: Schematic view shows the MCC and its compounds. 45

Chapter 5

- Figure 5.1: PTR-MS spectrum, the x-axis represents the mass (amu) and the y-axis represents the amplitude. 47
- Figure 5.2: Two graphs, which belong to the same measuring period: **(A)** graph belongs to propanenitrile ($m/z=56$) and **(B)** graph belongs to acetone ($m/z=59$). Each graph has different peaks, which indicate the ion counts of VOCs in counts per second (cps) for different breaths. The increase 49

	and decrease of acetone upon breathing into the PTR-MS can be directly reached.	
Figure 5.3:	The normalized counts of $m/z=59$ versus the normalized counts of $m/z=69$.	50
Figure 5.4:	Sketch of the isoprene model structure used to explain the dynamics of isoprene concentrations.	51
Figure 5.5:	Sketch of the acetone model structure used to explain the dynamic of acetone concentrations.	53
Figure 5.6:	The normalized counts of $m/z=59$ versus the normalized counts of $m/z=60$.	54
Figure 5.7:	Two-dimensional plot of Pearson's correlation coefficient where the color indicates the value of the correlation: (A) belong to vegans, (B) belong to volunteers and (C) belong to patients with liver diseases.	56
Figure 5.8:	The comparison between different health statuses for 200 m/z ratios: graph (A) and graph (B) show the same measurement but with different Y-scale.	57
Figure 5.9:	The flow chart for the optimization process of the measurement done with PTR-MS.	59
Figure 5.10:	The isotope of isoprene ($m/z=67$) shows a constant linear time dependence.	186
Figure 5.11:	The formaldehyde ($m/z=57$) shows an increasing linear time dependence.	187
Figure 5.12:	The isotope of methanol ($m/z=34$) shows a decreasing linear time dependence.	187
Figure 5.13:	The pentane ($m/z=71$) shows a rising kinetics.	188
Figure 5.14:	The methanol ($m/z=33$) shows a decaying kinetics.	189
Figure 5.15:	The LiMAX-Test values according to liver conditions.	60
Figure 5.16:	Some of the organosulfur compounds that found in the human bodies.	61
Figure 5.17:	The 1 st group of the organosulfur compounds.	62
Figure 5.18:	The 2 nd group of the organosulfur compounds.	63
Figure 5.19:	The 3 rd group of the organosulfur compounds.	64
Figure 5.20:	The 1 st part of the 4 th group of the organosulfur compounds.	65
Figure 5.21:	The 2 nd part of the 4 th group of the organosulfur compounds.	66
Figure 5.22:	The 1 st part of the 5 th group of the organosulfur compounds.	67
Figure 5.23:	The 2 nd part of the 5 th group of the organosulfur compounds.	68
Figure 5.24:	Some of the fatty acid compounds.	70
Figure 5.25:	The 1 st group of the fatty acid compounds.	70
Figure 5.26:	The 2 nd group of the fatty acid compounds.	71
Figure 5.27:	The classification of nitrogen containing organic compounds.	72
Figure 5.28:	The 1 st group of nitrogen containing organic compounds.	73
Figure 5.29:	The 1 st part of the 2 nd group of nitrogen containing organic compounds.	74
Figure 5.30:	The 2 nd part of the 2 nd group of nitrogen containing organic compounds.	75
Figure 5.31:	The 1 st part of the 3 rd group of nitrogen containing organic compounds.	76
Figure 5.32:	The 2 nd part of the 3 rd group of nitrogen containing organic compounds.	77
Figure 5.33:	The 4 th group of nitrogen containing organic compounds.	78
Figure 5.34:	The chemical structure of the nitrile compounds.	80
Figure 5.35:	The 1 st group of the nitrile compounds.	80
Figure 5.36:	The 2 nd group of the nitrile compounds.	81
Figure 5.37:	The classification of hydrocarbon organic compounds.	82
Figure 5.38:	The 1 st group of the alkanes of hydrocarbon organic compounds.	83

Figure 5.39:	The 2 nd group of the alkanes of hydrocarbon organic compounds.	84
Figure 5.40:	The 3 rd group of the alkanes of hydrocarbon organic compounds.	84
Figure 5.41:	The 1 st group of the alkenes of hydrocarbon organic compounds.	85
Figure 5.42:	The 2 nd group of the alkenes of hydrocarbon organic compounds.	86
Figure 5.43:	The 3 rd group of the alkenes of hydrocarbon organic compounds.	87
Figure 5.44:	The 4 th group of the alkenes of hydrocarbon organic compounds.	88
Figure 5.45:	The 1 st group of the aromatic of hydrocarbon organic compounds.	90
Figure 5.46:	The 2 nd group of the aromatic of hydrocarbon organic compounds.	91
Figure 5.47:	The 3 rd group of the aromatic of hydrocarbon organic compounds.	92
Figure 5.48:	The 4 th group of the aromatic of hydrocarbon organic compounds.	93
Figure 5.49:	The 5 th group of the aromatic of hydrocarbon organic compounds.	94
Figure 5.50:	The 6 th group of the aromatic of hydrocarbon organic compounds.	95
Figure 5.51:	The chemical structure of aldehyde and ketone organic compounds.	97
Figure 5.52:	The 1 st group of aldehyde and ketone organic compounds.	98
Figure 5.53:	The 2 nd group of aldehyde and ketone organic compounds.	99
Figure 5.54:	The 3 rd group of aldehyde and ketone organic compounds.	100
Figure 5.55:	The 4 th group of aldehyde and ketone organic compounds.	101
Figure 5.56:	The chemical structure of the alcohol compounds.	102
Figure 5.57:	The 1 st group of alcohol compounds.	102
Figure 5.58:	The 2 nd group of alcohol compounds.	103
Figure 5.59:	The 3 rd group of the alcohol compounds.	104
Figure 5.60:	The terpene and terpenoid compounds.	106
Figure 5.61:	The Organoselenium compounds.	106
Figure 5.62:	The organoselenium compounds.	107
Figure 5.63:	The methyl group.	190
Figure 5.64:	The water and water multimere.	191

Chapter 6

Figure 6.1:	The colour-code of the heatmap visualisation.	193
Figure 6.2:	The VisualNow window showing the RIP: (A) the main window, (B) the single chromatogram at the selected ion mobility on the right side of the main window and (C) the single spectrum at the selected retention time lower the main window.	194
Figure 6.3:	Two-dimensional MCC-IMS spectrum, the x-axis represents $1/k_0$ (Vs/cm^2) and the y-axis represents the RT (s).	195
Figure 6.4:	Chromatogram three-dimensional plot of MCC-IMS measurement: (A) a heatmap for the three-dimensional plot and (B) a schematic view of the three-dimensional plot.	196
Figure 6.5:	MCC-IMS chromatograms of (A) Raw, (B) Baseline Correction, (C) Compensate RIP-Tailing, (D) Norm Signal to RIP, (E) Smooth and (F) Median Smooth.	198
Figure 6.6:	(A) the spectra and (B) the chromatogram comparisons between: raw, baseline correction, compensate RIP-Tailing, norm signal to RIP, smooth, and median smooth for the same peak.	199
Figure 6.7:	MCC-IMS heatmap showing the effect of different diet statuses on three different analytes that characterized by their $1/k_0$ and RT.	201
Figure 6.8:	The different behaviours of three different analytes due to the different diet statuses in two parts of the device MCC (on the left) and IMS (on the right): — before eating, — after eating, — with mouthwash, — with tap water and — with chewing gum.	205

Figure 6.9:	MCC/IMS heatmap showing the effect of Tedlar bag on three different analytes.	206
Figure 6.10:	The different behaviours of three different analytes due to the way of breath in two parts of the device MCC (on the left) and IMS (on the right): — direct breath (1 st attempt), — indirect breath (Tedlar bag) and — direct breath (2 nd attempt).	207
Figure 6.11:	The three-dimensional view shows the effect of smoking and non-smoking on the spectra.	208
Figure 6.12:	The MCC/IMS heatmap for two different analytes showing the effect of the Tedlar bag and the smoking status.	209
Figure 6.13:	Box-and-Whisker-Plot showing the effect of the Tedlar bag and the smoking.	210
Figure 6.14:	The flow chart for the optimization process of the measurement done with IMS.	212
Figure 6.15:	An example of analytes that shows a constant linear time dependence: Sample No. 1 (fasting volunteer) with $1/k_0=0.577$ (Vs/cm ²) and RT=22.6(s).	213
Figure 6.16:	An example of analytes that shows an increasing linear time dependence: Sample No. 10 (normal volunteer) with $1/k_0=0.603$ (Vs/cm ²) and RT=8.9(s).	214
Figure 6.17:	An example of analytes that shows a decreasing linear time dependence: Sample No. 4 (normal volunteer) with $1/k_0=0.535$ (Vs/cm ²) and RT=7.9(s).	214
Figure 6.18:	: Two examples of analytes that show a rising kinetics: Sample No. 8 (smoking volunteer) with $1/k_0=0.485$ (Vs/cm ²) and RT=42.1(s) (on the left) and Sample No. 3 (after eating) with $1/k_0=0.644$ (Vs/cm ²) and RT=30.4(s) (on the right).	215
Figure 6.19:	Two examples of analytes that show a decaying kinetics: Sample No. 5 (after washing the mouth with Listerine mouthwash) with $1/k_0=0.650$ (Vs/cm ²) and RT=167.5(s) (on the left) and Sample No. 9 (after chewing peppermint gum) with $1/k_0=0.450$ (Vs/cm ²) and RT=5.6(s) (on the right).	216

List of Contents

Subjects	Page No.
1. Introduction	1-7
1.1. Volatile Organic Compounds (VOCs)	1
1.2. Breath Gas Analysis (BGA)	4
1.3. The Principle of The BGA	5
1.4. Common VOCs Apparatuses	7
2. Medical Background	8-13
2.1. CO ₂ Production Rate Measurement	8
2.2. Bicarbonate Kinetics Model	9
2.3. Stable Carbon-13 Isotope Breath Test	12
3. ¹³C-Methacetin for Monitoring the Liver Function	14-35
3.1. The Physiology of the Liver	14
3.2. Liver Function Breath Tests	17
3.3. ¹³ C-Methacetin Breath Analysis	17
3.4. Bicarbonate Kinetics of ¹³ C-Methacetin	19
3.5. The DOB-Kinetics	20
3.6. The LiMAx-Test	22
3.7. The Principle of FANci2	23
3.8. The Principle of FLIP	24
3.9. The Influence of O ₂ on the DOB Value	24
3.10. The Influence of Dosage and Sports on DOB-Kinetics and LiMAx-Test	25
4. Materials and Experimental Work	36-46
4.1. Breath Gas Sampling	36
4.2. Tedlar Bag and Teflon Tube	36
4.3. Effect of Tedlar Bag on VOCs	37
4.4. Identification of the VOCs	38
4.4.1. Proton-Transfer Reaction Mass Spectrometry (PTR-MS)	38
4.4.1.1. The Principle of PTR-MS Measurement	39
4.4.1.2. Measurement with PTR-MS	41
i. Vegan (People with Special Nutrition)	41
ii. Volunteers (Reference)	42
iii. Patients with Liver Diseases	42
4.4.2. Ion Mobility Spectrometry (IMS)	43
4.4.2.1. The Principle of IMS Measurement	44
4.4.2.2. Measurement with IMS	46
5. Results and Discussion of PTR-MS	47-107
5.1. PTR-MS Spectrum	47
5.2. Ion Counts Determination	48
5.3. Ion Counts Normalization	49

5.4. Paradigmatic Test Compounds	50
5.4.1. Isoprene Model	51
5.4.2. Acetone Model	51
5.4.3. Separating Overlapping Signals	53
5.5. Determination of Pearson's Correlation Coefficient (r)	55
5.6. VOCs Assessment	57
5.7. Influence of Tedlar Bags on VOCs Concentrations	58
5.8. Volatile Organic Compounds (VOCs) as Biomarkers	60
5.8.1. VOCs as Liver Diseases Biomarkers	60
5.8.1.1. Organosulfur Compounds	61
5.8.1.2. Volatile Fatty Acid Compounds	69
5.8.1.3. Nitrogen Containing Organic Compounds	72
5.8.1.4. Nitrile Compounds	80
5.8.1.5. Hydrocarbon Compounds	82
5.8.1.6. Aldehyde and Ketone Compounds	97
5.8.1.7. Alcohol Compounds	102
5.8.1.8. Terpene and Terpenoid Compounds	105
5.8.1.9. Organoselenium Compounds	106

Summary and Outlook	108-111
----------------------------	----------------

List of Publications	112
-----------------------------	------------

Appendices	113-216
-------------------	----------------

Part 1: Tables	113-185
-----------------------	----------------

Table 1: The data information that belong to Vegans according to PTR-MS measurement.	113
Table 2: The data information that belong to Volunteers according to PTR-MS measurement.	114
Table 3: The data information that belong to patients with liver diseases according to PTR-MS measurement	115-116
Table 4: The DOB and LiMAx values according to the type of liver disease for FANci and FLIP.	117-118
Table 5: The data information that belong to volunteers according to IMS measurement.	119
Table 6: Tentative assignments of some compounds at each protonated mass (m/z).	120-183
Table 7: The Organosulfur compounds.	184-185

Part 2:	186-189
----------------	----------------

5.7.1. Linear Time Dependence	186
5.7.1.1. Constant Linear Time Dependence	186
5.7.1.2. Increasing Linear Time Dependence	186
5.7.1.3. Decreasing Linear Time Dependence	187
5.7.2. Nonlinear Time Dependence	188
5.7.2.1. Rising Kinetics	188
5.7.2.2. Decaying Kinetics	188

Part 3:	190-191
----------------	----------------

5.8.2. Other VOCs Biomarkers	190
5.8.2.1. Methyl group-CH ₃	190

5.8.2.2. The Water and Water Multimere Peak Identification	190
Part 4: Results and Discussion of IMS	192-216
6.1. VisualNow Window	192
6.2. Data from MCC-IMS	194
6.3. The Pre-requisites for Sample Analysis	195
6.4. The Comparability of the Measurements	196
6.5. Comparisons within Spectra and Chromatograms	198
6.6. Peak Detection and Comparison	199
6.7. Factors Effecting on the VOCs Intensity	200
6.7.1. Comparative Study between Different Statuses of Diet	200
i. Before Eating (Fasting From the Day Before)	201
ii. After Eating	202
iii. After Washing the Mouth with Listerine Mouthwash	202
iv. After Washing the Mouth with Tap Water and Drinking Tap Water Many Time	203
v. After Chewing Peppermint Gum	204
6.7.2. Comparative Study between Direct Breath and Indirect Breath	206
6.7.3. Comparative Study between Smoker and non-Smoker	208
6.8. Influence of Tedlar Bags on VOCs concentrations	211
6.8.1. Linear Time Dependence	213
6.8.1.1. Constant Linear Time Dependence	213
6.8.1.2. Increasing Linear Time Dependence	213
6.8.1.3. Decreasing Linear Time Dependence	214
6.8.2. Nonlinear Time Dependence	215
6.8.2.1. Rising Kinetics	215
6.8.2.2. Decaying Kinetics	215

Bibliography

Acknowledgement

Curriculum Vitae (hidden for protection rule)

Erklärung der Selbstständigkeit

Chapter 1

Introduction

This chapter is an overview of the Volatile Organic Compounds (VOCs), the Breath Gas Analysis (BGA), the principle of the BGA and common VOCs apparatuses.

1.1. Volatile Organic Compounds (VOCs)

The substances (or chemicals) can enter the body by three ways: ingestion (food and/or beverage), inhalation (air), and topical contact (eyes, mouth and skin), as shown in Figure 1.1. These substances that enter the blood are metabolized and then distributed in the body or removed from the body through feces and/or urine.

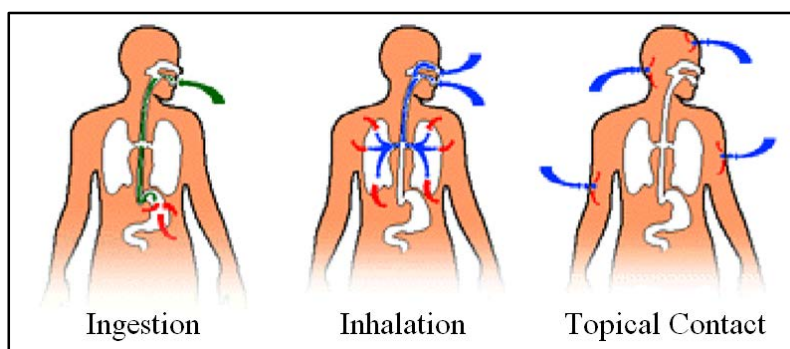


Figure 1.1: The three ways that the VOCs can enter the body: i) ingestion, ii) inhalation and iii) topical contact [1].

These absorbed substances (chemicals) are of two types: when they are exchanged with alveolar air and exhaled through the breath, they are called volatile. When their vapour pressure is too low they cannot be detected in the breath, and they are called non-volatile [2].

VOCs are organic chemical compounds which have under normal conditions a sufficient vapour pressure to vaporize and enter the atmosphere. There are many sources of VOCs in the atmospheric air such as pollution from vehicles and factories (CO₂, CO, hydrocarbons and etc.), human's breath (methanol, ethanol, acetone, isoprene and etc.) or plants releasing biogenic VOCs (isoprenoids and terpenes). The concentration of these VOCs in the atmospheric air can be as low as 1 ppbv (parts per billion volume) or even lower [3, 4].

Referring to exhaled breath, two different types of samples are recognized: i) exhaled breath vapour (EBV) that contains only volatile compounds and ii) exhaled breath condensate (EBC) that contains volatile and non-volatile compounds [5].

If the VOCs are used to diagnose the diseases, the origin of these compounds must be understood and if these compounds are present in the ambient surrounding. Figure 1.2 illustrates the sources of the VOCs. Some researchers subtract the environmental VOCs from the exhaled air sample while others do not [6, 7].

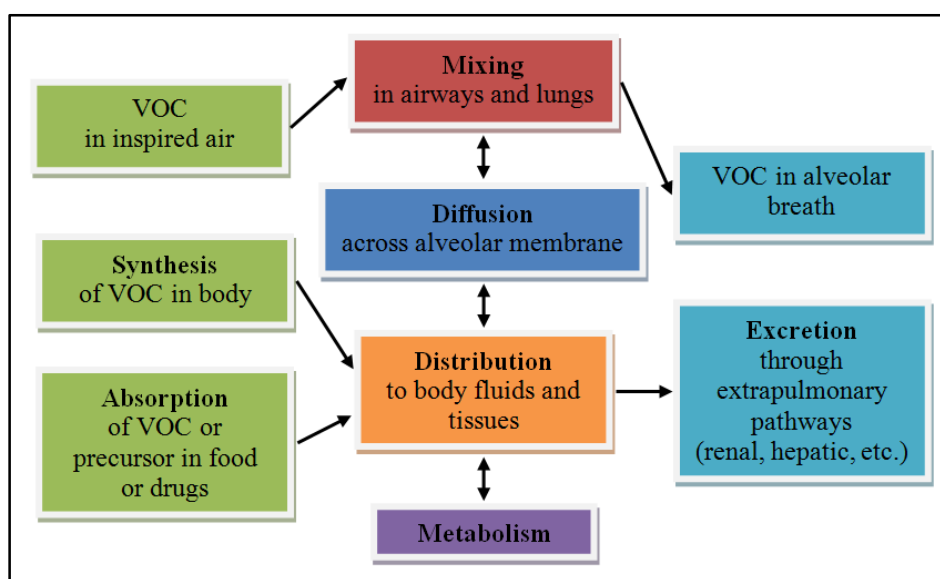


Figure 1.2: The sources of the VOCs in the breath [6, 7].

The gaseous and capillary VOCs equilibrium process in the alveoli varies with the phase of respiration, as shown in Figure 1.3. In the inspiratory phase, there is an equilibrium between the room air VOCs and pulmonary venous blood. In the expiratory phase, there is an equilibrium between the pulmonary arterial blood and VOCs in alveolar breath. The

extrapulmonary input of VOCs is primarily from endogenous synthesis, but the extrapulmonary output of VOCs is predominantly by metabolism in the liver and excretion in the kidneys [8].

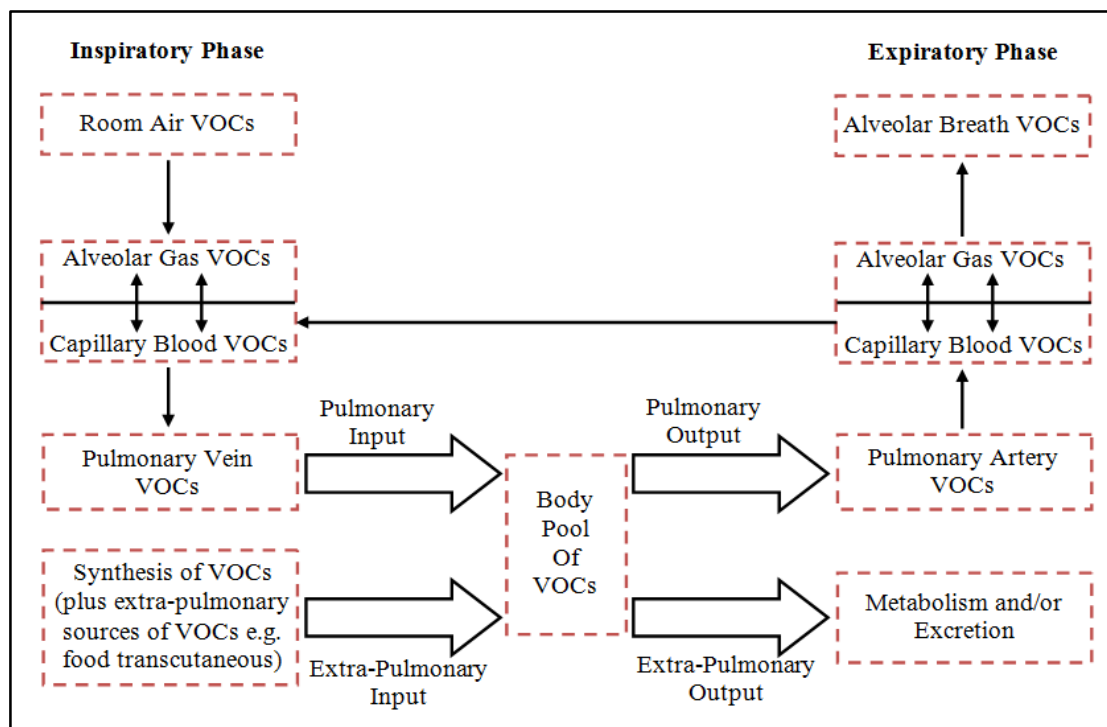


Figure 1.3: The VOCs pathways through different compartments of the body [8].

Nitrogen, oxygen, carbon dioxide, water, inert gases and VOCs mixture are the matrix of the breath [9], while acetone, isoprene, methanol and ethanol are considered the main VOCs that can be found in the breath of healthy subjects, which are endogenously produced due to metabolic process. There are other compounds that are found at very low levels [5, 9], (see Table 6 in Appendices). VOCs concentrations depend on food intake, state of physical condition, general health of the subject, and multiple environmental factors [10]. The intra- and intersubject variability in VOC emissions is essential and it has to be taken into account for data analysis [8, 10].

Additionally, exhaled NO, H₂, NH₃ and CO can reflect a potential disease of the individual or a recent exposure to a drug or an environmental pollutant [9, 11].

Most of VOCs origin and physiological function are still unknown, some of them originate from the subject's previous exposure to precursors, others are genuine metabolites of the organism itself or of its intestinal bacteria. In the first case, the precursors are taken up by inhalation, ingestion or skin contact then metabolized and exhaled by expiration. In the

second case, they are carried by the blood to the lungs and exhaled through the expiration [10].

If the source of VOC is inside the human body, it is called endogenous VOC, and if it is originated in the surrounding air, it is called exogenous VOC [3].

1.2. Breath Gas Analysis (BGA)

Breath tests are used for monitoring/detection diseases and/or to evaluate the drug metabolization, e.g. by CYP450 enzyme activity, because it offers a unique, rapid and a non-invasive diagnostic tool for tracking the biomarkers that are originated from both normal biochemical processes and pathological disorders [12, 13]. Breath test was used since the days of Hippocrates [12].

The ancient Greek physicians identified the disease from the odour of the exhaled breath [14]. In 1971, a great interest in analysing the VOCs from the breath has been shown, after explaining the breath gas analysis by Linus Puling using a gas-chromatography (GC) method [12, 14, 15]. He found out that, human breath is a complex gas mixture that contains more than 200 different VOCs. Since this time, the breath analysis is in use to monitor different types of diseases.

Breath Gas Analysis (BGA) is a non-invasive technique, which is important for monitoring and diagnosis the physiological status of people [16, 17]. BGA has many advantages comparing to other diagnostics methods such as blood, urine, biopsy, endoscopy and imaging as it is non-invasive, easier, fast and repeatable [18].

The concept of the BGA is based on the assumption that there is a correlation between the exhaled VOCs concentrations and the circulating blood concentrations, which is a reflection of the metabolic processes in the body [3, 19].

BGA is new field of medicine and medical instrumentation used for identification and quantification of the VOCs in human breath. It is classified into two groups: i) analysis of breath metabolites after administration of a drug or substrate and ii) analysis of breath compounds produced endogenously due to a particular physiological status [3, 17, 20].

The measurement of blood-borne VOCs occurs in the exhaled breath can be due to normal metabolic activities or due to pathological disorders [17].

According to many biological and technological processes, VOCs are used in several fields like environmental and atmospheric chemistry, plant biology, food science and technology and medical sciences [21].

1.3. The Principle of The BGA

The principle of breath gas analysis depends on the physiological phenomenon of gas exchange between blood and air [7]. The process of gas exchange between O_2 and CO_2 gases is a life process, which occurs in the lungs, the essential respiratory organ in the respiratory system, see Figure 1.4.

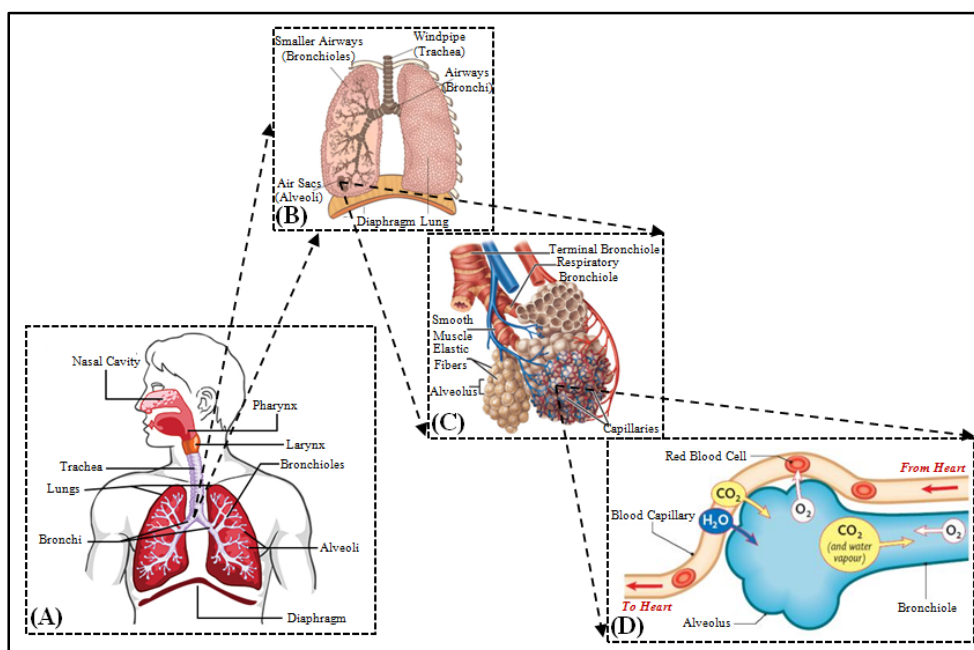


Figure 1.4: (A) A schematic view of the respiratory tract [22], (B) Anatomical view of the lungs that shows the position of the alveoli [23], (C) An enlarged view of the alveoli (gas sac) and pulmonary capillaries (blood vessels) [24] and (D) A close-up view of the O_2 and CO_2 exchange between the alveoli and pulmonary capillaries [25].

Figure 1.4.A shows the position of the lungs in the respiratory system. Figure 1.4.B shows the alveoli (singular=alveolus), the surface of numerous tiny chamber, present on the tip of the bronchiole in the lung. These alveoli are adapted well to their functions and each alveolus is covered with very thin membrane that is loaded with pulmonary capillaries, as shown in Figure 1.4.C.

As illustrated in Figure 1.4.D, the gas exchange occurs between the air in the alveolus and the blood in the pulmonary capillaries. A large surface area and a small distance associated with alveoli give the VOCs a chance to permeate from the air in the alveoli into the blood in the pulmonary capillaries. Another source of VOCs in the breath involves in the tissue surfaces of the nose, mouth and trachea through various biological processes.

The concentration gradient between the capillaries and the alveoli has a role in gas diffusion. For that, there are two types of processes: i) if the concentrations of the compounds in the air greater than that in the blood, the compounds move into the blood, but ii) if the concentrations of the compounds in the blood greater than that in the air, the compounds move into the air. Thus, the expired breath contains molecules from two different origins: i) from inspired air and ii) from the blood. Comparison between inspired air and expired air allows for identification of the origin of the VOCs. Typically, VOCs that are inhaled show a lower concentration in the exhaled air than in the inhaled air. This reflects the uptake of the blood of these VOCs.

According to Shaji *et al.* study [2], “The key challenge in the analysis of the breath is ‘separating the alveolar breath’, which contains analyte rich air delivered deep in the lungs from ‘the dead space’ air volume of breath contained in the upper airways namely mouth, and pharynx that is uninvolved in gas exchange, and another challenge is separating and identifying the volatile breath components which tend to be present at just picomolar level concentrations [8, 13]”.

King et al. reported that [17], “the concentrations of water-soluble, blood-borne substances in exhaled breath are influenced by:

- breathing patterns affecting gas exchange in the conducting airways,
- the concentrations in the tracheo-bronchial lining fluid,
- the alveolar and systemic concentrations of the compound”.

Here, I assume that these influences are negligible in our investigations.

1.4. Common VOCs Apparatuses

The analytical methods which are used to detect concentrations of VOCs emitted from the breath have been improved. Today, there are many methods in use for this purpose, for example [26]:

- Laser Absorption Spectroscopy (LAS), which was introduced with the Flow-through Fast Liver Investigation Packet (FLIP).
- Proton-Transfer-Reaction Mass Spectrometry (PTR-MS).
- Ion Mobility Spectrometry (IMS), mostly coupled to Multi-Capillary Columns (MCC/IMS).
- Gas-Chromatography with Mass Spectrometric detection (GC-MS), often combined with Thermal Desorption (TD-GC-MS).
- Differential Ion Mobility Spectrometry (DMS).
- Sensors or Sensor Arrays.

In this study, LAS, PTR-MS and IMS methods are used and discussed.

Chapter 2

Medical Background

This chapter introduces the ^{13}C breath test and discusses the influence of CO_2 production rate, and bicarbonate kinetics on this test.

2.1. CO_2 Production Rate Measurement

In ^{13}C breath tests a substance is administered that is metabolized to $^{13}\text{CO}_2$, so that carbon dioxide ($^{13}\text{CO}_2$) is an end-product in the catabolism of the administered compound. This process is effected by several factors, which may have an influence on the rate of appearance of $^{13}\text{CO}_2$ in the exhaled air.

Clearing dynamics are influenced for example by gastric emptying, rate of intestinal absorption and the bicarbonate pool for CO_2 [27].

The exhalation of the labelled CO_2 ($^{13}\text{CO}_2$) that is derived from the labelled compounds artificially or naturally has a useful means for various metabolic disorders diagnosis or estimation their oxidation rate quantitatively.

The CO_2 breath tests use the administration of carbon labelled substance that releases the labelled carbon isotopes through their metabolic pathways. The appearance rate of the label (^{13}C) in the exhaled CO_2 gives an information about the factors affecting the rate-limiting step of the metabolic route [27, 28].

2.2. Bicarbonate Kinetics Model

The bicarbonate kinetics are important for interpretation of the measured CO₂ isotopes in vivo [29].

The bicarbonate system has a crucial role in the measurement of the substrates' oxidation in the human body from the tracer data. In the process of oxidation, many substrates are metabolized and produce CO₂ that can be measured in the expired air. This measurement depends on the individual substrate metabolism as well as on the bicarbonate kinetics in the body [29, 30]. The bicarbonate distribution and metabolism knowledge is very important for the experimental interpretation correction to measure the carbon-labeled compounds' oxidation in vivo.

The bicarbonate kinetics models used in the studies of substrate oxidation tracer are linear compartmental models and are identified from an experiment involving an impulsive intravenous input of labeled bicarbonate (¹⁴C]-or [¹³C]NaHCO₃) and labeled CO₂ frequent sampling in the expired air.

Some of the tracer-labelled CO₂ is released or recovered in the breath and the other is equilibrated in slowly turning over pools such as bone and is released over a period of time. Theoretically, the entire released tracer in the oxidation process can be recovered when the breath sampling is done for a long period of time (in days), this procedure is not quite possible in human subjects additionally a non-respiratory losses of CO₂ can occur [31].

For that, it is necessary to apply a correction factor to the measured rate of labelled CO₂ evolution in expired air to correct and to determine the oxidation rate of the carbon labelled substrate accurately over a shorter period of time (for example 24 hrs.). This procedure is estimated by the proportion of the labelled bicarbonate dose, given intravenously or orally as a constant infusion or bolus, that appears in the expired air [31, 32].

It is often assumed that the administered labelled bicarbonate load and the labeled CO₂/HCO₃ that is generated by the substrate metabolic oxidation in the body share the same recovery (correction) factor [29]. It was demonstrated that both the respiratory and non-respiratory losses are located in the central vascular compartment, which is the pool where tracer input occurs [31].

It has been proposed that there are uncertainties in the two and three compartment model structures as well as for the influence of different output variables. Some important parameters for model parametrization such as specific activity, enrichment of CO₂, or the labelled CO₂ flux in the expired air are difficult to determine [29, 33, 34, 35].

The bicarbonate kinetics composite model can be constructed from the arterial and venous CO₂ levels estimations, the rates of tissue production, the bicarbonate and CO₂ levels and the rates of the organ blood flow. For construction of this model, there must be [32]:

- 1) Organs that are grouped into compartments depending on their CO₂ uptake and release rates.
- 2) HCO₃⁻-CO₂ compartments sizes that are calculated from the HCO₃⁻-CO₂ tissue levels.
- 3) Rates of fractional turnover that are determined from the arterial and venous CO₂ levels, the flow of the tissue blood and the rates of CO₂ production, assuming complete single-pass mixing of tissue and vascular HCO₃⁻-CO₂.
- 4) The fractional rate constant for the exchange of circulating bicarbonate with the sink of bone bicarbonate that is estimated from the levels of blood HCO₃⁻-CO₂, the rate of skeletal blood flow and the extraction ratio of bicarbonate from blood by bone.

The model that is displayed in Figure 2.1 consists of three pools of freely exchangeable bicarbonate: i) the vascular pool (2.111 μmol.kg⁻¹), which is considered the central pool, ii) the heart-brain-“other” pool (2.389 μmol.kg⁻¹), which is considered the slow pool and iii) the muscle pool (6.122 μmol.kg⁻¹), which is considered the fast pool. The CO₂ output rate is (153 μmol.kg⁻¹.min⁻¹), which is the result of CO₂ production from the heart-brain-“other” pool (127.5 μmol.kg⁻¹.min⁻¹) and the muscle pool (25.5 μmol.kg⁻¹.min⁻¹) [32].

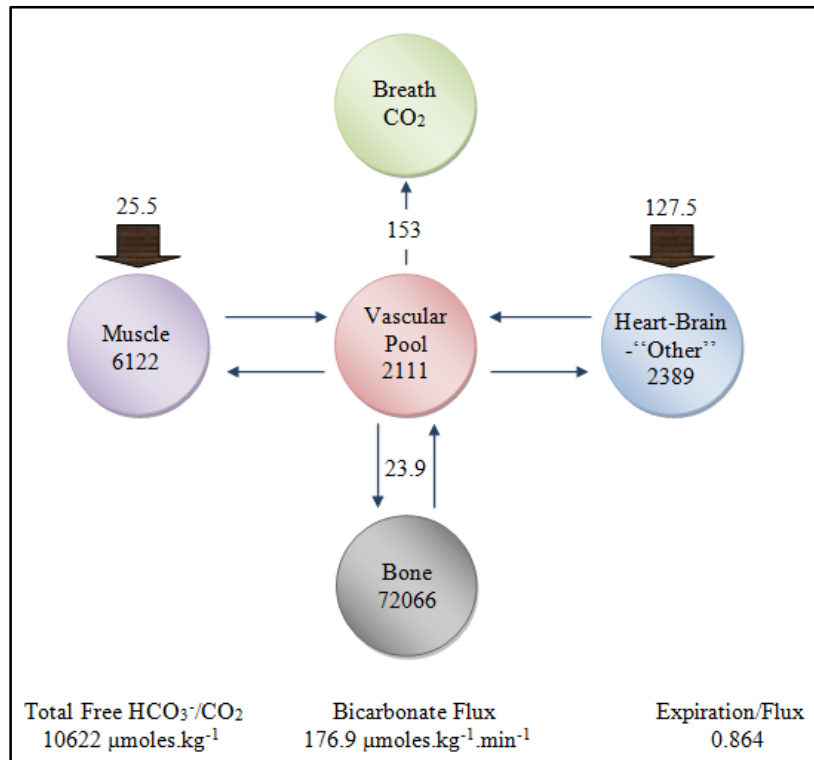


Figure 2.1: The physiological bicarbonate model that consists of three pools: i) the vascular pool, ii) the heart-brain-“other” pool and iii) the muscle pool [32].

There is an exchange between vascular bicarbonate and the large sink of bone bicarbonate ($72.066 \mu\text{mol.kg}^{-1}$) at a rate of ($23.9 \mu\text{mol.kg}^{-1}.\text{min}^{-1}$). ($23.9 \mu\text{mol.kg}^{-1}.\text{min}^{-1}$) value was estimated using skeletal blood flow rate that is equal to 5% of the cardiac output and a 30% of the bicarbonate extraction ratio between bone and blood [33, 36]. ($176.9 \mu\text{mol.kg}^{-1}.\text{min}^{-1}$) is the total flux of freely exchangeable bicarbonate of which 86.5% is accounted for by respiratory losses.

The unified model of the bicarbonate can provide us with a framework for future studies of the effect of age, nutritional and metabolic status, exercise and acidosis on bicarbonate kinetic parameters [32].

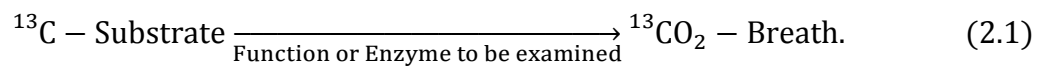
Fast and slow time constants related to the bicarbonate pool dynamics are reported to be about 3 minutes and 50 minutes [32].

2.3. Stable Carbon-13 Isotope Breath Test

Isotopes such as ^{13}C , ^{15}N and ^{18}O are stable isotopes, they are simple and safe. They can be used with children and pregnant women because they are non-radioactive isotopes and they contribute to the elemental content in human subjects.

^{13}C isotope is a non-radioactive isotope that has replaced its radioactive counterpart ^{14}C and it is naturally available for a non-invasive diagnosis. It ends up in the exhaled air or in the urine and provide us with the urine signal that is cumulated over time [37].

In ^{13}C -Breath test, the administered ^{13}C labeled substrate is metabolized by a specific enzyme system to $^{13}\text{CO}_2$ and released into the CO_2 pool of the body, which will equilibrate with the bicarbonate pool, as shown in the following equation:



When additional $^{13}\text{CO}_2$ is expired, one can quantify the tracer-released amount as enrichment product in the CO_2 expiration rate [31].

The ^{13}C -labeled substrates have been used as an investigation tool for the evaluation of different polymorphic enzyme activities. They enable us to measure gastro-intestinal, hepatological and metabolic functions directly under several physiological conditions. Figure 2.2 shows some possible ^{13}C -breath tests.

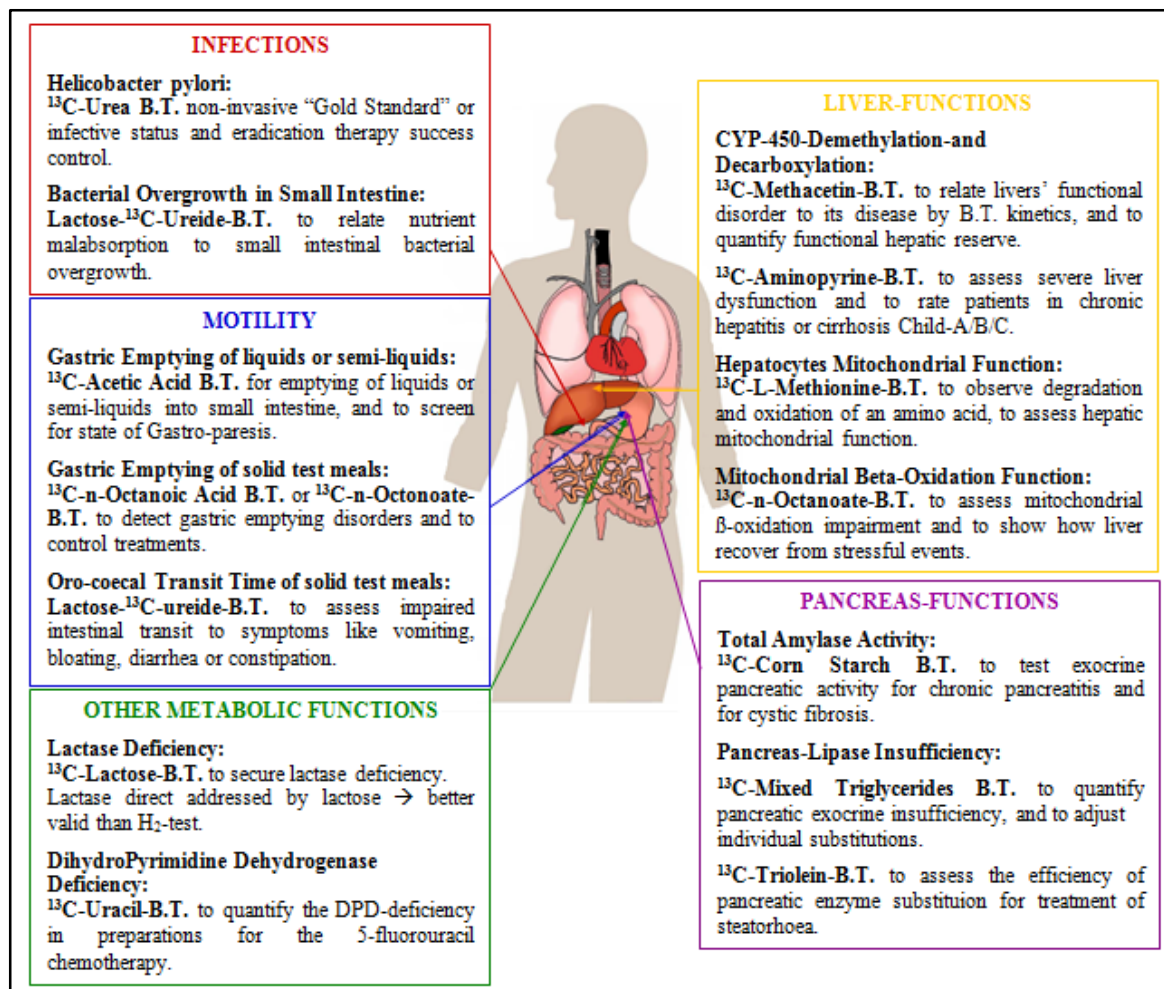


Figure 2.2: Some possible ^{13}C -Breath Tests [38].

Over 200 years ago CO_2 was identified as a breath analyte by Lavoisier. He examined the carbon dioxide in breath in 1784 [39], and 30 years since the first publications and many clinical applications later, the breath test is still unfamiliar as a diagnostic tool, and no general agreement concerning to its applications has been reached [7].

Chapter 3

¹³C-Methacetin for Monitoring the Liver Function

This chapter discusses the physiology of the liver, liver function breath tests, ¹³C-methacetin breath analysis, bicarbonate kinetics of ¹³C-methacetin, the DOB-Kinetics, the LiMAx-Test, the principle of FANci2, the principle of FLIP, the influence of O₂ on the DOB value as well as the influence of dose and sports on the DOB-Kinetics and the LiMAx-Test.

3.1. The Physiology of the Liver

Liver is the largest blood-rich organ in the body; it weighs nearly (1.3 kg to 1.4 kg) in the average adult and has a length of 7 cm to 10 cm. It has a wedge shape that occupies the right hypochondriac and epigastric regions, as shown in Figure 3.1.A. It is located in the abdominal cavity beneath the diaphragm and protected within the rib cage.

As illustrated in Figure 3.1.B, the liver has anatomically four lobes: i) the right lobe (the largest lobe), ii) the left lobe (the smallest lobe), which are separated by a deep fissure, iii) the caudate lobe and iv) the quadrate lobe, which are located inferior to the left lobe.

The liver is composed of functional units called liver lobules, which are sesame seed-sized structures, see Figure 3.1.C. This lobule has a roughly hexagonal (six-sided) structure consisting of plates of liver cells or hepatocytes. These hepatocyte plates radiate outward from a central vein running in the longitudinal axis of the lobule, see Figure 3.1.D.

The liver has the ability to regenerate itself in one week due to the mitotic division of the remaining hepatocytes.

The liver is considered one of the most important organ in the body associated with gallbladder and intestine, because it has many metabolic and regulatory roles. The digestive function of the liver is to produce bile, which is a fat emulsifier that breaks up fats into tiny particles and become more accessible to digestive enzymes that are stored and concentrated in the gallbladder before its discharge into the duodenum. The liver has a metabolic role rather than a digestive role, because it processes the nutrient-laden venous blood that is delivered to it directly from the digestive organs.

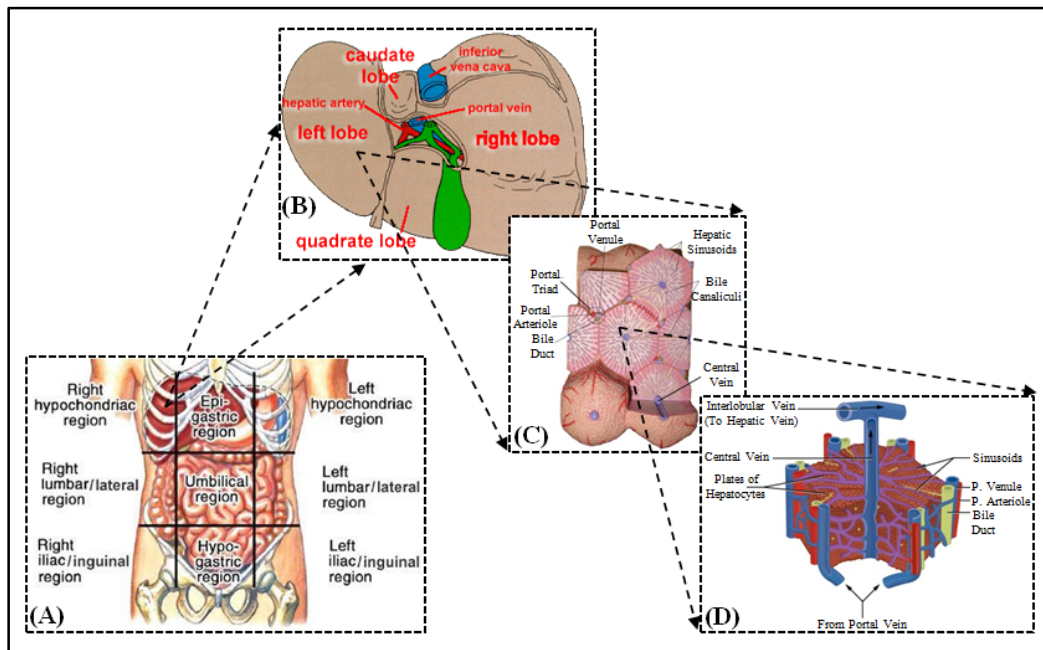


Figure 3.1: (A) A schematic view shows the location of the liver [40], (B) Anatomical view of the liver that shows the lobes [41], (C) An enlarged view of the functional unit of the liver [42] and (D) A close-up view of the hepatocytes plate [43].

The nutrient-rich venous blood, that is caused due to the absorption of the digestive products in the intestinal blood capillaries, is delivered to the liver that collects the absorbed nutrients for the metabolic processing or for the storage before entering the general circulation through the hepatic portal system, see Figure 3.2.

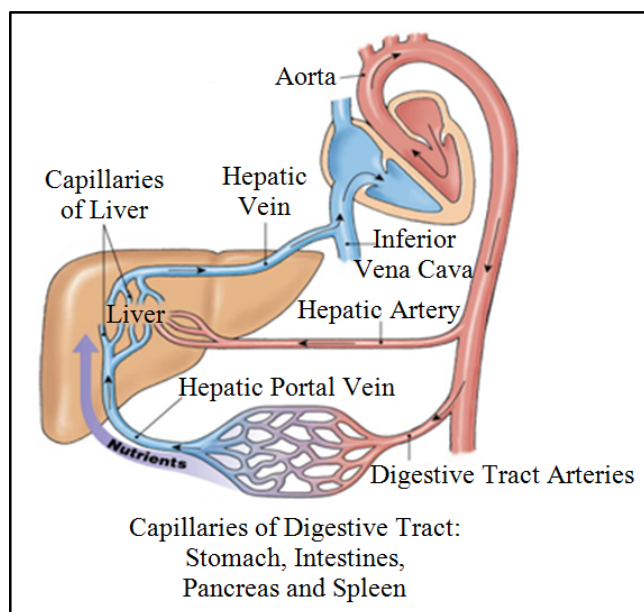


Figure 3.2: The hepatic portal circulation [44].

The hepatic portal vein connects the capillaries of the digestive system with the capillaries of the liver, so the blood exchange between these capillaries also receive the venous blood from the intestine, but through the hepatic artery the liver receives arterial blood.

In liver disease, the non-functional liver cells fail to produce the procoagulants and bile that are required for fat and vitamin K absorption. Figure 3.3 illustrates the types and the effects of liver diseases on the liver cells.

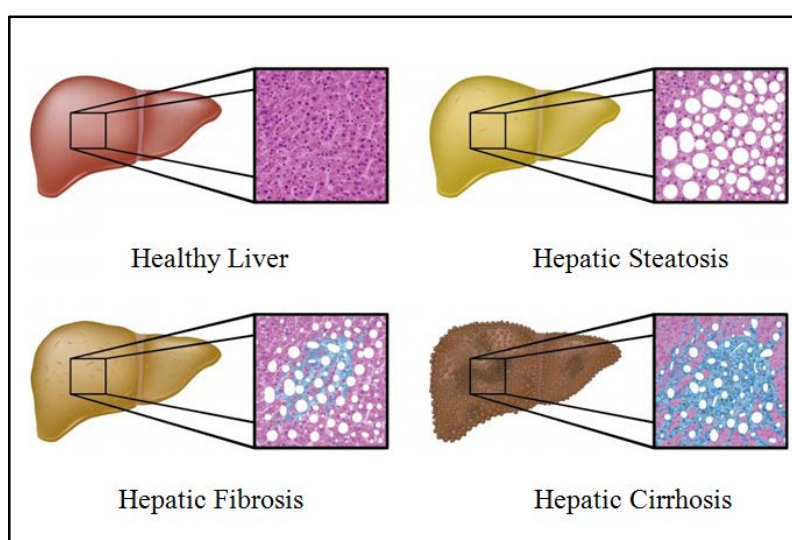


Figure 3.3: The types and the effects of liver diseases on the liver cells [45].

Liver disease is a major health problem concerned with a significant morbidity and mortality. The etiologies and the clinical presentation may differ from asymptomatic state to severe liver failure. Any damage to the liver cells will increase the concentration of toxic metabolites in the blood circulation, because liver plays a vital and complex role in various metabolic and synthetic functions.

3.2. Liver Function Breath Tests

To know how to manage patients with liver diseases, it is important to evaluate the liver function [46]. In clinical practice, diagnosis of liver disease is based on the results of physical examination, imaging techniques (ultrasonography, computed tomography, magnetic resonance, etc.) and biochemical investigations [47]. It is found that there is no single biochemical test able to predict the severity and prognosis of the hepatic diseases whether acute or chronic [48]. For that, several quantitative tests have been used to measure the residual hepatic function and numerous substrates to improve the diagnostic efficacy of biochemical tests [49].

Recently a breath test has been used to evaluate the liver function. The principle of the breath test is based on what happens to the injected substrate. When this substrate is injected, it goes through the blood circulation, then it is metabolized in the liver and then exhaled through the lungs. This procedure determines the liver metabolic function.

3.3. ¹³C-Methacetin Breath Analysis

From the breath test, we can easily assess the liver function based on the labelled substrates that are used and metabolized in the liver [50, 51]. ¹³C-methacetin breath test (¹³C-MBT) is the most suitable test for evaluation of the liver functional reserve compared to other tests [50, 52]. Comparing to other molecules that are used for breath tests, ¹³C-methacetin is a manageable substance, safe, cheap and has rapid clearance [50, 53]. ¹³C-methacetin can differentiate between healthy people and people with liver diseases in a short time.

Methacetin [N-(4-methoxyphenyl) acetamide], a derivative of phenacetin, undergoes O-demethylation through the hepatic mixed function oxidase system to become acetaminophen and CO₂, the latter ultimately being exhaled. Because of the rapid metabolism of ¹³C-methacetin in healthy people and the low toxicity in small doses, ¹³C-methacetin is well suited substance for breath test. The hepatic microsomal enzyme system (cytochrome P450 1A2) is evaluated by the metabolism of the ¹³C-methacetin labeled substrate to ¹³C-labelled CO₂ and paracetamol [54], as illustrated in Figure 3.4.

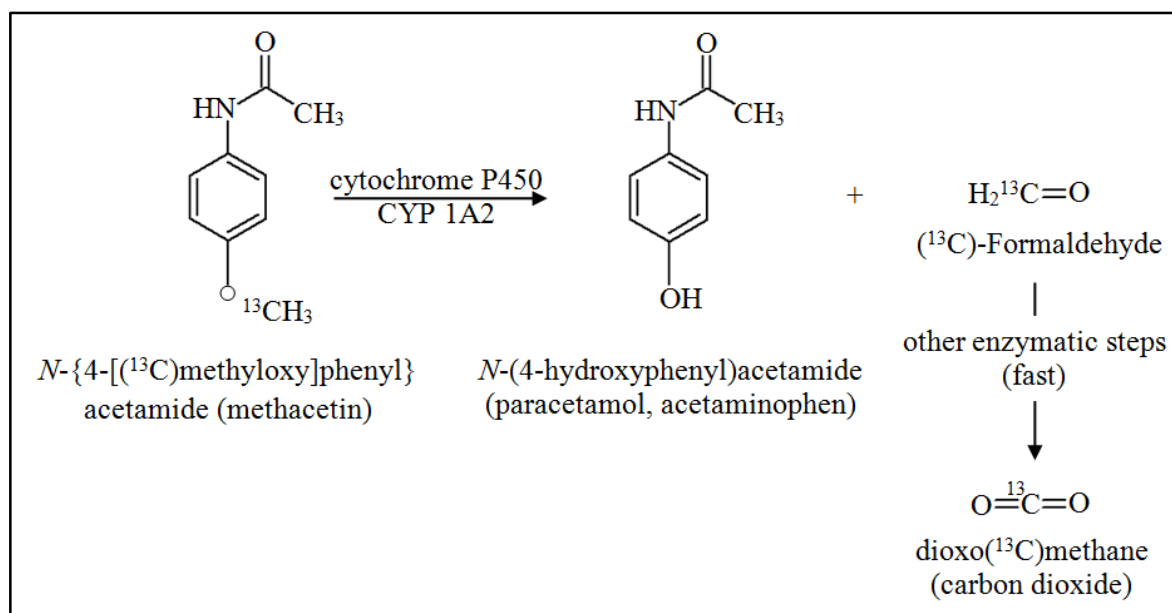


Figure 3.4: The conversion process of ¹³C-methacetin to paracetamol and CO₂ in the liver [54]. Formaldehyde is fast metabolized by formaldehyde dehydrogenase.

Cytochrome P450 1A2 (CYP1A2) is a hepatic enzyme that plays an important role in metabolizing drugs and xenobiotics like methacetin, theophylline, caffeine and clozapine [55].

¹³C-methacetin breath test belongs to the family of microsomal liver tests and it was first described by *Krumbiegel et al.* in 1985 [56, 57]. Since that time, it is considered a useful tool for assessing the degree of liver damage and estimating the functional reserve of the liver.

In the ¹³C-methacetin breath test procedure, the ¹³C-methacetin is delivered intravenously so it can detect the ¹³CO₂ quickly. Additionally, it is safer than the oral administration to avoid a gastro-intestinal tract resorption.

3.4. Bicarbonate Kinetics of ¹³C-Methacetin

The oxidation of substrates in the body is determined by the bicarbonate system. During the oxidation process these substrates are metabolized and produce CO₂ that can be measured from the expiration. When the influence factors like the physiological serum kinetics of the substrate and the bicarbonate kinetics are taken into account in the suitable test protocols development an accurate test result can be obtained from nBTs [58].

Three-compartment model has been used to describe the ¹³C-methacetin kinetics, as shown in Figure 3.5. This model describes (M) for ¹³C-methacetin, (C) for ¹³CO₂, it represents the total concentration of ¹³CO₂ and H¹³CO₃, which are in quasi-equilibrium due to the fast carboanhydrase reaction and (P) for paracetamol [59].

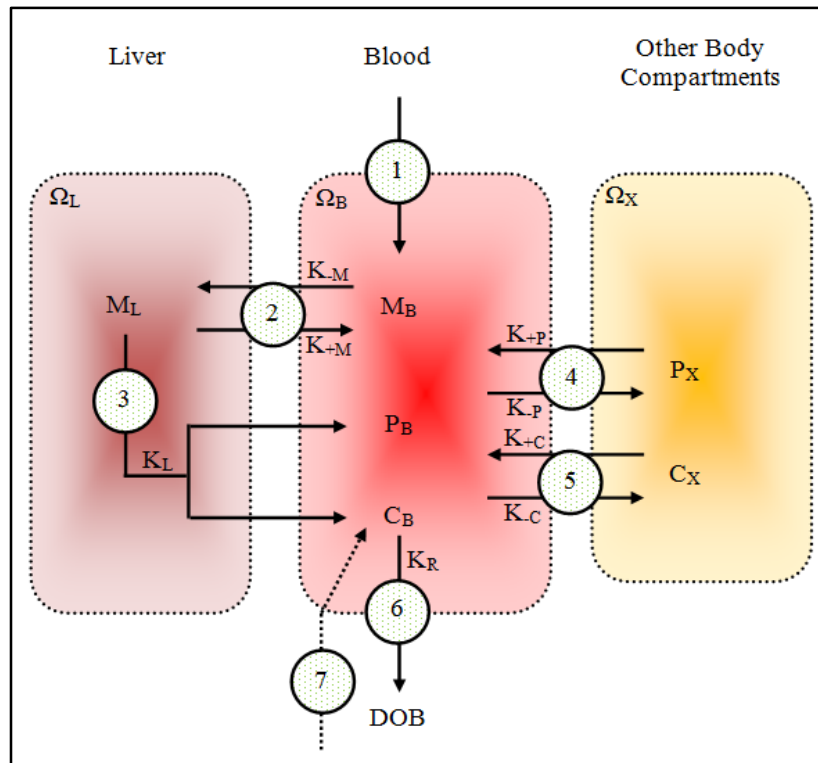


Figure 3.5: The schematic of the 3-compartment model uses to describe the observed kinetics of ¹³C-methacetin (M), paracetamol (P) and ¹³CO₂ (C) (quantified in the breath as DOB): (1) Injection of M into the blood, (2) reversible exchange of (M) between blood and liver, (3) hepatic metabolization of (M) to (P) and (C), (4) reversible exchange of (P) between blood and other body compartments, (5) reversible exchange of CO₂ between blood and other body compartments, (6) respiratory removal of (M) and (7) injection of H¹³CO₃ (in the proposed novel 2DOB-method). Ω_B, Ω_L and Ω_X denote the volume of the three compartments [59].

It was reported that, the exchange of the ¹³C-methacetin (M) in the plasma compartment (B) with the liver compartment (L) is reversible. The kinetic discrimination from exchange with the liver was not feasible from the measurements of plasma ¹³C-methacetin, so the exchange of methacetin with other body compartments was not considered [59].

Paracetamol (P) and ¹³CO₂ (C) may exchange reversibly between plasma compartment (B) and body compartment (X). Because the plasma half-life is (1.5-2.5) hrs. [59, 60], the excretion of the paracetamol was not considered, but by K_{+P} parameter the potential influence of paracetamol excretion on its plasma profile can be partially captured.

This model provides a suitable ansatz to explain the DOB-Kinetics we have investigated and that are presented in the next paragraph. In our experiment, we found additional ¹³CO₂ level on time scales after 2 hours.

3.5. The DOB-Kinetics

In the medical field, respiratory gas analysis is now increasingly being used because it is considered to be a non-invasive method that has a little impact on the patients. The patients' breath samples were collected in the bags and then analyzed in the laboratory with mass or infrared spectrometers.

The DOB kinetics reflect the change in ¹³CO₂/¹²CO₂ ratio R_(t) in the breath, where the isotope ratio is given by the following equation:

$$R_{(t)} = \frac{{}^{13}\text{CO}_2(t)}{{}^{12}\text{CO}_2(t)}. \quad (3.1)$$

DOB means Delta over Baseline in ‰, which is defined by to the following equation:

$$\text{DOB}_{(t)} = \frac{(R_{(t)} - R_{(0)})}{R_{\text{PDB}}} * 1000. \quad (3.2)$$

$$\text{DOB}_{(\text{max})} = \text{DOB}(t_{\text{max}}). \quad (3.3)$$

For the isotopic ratio the Pee Dee Belemnite standard is set with $R_{\text{PDB}} = 0.01123686$. In fact, the measured R_{PDB} -value is subjected to regional variations. Thus, for example:

- for Central Europeans:

$$R_{\text{M.E.}} = \frac{R_{\text{PDB}}}{1.025}. \quad (3.4)$$

- for Americans:

$$R_{\text{AM}} = \frac{R_{\text{PDB}}}{1.02}. \quad (3.5)$$

With the method that is currently used, the total CO_2 -production cannot be measured, because in the FANci measuring method, only a fraction of the total tidal volume is analysed. The FLIP method also does not detect the total CO_2 amount [61]. However, this is important because the DOB value describes the relative change of the CO_2 isotope ratio, but not the absolute $^{13}\text{CO}_2$ excess. Instead, the CO_2 production is estimated by equation 3.6, which depends on the body surface area of the patient and it has been accepted:

$$\text{CO}_2\text{Production} = 300 \left[\frac{\text{mm}}{\text{h} \cdot \text{m}^2} \right] * \text{BSA}[\text{m}^2] \quad \left[\frac{\text{mmol}}{\text{h}} \right] \quad (3.6)$$

The body surface area (BSA) as a function of the height (H) in cm and weight (W) in kg. It is calculated according to several formulas, which, however, provide comparable results.

In this work, BSA is calculated using the Du Bois formula [62]:

$$\text{BSA}(\text{m}^2) = 0.007184 * W^{0.425} * H^{0.725}. \quad (3.7)$$

A precise measurement of CO_2 production is, however, necessary for an accurate statement about the liver performance.

After administration of 2 mg ^{13}C -methacetin per kg body weight, the degree of the liver dysfunction can be verified concerning to the change in time of $R_{(t)}$ and the DOB kinetics.

3.6. The LiMAX-Test

LiMAX means Liver Maximum capacity. The LiMAX-test is a non-invasive technique that developed by Priv.-Doz. Martin Stockmann and is used in the Charité. It is based on the hepatocyte-specific metabolism of the ¹³C-labelled substrate (methacetin; Euriso-top, Saint-Aubin Cedex, France) by the cytochrome P450 1A2 enzyme, which is ubiquitously active throughout the liver [63, 64].

The LiMAX-test was assumed to represent an accurate surrogate parameter of liver function capacity, because the readouts were highly correlated with functional liver volume ($r=0,94$; $P<0.001$) [63, 65]. The LiMAX value can be calculated from the following formula [65]:

$$\text{LiMAX} = \frac{\text{DOB}_{\text{max}} * R_{\text{PDB}} * P_{\text{CO}_2} * M}{\text{BW}} \quad (3.8)$$

where:

$$\text{LiMAX} = \frac{\mu\text{g}}{\text{kg}} / \text{h}.$$

DOB_{max} = Maximum value of the DOB kinetics

$$R_{\text{PDB}} = 0.011237.$$

P_{CO_2} = The CO₂ production rate = 300 mmol/h*BSA m².

M = The molar mass of (¹³C-methacetin) = 166.19 g/mol.

BW = The body weight in kg.

When the labelled substrates are orally administrated the gastrointestinal absorption variations will occur and the maximal plasma levels will differ. This precludes a reliable kinetic analysis of the CYP1A2 activity as an actual metabolism depends on the available substrate [65]. To solve this problem the LiMAX test with intravenous bolus application was developed.

The LiMAX test procedure based on putting the patient in a resting horizontal position after at least 6 hours fasting. The baseline $^{13}\text{CO}_2/^{12}\text{CO}_2$ ratio is recorded ten minutes prior to the injection with ^{13}C -methacetin and the mean is used for the delta-over-baseline (DOB) calculation. ^{13}C -labeled methacetin is injected as a bolus of 2 mg/kg body weight over a maximum of 30 seconds into an intravenous catheter, followed by 20 mL 0.9% sodium chloride solution. Breath analysis is performed by a suitable device which is directly connected to the patient (online measurement), this procedure takes 60 min. Referring to Stockmann *at el.* study [63], “Mechanically ventilated patients were respired with 100% oxygen during the test to reduce interference with nondispersive isotope-selective infrared spectroscopy” [65, 66].

3.7. The Principle of FANci2

With a frequency of as approximately 1/min by a modified non dispersive isotope-selective infrared spectroscopy based device (FANci2-db16, Fischer ANalysen Instrumente GmbH, Leipzig, Germany) breath samples were automatically drawn and analyzed.

FANci2, which is a Fischer ANalysen Instrumente, is a photo-acoustic NDIR-Spectrometer for measuring the $^{13}\text{CO}_2$ to $^{12}\text{CO}_2$ ratio. As a light source, a black body radiator is used. Two detection chambers are filled with $^{13}\text{CO}_2$ or $^{12}\text{CO}_2$, in each of them there is a microphone. Between the light source and the detection chamber there is a chopper to modulate the IR radiation and the measuring chamber are filled with the gas to be tested. The molecules in the detection chambers absorb the modulated IR radiation and convert it to thermal energy. The so-modulated density fluctuations cause sound waves, and each is measured with a microphone.

The disadvantage of the device is that it is very sensitive to vibration and temperature changes. Also, the breath cannot be measured in the flow state, so instead of this an aluminum bag is used.

In standard mode, the breath is collected by bag and connected to the device, then it pumps the breath air into the measuring chamber. During blowing, it is important to make sure that only the alveolar air is used. The air that does not reach the alveoli has the CO_2 content of the inspired air would distort the values. With this measuring method an accuracy

of ± 2 DOB can be achieved according to the manufacturer, but it does not provide absolute values for exhaled CO₂ volumes [67].

3.8. The Principle of FLIP

Flip means Flow-through Fast Liver Investigation Packet. The FLIP can measure the ¹³CO₂/¹²CO₂ ratio in exhaled breath. It was developed by Prof. Dr. Karsten Heyne at Free University Berlin/Germany.

The ultra-sensitive laser spectroscopy system of the FLIP within the LiMAX-test can quickly and reliably determine the capacity of the liver function. The FLIP/LiMAX system, greatly improves the surgical intervention planning.

The laser based FLIP device detects a metabolic product of the enzymatic conversion of the drug methacetin in the liver in the exhaled air. This metabolic product is the ¹³CO₂ isotope, which is stable, non-radioactive and detected by the unique sensors in the device even at extremely low concentrations (100 ppb) in every single breath [68].

The FLIP measures in real-time a continuous flow of air. It has been developed in cooperation with medical professionals and is adapted to various clinical situations. The FLIP has unified the mobility, the usability and the practicality. It has been used successfully in various intensive care units, emergency rooms, operating theatres and outpatient stations.

3.9. The Influence of O₂ on the DOB Value

The DOB maximum value correlates well with the liver function capacity. It corresponds to the maximum of the metabolization rate of methacetin.

It is well known from the measurements in the Charité that pure O₂ ventilation leads to an increase of the measured DOB value of the patient. The reason for this has not yet been established.

To exclude the biological cause, gas mixture with the same ¹³CO₂ to ¹²CO₂ ratio but different oxygen concentrations from 7% to 90% were prepared and measured.

According to *Rubin's study* [67], “there was a good agreement for the influence of the oxygen on the DOB value of the patient [66] and the increased of the DOB value measured using FANci2 by 20 (1) when O₂ is used instead of N₂ as a residual gas”, as shown in Figure 3.6.

Particularly in the critical cases, the incorrect measured DOB increasing by the influence of oxygen is greater than the actual DOB signal. In the methodology that is developed by Rubin there is no influence on the DOB value by the presence of oxygen.

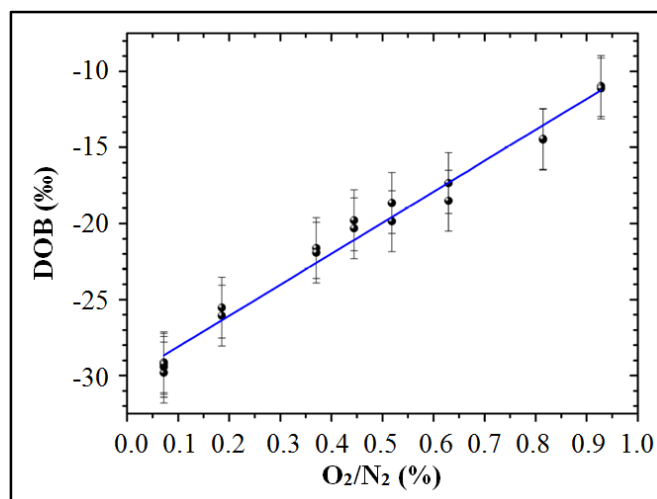


Figure 3.6: The influence of oxygen on the DOB measurement by using FANci2: The increase corresponds to 20 (1) DOB after replacing 100% N₂ with 100% O₂ as a residual gas [67].

3.10. The Influence of Dosage and Sports on DOB-Kinetics and LiMAX-Test

19 healthy volunteers with no known liver diseases (15 male / 4 female, mean age 30±7 years, range 21-47 years, mean body weight 75±13 kg, mean body mass index 23.2±2.9 kg/m², mean body surface area 1.9±0.2 m²) were recruited for the study from July 2008 to December 2008. The study protocol was prior approved by the faculty's (University Medicine Berlin - Charité; Germany) ethical review board and written informed consent was obtained from each individual.

The volunteers were injected with ¹³C-methacetin intravenously (IV) at the bend of the elbow (antecubital fossa), as explained in Figure 3.7.

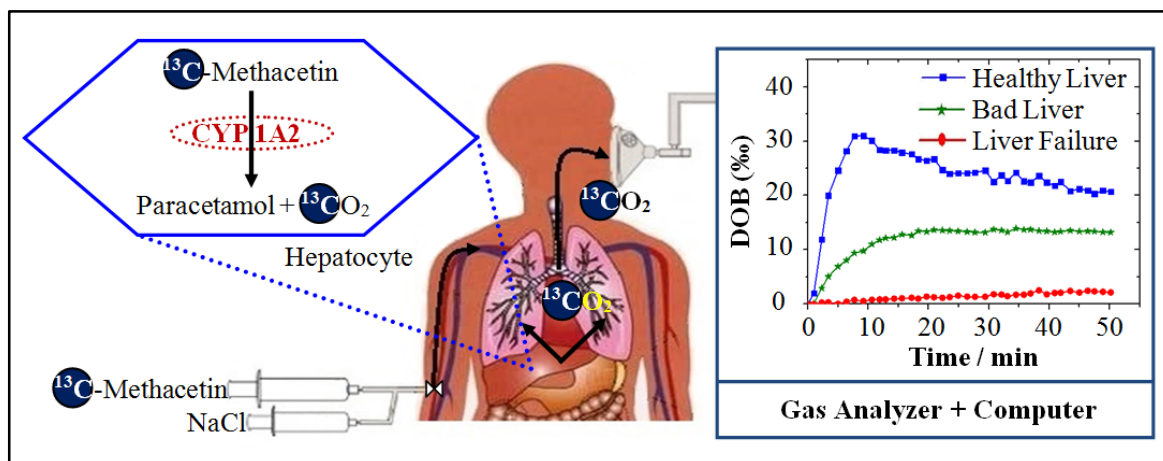


Figure 3.7: Scheme of ^{13}C -methacetin breath test / LiMAX test: iv administration of ^{13}C -methacetin and NaCl induces the metabolism (**upper left**) to paracetamol and $^{13}\text{CO}_2$; $^{13}\text{CO}_2$ is dissolved in the blood, transported to the lungs and exhaled; exhaled air is analyzed by a gas analyzer detecting the additional exhaled $^{13}\text{CO}_2$ plotted in ‰ as a function of time (**upper right**). The maximal DOB value indicates the liver status (healthy liver, bad liver and liver failure).

The DOB kinetics of $^{13}\text{CO}_2/^{12}\text{CO}_2$ ratio were measured for 60 mins. The $^{13}\text{CO}_2/^{12}\text{CO}_2$ ratio is standardized by the Pee Dee Belemnite standard.

Each subject performed the LiMAX test for five measurements in five different days with different doses and different cycling times, as shown in Figure 3.8.

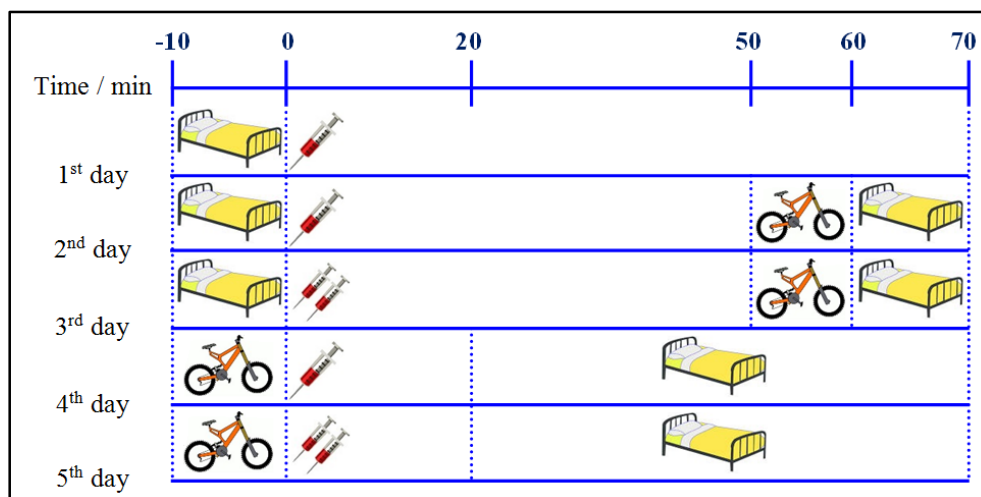


Figure 3.8: Measurement schemes for 5 days as a function of time in minutes with different dosages and different cycling times; bed: resting time; syringe: ^{13}C -methacetin iv bolus application; bicycle: cycling period.

We set a constant cycling load that was determined by a bicycle ergometer to a heart frequency of 1.9 times the resting heart rate, the power was about 50 W. The transition from resting to cycling and back was as fast as possible.

The Procedure:

*** In the 1st Day:**

The volunteers were injected with 2 mg/kg body weight ¹³C-methacetin without doing sports (normal LiMAx-test).

*** In the 2nd Day:**

The volunteers were injected with 2 mg/kg body weight ¹³C-methacetin and did sports from min(50) to min(60).

*** In the 3th Day:**

The volunteers were injected with 4 mg/kg body weight ¹³C-methacetin and did sports from min(50) to min(60).

*** In the 4th Day:**

The volunteers were injected with 2 mg/kg body weight ¹³C-methacetin and did sports from min(-10) to min(20).

*** In the 5th Day:**

The volunteers were injected with 4 mg/kg body weight ¹³C-methacetin and did sports from min(-10) to min(20).

The data were simulated with a maximum of three exponentials with the following formula:

$$DOB_{(t)} = -A_1 * \exp\left(-\frac{t}{\tau_1}\right) + A_2 * \exp\left(-\frac{t}{\tau_2}\right) + A_3 * \exp\left(-\frac{t}{\tau_3}\right) \quad (3.9)$$

Here, the amplitude $A_1 = -(A_2 + A_3)$ represents the maximal amount of metabolized ¹³C-methacetin. The first exponential τ_1 describes the rise of the ¹³CO₂ in the exhaled air due

to metabolization. This rise directly mirrors the fast metabolization of the ¹³C-methacetin. The time constants τ_2 , and τ_3 of the second and third exponentials reflect the decay of the ¹³CO₂ concentration in the bicarbonate pool to zero. In resting patients with single dosage of 2mg/kg we found typical values for τ_1 of (3.0±0.5) minutes, for τ_2 of (24±4) minutes and a fixed time constant τ_3 of 180 minutes [59].

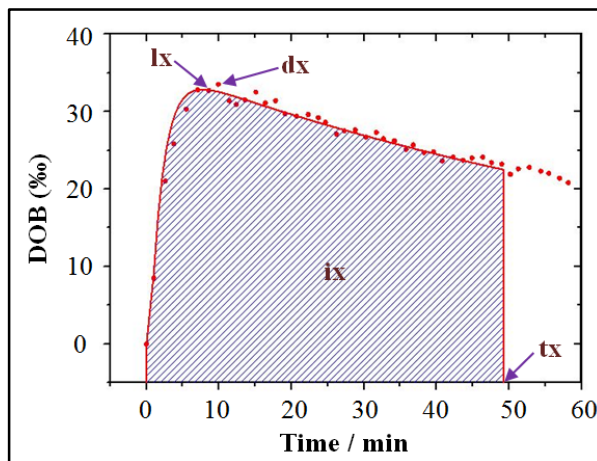


Figure 3.9: The typical DOB kinetics, **x**: the day of the measurement, **d**: the max. of the graph, **l**: the max. of the fitting, **i**: the integration of DOB, **t**: the time and **a**: the area (i/t).

Figure 3.9 shows the typical DOB kinetics. Three different measures to characterize the kinetics have been looked at, (i_x): the maximum of the fit curve, (d_x): the maximum point of the data and (i_x): the area below the fitting curve.

The reproducibility of the measured value was assessed by comparing (L_s): LiMAX value by simulating data and (L_d): LiMAX value by raw data of the different measurements with one another.

The result for $a(\text{min}20)$, $a(\text{min}50)$, data (d) and line (l), was (0.98±0.04) and for (A2+A3), the result was (0.98±0.05), so it is nearly the same. The $a(\text{min}50)$ has the smallest error and it is more reproducible, but the information of the DOB kinetic is lost.

The ¹³CO₂/¹²CO₂ ratio in the exhaled air was tracked for more than 60 minutes. Datapoints were taken every 1-2 minutes. The exhaled ¹³CO₂/¹²CO₂ ratio in DOB (delta over baseline) in ‰ is presented in Figure 3.10, which are shown the influence of dose and sports on the DOB-Kinetic and LiMAX-Test.

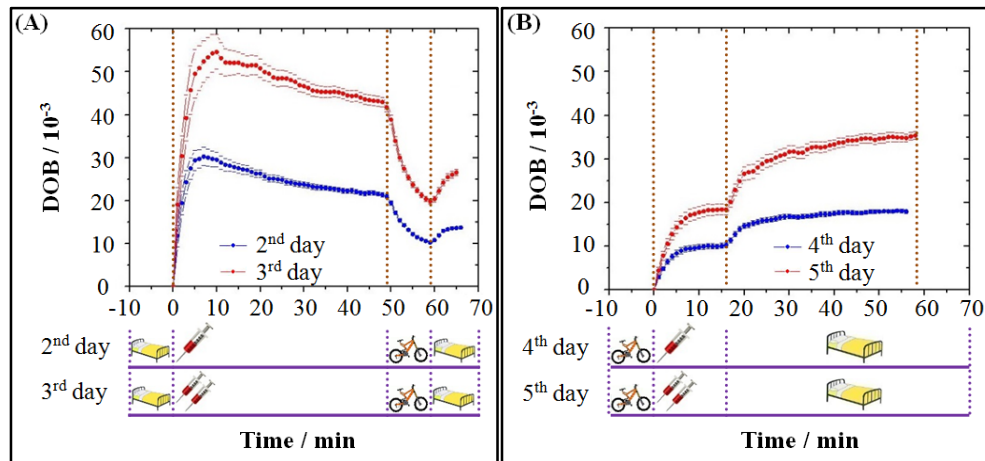


Figure 3.10: The effect of different doses of ¹³C-methacetin: **(A)** doing sports from min(50) to min(60) and **(B)** doing sports from min(-10) to min(20).

To investigate the dependency of the dosage ¹³C-methacetin was applied intravenously in a dosage of 2 mg/kg and 4 mg/kg and breath recovery was analyzed for 50 minutes to see the dependency of the dose. Figure 3.10.A illustrates the effect of double dose between the the 2nd measurement and the 3rd measurement and figure 3.10.B illustrates the effect of double dose between the 4nd measurement and the 5rd measurement.

When the doses are doubled from 2 mg to 4 mg, the results for a(20), a(50), data (d) and line (l) changed by (1.8±0.3) and for (A2+A3) the result changed to (1.9±0.4), so it nearly doubled. The doubled dose of methacetin nearly doubled the maximum DOB value due to the higher blood concentration of methacetin. The amount of methacetin metabolism is proportional to its concentration in the blood.

To investigate the influence of cycling all the cases underwent exercise (cycling) by an ergometer (~50 W) from min(50) to min(60) in the 2nd and 3rd measurement and from min(-10) to min(20) in the 4th and 5th measurement to see the influence of cycling, comparing Figure 3.10.A with Figure 3.10.B. With cycling our results for a(20), a(50), data (d) and line (l), were (0.33±0.08), nearly (1:3).

The DOB ratio decreases with sports since the muscles are producing CO₂ in significant amount, reducing relatively the ¹³CO₂ concentration supplied by the liver/methacetin. After sports completion, less CO₂ produced by the muscle leading to the recover of the DOB value.

The dose and the sports can be considered good indicators for the liver capacity. When the dose is increased, the average of the DOB increased in both cases within the time. This

indicates that ¹³C-methacetin is well absorbed and metabolized. When the exercise duration increase, the rate of mitochondrial CO₂ production decrease due to the slower rate of carbohydrate oxidation and faster rate of fat oxidation during exercise in the trained state and also bicarbonate recovery increased with exercise.

¹³C-methacetin as well as paracetamol blood levels were determined by HPLC at 0.5, 1, 2, 5, 10, 30 and 60 minutes after iv ¹³C-methacetin administration. Blood probes were drawn in a standardized manner as reported before: [59] 5 ml were discarded and a sample of 5 ml was drawn in a serum tube. Probes were centrifuged with 1,500 g for 4 minutes and the serum aliquot was separated. Blinded probes were analyzed for ¹³C-methacetin and paracetamol by high performance liquid chromatography (HPLC). HPLC analysis was performed using a Ultrashere ODS with a LC-6B system (Shimadzu) at a flow rate of 1.5 ml/min, with UV-detection at 260 nm. Samples of 50 µl serum were mixed with 100 µl of acetonitrile/methanol solution (1:1) and centrifuged at 10,000 g for 8 minutes before HPLC. Samples of each 10 µl were applied to the analyzer. A commercial HPLC-Test-Kit for measurement of levetiracetam was used for the analysis. The Kit-conditions were modified for estimation of methacetin and paracetamol. Chromatography was performed with the LC-6B system. The sensitivity was 0.5 µg/ml with proven test linearity up to a concentration of 100 µg/ml. The mean interassay variability was 6.8% for methacetin and 6.9% for paracetamol.

In Figure 3.11 the DOB kinetics (black and grey curves) and the clearing kinetics of ¹³C-methacetin (green and dark yellow curves) and the rise of paracetamol in the blood (red and magenta curves) are shown.

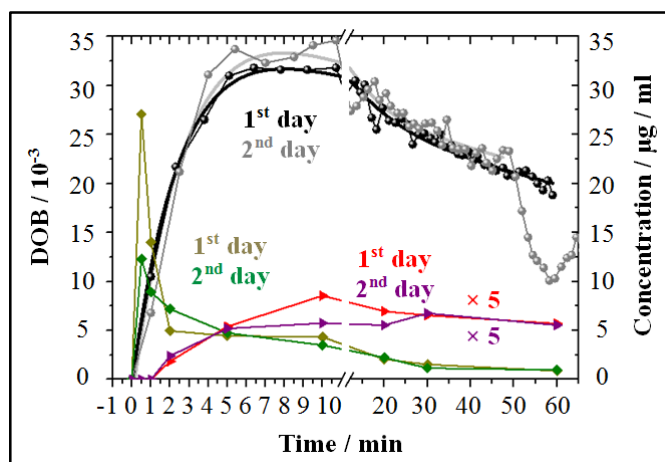


Figure 3.11: DOB kinetics, methacetin blood level and paracetamol blood level of the same person as a function of time after methacetin administration: **Day 1:** DOB kinetics (black dots) and simulation (black curve), methacetin blood level (dark yellow diamonds), and paracetamol blood level (red triangles); **day 2:** DOB kinetics (grey dots) and simulation (grey curve), methacetin blood level (green diamonds), and paracetamol blood level (magenta triangles). **Left:** Units for the DOB kinetics; **right:** Units for the blood levels.

We found matching time constants for the decay of ^{13}C -methacetin, and the rise of the DOB signal. This directly reflects the consumption of ^{13}C -methacetin and generation of $^{13}\text{CO}_2$. Unfortunately, fast and precise measurements of blood levels after ^{13}C -methacetin application is challenging, resulting in significant level deviations at early times as depicted in Figure 3.11 (green and dark yellow curves). Here, the maximal ^{13}C -methacetin blood levels vary from 27 $\mu\text{g}/\text{ml}$ to 12 $\mu\text{g}/\text{ml}$ thirty seconds after administration for the same measurement at two different days.

In contrast, the additional exhaled $^{13}\text{CO}_2$ (black and grey curves), and the paracetamol blood levels (red and magenta curves) displayed in Figure 3.11 are very reproducible. The paracetamol blood levels exhibit a delayed rise of ~ 1 minute with a slightly slower rise time compared to $^{13}\text{CO}_2$ [59]. The major part of ^{13}C -methacetin is metabolized on a short time scale of ~ 3 minutes (green and dark yellow curves). In the first 20 minutes the blood level of paracetamol appears to be at least a factor of five smaller than the methacetin level. Since, measurements on day 1 and day 2 are identical up to 50 minutes after administration, we can directly evaluate the reproducibility of the DOB_{max} values and the maximal paracetamol levels in the blood.

The correlation of the DOB_{max} values, the maximal paracetamol blood levels, correlation of DOB_{max} with maximal paracetamol blood level and the maximal methacetin blood levels are presented in Figure 3.12.

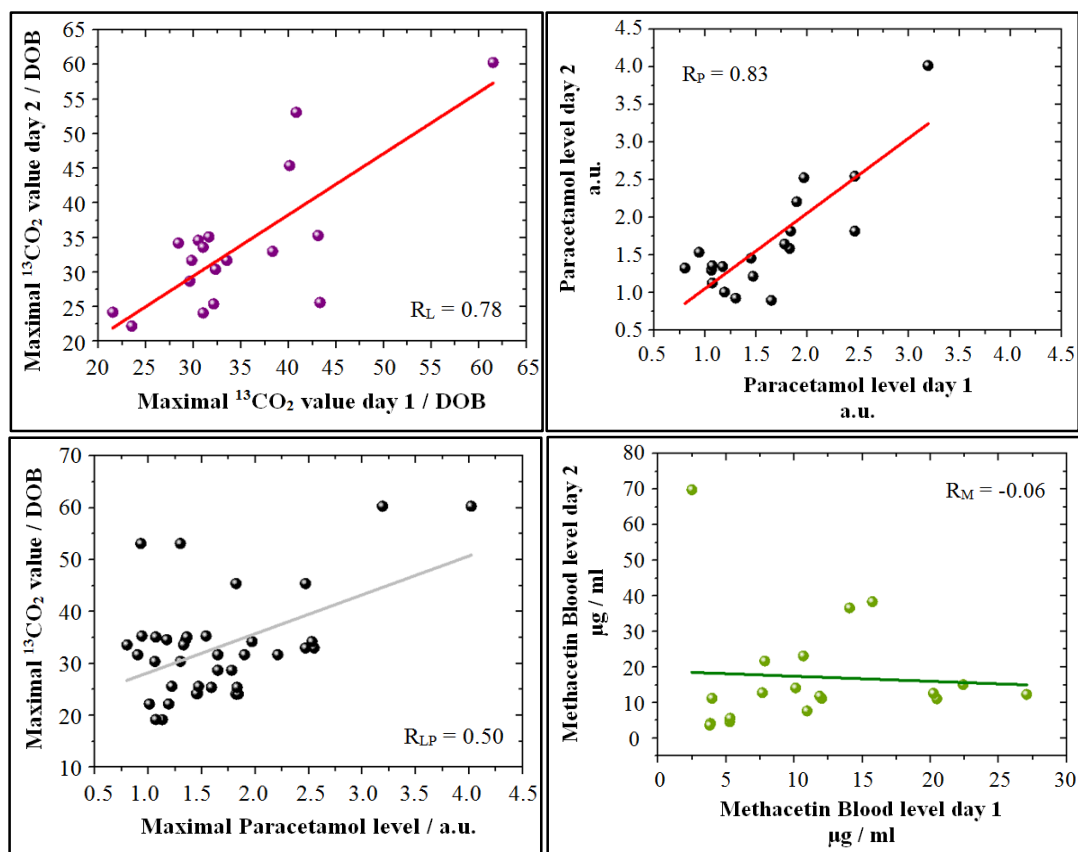


Figure 3.12: Analysis of the reproducibility of DOB_{max} , and maximal paracetamol blood level at two different days for the all subjects: DOB_{max} with correlation coefficient of $R_D=0.78$ (**upper left**), maximal paracetamol blood level with correlation coefficient of $R_p=0.83$ (**upper right**), correlation of DOB_{max} with maximal paracetamol blood level of $R_{DP}=0.5$ (**lower left**) and maximal methacetin blood level with correlation coefficient of $R_p=-0.06$ (**lower right**).

The Pearson coefficient show a very good correlation of $R_D=0.78$ and $R_p=0.83$ for the DOB_{max} values, and maximal paracetamol levels, respectively. The correlation between DOB_{max} value and maximal paracetamol level is depicted. Here, we found only a reasonable correlation with Pearson coefficient of $R_{DP}=0.5$, with a slope intersecting the y-axis at ~ 21 DOB. The reduced correlation could point to different diffusion properties of $^{13}CO_2$ and paracetamol in the liver cells. Moreover, paracetamol staying in the liver cells, while $^{13}CO_2$ is already distributed in the blood could account for the significant DOB value at the

intersection of the y-axis. In contrast, the maximal ¹³C-methacetin levels in the blood for repeated measurements show no correlation ($R_M = -0.06$).

The LiMAx values (L_d) of 19 subjects were determined by the maximum of the exhaled ¹³CO₂/¹²CO₂ ratio as a function of time (DOB kinetics) as presented in Figure 3.10 and 3.11 using equation 3.8 [63]. The LiMAx-values found, support normal liver function of the patients. The LiMAx value is proportional to the DOB_{max} value at time t_{max} , i.e. the maximum of the DOB transient. All other parameters in equation 3.8 stayed constant for the same patient. Thus, we used DOB_{max} in our analysis to investigate the dependence of DOB_{max} and LiMAx on several parameters.

Since the individual data points of the DOB kinetics exhibit error margins and fluctuations, we used a multi-exponential fit function to simulate the measured data, see Figure 3.11. From the simulated data we extracted the maximum of the DOB kinetics and used this value to determine the LiMAx value L_s . The DOB kinetics reflect the additional exhaled ¹³CO₂ due to ¹³C-methacetin metabolization after administration. Thus, integration of the simulated DOB kinetics from application to 20 minutes (A_{20}) or 50 minutes (A_{50}) after application reports the amount of metabolized and exhaled ¹³C-methacetin. Integration reduces the influence of random noise, increases the influence of fluctuations on a longer time scale, and is affected by the bicarbonate pool dynamics for longer integration times [29, 32].

Repeating the measurements for the same subjects at different days shows a very good average reproducibility of (99±4)% for L_s , (98±4)% for L_d , (98±4)% for A_{20} , and (98±3)% for A_{50} . For all measurements the average reproducibility of the values of L_s , L_d , A_{20} , and A_{50} agreed within the error margins.

The individual reproducibility for two consecutive measurements was identified by the Pearson correlation coefficient. We found a Pearson coefficient R of 0.80 for L_d , and L_s . For the amplitude A_1 , not influenced by the later bicarbonate pool dynamics we found a slightly smaller Pearson coefficient R of 0.78.

It was reported that the LiMAx value provides a linear correlation to the healthy liver volume of $R = 0.94$ [65]. Increasing the dosage could result in saturation effects. Here, we investigated the influence of doubling the dosage on the DOB kinetics. The LiMAx value was determined up to 50 minutes after application with dosage of 2 mg/kg body weight and 4 mg/kg body weight for day two and day three, respectively (Figure 3.8 and 3.10). Upon doubling the dosage the DOB kinetics were nearly doubled as presented in Figure 3.10.

Analysis of the LiMAX values L_d showed that the LiMAX values increased by (1.8 ± 0.1) upon doubling the dosage. This dependence deviates only slightly from linear behavior and points to small saturation effects for dosages as high as 4 mg/kg body weight.

After 50 minutes the patients started to cycle for 10 minutes and rested the following 10 minutes, see Figure 3.8 and 3.10. As depicted in Figure 3.10 upon cycling the exhaled $^{13}\text{CO}_2 / ^{12}\text{CO}_2$ ratio (DOB value) decreases nearly exponentially, followed by a DOB increase when the patient rests again. The DOB level does not fully recover to its original value upon resting on a time scale of 10 minutes.

Stable cycling conditions were used at day four and five when ^{13}C -methacetin was administered. As shown in Figure 3.10, the patients started cycling 10 minutes before administration and stopped 20 minutes thereafter. In this time window, the level of additionally metabolized $^{13}\text{CO}_2$ upon ^{13}C -methacetin metabolization rises with an averaged time constants of (6 ± 3) minutes for both dosages, see Figure 3.10. Upon resting the DOB level rises with an averaged rise time of (25 ± 20) minutes.

We found a reduction of LiMAX values L_s to (33 ± 2) % with respect to resting conditions, see Figure 3.10. Again, doubling the dosage result in nearly identical transients with nearly doubled DOB values, and increased LiMAX value by a factor of (1.82 ± 0.06) . Here, we observed a slightly smaller standard deviation in comparison to measurements under resting conditions.

After cycling, the DOB values rise with beginning of resting and levels of after ~ 50 minutes. We found an averaged rise time constants of (25 ± 20) minutes with DOB levels nearly matching the DOB levels of resting conditions (day 1 and day 2) upon single dosage, as shown in Figure 3.13.

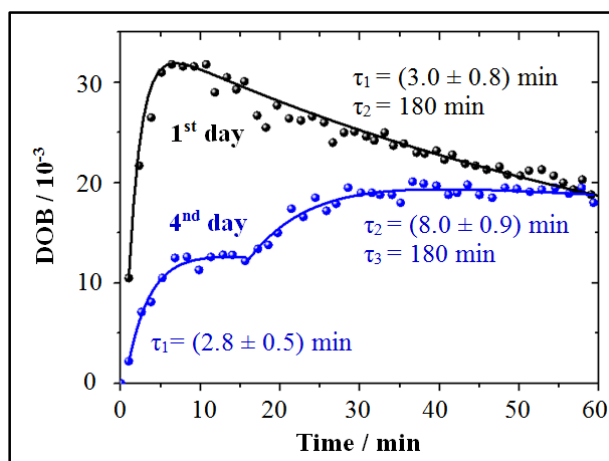


Figure 3.13: Example DOB kinetics and simulations with single dosage without sports (day 1: black dots and black curve) and with sports (day 4: blue dots and blue curve). Kinetics without sports have a single exponential rise and decay; kinetics with sports have a single rise time, followed by a slower rise time upon resting at about 20 min, followed by an exponential decay. The long decay constant is fixed to 180 minutes; time constants are given.

This nearly matching of DOB levels in all measurements comparing day 1 and day 4 indicates a reversible redistribution of CO₂ in the different body compartments upon physical activity within ~1 hour [29, 59].

Chapter 4

Materials and Experimental Work

This chapter explains the materials and the apparatus used in this study as well as the procedure we followed.

4.1. Breath Gas Sampling

After preparing the Tedlar bags and asking the people to take a deep breath, they were asked to blow direct into the bags. These bags were cleaned after each use with dry air (three times), to be sure that all the particles from the exhaled breath of the previous person were removed.

The collected breath samples contained breath from the alveolar phase, the transition phase and the anatomical dead space of an expiration cycle. People were asked to breathe normally and to blow into the Tedlar bags up to nearly filling the bags in one breath cycle.

4.2. Tedlar Bag and Teflon Tube

The breath samples were collected using 2 liter Tedlar bags, which are transparent and are possible to reuse (SUPELCO Analytical, USA). Tedlar bags are gas sample bags that are used because they are inert. They are made from Teflon (Polytetrafluoroethylene-PTFE) and are named Tedlar bags commercially. They are shown in Figure 4.1.A.

PTFE is a synthetic fluoropolymer of tetrafluoroethylene that has numerous applications, because of its many properties: it has excellent chemical and temperature resistance, good aging properties, remains tough and flexible over a broad temperature range, and contains no plasticizers. Hence, it is a highly viable material for breath testing. Tedlar film resists gas permeation both into and out of the bag. Tedlar bags are rated for continuous use, from -72 to 107 °C, so they are used in very cold or very hot environments.

The Teflon tube as shown in Figure 4.1.B, which is (153 cm) long, (3 mm) outer diameter and (1 mm) inner diameter was used in our measurement with Ion Mobility Spectrometry (IMS) to pump the air from Tedlar bag into the measuring device.

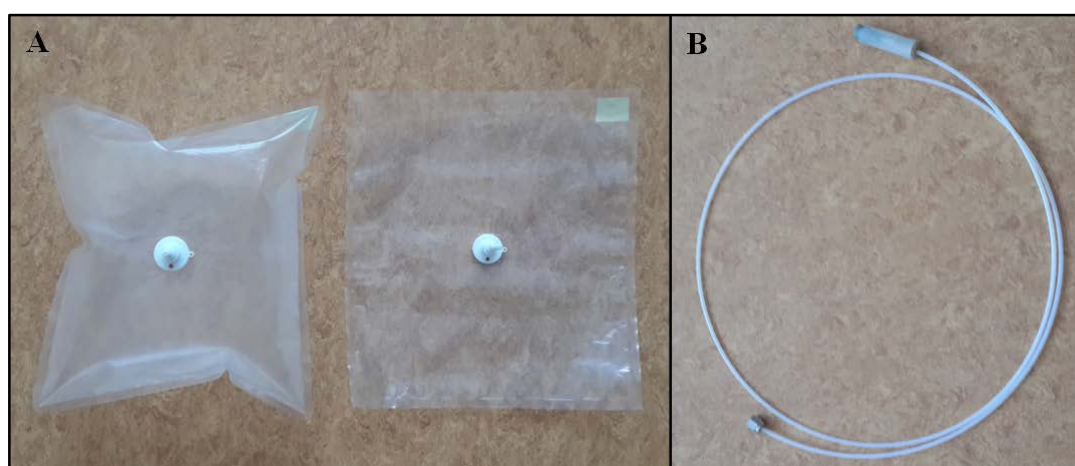


Figure 4.1: (A) two Tedlar bags one of them is inflated with breath and the other is not and (B) the Teflon tube.

4.3. Effect of Tedlar Bag on VOCs

According to *Thekedar et al.* [69], “it was found that with Tedlar bags ~80% of the CO₂ is lost during 3 days, this decreases the concentration of protonated water dimers in the drift tube and decreases the concentration of VOC. For that, the loss of humidity from the bag has more critical role than the CO₂ and humidity variation during breath sampling”.

Possible reasons for this variation may be referred to the presence of N,N-dimethylacetamide [70] and phenol, which are emitted from the Tedlar bag (Amman, private communication, Di Francesco, private communication) [71].

The sample storage time with Tedlar bags also effects the VOCs concentration due to diffusion through the bag materials. It found that only water can permeate through the wall until the relative humidity inside the bags reaches the ambient air values.

Beauchamp at al. [72] found that some VOCs concentrations increased even with unused and cleaned Tedlar bags. This may denote to the diffusion into the bags especially when the concentration of these compounds in the room air is higher than in the bags.

4.4. Identification of the VOCs

The VOCs were identified in exhaled breath samples by using two types of spectrometers. These two types of spectrometers are described as follows:

4.4.1. Proton-Transfer Reaction Mass Spectrometry (PTR-MS)

The details of the PTR-MS were first described in 1995, but it was invented by Professor Werner Lindinger and his colleagues at the University of Innsbruck in Austria in the middle of the 1990s for the monitoring of the VOCs in air. It is a useful device for online measurement of the VOCs. This device has a wide range of applications especially in medical diagnosis and food science. It is also used in atmospheric compounds analysis.

For the measurements, a standard PTR-MS instrument was used in this study which is commercially available instrument manufactured by IONICON (GmbH, Innsbruck, Austria). PTR-MS consists of three different parts: ion source, drift tube reaction chamber and quadrupole mass analysing system, which consists of a Quadrupole Mass Spectrometer (QMS) and a Secondary Electron Multiplier (SEM).

PTR-MS is a type of mass spectrometer that operates under low pressure to prevent collisions between ions or between ions and contaminants that would lead to the loss of analyte as neutral species and will not pass through the mass analyzer and hit the detector.

4.4.1.1. The Principle of PTR-MS Measurement

The VOCs enter the drift tube of the PTR-MS unit through the breath gas inlet to react with the H_3O^+ that comes from the ion source. Then these VOCs are detected in the quadrupole based system. The analysed data are shown on a computer by a special program. These steps of measurement are illustrated in Figure 4.2.

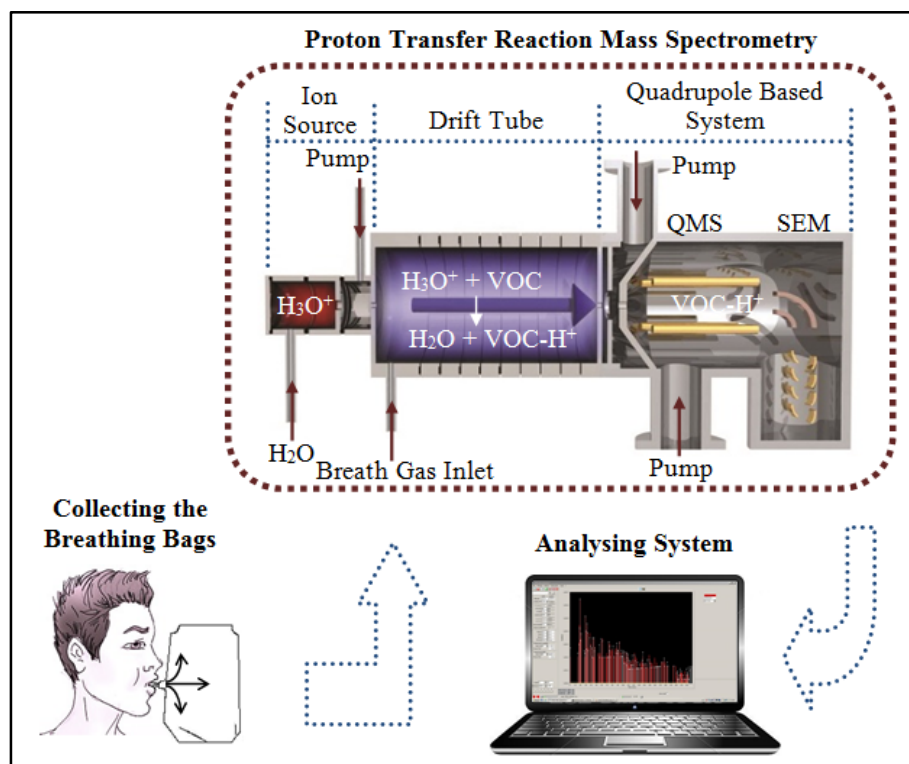


Figure 4.2: Schematic view shows the steps of measurement with PTR-MS [73].

PTR-MS uses the constituents of the exhaled air (VOCs) in the drift tube by reaction with the ions of hydronium (H_3O^+), which has previously been produced in the discharge ion source. This allows to detect the protonated VOCs, which are separated by a mass selective quadrupole detector according to their mass/charge ratio and detected by an ion detection unit.

Munson and Field [74] had introduced that “the PTR-MS linked with chemical ionization. This chemical ionization (CI) is based on the proton-transfer reactions. For that, H_3O^+ is the most suitable primary reaction ion used for analysing the complex air samples even if there are other precursor ions available such as NO^+ and O_2^+ ”.

There is no reaction with any of the natural components of air such as O₂ or N₂, because their proton affinities are lower than that for H₂O, and the reaction depends on the proton affinity as well as on the other factors like the collision rate constant, the reaction time and the kinetic energy of the ions.

As shown in Figure 4.3, the PTR-MS unit is divided into two parts: the first part for charging the VOCs, which is represented by the ion source section and the drift tube reaction chamber section, the second part for mass/charge ratio separation and detection, which is illustrated by the quadrupole mass system and the secondary electron multiplier of the quadrupole mass analysing system.

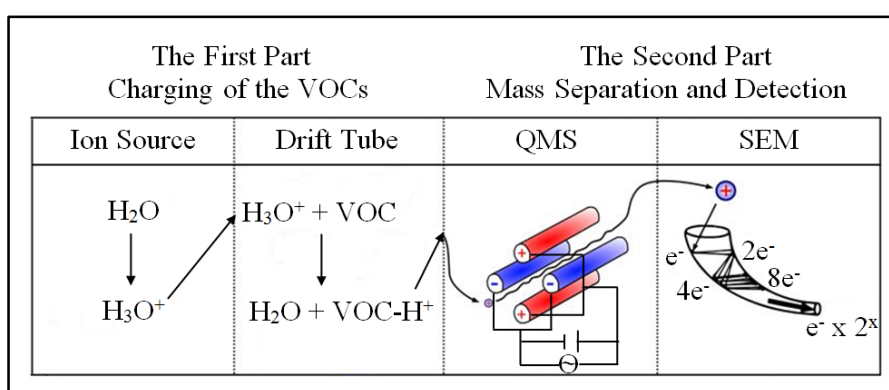
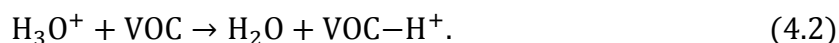


Figure 4.3: The process of the measurement with PTR-MS [75].

In the first part of the PTR-MS unit, H₃O⁺ (with a high purity > 99%) is produced from the very pure water vapour via a hollow cathode. This part of protonation occur in the ion source, as illustrated in the following equation:



This pure H₃O⁺ moves to the drift tube reaction chamber by a high electrical field to interact with the gas mixture that contains the VOCs, as illustrated in the following equation:



In the second part of the PTR-MS unit, which is operated at a high vacuum, the ions are separated according to their mass to charge ratio by oscillating electrical fields.

The quadrupole mass system consists of four parallel rods, each two facing rods pairs are connected to the DC source electrically have the same charge (positive and negative).

Additionally an oscillating radio-frequent field is applied. By increasing the field voltage and keeping the ratio between the field constant, the trajectories of the ions that are accelerated through the mass filter will alter.

The ions will enter the electric field. Thus, the ions with a high mass to charge ratio (m/z) will pass this part of the device but the ions with a low mass to charge ratio (m/z) will hit one of the rod that has an opposite charge and will be neutralized.

The ions that passed the previous section (m/z filter) will be delivered to the secondary electron multiplier. It has many discrete plates, which are connected by means of a chain of resistors. In the secondary electron multiplier, by applying a high voltage, the incoming electron will trigger a cascade: it strikes the first plate and generates an ion beside the original ion, then these two electrons strike the next plate and release more electrons, and so on.

This detector cascade induces the electrical signal measured with the detectors.

4.4.1.2. Measurement with PTR-MS

For this device, the exhaled breath samples were collected from different case groups (health statuses) to examine the typical odor that caused by VOCs from those with oral malodor as a differential diagnosis.

i. Vegan (People with Special Nutrition)

33 vegans were tested in this procedure (4 males and 29 females); their age between (21-71) years old in a good health condition. They were put on a vegan diet for two months (with the expectation of lowest concentrations of toxic substances in their bodies). One breath sample (Tedlar bag) was collected from each person, (see Table 1 in Appendices).

Vegans are like Vegetarians, that do not eat any dead animals, or parts of them. This means vegetarians do not eat meat, poultry (chickens, turkeys, ducks, etc.), fish or other water animals (like shrimp and crabs), or any by-products of these animals, like gelatin or animal fats or cheeses made from rennet taken from the stomach of calves. Vegans do not eat any of these either but they also strive to avoid all animal products for food (milk and milk products, eggs and honey) since these cause pain and suffering. They also often avoid animal products-leather, silk, pearls, wool or even paint brushes made of animal hair, as well as products that have been tested on animals.

ii. Volunteers (Reference)

20 volunteers were participated in this procedure (10 males and 10 females); their ages between (21-49) years and they did not suffer from any known diseases. Two breath samples (Tedlar bags) were collected from each volunteer; the time between these two samples was about 2-3 min. to assess the accuracy and the reproducibility of our measurements. The Tedlar bags were collected early in the morning, so they had not eaten for nearly 6 hours. This allows a comparative study with the patients suffering from liver diseases, who are submitted to the LiMAX-Test, and must have fasted for at least 6 hours before the test, (see Table 2 in Appendices).

In our measurements, we took the average of two breath samples (Tedlar bags) for each volunteer.

iii. Patients with Liver Diseases

59 patients with liver diseases were submitted to this procedure (35 males and 24 females); their age between (23-80) years old and they had fasted for at least 6 hours before submitting to the LiMAX-Test. Two breath samples (Tedlar bags) were collected from each patient, the first one before submitting to the LiMAX-Test and the second one after submitting to the LiMAX-Test, (see Table 3 in Appendices).

In our measurements, we took the average of two breath samples (Tedlar bags) for each patient.

4.4.2. Ion Mobility Spectrometry (IMS)

IMS is used to detect the gas sample characterisation with a low limit, because it is considered a fast and highly sensitive method. It quantifies the analytes and displays the unknown compounds.

For the measurements, an IMS (ISAS Institute for Analytical Sciences, Dortmund, Germany) was used. IMS has two regions: the ionisation and reaction region and the drift region.

IMS is applied with radioactive source, the most favourite radioactive source is the Nickel (^{63}Ni), because it is a (β^-) emitter, efficient, simple, stable, reliable and it has a long life time. The electron emitted from the Nickel (^{63}Ni) has a maximum energy of 67keV.

Despite the fact that a negative particle is released, the Nickel-63 creates both positive and negative ions. Positive ions are created by the high-energy electron striking a neutral gas molecule and knocking off an electron from the molecule, thus leaving the molecule positively charged, introducing an additional low-energy electron into the gas and leaving the impact electron with only a slightly lower energy. This low-energy electron then attaches itself to another molecule to create a negative ion. Just one 67 keV beta particle emitted from Nickel-63 has enough energy to generate about 1000 negative and positive ion pairs. The analyte molecules are ionized by charge exchange with the initial ions that are created by the emitted beta particle.

When these electrons are generated, they interact with the air (carrier gas) forming a reactive ion peak (RIP), which is a stable intermediate ion that has positive and negative charge. By collisions, they transfer their charge to neutral molecules. The RIP is used as one calibration point in the IMS (strong line on the computer in Figure 4.4).

The basic function of the IMS is to ionize the gaseous analytes in the ionisation and reaction region, and then by applying the electrical field, the characteristic drift time is detected.

Currently, IMS is coupled with a Multi-Capillary Column (MCC) to pre-separate the analytes before entering the IMS and separate the analytes by their chemical interactions with the column. This reduces the complexity of the signal and result in a 3D plot as depicted in figure 6.5 in Appendices.

4.4.2.1. The Principle of IMS Measurement

The VOCs enter the ionisation and reaction region (the first part of the device) through the breath gas inlet and are ionized by the radioactive source (^{63}Ni). Then they enter the drift region (the second part of the device) through the ion shutter to be detected by a Faraday plate. The analysed data are shown on a computer by a special program, these steps of measurement are shown in Figure 4.4.

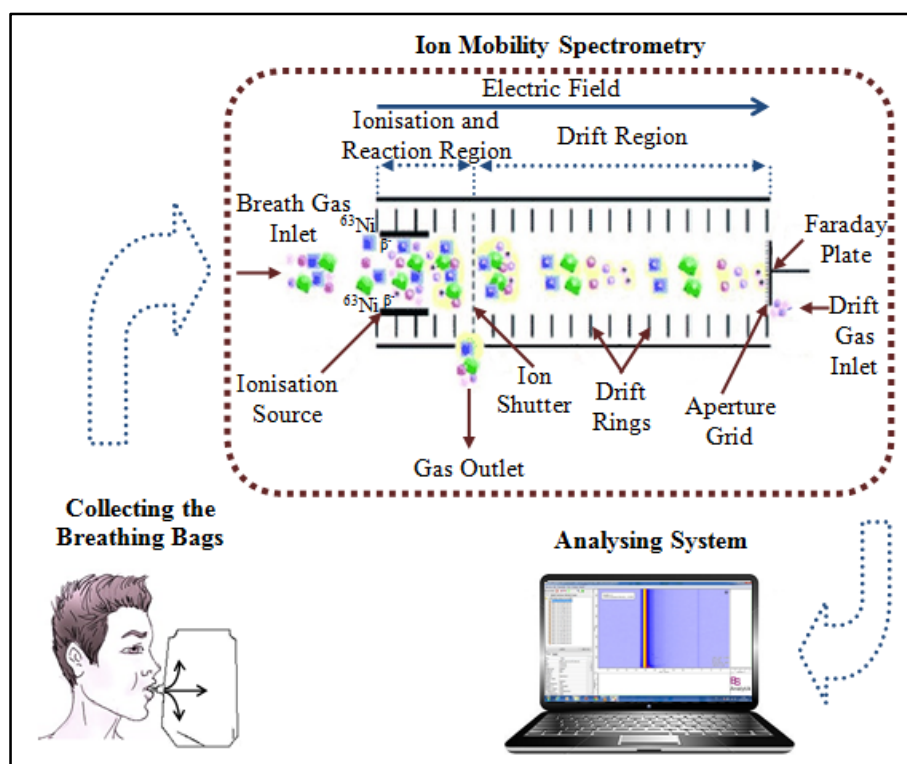


Figure 4.4: Schematic view shows the steps of the measurement with IMS [76].

In the IMS unit, the sample breath enters the ionization and reaction region (the first part of the device) through the breath gas inlet. In the ionization and reaction region, the molecules are ionized by Nickel (^{63}Ni) as (ionization source) that emits β^- particles. After the ionization, the molecules are driven to the drift region (the second part of the device) passing through the ion shutter that is opened for a short time (every 100 ms) letting only a small amount of molecules enter the drift region.

In the drift region, the ions drift towards the Faraday plate, which is located at the end of the drift region, by the influence of the electrical field and collide with the drift gas molecules that come from the opposite direction. Because of these collisions, the ions are

decelerated in a different manner depending on their structure and reach to a steady drift velocity.

It is found that coupling the IMS with the MCC is suitable for human breath investigation. With the complex biological samples, the IMS alone does not give a good identification and quantification of the sample due to the overlap of different analyte peaks.

MCC as shown in Figure 4.5, consists of a single glass tube with 1000 parallel capillaries with a diameter (40 μm). These capillaries are coated with a gel, which is OV-5 phase (5% Phenyl, 95 % dimethyl polysiloxane) on the inside with a thickness of 200 nm.

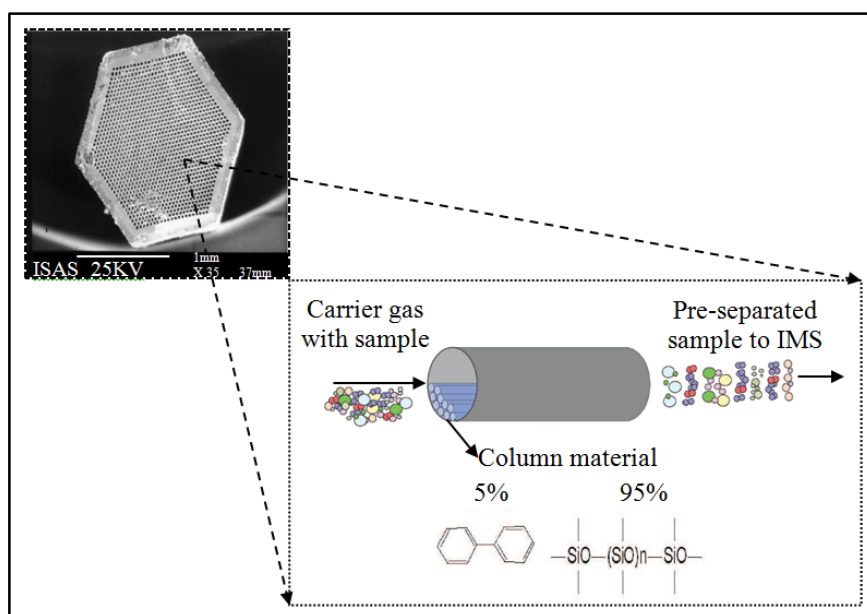


Figure 4.5: Schematic view shows the MCC and its compounds [77].

When the analytes enter the MCC, they bind to the gel depending on their affinity. The higher binding affinity compounds need more time to pass the MCC than others.

The sequence of IMS spectra measurement called MCC/IMS measurement and it takes 10 min. for complete measurement. The time that the compound needs to pass the MCC is called retention time and it is measured in seconds and the time that the compound needs to pass the drift tube in IMS is called drift time and it is measured in milliseconds.

4.4.2.2. Measurement with IMS

For this device, the exhaled breath samples were collected only from the volunteers. 10 volunteers were contributed in this procedure (4 males and 6 females); their age varied between (24-40) years and they did not suffer from any known diseases. One breath sample (Tedlar bag) was collected from each volunteer and they also blow direct into the device two times: i) before collecting the breath sample and ii) after collecting the breath sample, (see Table 5 in Appendices).

Chapter 5

Results and Discussion of PTR-MS

The data that obtained from analyzing the breath samples by using PTR-MS are presented and discussed in this chapter.

After collecting the data from the PTR-MS device, it was analyzed by a high-level script language Python program. The structure of the Python language can provide clear programs on small and large scales and work efficiently with large matrices.

5.1. PTR-MS Spectrum

The spectrum window of the PTR-MS program is illustrated in Figure 5.1, which is represented by the mass (x-axis) and the amplitudes (y-axis).

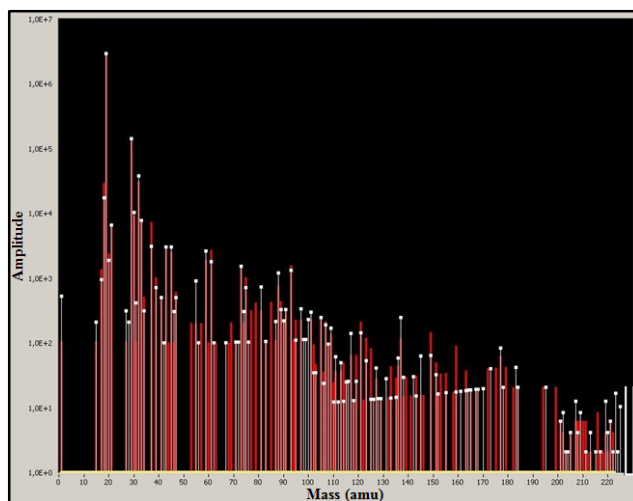


Figure 5.1: PTR-MS spectrum, the x-axis represents the mass (amu) and the y-axis represents the amplitude.

After connecting the Tedlar bag that contains the breath sample the program is run, the VOCs are detected by their mass and amplitude.

5.2. Ion Counts Determination

The measurement time for the experiment and the number of measured counts, depend on many factors, the most important one is the mass spectrometer's cycle-time.

The mass spectrometer's cycle-time is the time that the instrument needs to cycle through separation and detection of a set of m/z ratios. The dwell-time is the time needed to analyse each electric pulse and it is defined as the amount of time where one mass analyser is detecting and measuring one ion only. It has a significant impact, not only for the ion count signal number that one can measure in any experiment but also for the detection sensitivity.

Dwell-time and cycle-time are directly proportional to each other and they effect the sensitivity. In a more sensitive measurement, the dwell-time increases. On the other hand, more sensitive measurement is at the cost of increasing the cycle-time, this will lead to decrease the number of m/z ratios measured , i.e. the productivity of the MS run.

Traditionally, the dwell-time is optimized in a manner that each transition is being scanned and analysed at least twice [78].

Figure 5.2 illustrates two graphs that related to two different VOCs having different m/z ratios. This procedure was carried out for all of the samples to create the database of the VOCs.

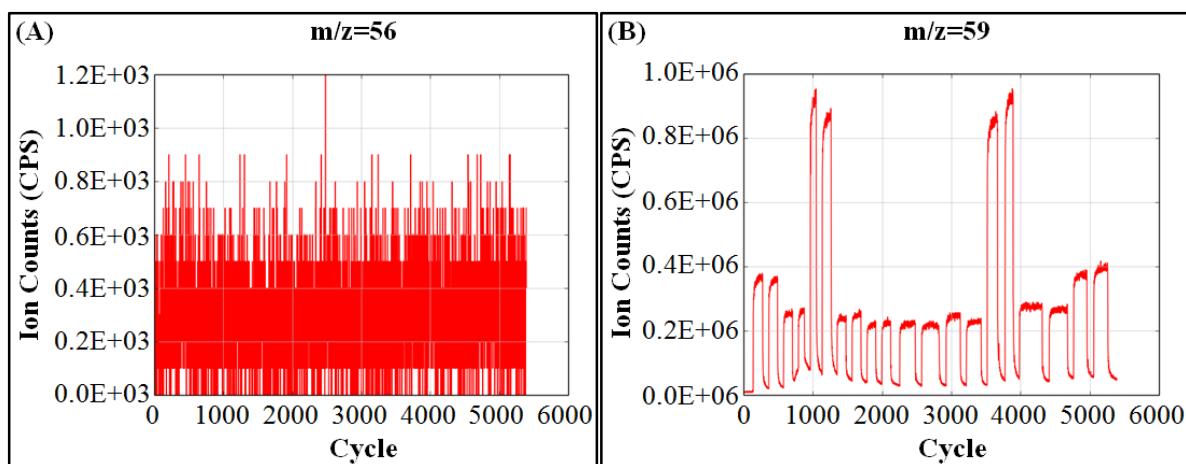


Figure 5.2: Two graphs, which belong to the same measuring period: (A) graph belongs to propanenitrile ($m/z=56$) and (B) graph belongs to acetone ($m/z=59$). Each graph has different peaks, which indicate the ion counts of VOCs in counts per second (cps) for different breaths. The increase and decrease of acetone upon breathing into the PTR-MS can be directly reached.

5.3. Ion Counts Normalization

The source for ionized VOCs are the H_3O^+ ions in drift tube. Increasing the H_3O^+ concentration results in higher ion count for the VOCs. Then, ion counts of the VOCs were normalized to compensate for altered H_3O^+ contribution. This effect comes from H_3O^+ ($m/z=19$) and $H_3O^+ \cdot H_2O$ ($m/z=37$). The normalized counts for the VOCs were calculated by using the following equation:

$$\text{Normalized Counts for VOCs} = \frac{\text{CPS}_{\text{VOCs}}}{\text{CPS}_{(m/z=19)} + \text{CPS}_{(m/z=37)}}. \quad (5.1)$$

Where CPS (counts per second) is the ion counts of the VOCs that measured by the device.

Water vapour is detected in the drift tube of the PTR-MS at the $H_3O^+ \cdot H_2O$ ($m/z=37$), this water vapour comes from the ion source and from water vapour in the breath sample.

5.4. Paradigmatic Test Compounds

In this part of the study the normalized counts of two prototypic compounds, acetone ($m/z=59$) and isoprene ($m/z=69$), was compared, for 33 vegans, 20 volunteers and 59 patients with liver diseases. This part of the study provides reference datasets for future examinations of VOC profiles, potentially involving a wider range of VOCs, as shown in the Figure 5.3.

It was reported that, there is a linear correlation between these two types of VOCs, which were fitted by a linear equation ($y=a+b*x$).

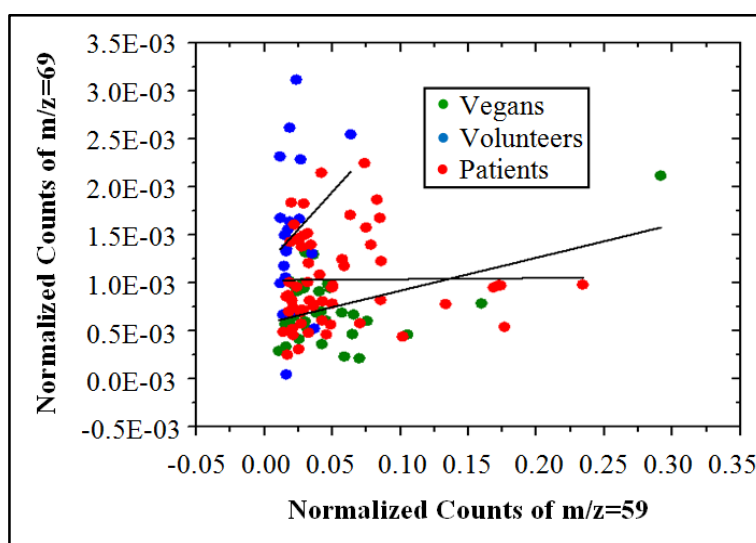


Figure 5.3: The normalized counts of $m/z=59$ versus the normalized counts of $m/z=69$.

From figure 5.3 we found the following correlations: for vegans, which is denoted by green dots, $r^2=0.21049$ and the slope= 0.00344 , for volunteers, which is denoted by blue dots, $r^2=0.00828$ and the slope= 0.01559 and for patients with liver diseases, which is denoted by red dots $r^2=-0.01741$ and the slope= $1.11236E-4$.

Acetone and isoprene models were studied because they are the most abundant endogenous trace gases in human breath.

This comparison between isoprene and acetone is important for several reasons: i) both of them are endogenous in their origin and highly abundant in normal human breath, ii) their physico-chemical properties are contrary, isoprene is lipophilic and its blood solubility is low, but acetone is hydrophilic and its blood solubility is high and iii) both are reliably quantifiable by virtue of several distinct analytical techniques [79, 80].

Our data indicate no relevant correlation between isoprene and acetone.

5.4.1. Isoprene Model

Isoprene is lipophilic and has a low solubility in blood (as reflected by a small blood: gas partition coefficient $\lambda_{b:air} \approx 0.75$) and is presumed to be involved in the cholesterol biosynthesis. Isoprene exchange occurs in alveolar region due its volatility and due to the low affinity for water and blood. Physical activity causes marked changes in exhaled breath isoprene concentrations of humans [80, 81].

Figure 5.4 illustrates the isoprene model, it consists of three compartments: i) alveolar/end-capillary compartment (gas exchange), ii) richly perfused tissue (metabolism and production) and iii) peripheral tissue (storage, metabolism and production).

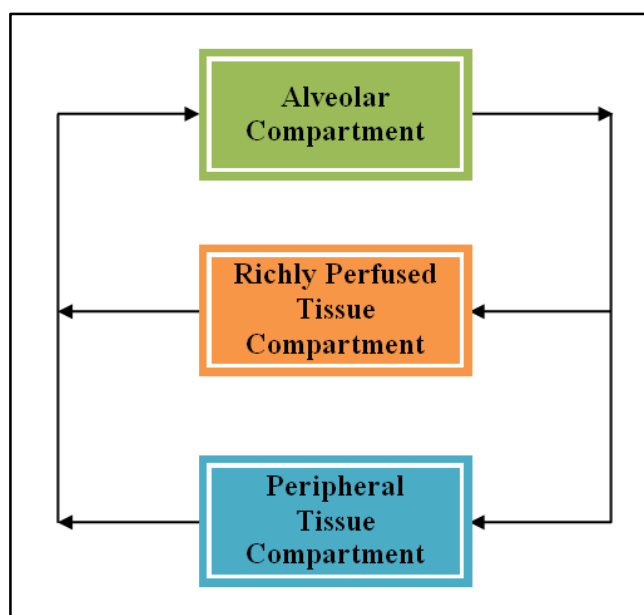


Figure 5.4: Sketch of the isoprene model structure used to explain the dynamics of isoprene concentrations [80].

5.4.2. Acetone Model

Acetone is more soluble in blood ($\lambda_{b:air} \approx 340$) and has been linked to fat catabolism. Acetone is a product of the conversion of acetoacetate by elimination of CO_2 and it is a hydrophilic

compound interacts with the water-like mucus membrane lining the conductive airways and cause an effect known as wash-in/wash-out behavior [80, 81].

The term wash-in/wash-out, as defined by *King et al.* [80] refers to the fact that “while fresh air is being inhaled, it becomes enriched with hydrophilic VOCs stored in the airway surface walls of the peripheral bronchial tract, thus leading to a decrease of the respective pressure/tension gradient between the gas phase and capillary blood in the alveolar space. This causes an effective reduction of the driving force for gas exchange in the alveoli and minimizes the unloading of the capillary VOC level. Correspondingly, during exhalation the aforementioned diffusion process is reversed, with a certain amount of hydrophilic VOCs being stripped from the air stream and redepositing onto the previously depleted mucus layer”.

As a phenomenological consequence, exhaled breath concentrations of such VOCs tend to be diminished on their way from the deeper respiratory tract to the airway opening. The resulting discrepancies between the “true” alveolar and measured breath concentrations can be substantial (even if breath samples are drawn in a strictly standardized manner, e.g. by employing CO₂-controlled sampling) and will depend on a variety of factors such as airway temperature profiles, airway perfusion and volumetric flow.

Figure 5.5 illustrates the acetone model, it consists of four compartments: i) bronchial/mucosal compartment (gas exchange), ii) alveolar/end-capillary compartment (gas exchange), iii) liver (metabolism and production) and iv) tissue (storage).

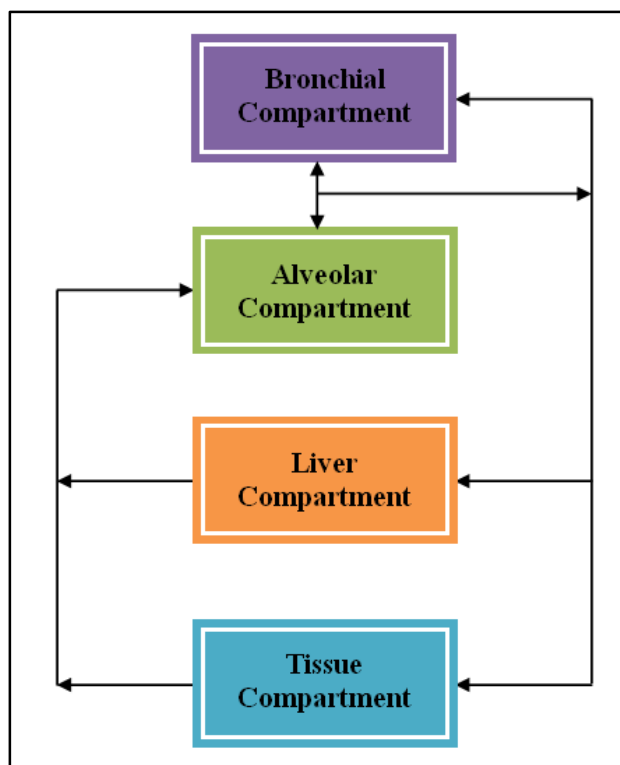


Figure 5.5: Sketch of the acetone model structure used to explain the dynamic of acetone concentrations [80].

5.4.3. Separating Overlapping Signals

The separating of the PTR-MS cannot distinguish between molecules which similar, but different masses as acetone ($m/z=59$) and butane ($m/z=59$). Thus, it cannot be guaranteed that the signal at ($m/z=59$) stems from acetone.

Acetone identified by comparing the normalized counts of ($m/z=59$) to the normalized counts of ^{13}C -isotopes ($m/z=60$), for 33 vegans, 20 volunteers and 59 patients with liver diseases, as shown in the Figure 5.6.

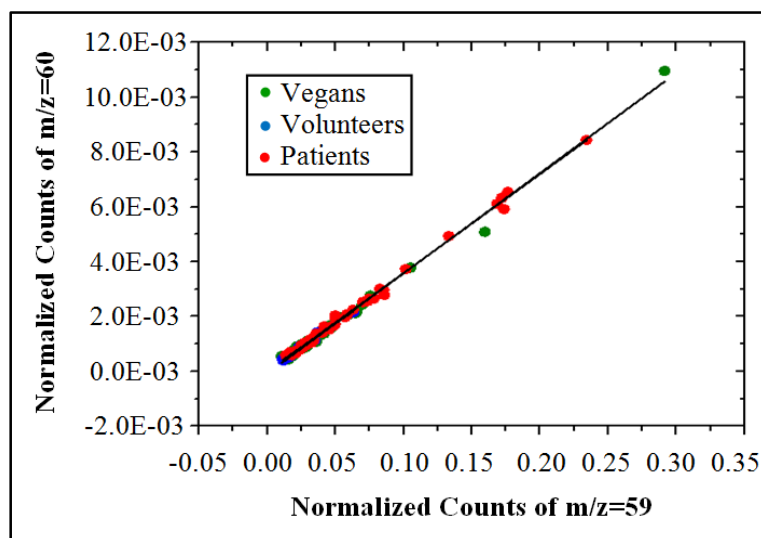


Figure 5.6: The normalized counts of $m/z=59$ versus the normalized counts of $m/z=60$.

The network abundance of stable isotopes result in contribution at different m/z ratios. For acetone we found that, there is a linear correlation between these two isotopes, which were fitted by $(y=a+b*x)$ equation. For vegans, which is denoted by green dots, $r^2=0.99$ and the slope=0.037, for volunteers, which is denoted by blue dots, $r^2=0.98$ and the slope=0.034 and for patients with liver diseases, which is denoted by red dots $r^2=0.997$ and the slope=0.0361.

Acetone, propanal and butane have molecular weights of 58.08 g/mol, 58.08 g/mol and 58.12 g/mol, respectively. These molecules plus H^+ are detected at a m/z ratio of 59 Thomson, with $m/z=59$ there is a significant contribution at $m/z=60$, due to isotopes of acetone. Acetone and propanal have the same molecular formula C_3H_6O and are treated as one molecule acetone. Thus, they are not distinguishable by mass spectrometer. Butane has the formular C_4H_{10} and exhibits a different isotope pattern than C_3H_6O .

The natural abundance of ^{13}C is 1.1%, of 2H is 0.0115% and of ^{18}O is 0.2%. From the natural abundances one can calculate the relative contributions of acetone and butane at 60 Thomson. The main contribution for acetone is due to a single ^{13}C isotope in the molecule, resulting in $3 \times 1.1\%$ for every carbon atom. The next strongest contribution comes from deuterium in acetone. Since acetone exhibits six hydrogen atoms the isotopic contribution is $6 \times 0.0115\%$, resulting in 3.369% at 60 Thomson. The oxygen isotope ^{18}O would change the mass. Therefore, 0.2% of the 3.369% are found at 62 Thomson. In addition, the probability of

having two ^{13}C atoms in the molecule is $3 \times (0.011)^2$. In summary, at a m/z ratio of 60 Thomson 3.325% of the acetone signal should be detected as a result of isotope probability.

Butane has four carbons, ten hydrogens and no oxygen. Thus, the isotope contribution at 60 Thomson is calculated as $4 \times 1.1\%$ plus $10 \times 0.0115\%$, resulting in 4.515% of the butane signal at 59 Thomson. In addition, the probability of having two ^{13}C atoms in the molecule is $6 \times (0.011)^2$. In summary, at a m/z ratio of 60 Thomson 4.44% of the butane signal should be detected as a result of isotope probability.

By comparing these values (3.325%) and (4.44%) with the slope (0.0357 ± 0.0007), we can conclude that the slope is nearly the same and thus represents acetone and propanal in the breath.

5.5. Determination of Pearson's Correlation Coefficient (r)

Pearson's correlation coefficient is a measure of the strength of the association between two variables x and y and it is calculated by:

$$r = \frac{\sum_i (x_i - \bar{x})(y_i - \bar{y})}{\sqrt{\sum_i (x_i - \bar{x})^2} \sqrt{\sum_i (y_i - \bar{y})^2}} \quad (5.2)$$

where: -

x_i and y_i = The variables.

\bar{x} and \bar{y} = The mean values for x_i and y_i variables.

r is Pearson's correlation coefficient. If the value of $r = 1$, the variables are correlated to each other, and when the value of $r = 0$, the variables are not correlated to each other, but if the value of $r = -1$, the variables are anti-correlated.

The Pearson's correlation coefficient was used to see how exhaled VOCs are related to each other in different cases, for 33 vegans, 20 volunteers and 59 patients with liver diseases.

200 m/z ratios were compared with 200 m/z ratios for each health status, as shown in the Figure 5.7.

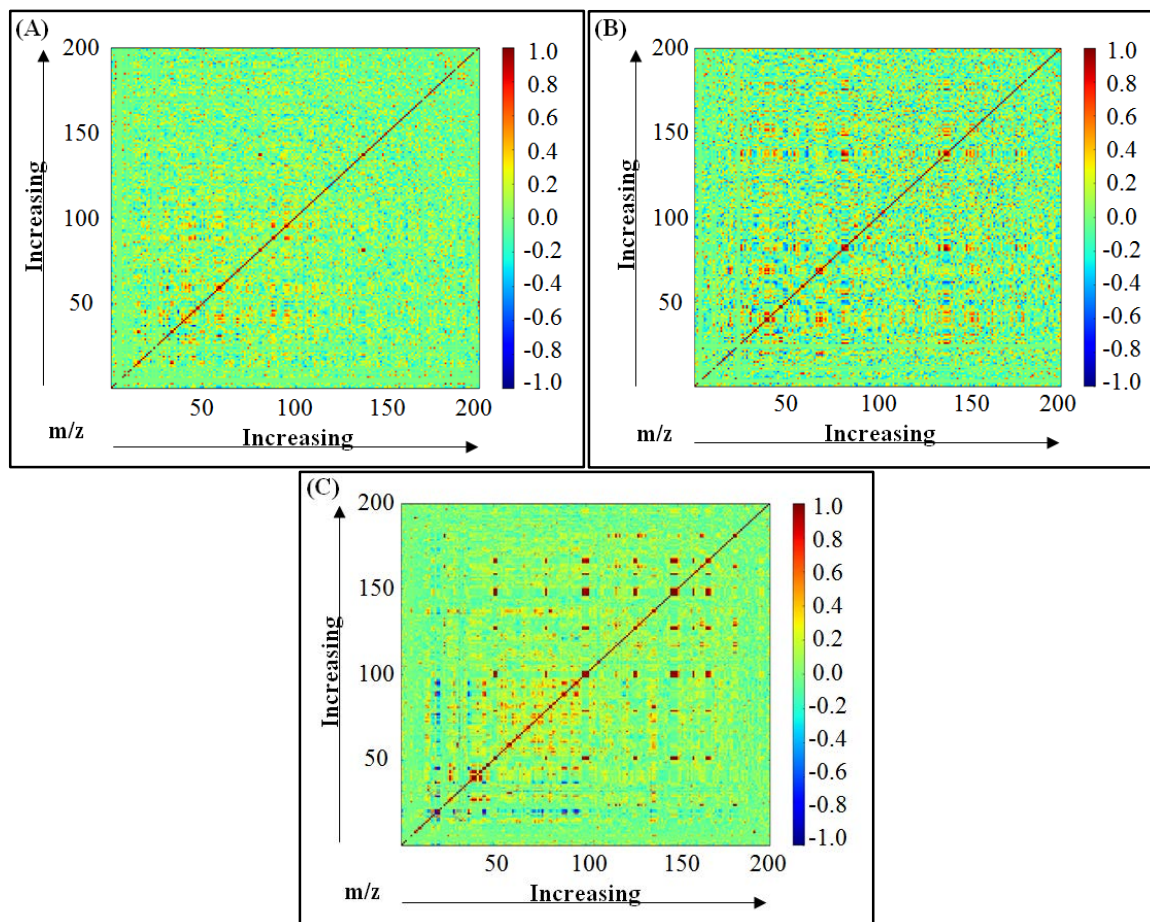


Figure 5.7: Two-dimensional plot of Pearson’s correlation coefficient where the color indicates the value of the correlation: (A) belong to vegans, (B) belong to volunteers and (C) belong to patients with liver diseases.

From Figure 6.7, it can be seen that the relationship between the concentrations of VOCs to each other differ between the three study groups due to the differences in their concentrations [82].

According to *Hauschild et al.* [83], “Pearson’s correlation coefficient can be used: i) to find sets or clusters of related metabolites exposing the same behavior and ii) to reduce the data set by selecting representatives for each cluster. Moreover, it would be interesting to investigate whether a set of metabolites showing the same pattern also originates from the same pathway”.

The further analysis of the complete dataset by using correlated factors is not within the scope of this work.

5.6. VOCs Assessment

It has become possible to separate and study the VOCs from the breath according to their m/z ratios with the development of several analytical techniques, (see Table 6 in Appendices).

It has been shown that most of the VOCs origin is not endogenous, in spite of the fact that the biological origins of these VOCs are mostly unknown.

The endogenous VOCs analysis from the exhaled breath can provide different informations about the pathological disorders. Figure 5.8 illustrates the differences in VOCs concentrations according to the different health statuses (33 vegans, 20 volunteers and 59 patients with liver diseases) by comparing the average of their normalized counts for different m/z ratios.

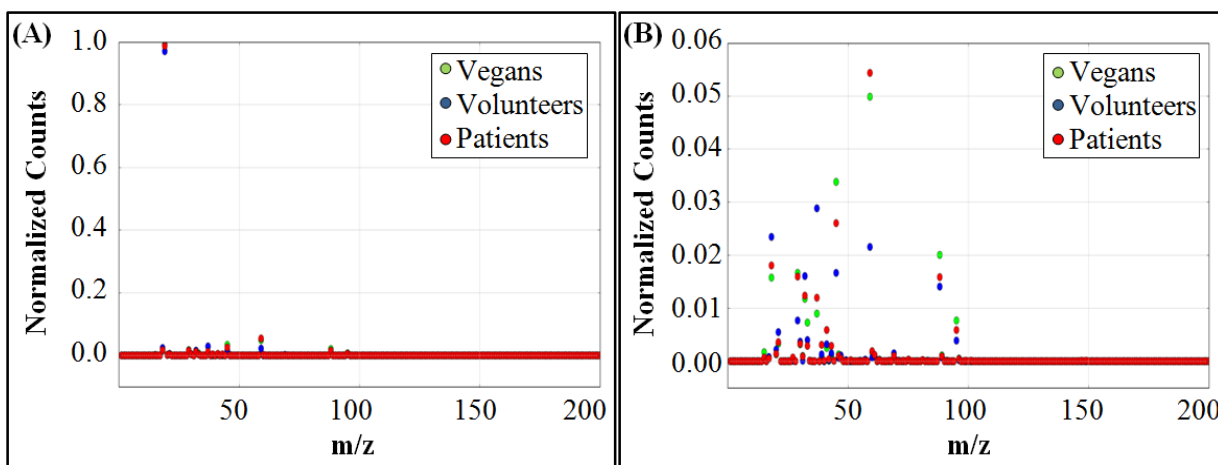


Figure 5.8: The comparison between different health statuses for 200 m/z ratios: graph (A) and graph (B) show the same measurement but with different Y-scale.

5.7. Influence of Tedlar Bags on VOCs Concentrations

In this part of the study, four Tedlar bags were collected from two volunteers, two Tedlar bags from each volunteer. After collecting the breath samples, they were analyzed on different days to study their changes over the time. The measurements were taken repeatedly over 160 hr period (approximately one week), in order to study the variability and the stability of the VOCs in time [84].

With PTR-MS, each sample has 200 compounds (VOCs), the average for the samples is taken and fitted with a linear exponential function using the OriginLab program.

Figure 5.9 shows the flow chart for the optimization process of the measurement done with PTR-MS.

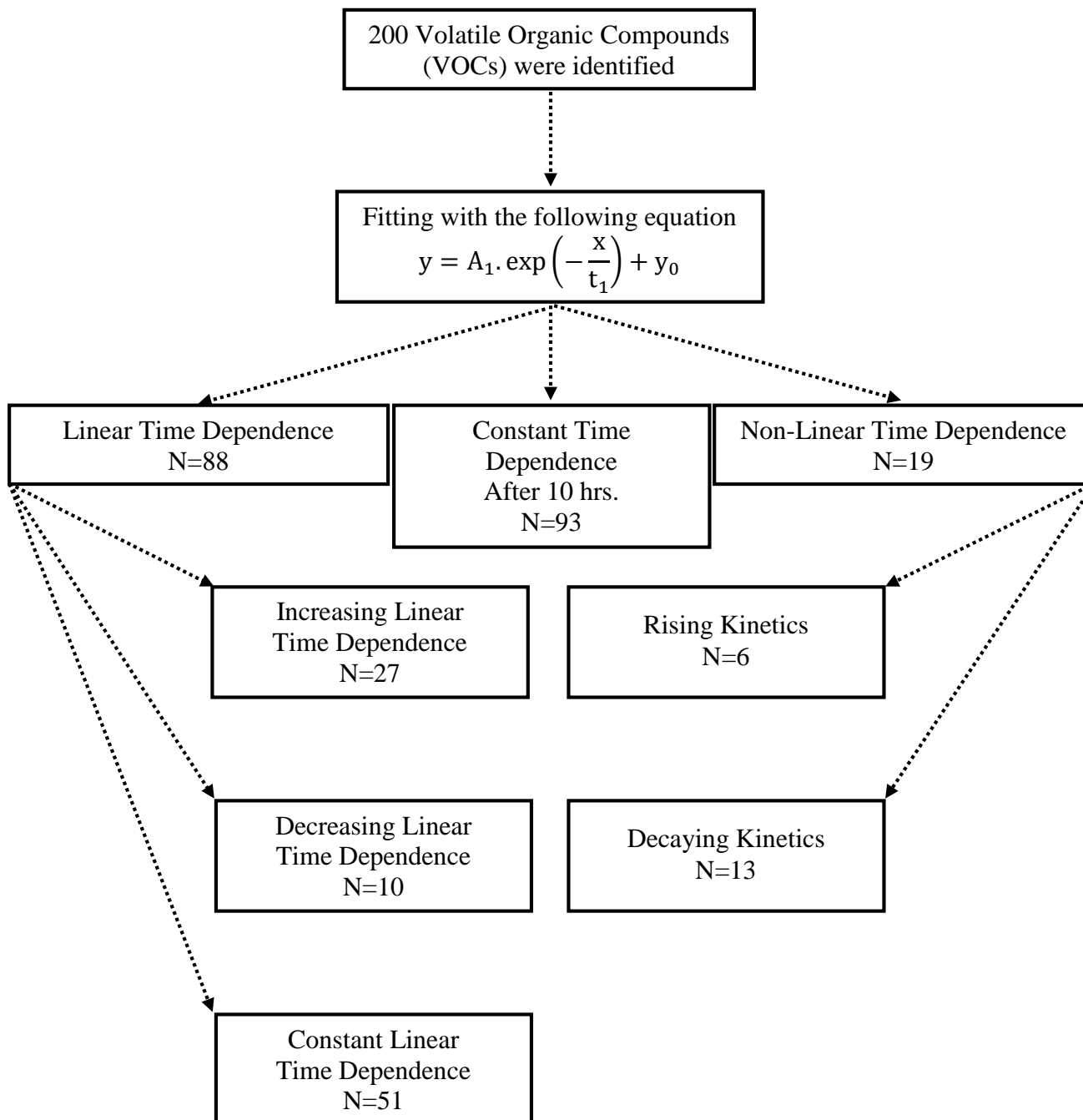


Figure 5.9: The flow chart for the optimization process of the measurement done with PTR-MS.

The data are presented in (Part 2 in Appendices). For all measurements the influence of the Tedlar bags on the VOCs concentrations can be neglected. The m/z values, where a deviation of less than 30% can occur are marked in (Table 6 in Appendices).

5.8. Volatile Organic Compounds (VOCs) as Biomarkers

Biomarkers are molecules indicating a specific metabolism process or disease. For example, halitosis is caused by exhalation of volatiles that are observed organoleptically. According to the literature, these extraoral causes are sometimes associated with a typical odor as a result of specific VOCs in breath [11, 85, 86].

5.8.1. VOCs as Liver Diseases Biomarkers

Here the biomarkers for detecting liver diseases are investigated. The liver plays an important role in metabolism. When damage or failure of the liver occurs, the concentration of some toxic metabolites will increase in the blood. Some of these metabolites may give us a smelly breath when it is exhaled due to the metabolic and pathological processes [20, 87]. A sweet, musty or slightly fecal aroma of the breath may acquire in patients with various degrees of hepatocellular failure and portosystemic shunting of blood, termed fetor hepaticus, which has been mainly attributed to sulfur compounds [86, 88]. Many studies identify numbers of VOCs in breath as biomarkers of certain diseases.

In our study, we compared the VOCs that belong to patients with liver diseases to the VOCs that belong to volunteers as a healthy people and vegans as super healthy people to investigate the VOCs that are correlated to liver diseases and are considered as biomarkers.

Additionally, another comparison was done. The VOCs values were compared to the LiMAX-Test values for the patients with liver diseases to study the effect of liver conditions on VOCs. Figure 5.15 illustrates the LiMAX-Test values according to the liver conditions.

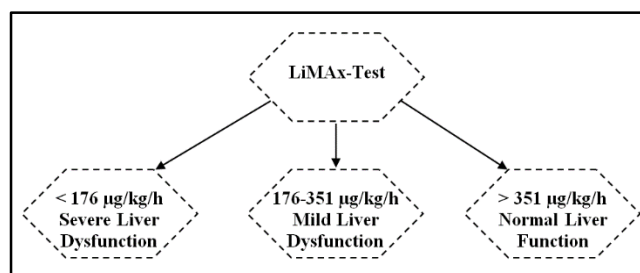


Figure 5.15: The LiMAX-Test values according to liver conditions.

With the help of these two comparisons, we can identify the VOCs that are actually affected by liver diseases and can be considered as biomarkers. These VOCs were studied in different groups:

5.8.1.1. Organosulfur Compounds

They are organic compounds that contain sulfur, which are essential for life like antibiotics penicillin and sulfa drug that contain sulfur. It occurs in the body in the form of the amino acids (cysteine and methionine), the tripeptide (glutathione), enzymes, coenzymes, vitamins and hormones. The organosulfur compounds are classified into several classes. Some of them are found in the body, as illustrated in Figure 5.16 and also (see Table 7 in Appendices).

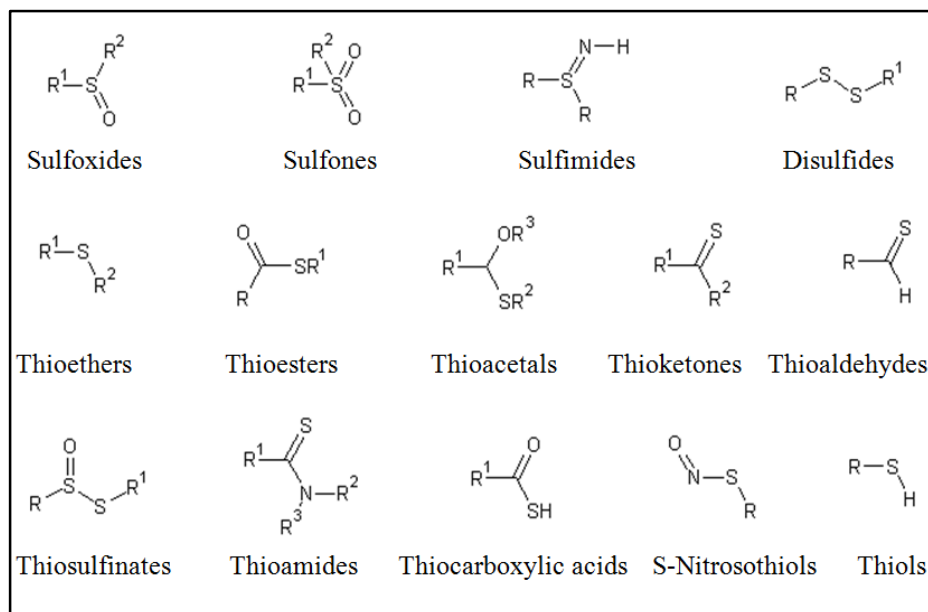


Figure 5.16: Some of the organosulfur compounds that found in the human bodies.

In our measurement, the organosulfur compounds are hydrogen sulfide ($m/z=35$), carbonyl sulfide ($m/z=61$), dimethyl sulfide ($m/z=63$), carbon disulfide ($m/z=77$), dimethyl sulfoxide ($m/z=79$), dimethyl disulfide ($m/z=95$), allyl isothiocyanate ($m/z=100$), S-methyl thioacrylate ($m/z=102$), bis-(methylthio)methane ($m/z=109$), taurine ($m/z=126$), homocysteine ($m/z=136$), methionine ($m/z=150$), sulfur mustard ($m/z=160$), allicin ($m/z=163$), dibenzothiophene ($m/z=185$) and thiols.

Thiols are sometimes called mercaptans, because of the strong bond between thiolate group and mercury compounds to form mercaptides. Thiols have a general structure (R-S-H) as denoted before in Figure 5.16.

Thiols in our measurement are methanethiol ($m/z=49$), butyl mercaptan ($m/z=91$), thiophenol ($m/z=111$), cysteine ($m/z=122$), dithiothreitol/dithioerythritol as epimeric pair ($m/z=155$), grapefruit mercaptan ($m/z=171$) and dimercaptosuccinic acid ($m/z=183$).

Figure 5.17 shows two types of comparisons for three compounds, $m/z = 61$, 102 and 109: (**on the left**), the counts of these compounds are high in patients group and (**on the right**), they show a decrease in their counts according to LiMAX-test value.

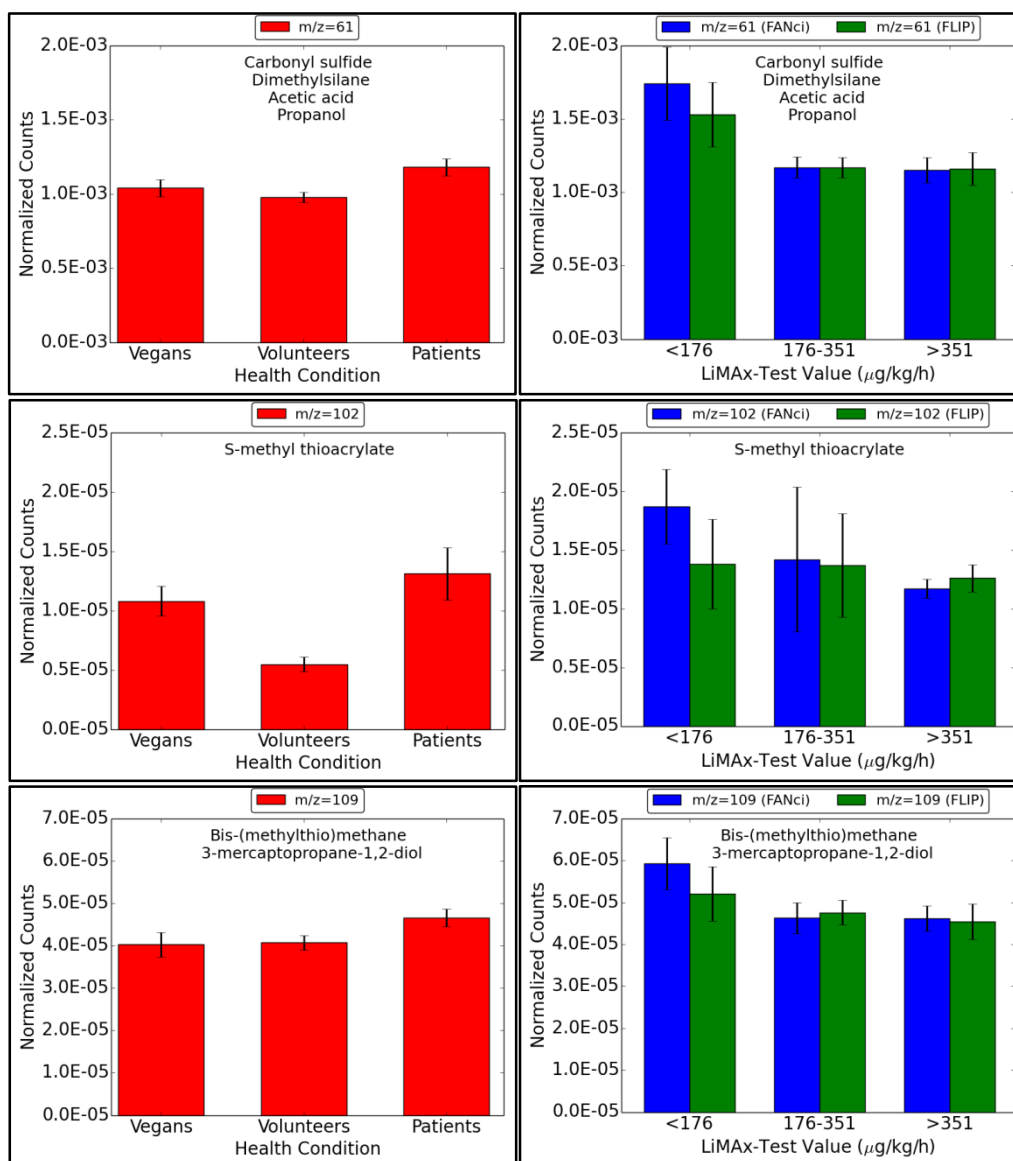


Figure 5.17: The 1st group of the organosulfur compounds.

The VOC at (61 Th) is identified as carbonyl sulfide and other compounds, at (102 Th) is S-methyl thioacrylate and at (109 Th) we found bis-(methylthio)methane and other compound. These VOCs are **good biomarkers** for liver diseases, because in the first comparison they have the highest values in patients compared to volunteers and vegans and in the second comparison the values decrease when the liver condition improves.

Figure 5.18 shows two types of comparisons for four compounds, $m/z = 79$, 100, 150 and 163: (**on the left**), the counts of these compounds are high in patients group and (**on the right**), their counts are high with bad liver function ($<176\mu\text{g/kg/h}$) and low with good liver function ($>351\mu\text{g/kg/h}$), but in the LiMAX range ($176\text{--}351\mu\text{g/kg/h}$) they show an increase in their counts compared to bad liver function.

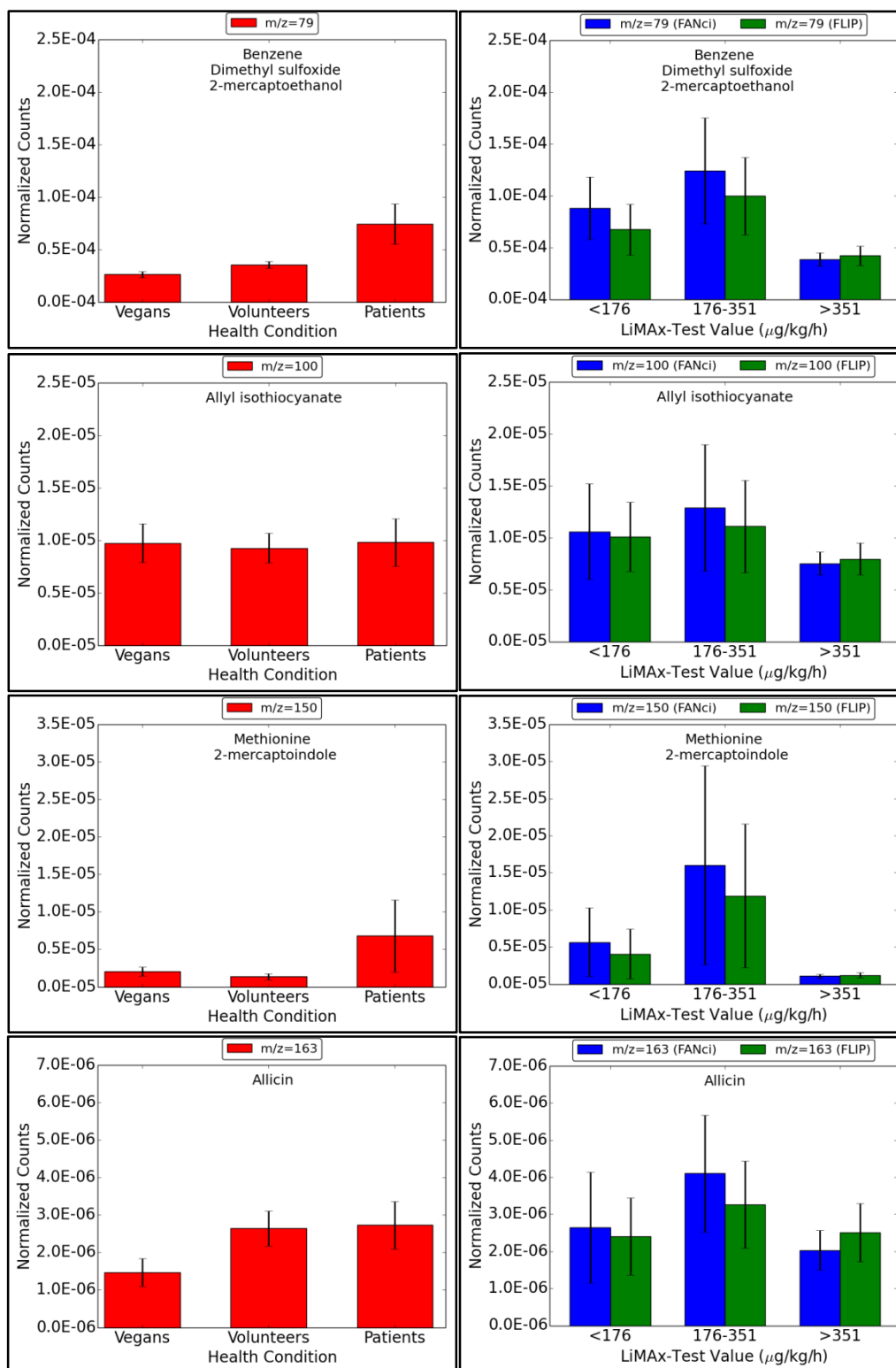


Figure 5.18: The 2nd group of the organosulfur compounds.

The VOC at (79 Th) we found dimethyl sulfoxide and other compounds, at (100 Th) is allyl isothiocyanate, at (150 Th) is identified as methionine and other compound and at ($m/z=163$) is recognized as allicin. All of them are **not good biomarkers** for liver diseases, because their values do not show a good correlation with LiMAx-test value in the second comparison even they show the highest values in patients compared to volunteers and vegans in the first comparison.

Figure 5.19 shows two types of comparisons for two compounds, $m/z = 111$ and 160: (**on the left**), the counts of these compounds are high in patients group and (**on the right**), they show an increase in their counts according to LiMAx-test value.

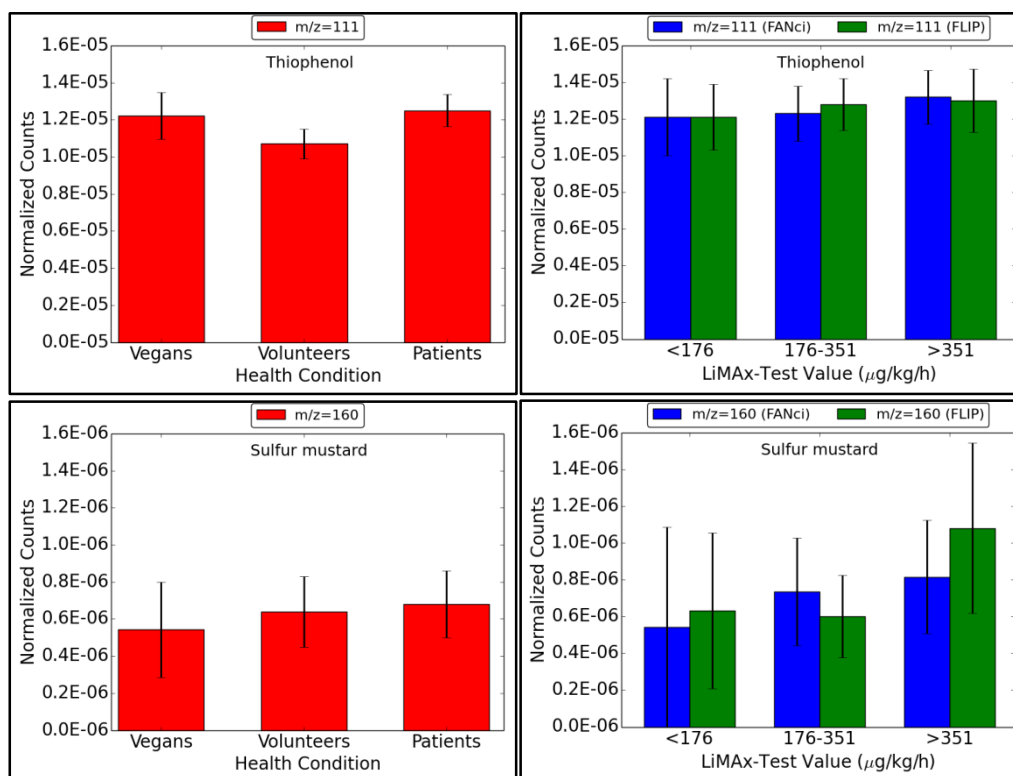


Figure 5.19: The 3rd group of the organosulfur compounds.

The VOC at (111 Th) is identified as thiophenol and at (160 Th) is sulfur mustard. These VOCs are **not good biomarkers** for liver diseases, because their values increase when the liver condition improves in the second comparison even they show the highest values in patients compared to volunteers and vegans in the first comparison.

Figure 5.20 and figure 5.21 show two types of comparisons for six compounds, $m/z = 63, 77, 91, 95, 136$ and 171: (**on the left**), the counts of these compounds are high in vegans group and (**on the right**), their counts are high in bad liver function.

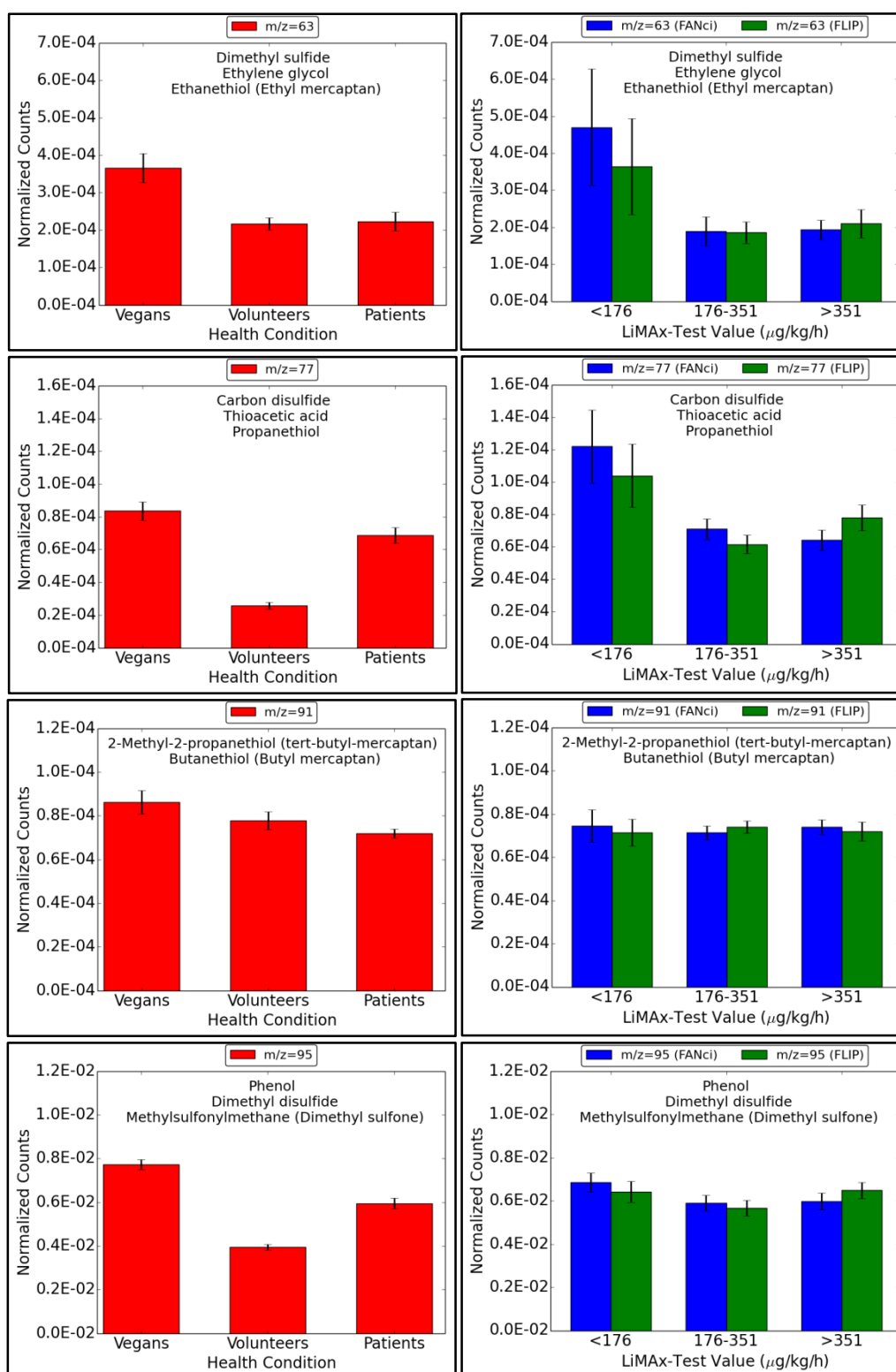


Figure 5.20: The 1st part of the 4th group of the organosulfur compounds.

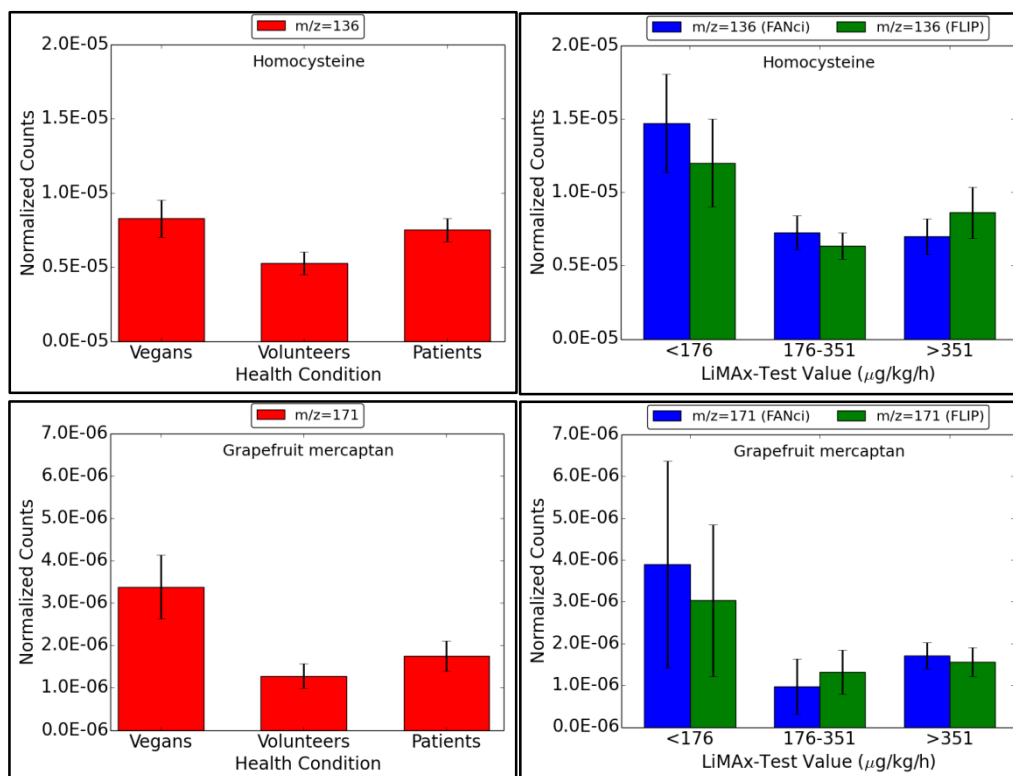


Figure 5.21: The 2nd part of the 4th group of the organosulfur compounds.

The VOC at (63 Th) is recognized as dimethyl sulfide and other compounds, at (77 Th) is defined as carbon disulfide and other compounds, at (91 Th) we found butyl mercaptan and other compound, at (95 Th) dimethyl disulfide and other compounds, at (136 Th) homocysteine and at (171 Th) grapefruit mercaptan. All of them are **not good biomarkers** for liver diseases, because they have the highest value in vegans. Even when dimethyl sulfide, carbon disulfide and dimethyl disulfide in patients are higher comparing to vegans, similar to *Velde et al.* finding [86], but they are lower than vegans and in comparison according to liver condition they show bad correlation especially with dimethyl disulfide.

Figure 5.22 and figure 5.23 show two types of comparisons for seven compounds, $m/z = 35, 49, 122, 126, 155, 183$ and 185 : (**on the left**), the counts of these compounds are high in volunteers group and (**on the right**), their counts are high in bad liver function.

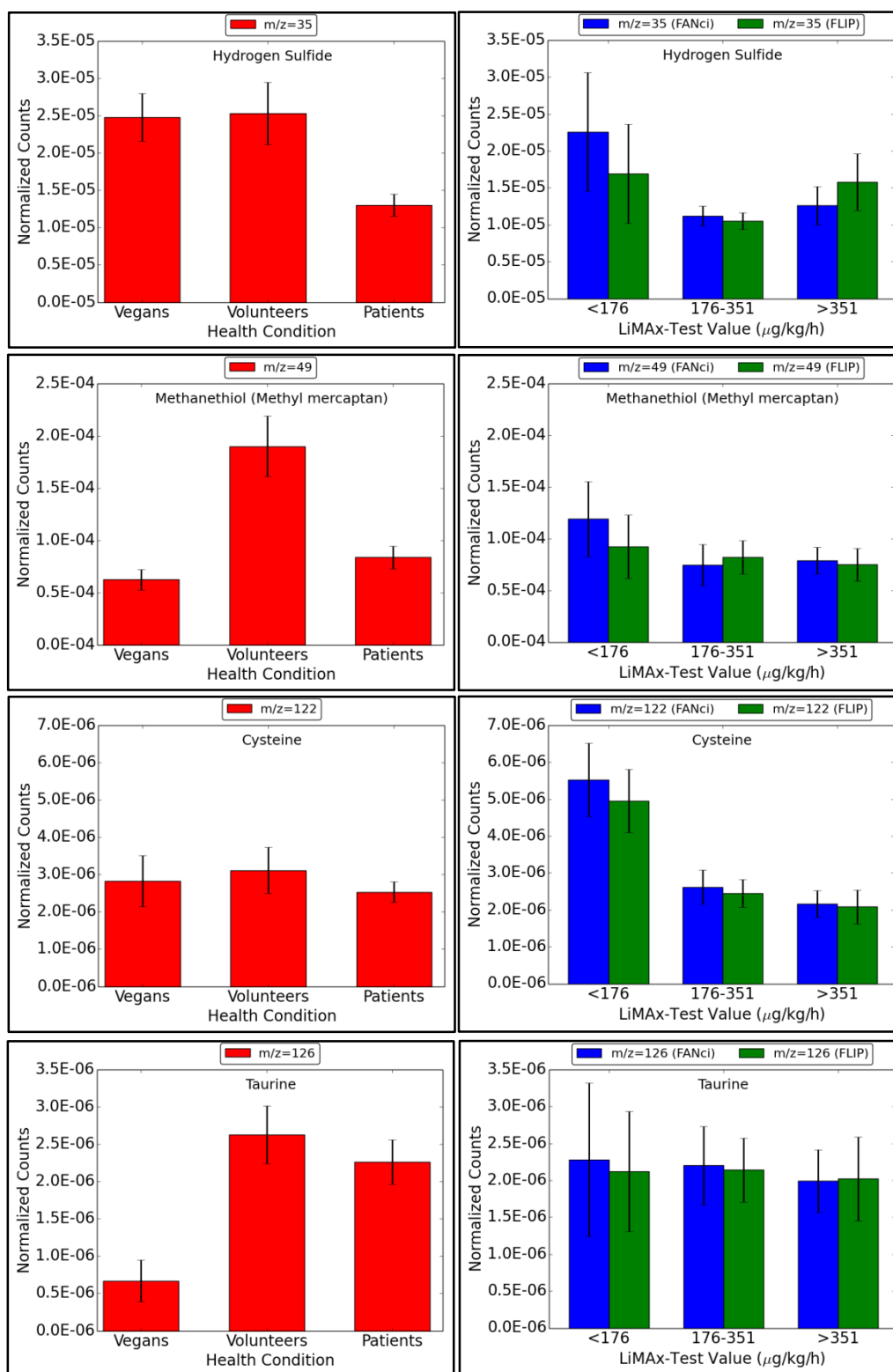


Figure 5.22: The 1st part of the 5th group of the organosulfur compounds.

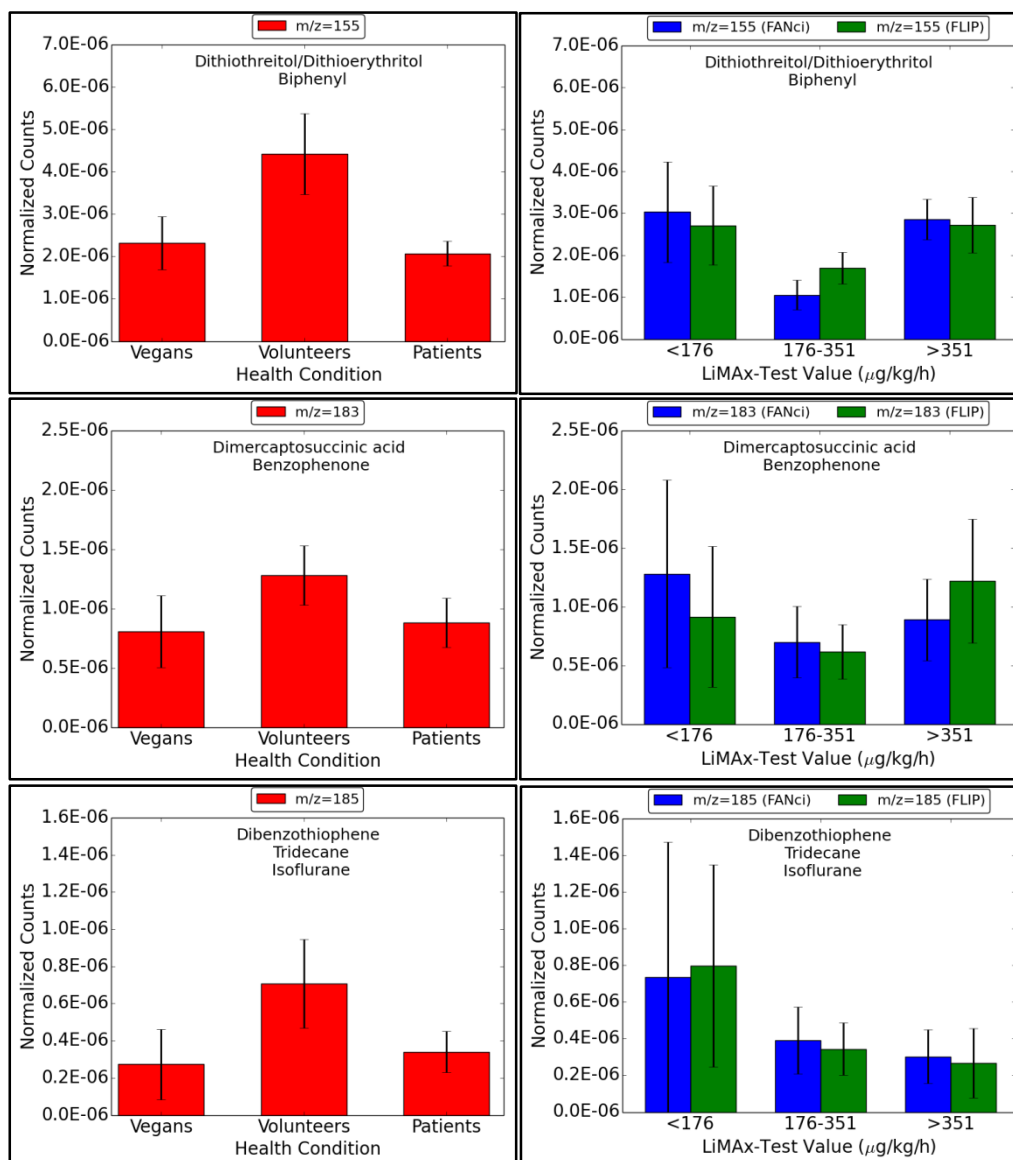


Figure 5.23: The 2nd part of the 5th group of the organosulfur compounds.

The VOC at (35 Th) is hydrogen sulfide, at (49 Th) we found methanethiol, at (122 Th) is defined as cysteine, at (126 Th) taurine, at (155 Th) dithiothreitol/dithioerythritol as epimeric pair and other compound, at (183 Th) dimercaptosuccinic acid and other compound and at (185 Th) dibenzothiophene and other compounds. These VOCs are **not good biomarkers** for liver diseases, because they have the highest value in volunteers.

Sulfur containing compounds are considered biomarkers for liver disease, because these compounds increase in the circulatory and respiratory systems due to the incomplete metabolism in the transamination pathway in the case of liver function impairment, this will lead to an increase of these compounds in breath [89].

Patients with liver disease have a special smell in their breath. It found that dimethyl sulfide (DMS) is the primary cause of the fetor hepaticus. DMS is a natural molecule that is stable in blood and can be transported into the alveolar and exhaled in contrast to other sulfur containing compounds [89, 90].

For some metabolites, we saw that their levels in vegans group or even in volunteers group are higher than in patients group. This may be due to nature of their food that contain sulfur containing amino acids (SAAs) analysis and protein supplementations to avoid the risk of SAA deficiency especially in vegans or because of their dietary status (not fasted for 6-12 hrs).

The dietary source is either an *Allium* species that contribute enzymatically-derived flavors (garlic, onion, chive) or a Cruciform families (Brussels sprouts, broccoli, cabbage, cauliflower), and the flavors that are thermally-generated such as roasted meat, chicken, seafood and coffee. Volatile sulfur compounds have an important role in the aromas of bread, popcorn, nuts, potato products and wine, and they give a subtle flavor to cheddar cheese, chocolate and tropical fruit.

In healthy individuals, the metabolism of methionine ($m/z=150$) produced S-adenosylmethionine (SAME) which regulates hepatocytes growth, differentiation and death. Low biosynthesis of SAME, as a result of impaired methionine metabolism, may have a causative role in liver cirrhosis [87].

5.8.1.2. Volatile Fatty Acid Compounds

They are carboxylic acids that have a long unbalanced aliphatic tail. There are two types of fatty acids, saturated, which are without double bond or without any other functional group, and unsaturated, which have one or more alkenyl functional groups.

The volatile fatty acids are biomarkers for liver diseases, these acids are derived from the action of the intestinal bacteria on carbohydrates and amino acids.

The volatile fatty acids are propionic acid ($m/z=75$), butyric acid ($m/z=89$) or isobutyric acid ($m/z=89$), isovaleric acid ($m/z=103$) and decanoic acid ($m/z=173$), as illustrated in Figure 5.24.

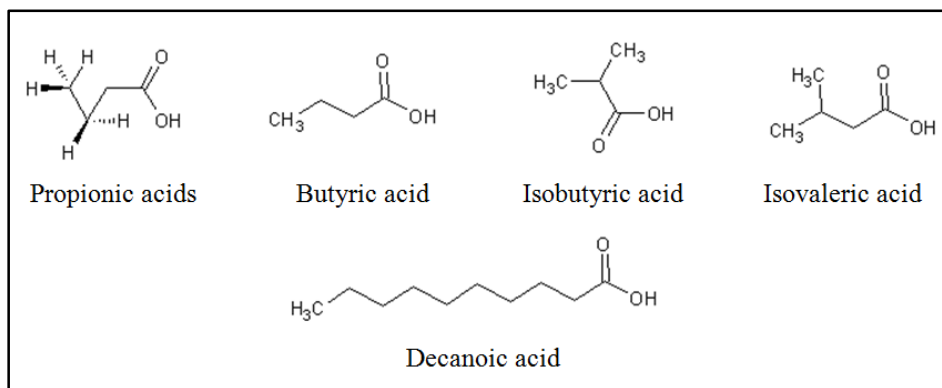


Figure 5.24: Some of the fatty acid compounds.

Figure 5.25 shows two types of comparisons for compound, $m/z = 103$: (**on the left**), the counts of this compound is high in volunteers group and (**on the right**), it shows a decrease in its counts according to LiMAX-test value.

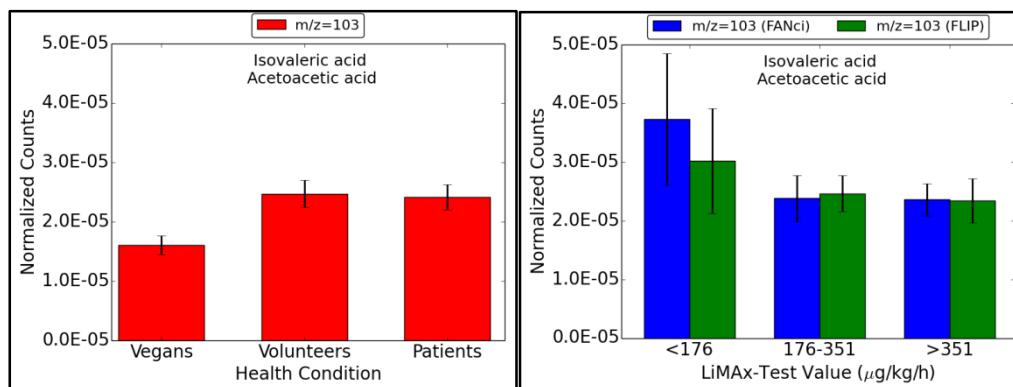


Figure 5.25: The 1st group of the fatty acid compounds.

The VOC at (103 Th) is defined as isovaleric acid and other compound. It is **not a good biomarker** for liver diseases, because it has the highest value in volunteers.

Figure 5.26 shows two types of comparisons for three compounds, $m/z = 75$, 89 and 173: (**on the left**), the counts of these compounds are high in vegans group and (**on the right**), their counts are high in bad liver function.

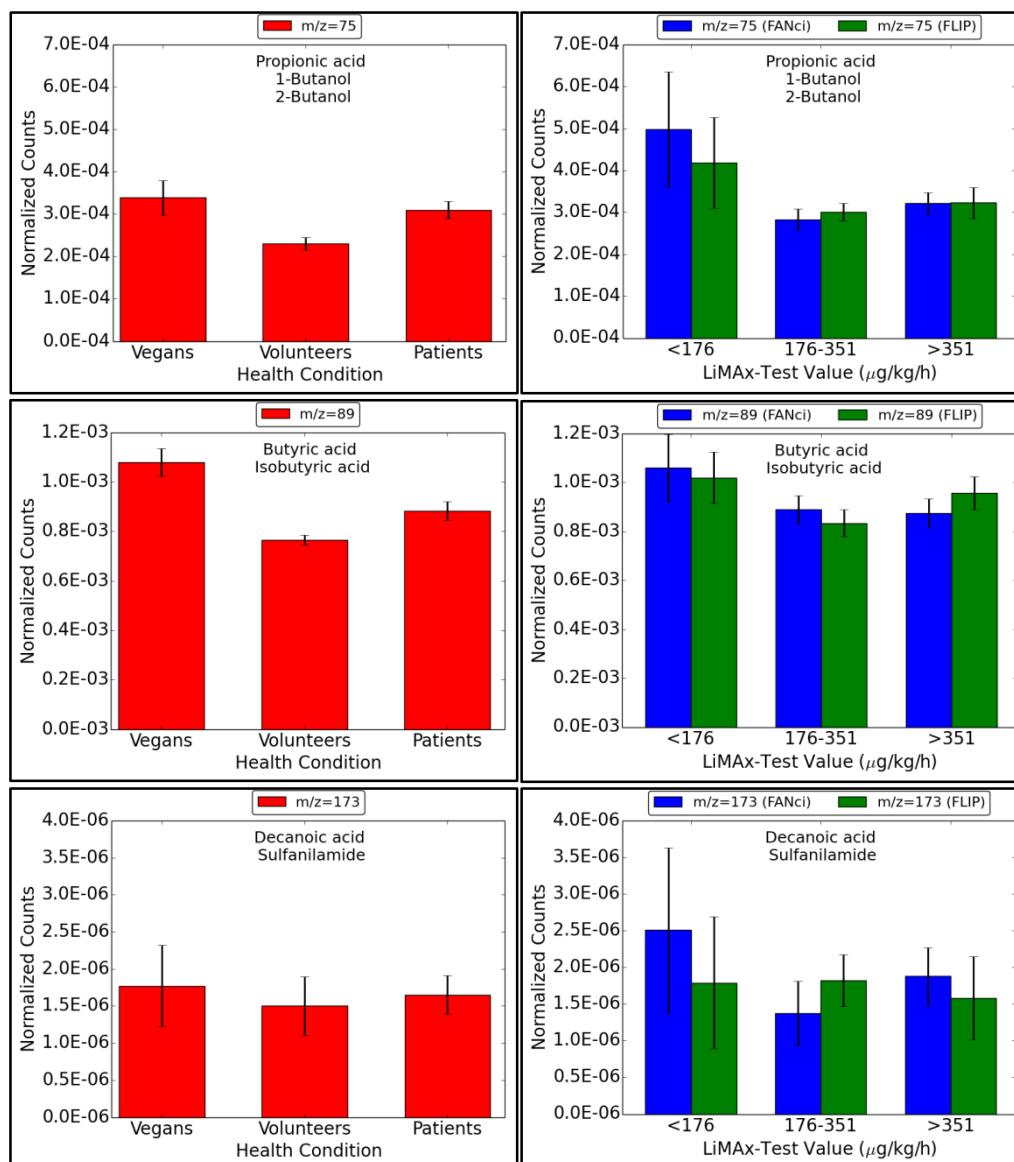


Figure 5.26: The 2nd group of the fatty acid compounds.

The VOC at (75 Th) we found propionic acids and other compounds, at (89 Th) is defined as butyric acid and other compound and at (173 Th) is decanoic acid and other compound. All of them are **not good biomarkers** for liver diseases, because they have the highest value in vegans.

The major sites of fatty acid synthesis are adipose tissue and the liver. They are transported to the liver as free fatty acids (FFA) and undergo β -oxidation in the liver to produce ketone bodies. These ketone bodies can not be used by the liver but are exported to extra-hepatic tissues to be used for energy production. In the case of liver disease or liver

failure, the fatty acids do not oxidize leading to increase these compounds in blood and breath.

The increase in the level of these volatile fatty acids may refer also to their dietary (omega-3 and omega-6) that contain volatile fatty acids (VFA) or supplements to avoid the fatty acid deficiency especially in vegans or because of their dietary status (not fasted for 6-12 hrs). Fatty acids are found in sunflower seeds, pumpkin seeds, sesame seeds, walnuts, wheat germ soy foods and etc.

5.8.1.3. Nitrogen Containing Organic Compounds

Nitrogen containing organic compounds or (amines) are organic compounds that are derivatives of ammonia (NH_3). Amines are found in different classes depending on the number of alkyl or aryl groups that attached to nitrogen, as illustrated in Figure 5.27.

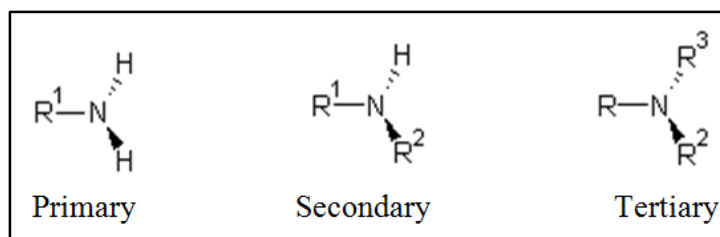


Figure 5.27: The classification of nitrogen containing organic compounds.

The exhaled breath contains volatile organic amines. Volatile organic amines are ammonia ($m/z=18$), methylamine ($m/z=32$), vinylamine ($m/z=44$), dimethylamine ($m/z=46$), trimethylamine ($m/z=60$), n-butylamine ($m/z=74$), glycine ($m/z=76$), alanine ($m/z=90$), serine ($m/z=106$), proline ($m/z=116$), threonine ($m/z=120$), cysteine ($m/z=122$) which is discussed previously with sulfur containing compounds, octylamine ($m/z=130$), ornithine ($m/z=133$), glutamine ($m/z=147$), glutamic acid ($m/z=148$), carnitine ($m/z=162$), selenocysteine ($m/z=169$) and arginine ($m/z=175$).

Figure 5.28 shows two types of comparisons for three compounds, $m/z = 44$, 74 and 106: (**on the left**), the counts of these compounds are high in patients group and (**on the right**), they show a decrease in their counts according to LiMAX-test value.

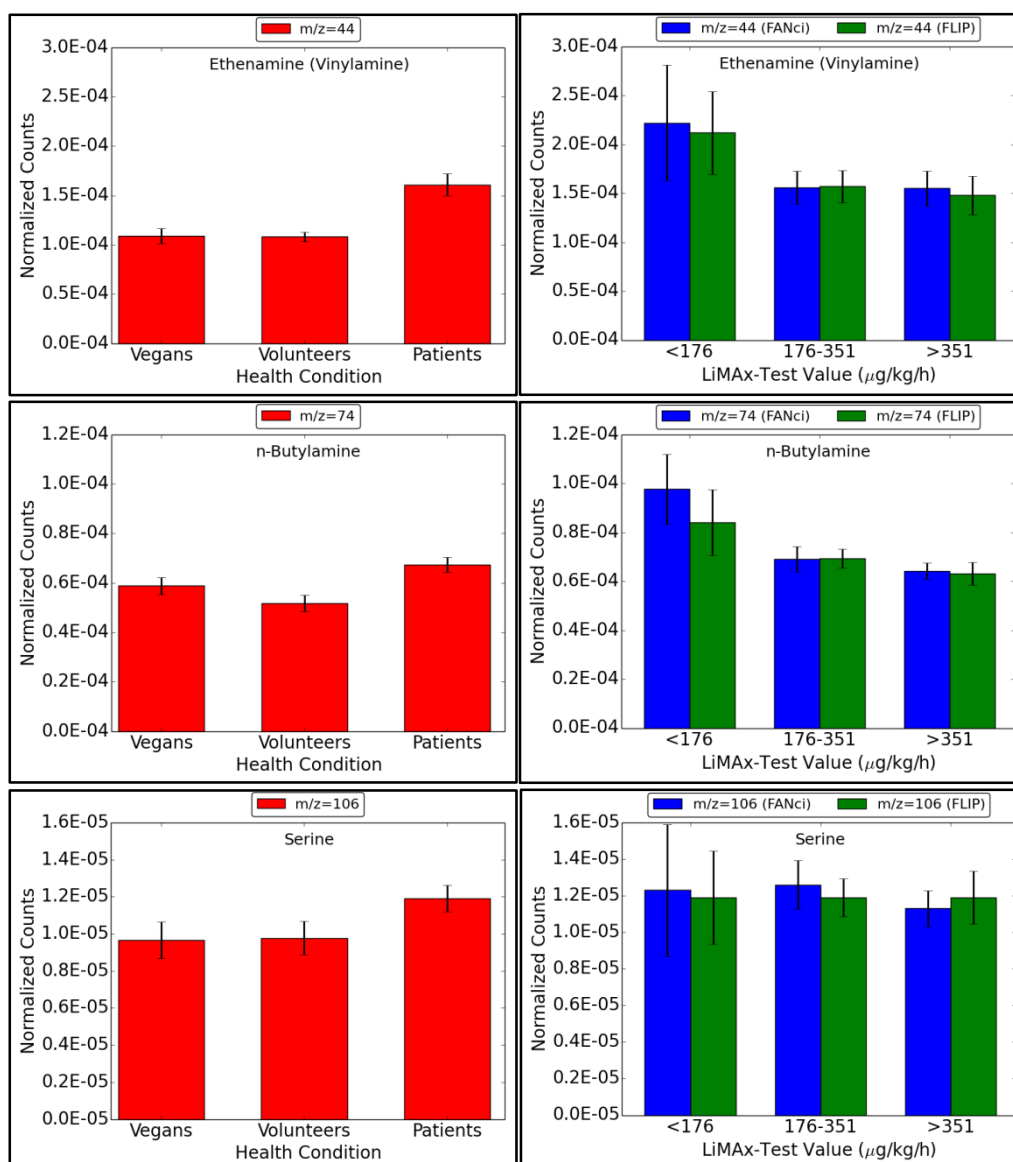


Figure 5.28: The 1st group of nitrogen containing organic compounds.

The VOC at (44 Th) is vinylamine, at (m/z=74) is defined as n-butylamine and at (m/z=106) is recognized as serine. These VOCs are **good biomarkers** for liver diseases, because in the first comparison they have the highest value in patients compared to volunteers and vegans and in the second comparison the values decrease when the liver condition improves.

Figures 5.29 and figure 5.30 show two types of comparisons for eight compounds, m/z = 60, 76, 120, 130, 133, 147, 148 and 169: (**on the left**), the counts of these compounds are high in patients group and (**on the right**), their counts do not show any relation with LiMAX-test value.

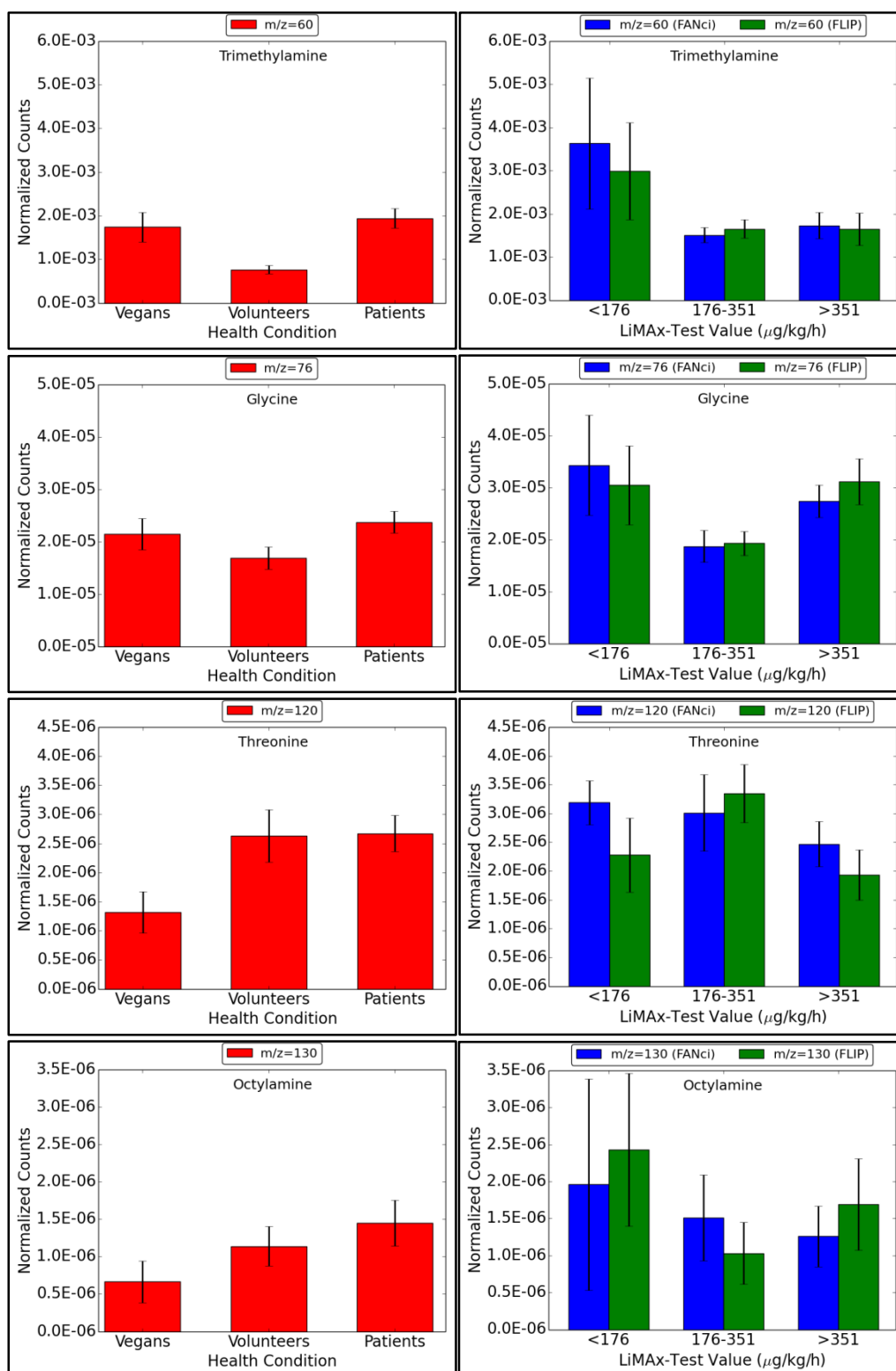


Figure 5.29: The 1st part of the 2nd group of nitrogen containing organic compounds.

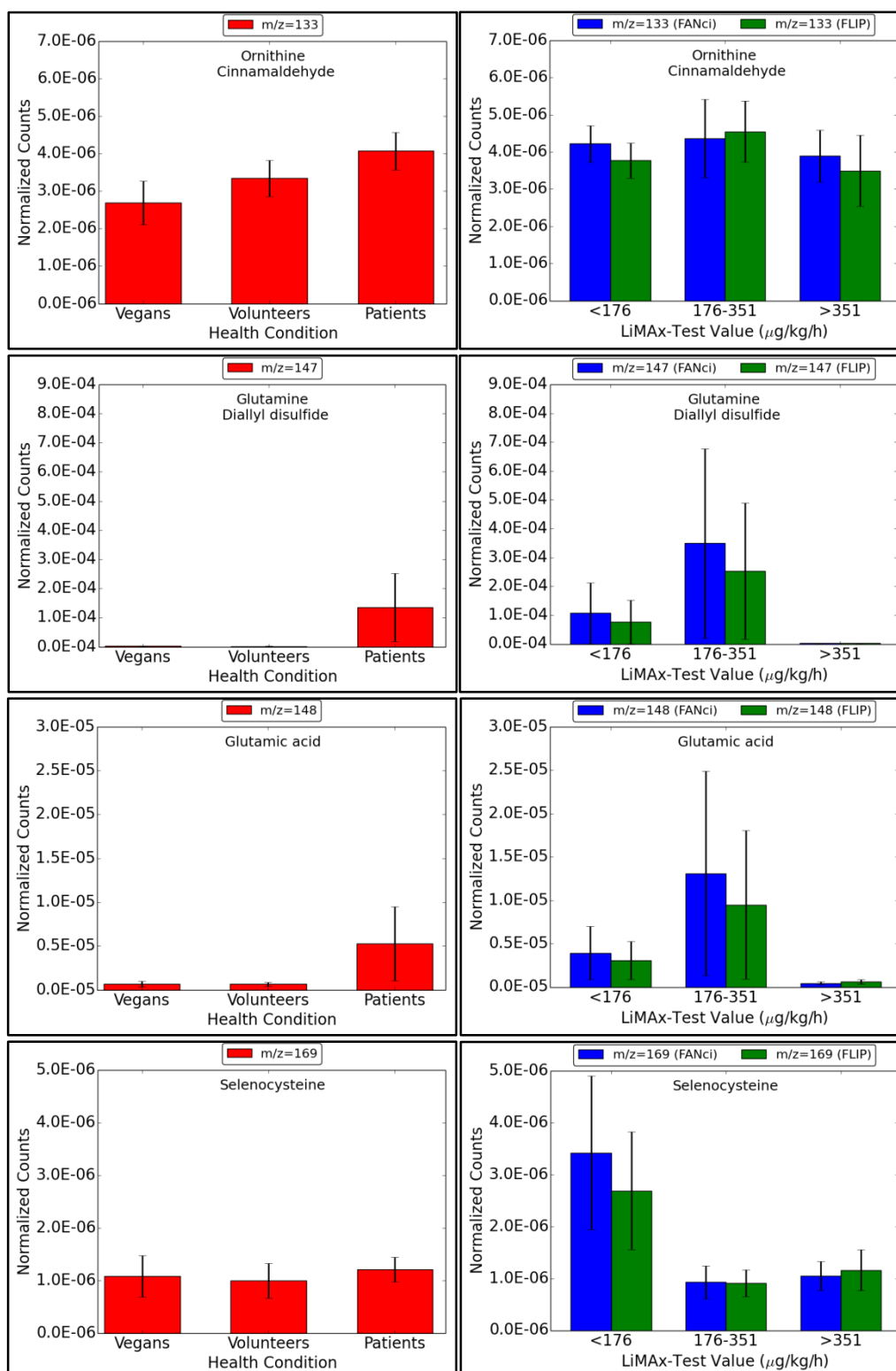


Figure 5.30: The 2nd part of the 2nd group of nitrogen containing organic compounds.

The VOC at (60 Th) is known as trimethylamine, at (76 Th) we found glycine, at (120 Th) is threonine, at (130 Th) is defined as octylamin, at (133 Th) ornithine and other compound, at (147 Th) glutamine and other compound, at (148 Th) glutamic acid and at (169 Th) selenocysteine. All of them are **not good biomarkers** for liver diseases, because their values do not show good correlations with LiMAX-test value in the second comparison even they show the highest values in patients compared to volunteers and vegans in the first comparison.

Figure 5.31 and figure 5.32 show two types of comparisons for five compounds, $m/z = 46, 90, 116, 162$ and 175 : (**on the left**), the counts of these compounds are high in vegans group and (**on the right**), their counts are high in bad liver function.

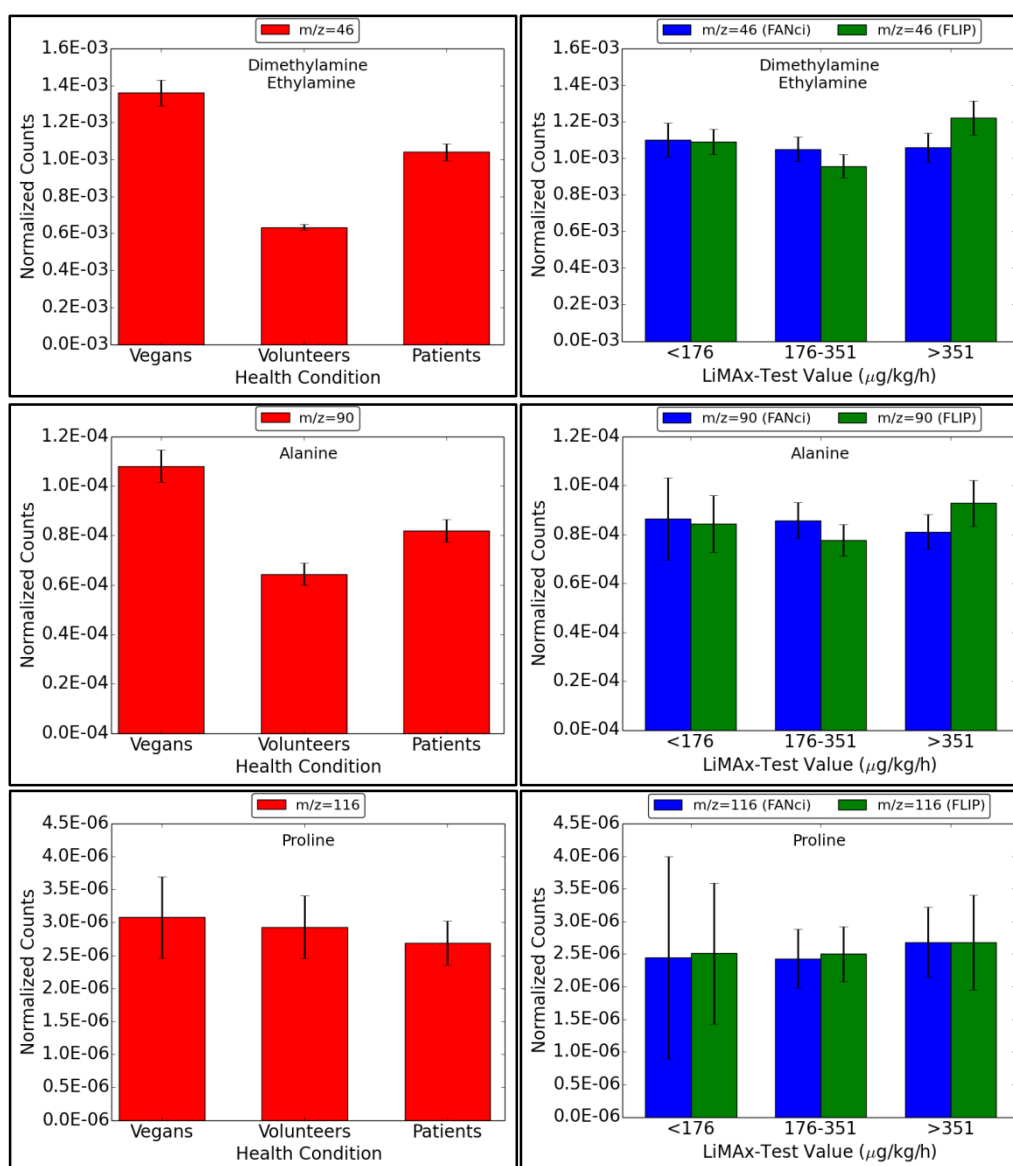


Figure 5.31: The 1st part of the 3rd group of nitrogen containing organic compounds.

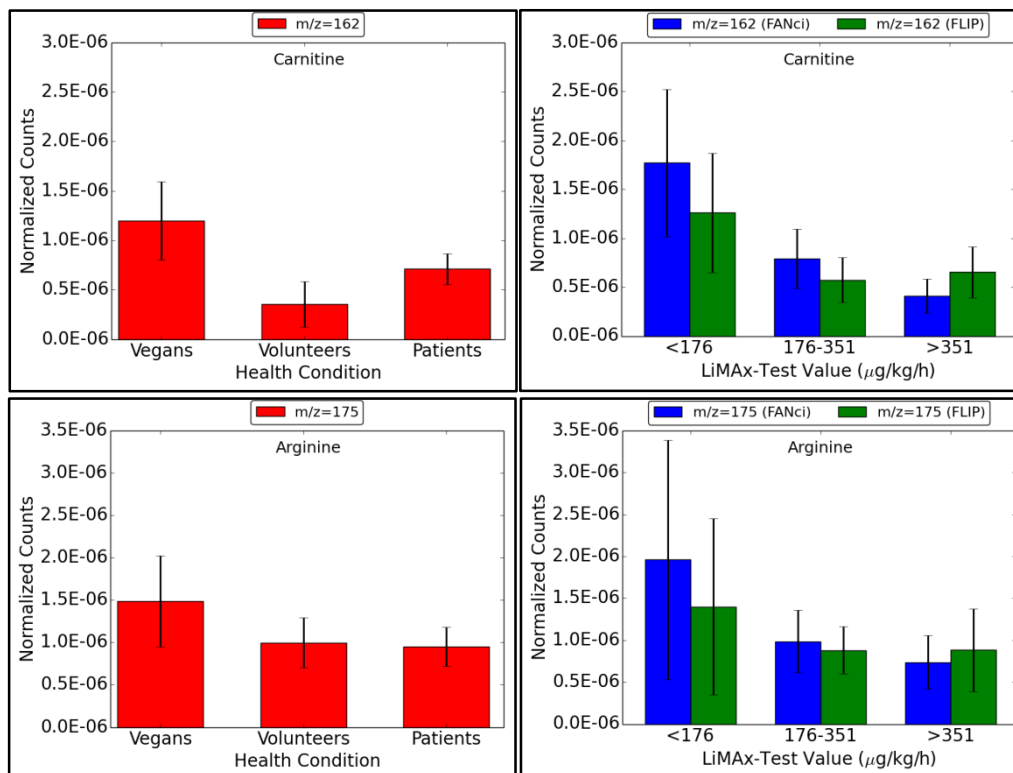


Figure 5.32: The 2nd part of the 3rd group of nitrogen containing organic compounds.

The VOC at (46 Th) is defined as dimethylamine and other compound, at (90 Th) is known as alanine, at (116 Th) is proline, at (162 Th) carnitine and at (175 Th) arginine. All of them are **not good biomarkers** for liver diseases, because they have the highest value in vegans.

Figure 5.33 shows two types of comparisons for two compounds, $m/z = 18$ and 32 : (**on the left**), the counts of these compounds are high in volunteers group and (**on the right**), their counts do not show any relation with LiMAX-test value.

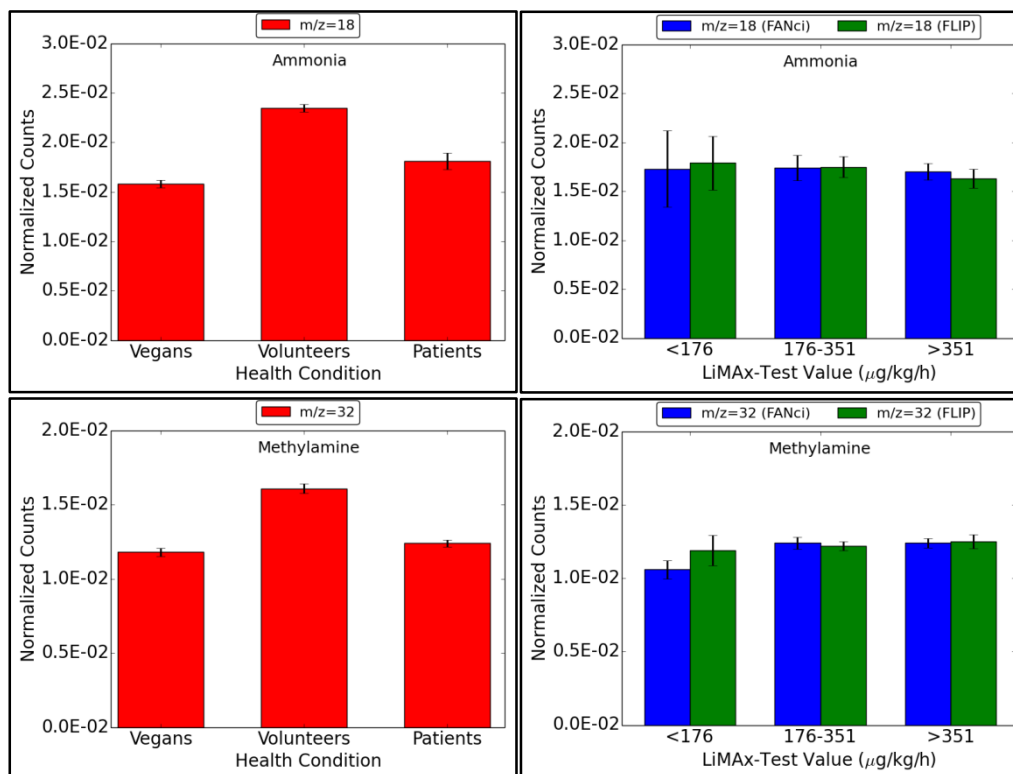


Figure 5.33: The 4th group of nitrogen containing organic compounds.

The VOC at (18 Th) is known as ammonia and at (32 Th) is methylamine. These VOCs are **not good biomarkers** for liver diseases, because they have the highest value in volunteers.

Ammonia is produced systematically by breaking-down the protein products that originate from the degradation of proteins by the intestinal bacteria. Ammonia is generated in the liver from glutamate and then is converted into urea that is eliminated through urine; some of them are exhaled in the breath and others are emitted from the skin.

Since muscle is a site for extrahepatic ammonia removal, a common occurrence in cirrhotic patients is muscle wasting that may also elevate the arterial ammonia level.

Almost all the ammonia found in the blood comes from the intestine. This blood is carried to the liver by the portal vein where a high percentage of ammonia is converted to urea.

There are many factors that cause the ammonia level to increase: it may increase due to the increase in its production (convulsive seizures with increased muscle production) or its

clearance is impaired (hepatocellular dysfunction, portosystemic shunting, or both, with subsequent impaired hepatic detoxification of ammonia [91].

By ingestion of protein and/or Niacin (Vitamin B3) an increase of systemic ammonia can be induced [92, 93].

The increase in the level of ammonia may also refer to a confounding factor, poor oral hygiene, that can be modified by an appropriate mouth washing or eliminated by washing the mouth with water before collecting the sample.

Referring to *Spandel et al.* [94], “the speed of production of ammonia indicates that it is presumably due to the action of salivary and bacterial ureases in the urea”.

Glutamine ($m/z=147$) flux is increased in cirrhosis through hepatic glutaminase 4- to 6-fold. The concentration of blood ammonium is elevated in hepatic cirrhosis patients, especially with those which have a transjugular intrahepatic portosystemic shunt, after oral administration of amino acids such as glutamine ($m/z=147$), glycine ($m/z=76$), serine ($m/z=106$), and threonine ($m/z=120$) when compared to healthy subjects due to deficient handling of ammonium in the case of liver disease.

Carnitine ($m/z=162$) compound is synthesized from lysine and methionine as a methyl donor by the liver and it is derived from dietary protein. It must be oxidized to transfer medium- and long- chain fatty acids across the mitochondrial membrane.

The concentration of plasma carnitine is increased in alcohol-induced cirrhosis patients due to the increase of carnitine biosynthesis because of increased skeletal muscle protein turnover.

The hydrolysis of arginine ($m/z=175$) is catalyzed to ornithine and urea by the arginase enzyme. Two isoenzymes of arginase are known in human, AI, which is a cytosolic enzyme and AII, which is located in the mitochondrion and viewed as biosynthetic. Arginase-AI isoenzyme is found in liver and red blood cells while arginase-AII isoproteins is found in kidney, brain, gastrointestinal tract and prostate [95].

Due to the depletion of ornithine ($m/z=133$) and arginine ($m/z=175$) in liver mitochondria, the recurring of postprandial hyperammonemia may happen. The metabolism of citrulline ($m/z=176$) to arginine ($m/z=175$) and then to ornithine ($m/z=133$) leads to improve the urea cycle performance and ameliorate the postprandial rise of plasma ammonium.

In contrast to healthy humans, the peripheral arteriovenous difference for glutamine ($m/z=147$) is threefold greater than that for alanine ($m/z=90$) in patients with hepatic insufficiency. When the released alanine is more than glutamine, this proposed that the major fraction of ammonium in patients with liver diseases are taken up by the muscle is released as glutamine.

The aromatic amino acids are metabolized in the liver. If there is an impairment in liver function, these compounds do not metabolize correctly then lead to increase the free tyrosine and tryptophan in the body.

5.8.1.4. Nitrile Compounds

They are organic compounds that have $-C\equiv N$ functional group, as illustrated in Figure 5.34. In inorganic compounds the $-C\equiv N$ functional group is called cyanides instead of nitrils.

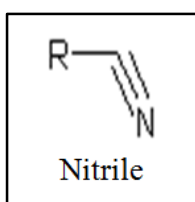


Figure 5.34: The chemical structure of the nitrile compounds.

Cyanide ($m/z=27$), hydrogen cyanide ($m/z=28$) and acetonitrile ($m/z=42$) are examples of this group.

Figure 5.35 shows two types of comparisons for compound, $m/z = 28$: (**on the left**), the counts of this compound is high in patients group and (**on the right**), it shows a decrease in its counts according to LiMAX-test value.

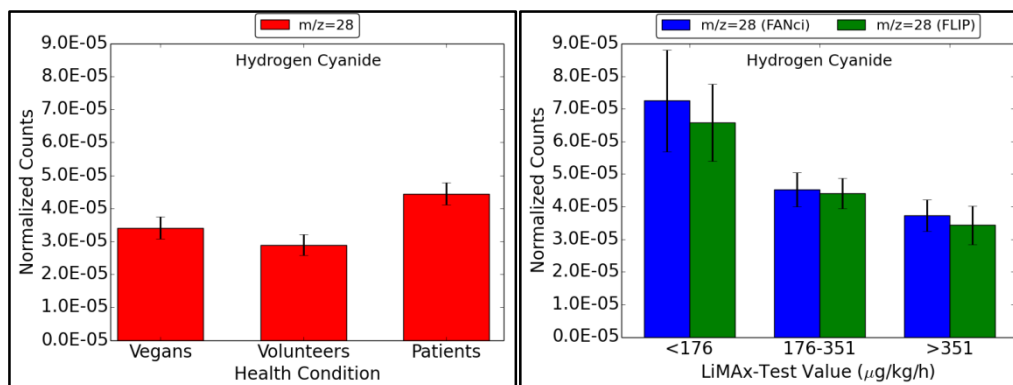


Figure 5.35: The 1st group of the nitrile compounds.

The VOC at (28 Th) is defined as hydrogen cyanide, which is a **good biomarker** for liver diseases, because in the first comparison it has the highest value in patients compared to volunteers and vegans and in the second comparison the value decreases when the liver condition improves.

Figure 5.36 shows two types of comparisons for two compounds, $m/z = 27$ and 42: (**on the left**), the counts of these compounds are high in patients group and (**on the right**), their counts do not show any relation with LiMAX-test value.

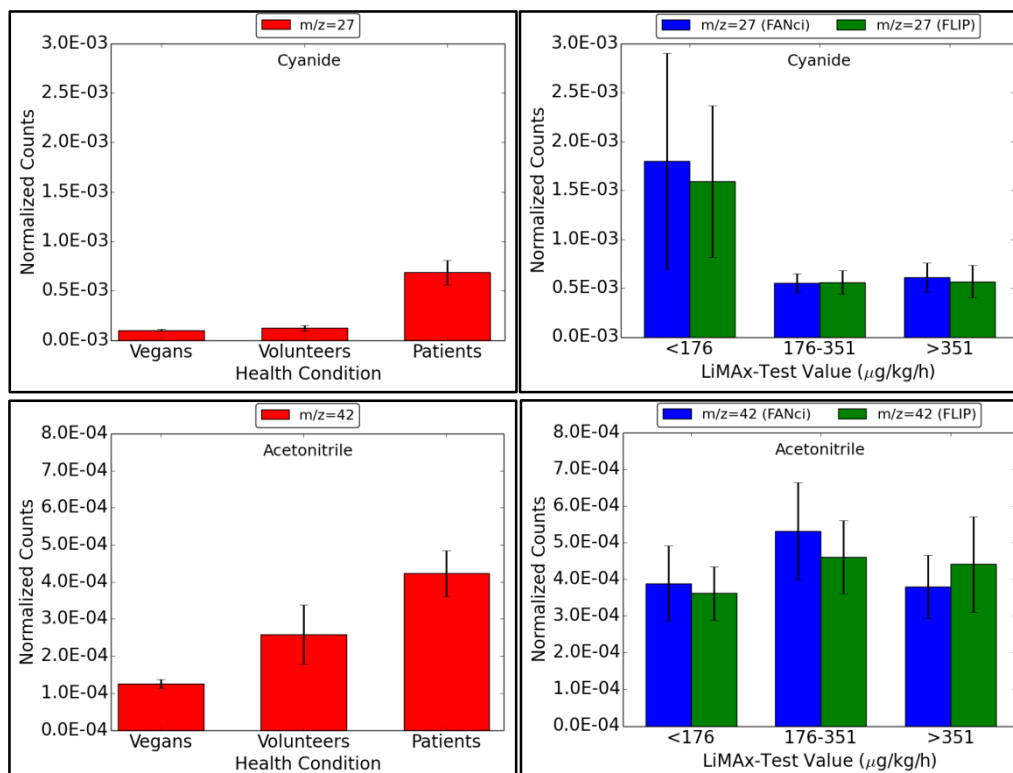


Figure 5.36: The 2nd group of the nitrile compounds.

The VOC at (27 Th) is recognized as cyanide and at (42 Th) is known as acetonitrile. These VOCs are **not good biomarkers** for liver diseases, because their values do not show a good correlation with LiMAX-test value in the second comparison even they show the highest values in patients compared to volunteers and vegans in the first comparison.

As denoted by WHO [96], “The major route of metabolism for hydrogen cyanide ($m/z=28$) and cyanide ($m/z=27$) is detoxification in the liver by the mitochondrial enzyme rhodanese, which catalyses the transfer of the sulfane sulfur of thiosulfate to the cyanide ion to form thiocyanate, about 80% of cyanide is detoxified by this route [97]”. Cyanide can be combined with the hydroxocobalamin (vitamin B12a) to yield cyanocobalamin (vitamin B12)

and non-enzymatic combination of cyanide with cysteine to form 2-iminothiazoline-4-carboxylic acid, which is excreted without further change [98].

When there is a health problem or a liver failure, hydrogen cyanide ($m/z=28$) and cyanides ($m/z=27$) do not detoxify leading to an increase of their concentrations in the body and in the exhaled breath.

5.8.1.5. Hydrocarbon Compounds

They are organic compounds that consist of hydrogen and carbon. Hydrocarbons are divided into four groups according to IUPC nomenclature of organic chemistry, as illustrated in Figure 5.37. Hydrocarbons can be found in different forms like gases, liquids, waxes and/or polymers.

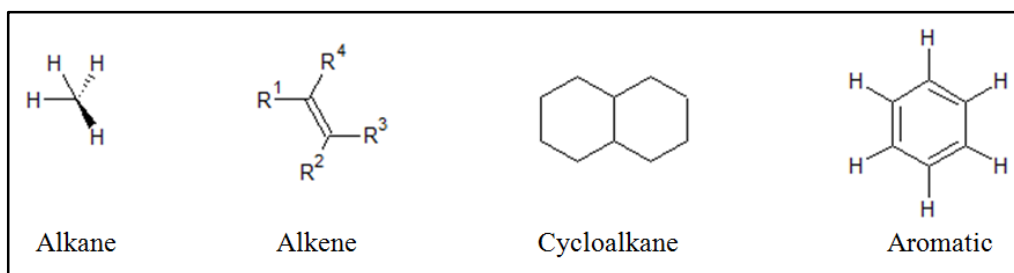


Figure 5.37: The classification of hydrocarbon organic compounds.

Alkanes are saturated hydrocarbons that consist of hydrogen and carbon atoms and all bonds are single.

Alkane compounds are ethane ($m/z=31$), octane ($m/z=115$), nonane ($m/z=129$), decane ($m/z=143$) and tetradecane ($m/z=199$).

Figure 5.38 shows two types of comparisons for two compounds, $m/z = 115$ and 199 : (**on the left**), the counts of these compounds are high in patients group and (**on the right**), they show a decrease in their counts according to LiMAx-test value.

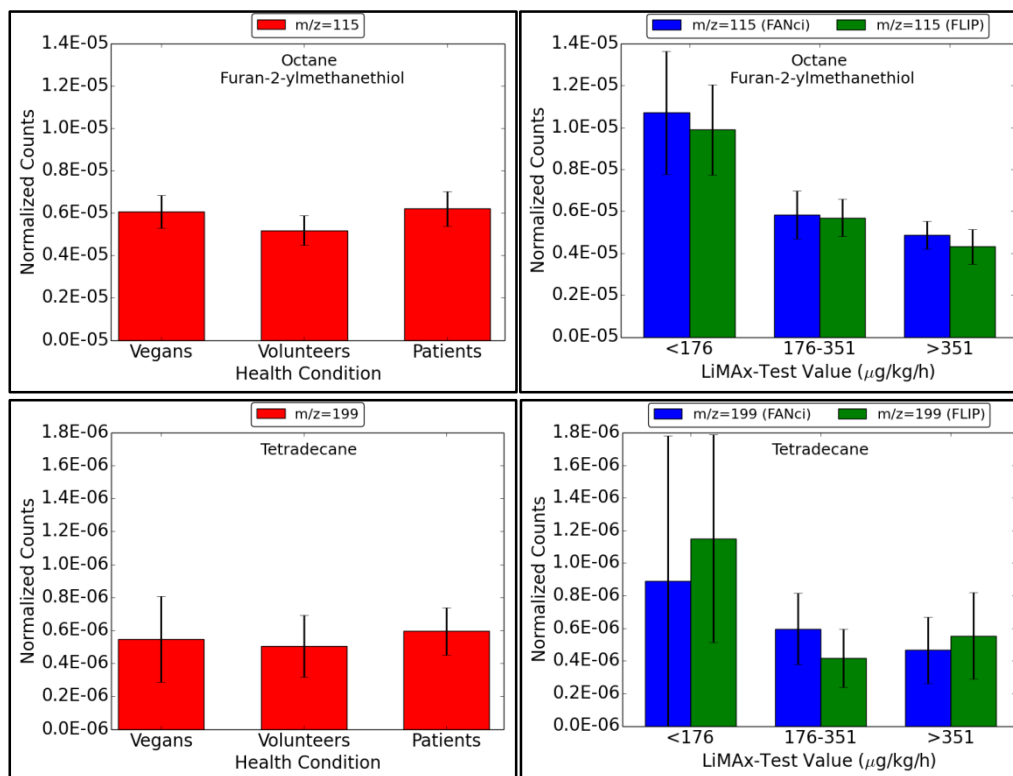


Figure 5.38: The 1st group of the alkanes of hydrocarbon organic compounds.

The VOC at (115 Th) is octane and other compound and at (199 Th) is tetradecane. These VOCs are **good biomarkers** for liver diseases, because in the first comparison they have the highest value in patients compared to volunteers and vegans and in the second comparison the values decrease when the liver condition improves.

Figure 5.39 shows two types of comparisons for two compounds, $m/z = 129$ and 143 : (**on the left**), the counts of these compounds are high in patients group and (**on the right**), their counts do not show any relation with LiMAX-test value.

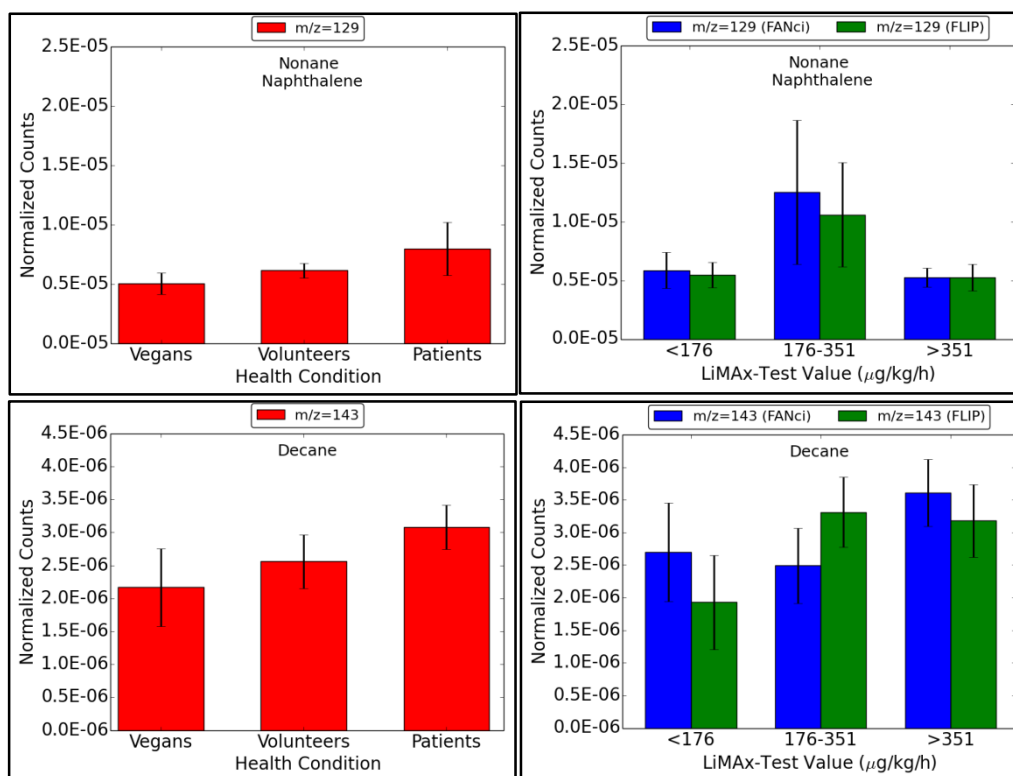


Figure 5.39: The 2nd group of the alkanes of hydrocarbon organic compounds.

The VOC at (129 Th) is defined as nonane and other compound and at ($m/z=143$) is decane. These VOCs are **not good biomarkers** for liver diseases, because their values do not show a good correlation with LiMAX-test value in the second comparison even they show the highest values in patients compared to volunteers and vegans in the first comparison.

Figure 5.40 shows two types of comparisons for compound, $m/z = 31$: (**on the left**), the counts of this compound is high in vegans group and (**on the right**), its counts is high in bad liver function.

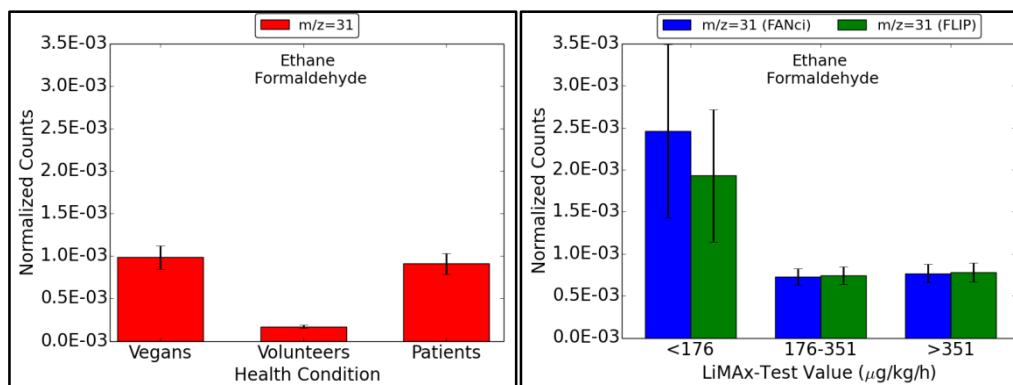


Figure 5.40: The 3rd group of the alkanes of hydrocarbon organic compounds.

The VOC at (31 Th) is defined as ethane and other compound. It is **not a good biomarker** for liver diseases, because it has the highest value in vegans.

Alkenes are unsaturated hydrocarbons that have at least one carbon-carbon double bond.

Alkene compounds are ethene ($m/z=29$), isoprene ($m/z=39$, 22.6% of $m/z=69$), isoprene ($m/z=41$, 88.7% of $m/z=69$), propene ($m/z=43$), acrolein ($m/z=57$), isoprene ($m/z=67$, 3.8% of $m/z=69$), isoprene ($m/z=69$), pentene ($m/z=71$), hexene ($m/z=85$), heptene ($m/z=99$), octene ($m/z=113$) and nonene ($m/z=127$).

Figure 5.41 shows two types of comparisons for two compounds, $m/z = 41$ and 43: (**on the left**), the counts of these compounds are high in patients group and (**on the right**), they show a decrease in their counts according to LiMAX-test value.

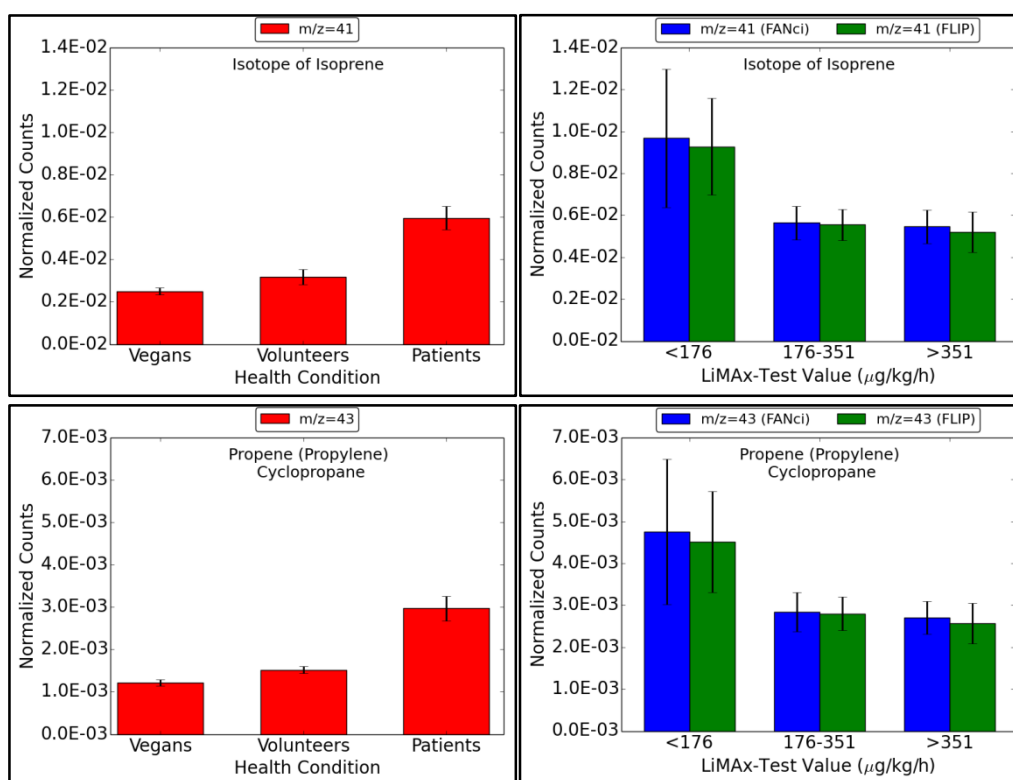


Figure 5.41: The 1st group of the alkenes of hydrocarbon organic compounds.

The VOC at (41 Th) is isotope of isoprene (88.7% of $m/z=69$) and at (43 Th) we found propene and other compound. They are **good biomarkers** for liver diseases, because in the first comparison they have the highest value in patients compared to volunteers and vegans and in the second comparison the values decrease when the liver condition improves.

Figure 5.42 shows two types of comparisons for four compounds, $m/z = 39, 67, 99$ and 127 : (**on the left**), the counts of these compounds are high in patients group and (**on the right**), their counts do not show any relation with LiMAX-test value.

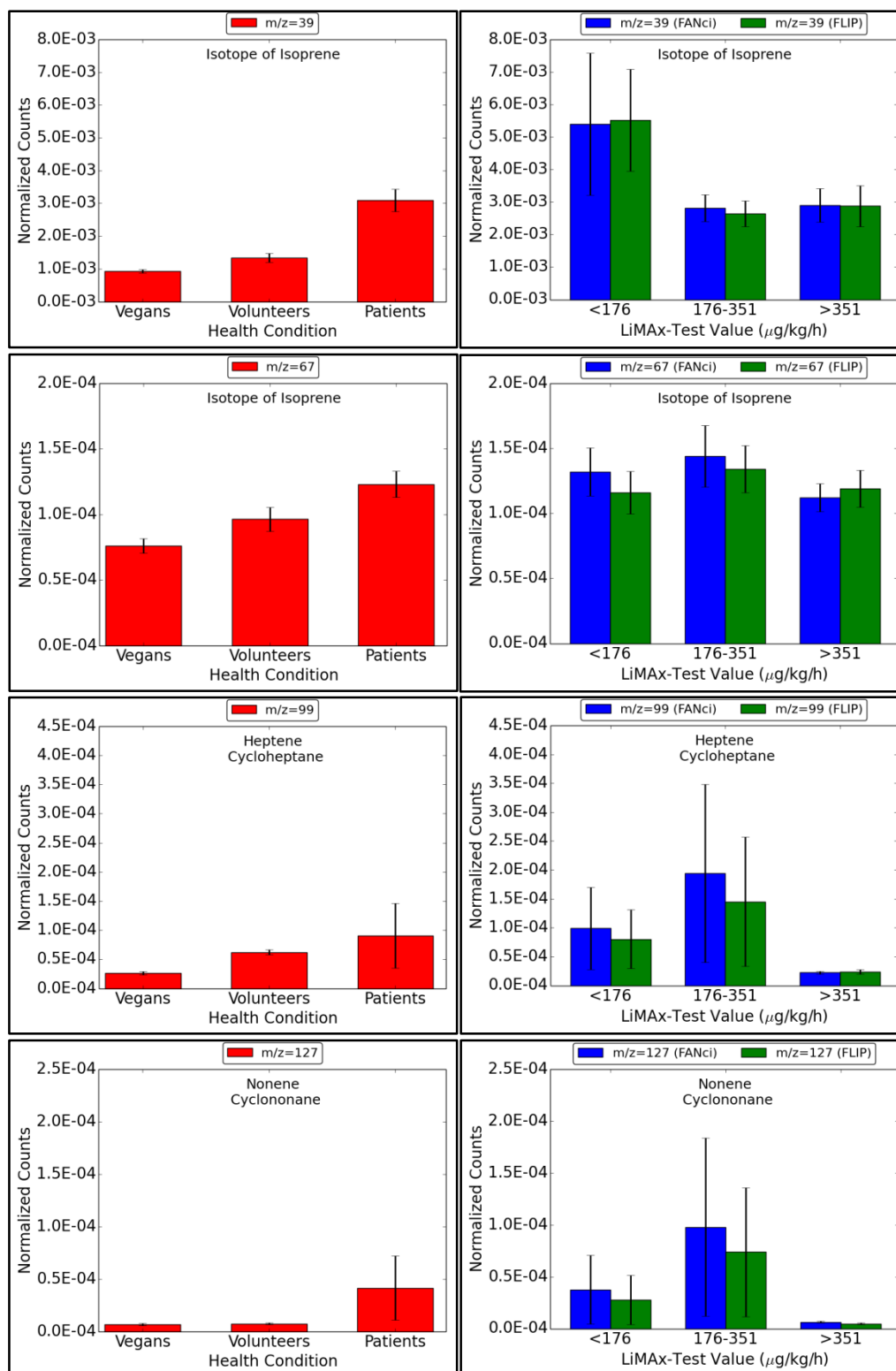


Figure 5.42: The 2nd group of the alkenes of hydrocarbon organic compounds.

The VOC at (39 Th) is isotope of isoprene (22.6% of $m/z=69$), at (67 Th) we found isotope of isoprene (3.8% of $m/z=69$), at (99 Th) is defined as heptene and other compound and at ($m/z=127$) nonene and other compound. All of them are **not good biomarkers** for liver diseases, because their values do not show a good correlation with LiMAX-test value in the second comparison even they show the highest value in patients compared to volunteers and vegans in the first comparison

Figure 5.43 shows two types of comparisons for compound, $m/z = 29$: (**on the left**), the counts of this compound is high in vegans group and (**on the right**), its counts is high in bad liver function.

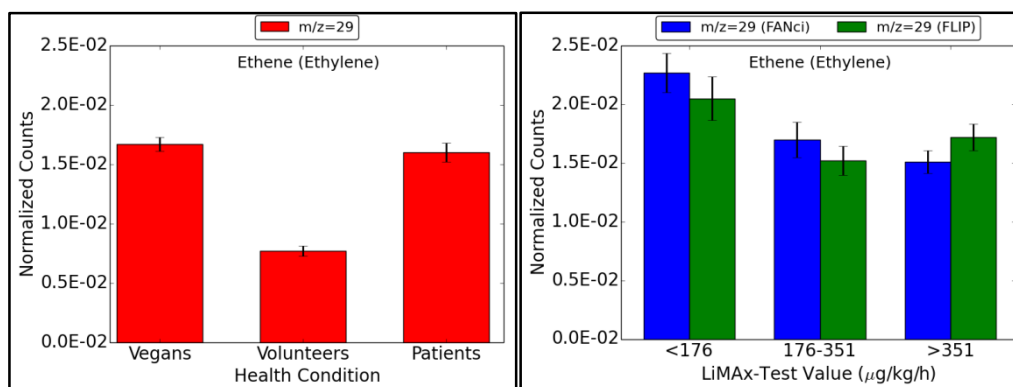


Figure 5.43: The 3rd group of the alkenes of hydrocarbon organic compounds.

The VOC at (29 Th) is ethane, which is **not a good biomarker** for liver diseases, because it has the highest value in vegans.

Figure 5.44 shows two types of comparisons for five compounds, $m/z = 57, 69, 71, 85$ and 113: (**on the left**), the counts of these compounds are high in volunteers group and (**on the right**), their counts do not show any relation with LiMAX-test value.

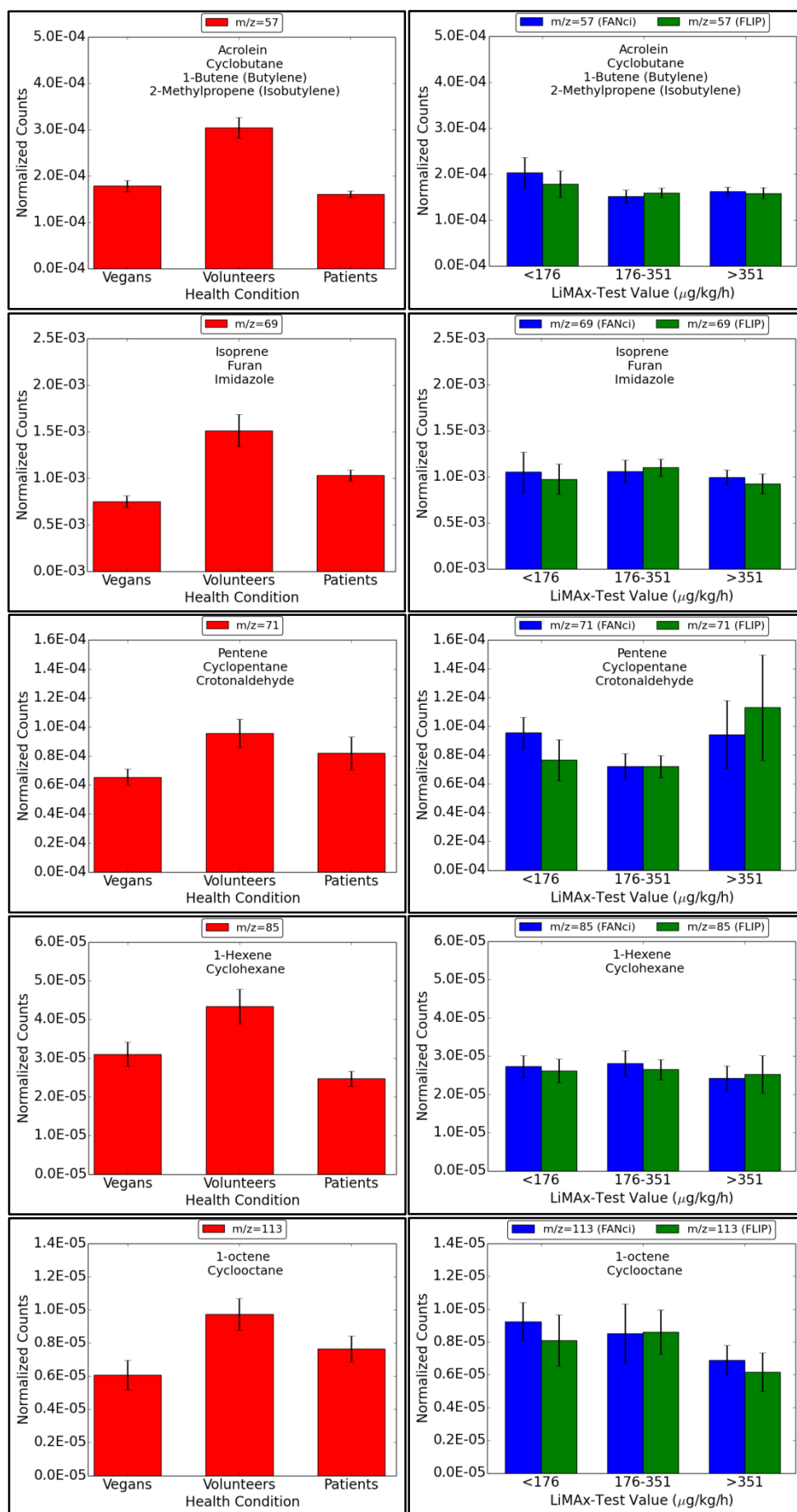


Figure 5.44: The 4th group of the alkenes of hydrocarbon organic compounds.

The VOC at (57 Th) is defined as acrolein and other compounds, at (69 Th) is known as isoprene and other compounds, at (71 Th) we found pentene and other compounds, at (85 Th) is 1-hexene and other compound and at (113 Th) 1-octene and other compounds. All of them are **not good biomarkers** for liver diseases, because they have the highest value in volunteers.

Cycloalkanes are compounds which have in their chemical structure one or more rings of carbon atoms.

Cycloalkane compounds are cyclo-propane ($m/z=43$), cyclo-butane ($m/z=57$), cyclo-pentane ($m/z=71$), cyclo-heptane ($m/z=99$) and cyclo-octane ($m/z=113$).

Aromatics are compounds with alternating double and single bond between the carbon atoms forming rings.

Aromatic compounds are benzene ($m/z=79$), pyridine ($m/z=80$), pyrimidine ($m/z=81$), toluene ($m/z=93$), aniline ($m/z=94$), phenol ($m/z=95$), benzonitrile ($m/z=104$), styrene ($m/z=105$), ethyl benzene ($m/z=107$), indole ($m/z=118$), 4-ethylphenol ($m/z=123$), skatole ($m/z=132$), durene ($m/z=135$), limonene ($m/z=137$), oxindole ($m/z=134$), isotope of 1,2-dichlorobenzene ($m/z=151$) and anthracene ($m/z=179$).

Figure 5.45 shows two types of comparisons for four compounds, $m/z = 81, 93, 104$ and 151 : (**on the left**), the counts of these compounds are high in patients group and (**on the right**), they show a decrease in their counts according to LiMAX-test value.

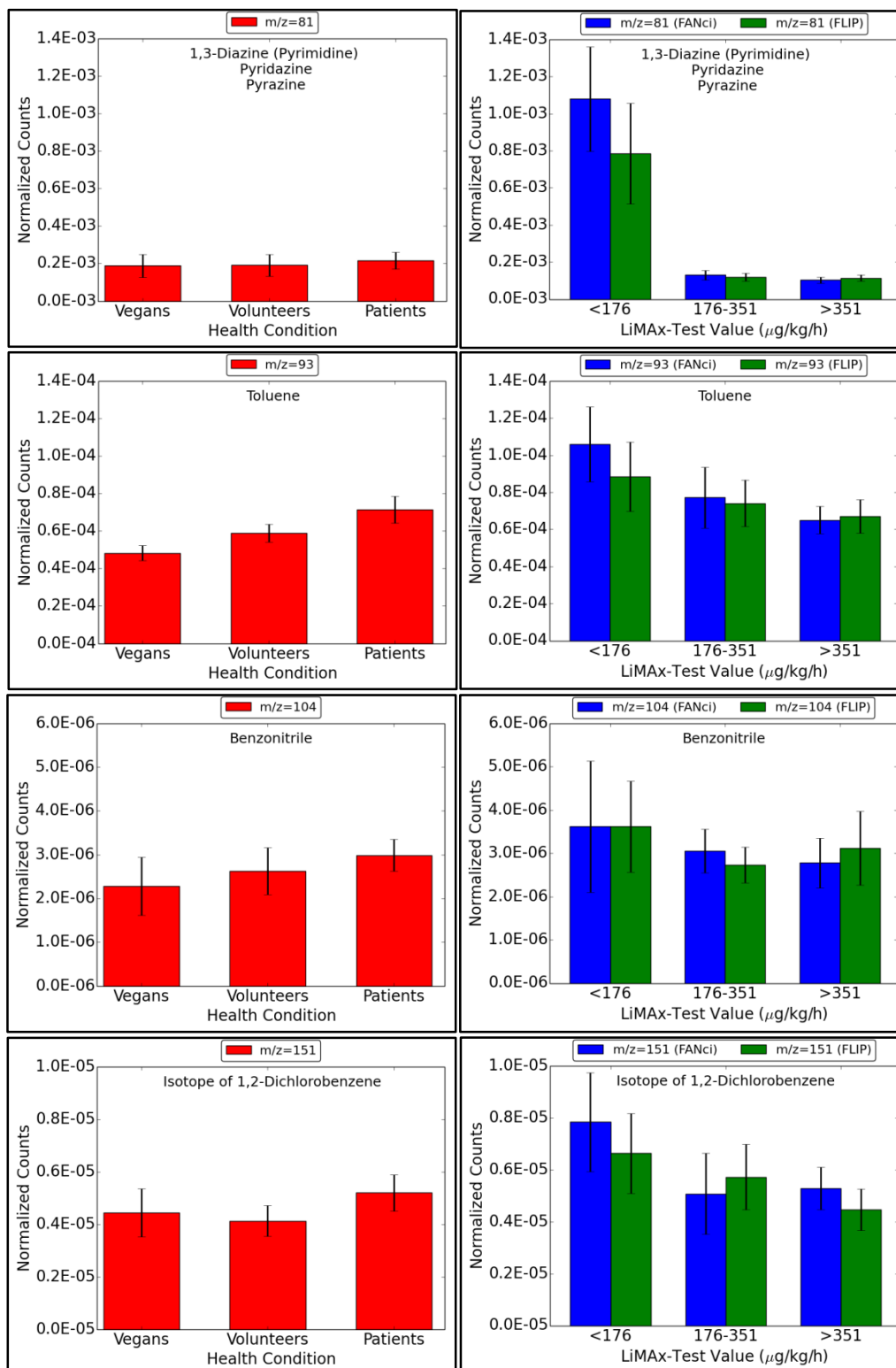


Figure 5.45: The 1st group of the aromatic of hydrocarbon organic compounds.

The VOC at (81 Th) is known as pyrimidine and other compounds, at (93 Th) we found toluene, at (104 Th) is defined as benzonitrile and at (151 Th) isotope of 1,2-dichlorobenzene.

These VOCs are **good biomarkers** for liver diseases, because in the first comparison they have the highest value in patients compared to volunteers and vegans and in the second comparison the values decrease when the liver condition improves.

Figure 5.46 shows two types of comparisons for compound, $m/z = 118$: (**on the left**), the counts of this compound is high in patients group and (**on the right**), it shows an increase in its counts according to LiMAX-test value.

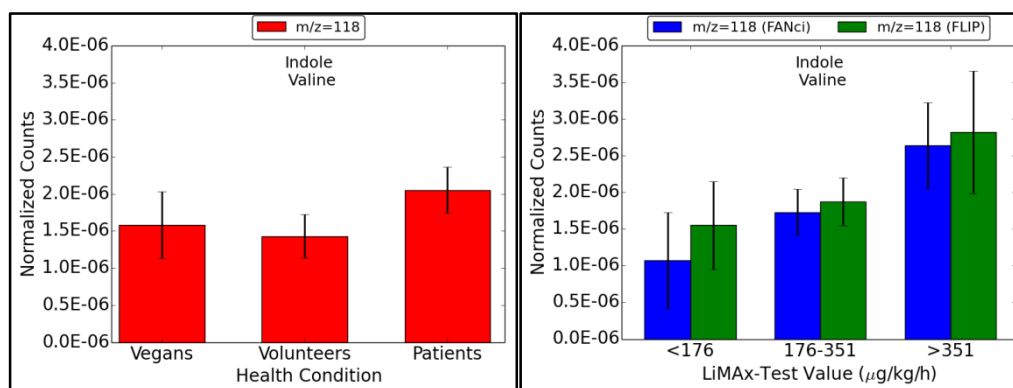


Figure 5.46: The 2nd group of the aromatic of hydrocarbon organic compounds.

The VOC at (118 Th) is defined as indole and other compound, which is **not good biomarker** for liver diseases, because its value increases when the liver condition improves in the second comparison even it shows the highest value in patients compared to volunteers and vegans in the first comparison. This finding is in contrast to *Velde et al.* [86] finding, because in their study they found that indole in patients breath is lower than in healthy breath.

Figure 5.47 shows two types of comparisons for five compounds, $m/z = 79, 80, 123, 132$ and 135 : (**on the left**), the counts of these compounds are high in patients group and (**on the right**), their counts do not show any relation with LiMAX-test value.

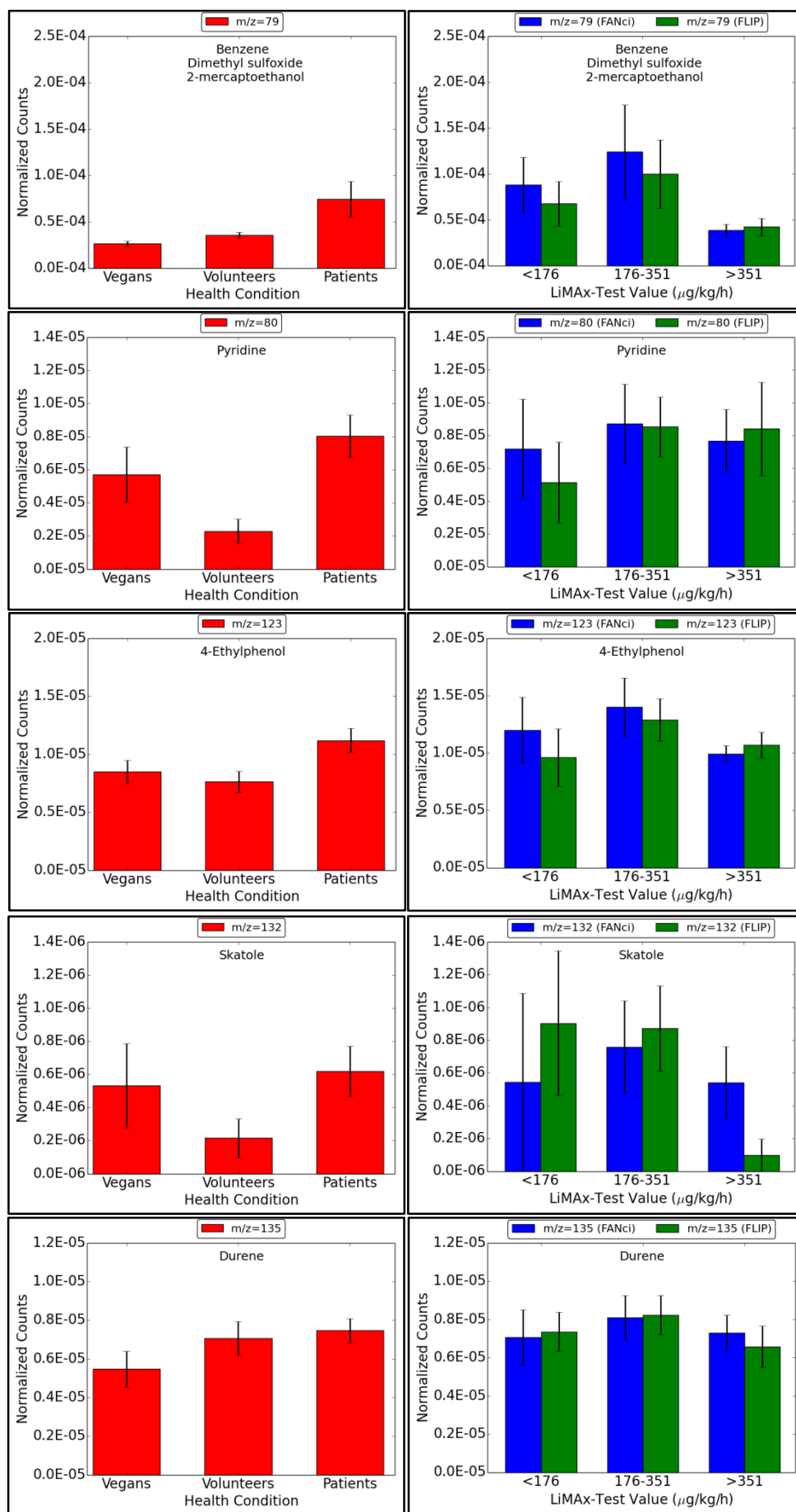


Figure 5.47: The 3rd group of the aromatic of hydrocarbon organic compounds.

The VOC at (79 Th) is known as benzene and other compounds, at (80 Th) we found pyridine, at (123 Th) is 4-ethylphenol, at (132 Th) skatole and at (135 Th) durene. All of them are **not good biomarkers** for liver diseases, because their values do not show a good correlation with LiMAx-test value in the second comparison even they show the highest value in patients compared to volunteers and vegans in the first comparison.

Figure 5.48 shows two types of comparisons for three compounds, $m/z = 94$, 95 and 179: (**on the left**), the counts of these compounds are high in vegans group and (**on the right**), their counts are high in bad liver function.

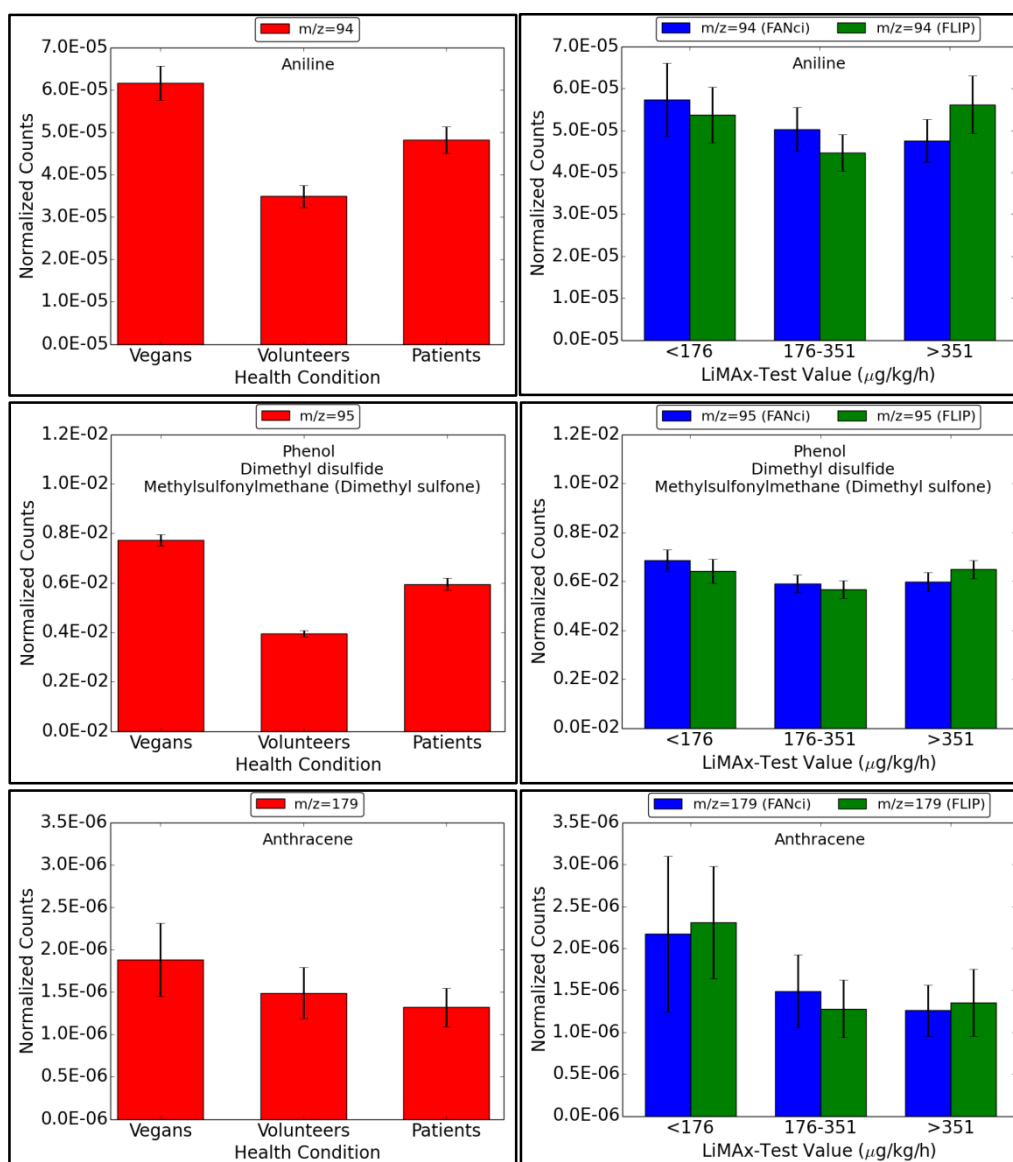


Figure 5.48: The 4th group of the aromatic of hydrocarbon organic compounds.

The VOC at (94 Th) is aniline, at (95 Th) we found phenol and other compounds and at (179 Th) anthracene. These VOCs are **not good biomarkers** for liver diseases, because they have the highest value in vegans.

Figure 5.49 shows two types of comparisons for three compounds, $m/z = 105$, 107 and 134: (**on the left**), the counts of these compounds are high in volunteers group and (**on the right**), their counts do not show any relation with LiMAX-test value.

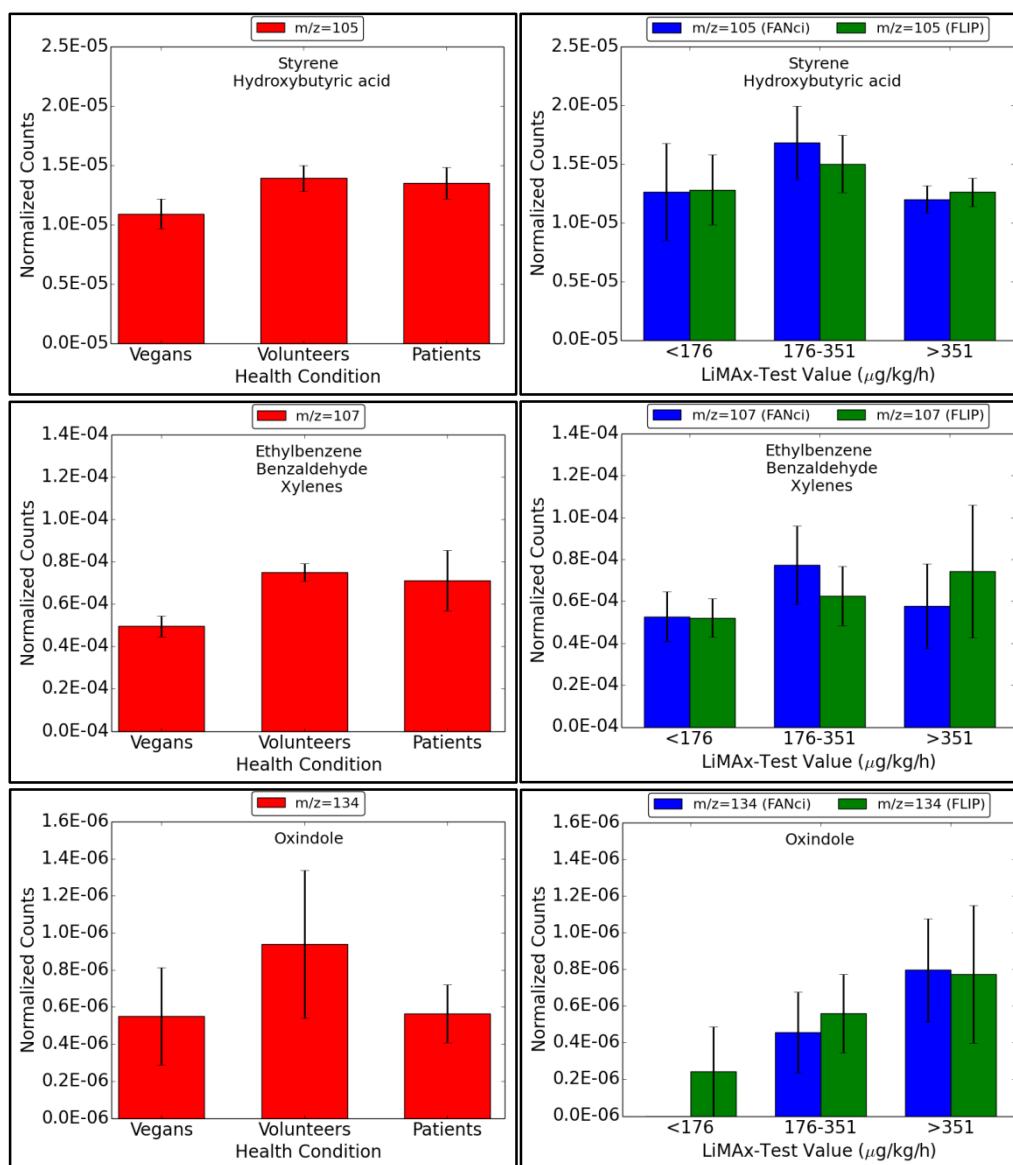


Figure 5.49: The 5th group of the aromatic of hydrocarbon organic compounds.

The VOC at (105 Th) is recognized as styrene and other compound, at (107) is known as ethyl benzene and other compounds and at (134 Th) is oxindole. These VOCs are **not good biomarkers** for liver diseases, because they have the highest value in volunteers.

Figure 5.50 shows two types of comparisons for compound, $m/z = 137$: (**on the left**), the counts of this compound in patients group is equal to volunteers group, which is higher than vegans group and (**on the right**), its counts is very high in bad liver function compared to other conditions.

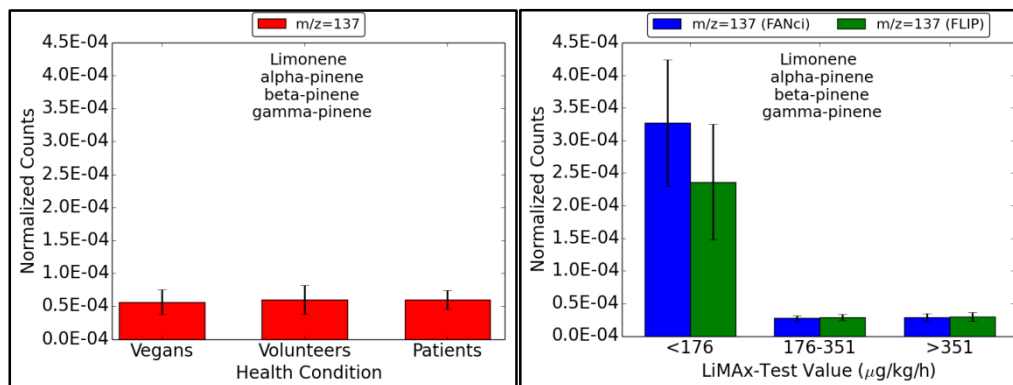


Figure 5.50: The 6th group of the aromatic of hydrocarbon organic compounds.

The VOC at (137 Th) is defined as limonene and other compounds, which is **not a good biomarker** for liver diseases, because the patients' value same as vegans' value.

The reductive dehalogenation of polyhalogenated alkanes is by microsomal cytochrome P450 [99]. If there is a defect or a deficiency in the liver function the concentration of alkanes increases in the body and breath.

2-Methyl-1-propene ($m/z=57$) or isobutene is a compound occurring normally in human breath. It has been proven with animal models that isobutene metabolized by P450 enzymes and converted to epoxides. The main portion of metabolized terpenes, which are the source of the isobutene compound, that are metabolized by cytochrome P450-enzymes in the liver are excreted in the urine and a small fraction exhaled in the breath. In the case of liver disease or liver failure, a change in the metabolism will occur, which leads to an increase in the concentration of this compound in the blood and breath.

The basic unit of terpenes is isoprene ($m/z=69$), which is the most common hydrocarbon in breath that is formed along the mevalonic pathway of cholesterol synthesis. Isoprene is probably metabolized by liver monooxygenase and is converted to mono-epoxides, because its concentration decreases in hepatic venous blood. There are also peripheral origins of isoprene such as muscle cells due to high mixed venous concentration.

The increased level of these compounds may also be due to the nature of their food or after smoking. It has been found that isoprene is a biomarker for oxidative stress and many other conditions causing an increase of these compounds in breath.

A previous study showed that styrene ($m/z=105$) level decreases in liver cirrhosis, because it is oxidized by cytochrome P450 (CYP) to styrene-7,8-oxide. CYP2E1 is the main isoform that is responsible for styrene metabolism in humans [100]. In the case of liver disease, isoprene is not completely metabolized in the liver, this leads to an increase in its concentration in the blood and breath.

The increased level of styrene may also be due to the nature of their food and it is found that styrene is a biomarker for smokers. There are other conditions that cause an increase of these compounds in breath.

Phenol ($m/z=95$) and indole ($m/z=118$) are derived from the catabolism of tyrosine and tryptophan, respectively.

When phenol and indole compounds increase other compound like oxindole, the potential mediator in hepatic encephalopathy will also increase. Because of the binding of phenol and indole to albumin in blood, the breath levels of these compounds will decrease due to the low serum albumin and/or due to low albumin binding capacity [89].

A previous study showed when the mice (mouse liver and brain tissue) are exposed to carbon tetrachloride, there is an increase in the amount of ethane ($m/z=31$) and ethylene ($m/z=29$) [101]. The metabolism of carbon tetrachloride is proposed that these compounds are markers of lipid peroxidation, which known as hepatotoxin, that is involved in free radical generation.

Ethane ($m/z=31$) and pentane ($m/z=73$) are red the better compounds that correlate with alcohol induced hepatic injury than others; this may refer to the increased induction of cytochrome P450 by alcohol which cause an increase in the oxygen radicals production [87].

Ethane and pentane compounds are the end products of omega-3 and omega-6 poly unsaturated fatty acid peroxidation and are considered to be a non-invasive method for lipid peroxidation measurement. The increase in their levels in vegans may refer to supplements, discussed previously with fatty acid, or because of the nature of their food.

In normal liver function, the saturated hydrocarbons are metabolized to alcohol by hepatic enzymes (cytochrome P450), but in the case of bad liver function, there will be incomplete metabolism that causes an increase of hydrocarbons in blood and also in exhaled breath.

Concerning to cytochrome P450 2E1 activity, benzene ($m/z=79$) is metabolized in human liver microsomes to a variety of hydroxylated and ring-opened products then it is transported to the bone marrow for other subsequent secondary metabolism.

In case of liver dysfunction, benzene ($m/z=79$) is not metabolized correctly, this will increase its concentration in the body and breath.

Toluene ($m/z=93$) is metabolized by cDNA-expressed human cytochrome P450s (CYPs) to benzyl alcohol and slightly to o- and p- cresol in the liver microsomes. In case of liver disease, there is an increase in the level of toluene in the body and in the breath due to incomplete metabolism and it is considered to be a biomarker of liver disease.

Skatole ($m/z=132$) or 3-methylindole is metabolized in the liver by specific human cytochrome P450 enzymes.

Indole and skatole are by-products of the metabolic break down of tryptophan in the digestive tract but can also be produced by bacteria in the mouth.

Limonene ($m/z=137$) compound is metabolized by cytochrome P450 (CYP) enzymes to carveol metabolites or perillyl alcohols metabolites in the liver. In the case of liver function impairment, the biotransformation of the limonene will decrease and will accumulate in the original form leading to increase its concentration in the body and in the exhaled breath.

5.8.1.6. Aldehyde and Ketone Compounds

They are organic compounds that have a carbonyl functional group ($C=O$). In this group, the carbon atom has two remaining bonds, which are occupied by substituents. The compound is an aldehyde when at least one substituent is hydrogen and it is a ketone if neither is hydrogen. Aldehydes and ketones are illustrated in Figure 5.51.

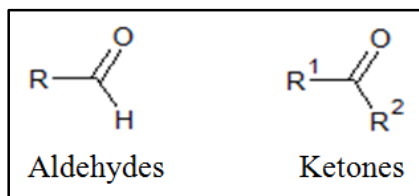


Figure 5.51: The chemical structure of aldehyde and ketone organic compounds.

Aldehyde compounds are acetaldehyde ($m/z=45$), furan-2-carboxaldehyde ($m/z=97$), 4-methylbenzaldehyde ($m/z=121$) and 4-Hydroxynonanal ($m/z=157$).

Ketone compounds are acetone ($m/z=59$), butanone ($m/z=73$), 2-pentanone ($m/z=87$) and methyl isobutyl ketone ($m/z=101$).

Figure 5.52 shows two types of comparisons for two compounds, $m/z = 59$ and 73 : (**on the left**), the counts of these compounds are high in patients group and (**on the right**), they show a decrease in their counts according to LiMAX-test value.

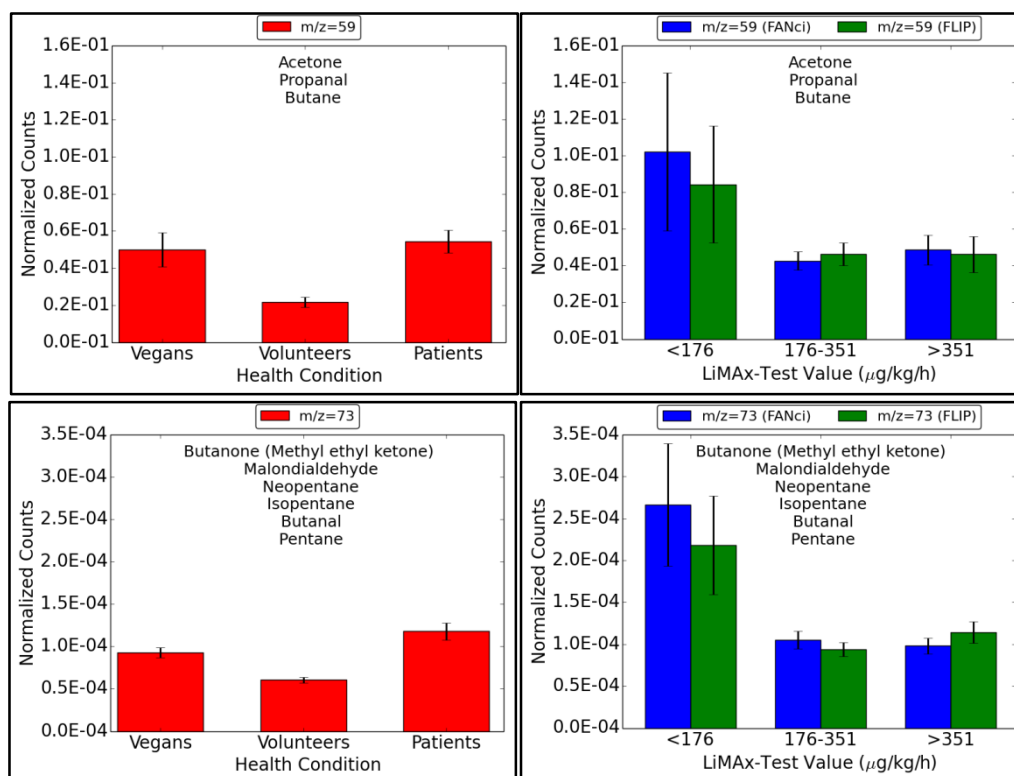


Figure 5.52: The 1st group of aldehyde and ketone organic compounds.

The VOC at (59 Th) is acetone and other compounds and at (73 Th) we found butanone and other compounds. They are **not good biomarkers** for liver diseases, because in the first comparison they have similar strong signals for vegans than for patients with liver diseases especially for acetone and in the second comparison their values do not show good correlation with LiMAX-test value. This finding do not agree with *Velde et al.* [86] finding, they identified acetone as a biomarker for liver diseases with increasing signals for patients comparing to healthy persons.

Figure 5.53 shows two types of comparisons for compound, $m/z = 101$: (**on the left**), the counts of this compound is high in patients group and (**on the right**), its counts does not show any relation with LiMAX-test value.

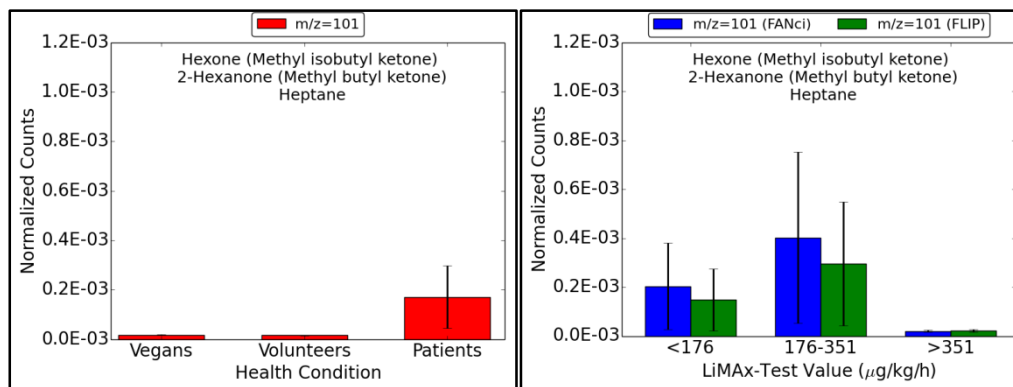


Figure 5.53: The 2nd group of aldehyde and ketone organic compounds.

The VOC at (101 Tn) is defined as methyl isobutyl ketone and other compounds, which is **not a good biomarker** for liver diseases, because its value does not show a good correlation with LiMAX-test value in the second comparison even it shows the highest value in patients compared to volunteers and vegans in the first comparison.

Figure 5.54 shows two types of comparisons for three compounds, $m/z = 45, 87$ and 97 : (**on the left**), the counts of these compounds are high in vegans group and (**on the right**), they show a decrease in their counts according to LiMAX-test value.

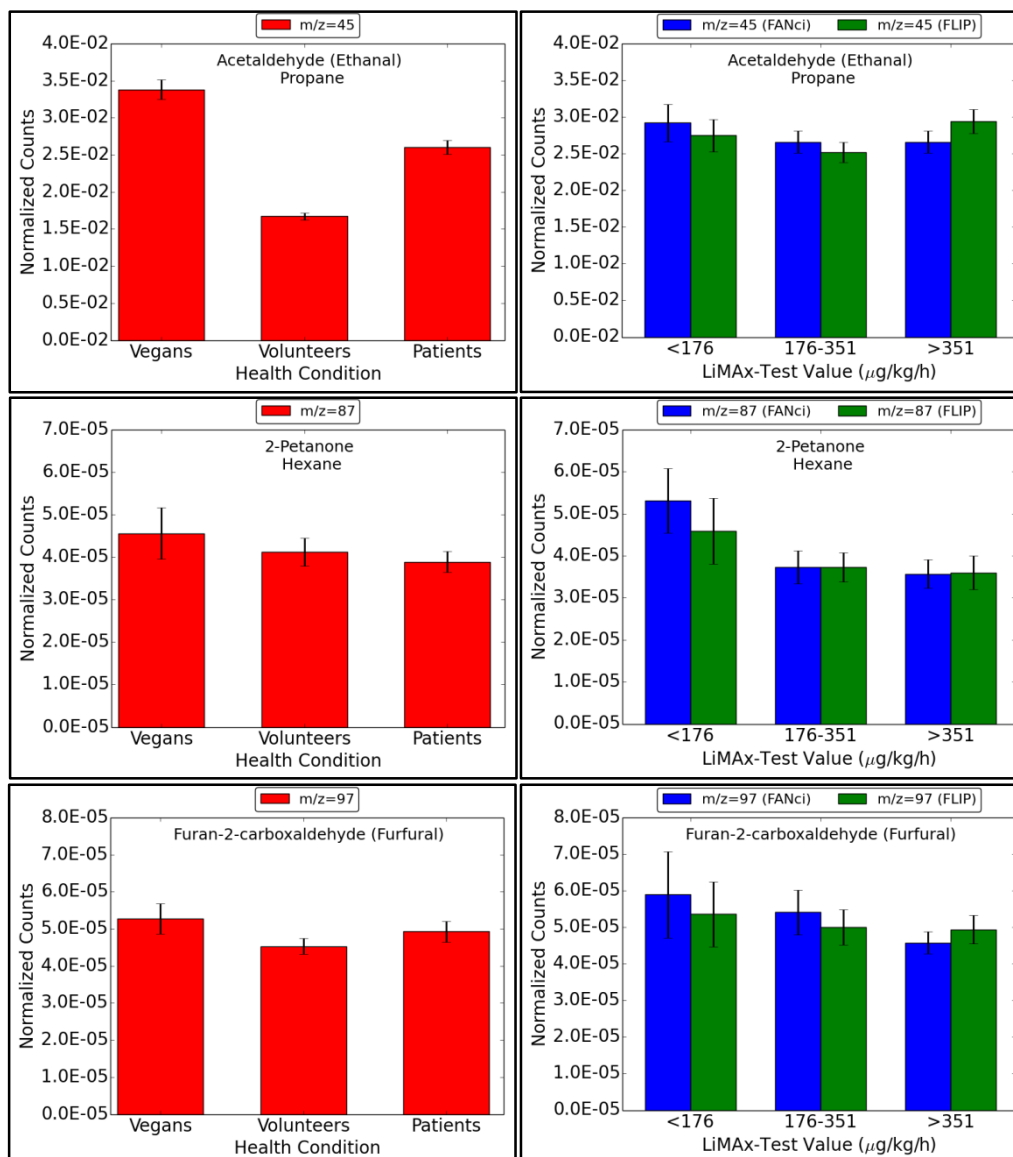


Figure 5.54: The 3rd group of aldehyde and ketone organic compounds.

The VOC at (45 Th) is known as acetaldehyde and other compound, at (87 Th) is defined as 2-pentanone and other compound and at (m/z=97) is furan-2-carboxaldehyde. All of them are **not good biomarkers** for liver diseases, because they have the highest value in vegans. The finding with 2-pentanone is in contrast with *Velde et al.* [86] finding, because in their study they found that 2-pentanone in patients breath is higher than in healthy breath.

Figure 5.55 shows two types of comparisons for two compounds, m/z = 121 and 157: (**on the left**), the counts of these compounds are high in volunteers group and (**on the right**), they show different relations with LiMAX-test value.

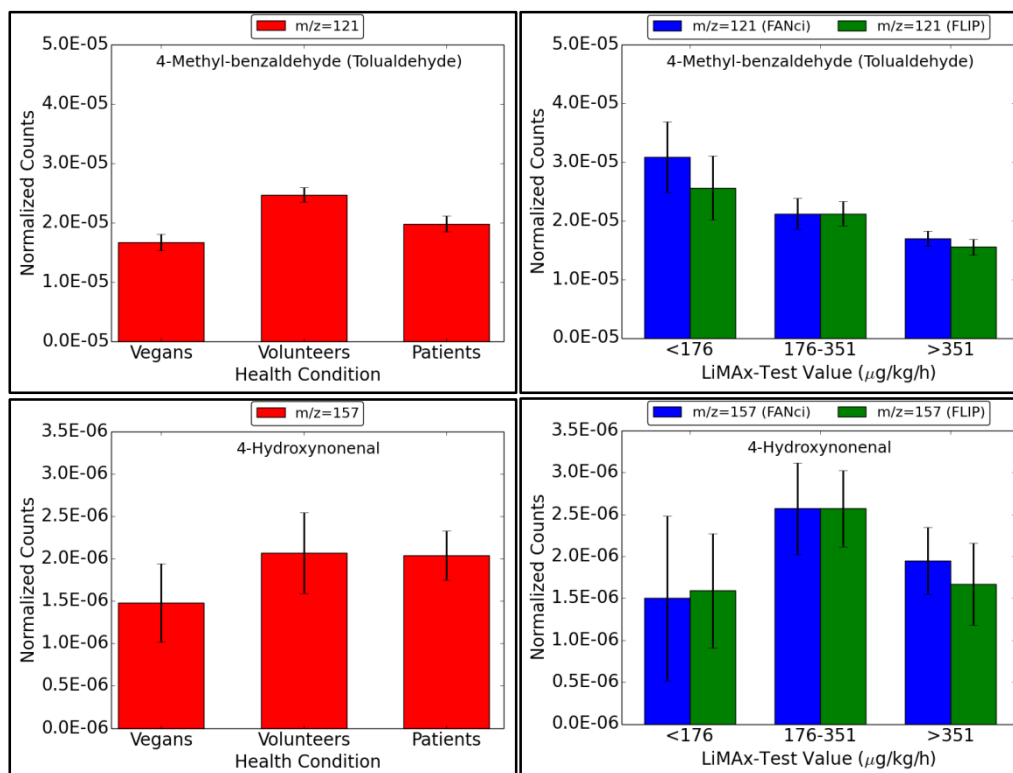


Figure 5.55: The 4th group of aldehyde and ketone organic compounds.

The VOC at (121 Th) is 4-methylbenzaldehyde and at (157 Th) we found 4-hydroxynonenal. These VOCs are **not good biomarkers** for liver diseases, because they have the highest value in volunteers.

Hepatic insulin resistance is a common complication of the cirrhotic patient. Due to hepatic insulin resistance there will be an increase in the triglycerides, free fatty acids and ketones (acetone and 2-butanone) formed during lipolysis. A previous research on rats showed that acetone (m/z=59) and butanone (m/z=73) are increased in breath due to CYP2E1 inhibition [102].

In human liver, only NAD-dependent aldehyde dehydrogenase located in the liver mitochondrial matrix space catalyses the oxidation of acetaldehyde (m/z=45). The deficiency in the liver function will lead to impairment in the acetaldehyde oxidation then increasing its concentration in the body and exhaled breath.

There is an increase in the level of acetaldehyde in vegans group compared to others; this may be due to the types of their food (many fruits and vegetables contain acetaldehyde) and/or because they are not fasted for 6-12 hrs. It was confirmed that all fresh and processed (single-strength) juices showed a higher concentration of acetaldehyde than of ethanol and methanol.

5.8.1.7. Alcohol Compounds

They are compounds that have a hydroxyl group (-OH) bound to a carbon atom, as illustrated in Figure 5.56. The center carbon must be saturated and have single bond to other three atoms.

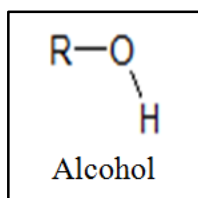


Figure 5.56: The chemical structure of the alcohol compounds.

Methanol ($m/z=33$), isotope of methanol ($m/z=34$, 1.2% of $m/z=33$), ethanol ($m/z=47$), isotope of ethanol ($m/z=48$), water cluster of methanol ($m/z=51$, 0.7% of $m/z=33$), and octanol ($m/z=131$) are examples of alcohol compounds.

Figure 5.57 shows two types of comparisons for two compounds, $m/z = 34$ and 51: (**on the left**), the counts of these compounds are high in patients group and (**on the right**), their counts do not show any relation with LiMAXtest value.

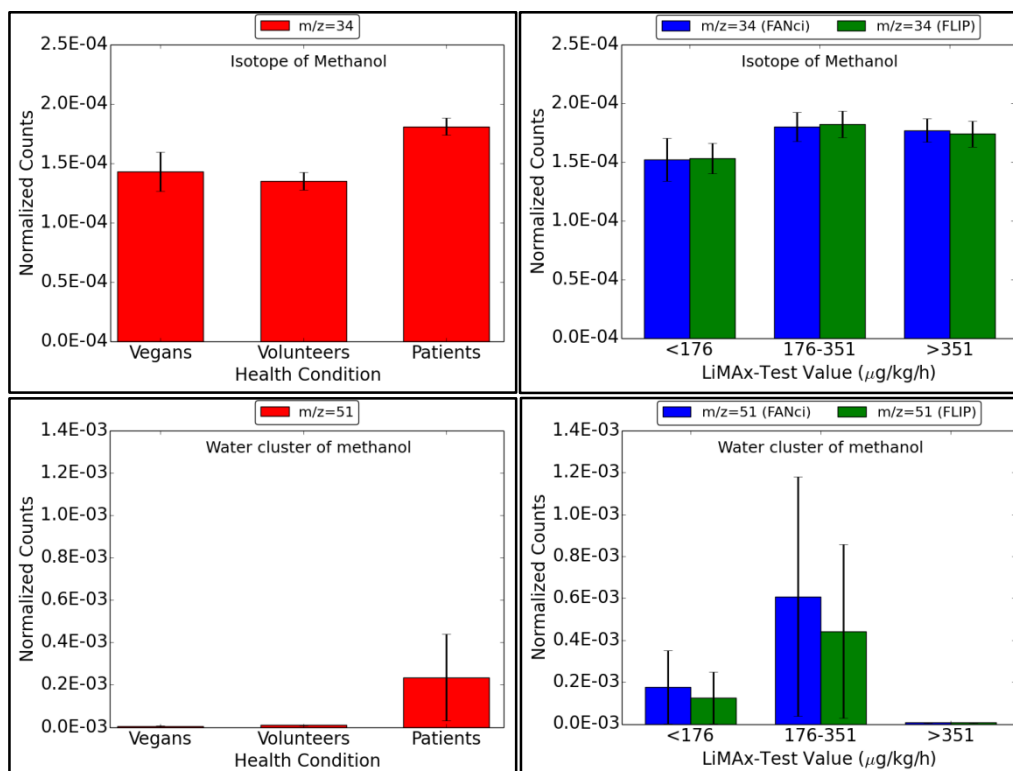


Figure 5.57: The 1st group of alcohol compounds.

This VOC at (34 Th) is known as isotope of methanol (1.2% of $m/z=33$) and at (51 Th) is water cluster of methanol (0.7% of $m/z=33$). They are **not good biomarkers** for liver diseases, because their values do not show a good correlation with LiMAx-test value in the second comparison even they show the highest value in patients compared to volunteers and vegans in the first comparison.

Figure 5.58 shows two types of comparisons for compound, $m/z = 33$: (**on the left**), the counts of this compound is high in vegans group and (**on the right**), its counts is high in bad liver function.

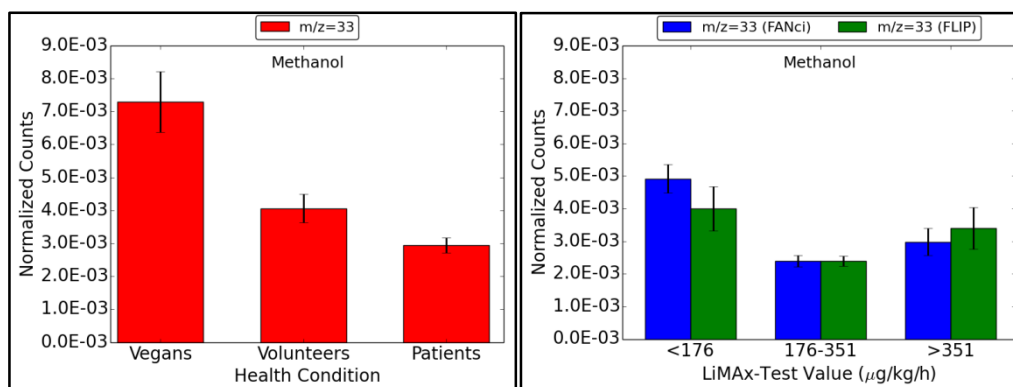


Figure 5.58: The 2nd group of alcohol compounds.

The VOC at (33 Th) is methanol, which is **not a good biomarker** for liver diseases, because it has the highest value in vegans.

Figure 5.59 shows two types of comparisons for three compounds, $m/z = 47$, 48 and 131: (**on the left**), the counts of these compounds are high in volunteers group and (**on the right**), they show different relations with LiMAx-test value.

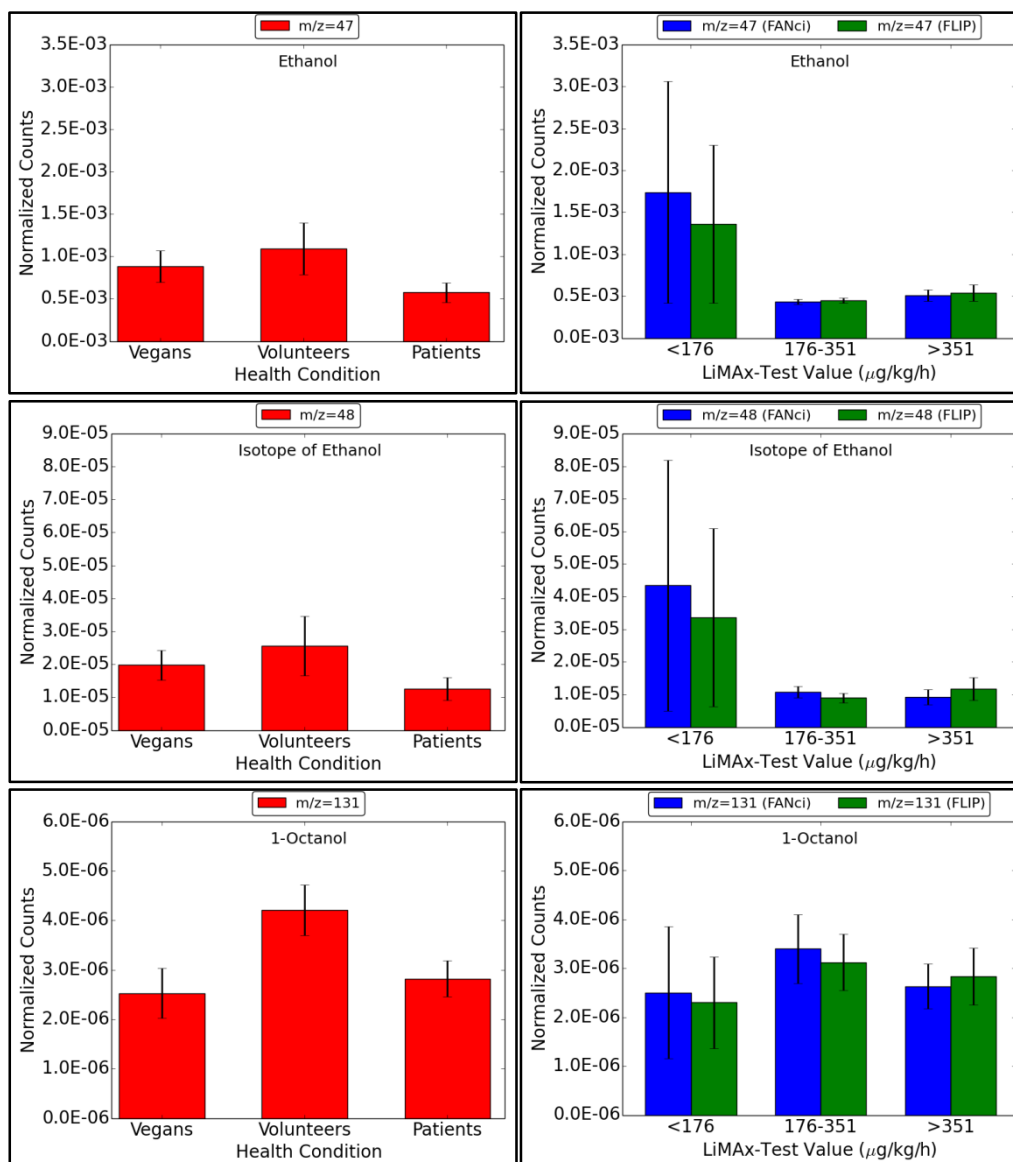


Figure 5.59: The 3rd group of the alcohol compounds.

The VOC at (47 Th) is defined as ethanol, at (48 Th) is isotope of ethanol and at (131 Th) 1-octanol. All of them are **not good biomarkers** for liver diseases, because they have the highest value in volunteers.

Liver is the primary site of methanol (m/z=33) metabolism by a series of oxidative steps. Methanol is oxidized to methanal by alcohol dehydrogenase enzyme then to methanoic acid by aldehyde dehydrogenase enzyme and finally is detoxified to carbon dioxide by folate dependent mechanisms [103]. Any defect or impairment in the liver function will reduce the methanol oxidation leading to an increase in its concentration in the body and in the exhaled breath.

The increased level of methanol in volunteers or vegans may be due to the nature of their food. It is found that methanol occurs naturally in fruits and vegetables like dried beans, split peas, lentils, fresh or canned orange juice and fresh grapefruit juice. This compound is also found when the fruits or vegetables are sliced, chopped, pureed and/or juiced. After eating fruits and/or vegetables, the microorganisms in the digestive tract will break down the pectin, which is a structural heteropolysaccharide contained in the primary cell walls of terrestrial plants [104] and release methanol.

The microsomal ethanol-oxidizing system (MEOS) is the pathway of ethanol ($m/z=47$) metabolism in the liver. MEOS will increase its activity in the case of chronic alcohol consumption that involves CYP2E1, a specific cytochrome P450, and catalyzes the ethanol metabolism and activates some of the hepatotoxic agents.

The level of ethanol in volunteers and vegans may be due to the nature of their food. The ethanol level increases in breath after sugary drinks or even after drinking a cup of sweetened tea before 2 hr. period before the test [94]. It is also found in cereal grains and especially corn, potato, sweet potato, yam, Jerusalem artichoke and cassava (used in Brazil). Sugarcane, sugarbeet, sweet sorghum and fodder beet (mangold) give higher alcohol (Yield/Acre) than the starch crops, but grains have been the main source of alcohol.

5.8.1.8. Terpene and Terpenoid Compounds

Terpene are organic compounds that are the result of isoprene unit combination. While terpenoid are organic compounds that include some oxygen functionality or some rearrangements and they are related to terpenes.

Alpha-pinene ($m/z=137$), beta-pinene ($m/z=137$) and gamma terpinene ($m/z=137$) are examples of terpene and terpenoid compounds.

Figure 5.60 shows two types of comparisons for compound, $m/z = 137$: (**on the left**), the counts of this compound in patients group is equal to volunteers group which is higher than vegans group and (**on the right**), its counts is very high in bad liver function compared to other conditions.

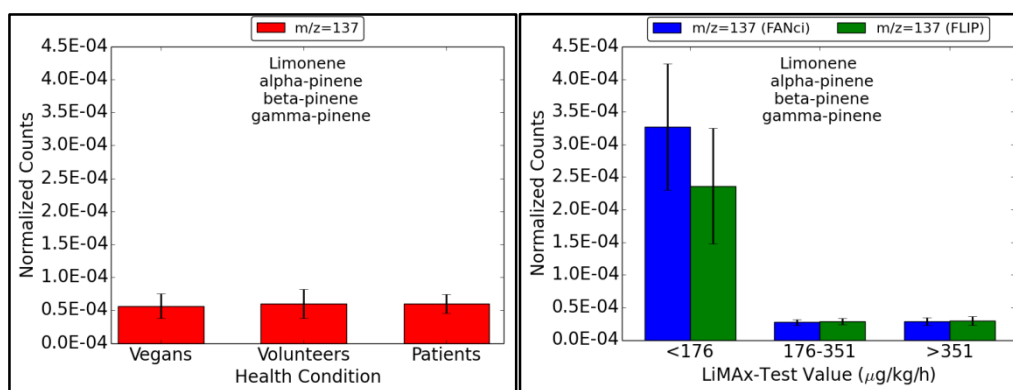


Figure 5.60: The terpene and terpenoid compounds.

The VOC at (137 Th) is pinene and other compound, which is **not a good biomarkers** for liver diseases, because the patients' value same as vegans' value.

Because isoprene ($m/z=69$), which is the most common hydrocarbon in breath and the basic unit of terpenes as mentioned previously, is formed in the mevalonic pathway of cholesterol synthesis, it is suggested that isoprene is metabolized by liver monooxygenase and is converted to mono-epoxides, since its counts decreases in hepatic venous blood. For that, the levels of these compounds increase when there is a liver disease or damage due to incomplete metabolism.

5.8.1.9. Organoselenium Compounds

Organoselenium are organic compounds that have a carbon-selenium chemical bond. Dimethyl selenide ($m/z=110$) is an example of this compound, as illustrated in Figure 5.61.

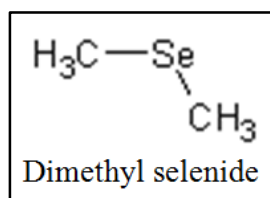


Figure 5.61: The Organoselenium compounds.

Figure 5.62 shows two types of comparisons for compound, $m/z = 110$: (**on the left**), the counts of this compound is high in patients group and (**on the right**), it shows an increase in its counts according to LiMAX-test value.

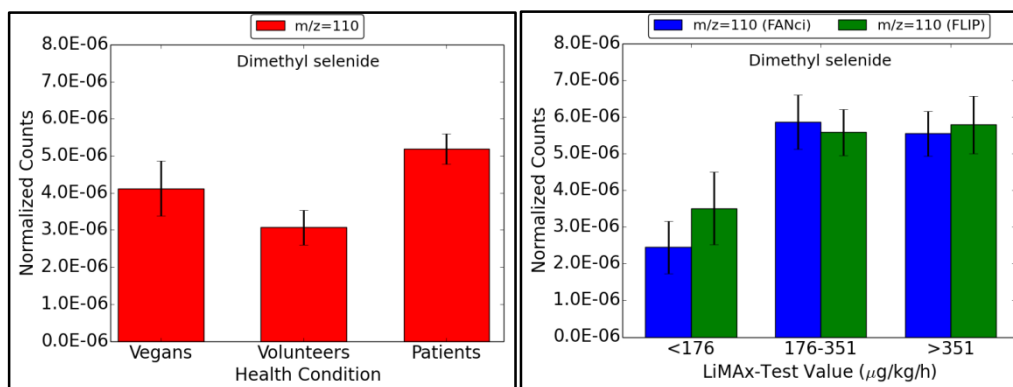


Figure 5.62: The organoselenium compounds.

The VOC at (110 Th) is defined as dimethyl selenide, which is **not a good biomarker** for liver diseases, because its value increases when the liver condition improves in the second comparison even it shows the highest value in patients compared to volunteers and vegans in the first comparison. This finding is in contrast to *Velde et al.* [86] finding, according to their study, dimethyl selenide in patients breath is lower than in healthy breath.

Dimethyl selenide ($m/z=110$) is a byproduct of selenium fed as selenite in the liver and exhaled through the lung. Selenium in selenomethionine is not seemed to be converted to dimethyl selenide, it is rapidly incorporated into protein which it is may be responsible for differences in tissue accumulation [105, 106]. Previous study showed that when there is an increase in the intensity of hepatic injury, the level of serum selenium will directly decrease [107], which causes a reduction in dimethyl selenide concentration in the body and in the exhaled breath.

5.8.2. Other VOCs Biomarkers

This study is presented in (Part 3 in Appendices).

Summary and Outlook

In my work, I have studied breath gas analysis (BGA) with absorption spectroscopy and mass spectrometry to investigate the diverse possibilities of these methods to acquire information on the health status of human beings.

Absorption spectroscopy was used to evaluate the additionally exhaled $^{13}\text{CO}_2$ to calculate the LiMAX-value after administration of ^{13}C -methacetin. The LiMAX-test (**L**iver **M**aximal Capacity) is a new methacetin breath test for personalized and quantitative assessment of the liver status. This breath-test allows a precise distinction of the metabolic power of the liver volume that decreases from healthy to liver damage. The precision of this test is high enough to detect reduced function upon cirrhosis, and can directly monitor liver damage and liver failure.

The LiMAX-test is based on administration of ^{13}C -methacetin solution, that is solely metabolized in healthy liver cells to paracetamol and $^{13}\text{CO}_2$. The generated $^{13}\text{CO}_2$ is solved in the blood, transported to the lungs and exhaled. The metabolization can be tracked in real time in the breath by monitoring the relative increase of $^{13}\text{CO}_2$. Fluctuations in the breath are corrected by detecting the $^{13}\text{CO}_2/^{12}\text{CO}_2$ ratio over time, which is called DOB kinetics. The LiMAX-value uses the maximal value of the DOB kinetics to evaluate the liver function capacity. In cooperation with the Charité-Universitätsmedizin (AG Stockmann) a study was performed, where the influence of the dosage and physical activity on the LiMAX-value was investigated.

My analysis of the data showed a nearly linear dependence of the LiMAX-value of (1.8 ± 0.3) on doubling the dosage from 2 mg/kg to 4 mg/kg body weight. Sports changes the DOB kinetics dramatically, because of the additional generation of CO_2 , thereby increasing the $^{13}\text{CO}_2/^{12}\text{CO}_2$ ratio. Resting after sports leads to a recovery of the $^{13}\text{CO}_2/^{12}\text{CO}_2$ ratio by about 80% with a time constant of several ten minutes.

When the ^{13}C -methacetin is administered while doing sports, the DOB kinetics are similar, but exhibits a smaller amplitude. Nevertheless, doubling the dosage result in an increase of the LiMAx-value of (1.8 ± 0.3) .

Comparison of the DOB kinetics with blood level concentrations of methacetin and paracetamol, obtained by HPLC showed that the reproducibility of the maximal DOB value is $R_D=0.78$. For the maximal blood levels we found Pearson correlation coefficients of $R_M=-0.06$ and $R_P=0.83$ for methacetin and paracetamol, respectively. Nevertheless, detection of paracetamol blood levels shows an about 5 times smaller signal compared to methacetin blood levels, and a delayed rise of the blood level of ~ 1 minute. We concluded that paracetamol persists longer in the liver cells, and is, thus, not a suitable parameter to track the metabolization of the liver. Blood levels of methacetin display a strong fast and a slow kinetic component, and strongly fluctuating maximal value. The fast component decays within ~ 3 minutes accompanied by the rise of the DOB kinetics with a 3 minute time constant. This indicates the fast component to reflect the methacetin metabolization to paracetamol and $^{13}\text{CO}_2$. Thus, DOB kinetics allow direct tracking of methacetin metabolization by the liver cells.

Slower time constants in the DOB kinetics reflect redistribution processes of the bicarbonate pool and equilibrium processes and are difficult to connect to liver metabolization processes.

BGA of VOCs can be used to identify unusual metabolites in the blood, e.g. alcohol breath test. The breath contains both volatile and non-volatile substances. In this work, $^{13}\text{CO}_2$ was used successfully to assess the liver function capacity of humans. VOCs are much more numerous but not necessarily unique to a specific process in the human body. Nevertheless, most processes in the human body generate VOCs which can be detected in the breath. On account of the large number of VOCs and their non-unique origin signatures, different mass spectrometry techniques were tested, and a new method to verify the impact on the liver condition was introduced.

Two types of mass spectrometers were used to measure and quantify the VOCs in the breath: The Ion Mobility Spectrometry (IMS) and Proton Transfer Reaction Mass spectrometry (PTR-MS).

The Ion Mobility Spectrometry (IMS) offers the possibility to highly resolve VOCs in the breath by their retention time in a Multi Capillary Column (MCC) as a function of the

drift time in an electric field. The advantage of this method is that molecules of the same molecular formula, but with a different collision cross sections can be distinguished by different drift times. Additionally, chemical properties are reflected by the retention time due to different interactions with the column. First investigations with the IMS were performed successfully. Smokers can be identified by an acetonitrile peak as reported, as well as other influences (see Chapter 6 in Appendences). Since the aim was to study the breath of patients with liver disease, and the device had no certification for the hospital, I tested the influence of Tedlar bags on the IMS measurements. The Tedlar bags were used to collect the breath (~2 liters) of the patients and transport it to the device. I tested, whether the time delay between collecting the breath and performing the measurement has an influence on the signal strength. For this investigation the time delay was varied from some hours to 180 hours. Indeed, I found that the signal strengths for some VOCs decay while others rise.

The IMS measurements were not used for analyzing the breath of patients, because there is no stable or easy way to identify the specific molecules by their drift time and retention time. Furthermore, we observed a change of calibration at different days, resulting in a shift of peak positions. Hence, the reproducibility and precision could not be guaranteed.

Proton Transfer Reaction Mass spectrometry allows for detection of VOCs with high proton affinity. I used a spectrometer with quadrupole mass filter with a resolution of 1 mass over charge (1 Thomson). I performed similar investigations to check, whether the use of Tedlar bags would influence the results. Since nearly all measurements were performed between 10 and 20 hours after breath collection, my results indicate that the use of Tedlar bags has negligible influence on the comparison of relative VOCs concentrations.

Most investigations to identify biomarkers were performed with two collectives, a patient group and a group of healthy persons. Since Attila Hildman performed a pilot study for his Diploma work in our group, using PTR-MS to investigate the influence of vegan nutrition on the exhaled VOCs, I also took breath samples of the vegans for comparison.

I compared the amount of VOCs in the exhaled air for three groups, patients with known liver disease, volunteers and vegans as a reference for super healthy persons. My results clearly show that diet has a major influence on the VOCs in the breath. Acetone for example (Figure 5.52) was identified as a biomarker for liver diseases with increasing signals for patients compared to healthy persons. When I compared the acetone signals I found

similar strong signals for vegans, than for patients with liver disease, clearly demonstrating that such simple comparisons can be misleading.

We introduced the LiMAx-test, and compared the VOCs signals as a function of the liver status. Here, we found that the LiMAx-test reproduces known dependences, for example the increase of Dimethyl sulfide (DMS) in patients with severe liver damage. Nevertheless, the DMS signal is higher in vegans compared to patients (Figure 5.20). Thus, we developed a new definition for good biomarker for liver disease: The VOCs signals have to be significantly higher than for volunteers and persons with special diet, and the VOCs signal has to increase with decreasing LiMAx-value.

This new definition should allow for reliable identification of good biomarkers for liver disease such as n-Butylamine (Figure 5.28). Nevertheless, the mass resolution of the used PTR-MS is not good enough to assign the VOCs unequivocally. Therefore, measurements should be repeated for the identified VOCs with mass spectrometer of a higher resolution. This should result in identification of new biomarkers for liver diseases.

List of Publications

- Article: S. Adel, T. Rubin, P. Taheri, M. Stockmann, J. F. Lock and K. Heyne, 'Fast liver metabolization: Influence of Dosage and Sports on the LiMAx-Test for Liver Function Capacity Assessment', submitted to the Journal of Breath Research (2015).
- Workshop: S.A. Al-Ani, T. von Haimberger, A. Hildmann, A. Heyne, M. Stockmann and K. Heyne, 'Identifizierung und Ausschluss von möglichen Markersubstanzen für Leberkrankheiten und Leberschäden', Beitrag: 6. Symposium "Metaboliten in der Prozessabluft und Ausatemluft" am 22. und 23.9.2015 am LFZ PA&T der Hochschule Reutlingen.

Appendices

Part 1: Tables

Table 1: The data information that belong to Vegans according to PTR-MS measurement.

Name	Date of Birth	Sex	Height (cm)	Weight (kg)	Smoking	Date of Collecting the Tedlar Bag	Time of Collecting the Tedlar Bag	Nr. of the Bag
V-001	04.06.1992	f	162	59	0	31.08.2013	09:30	1
V-002	05.12.1959	f	170	82,7	0	31.08.2013	09:33	2
V-003	13.03.1962	f	173	88,5	0	31.08.2013	10:10	3
V-004	28.01.1942	f	163	74,8	0	31.08.2013	10:52	4
V-005		f	166	72	0	31.08.2013	10:59	5
V-006		m	187	91	0	31.08.2013	11:00	6
V-007	10.05.1964	f	164	108	0	31.08.2013	11:24	7
V-008	03.02.1964	f	175	68	0	31.08.2013	12:54	8
V-009	02.09.1960	f	167	81	0	31.08.2013	12:56	9
V-010	10.05.1974	f	172	120	0	31.08.2013	13:35	11
V-011	13.08.1969	f	164	72,8	0	31.08.2013	13:38	12
V-012	02.05.1969	f	166	56,6	0	31.08.2013	13:12	10
V-013		f				31.08.2013	13:41	13
V-014	08.07.1977	f	168	58,5	0	31.08.2013	13:56	14
V-015	30.01.1958	m	178	93,5	0	31.08.2013	14:22	15
V-016	29.10.1952	f	173	86,5	0	31.08.2013	15:02	16
V-017	17.06.1988	f	162	77	0	31.08.2013	15:58	17
V-018	07.05.1970	f	164	65,7	0	31.08.2013	16:18	18
V-019	07.02.1980	f	164	73,5	0	01.09.2013	10:14	19
V-020	22.12.1968	f	164	83	0	01.09.2013	10:37	20
V-021	07.12.1964	f	172	82	0	01.09.2013	10:52	1
V-022		f	173	80	0	01.09.2013	11:07	2
V-023	10.04.1966	f	170	93	0	01.09.2013	11:16	3
V-024	03.08.1983	f	169	91	0	01.09.2013	11:47	4
V-025	02.03.1963	f	176	71	0	01.09.2013	12:02	5
V-026	19.09.1964	m	183	95	0	01.09.2013	12:31	6
V-027	30.10.1965	m	202	113	0	01.09.2013	12:57	7
V-028		f	168	57	0	01.09.2013	12:58	8
V-029	04.08.1966	f	175	90	1	01.09.2013	13:25	9
V-030	21.11.1979	f	169	84,8	0	01.09.2013	14:17	10
V-031	19.03.1970	f	180	140	0	01.09.2013	14:20	11
V-032		f	168	62	0	01.09.2013	14:35	12
V-033		f	168	75	0	01.09.2013	14:55	13

Table 2: The data information that belong to Volunteers according to PTR-MS measurement.

Name	Date of Birth	Sex	Height (cm)	Weight (kg)	Smoking	Alcohol	Date of Collecting the Tedlar Bag	Time of Collecting the 1 st Tedlar Bag	Nr. of the Bag	Time of Collecting the 2 nd Tedlar Bag	Nr. of the Bag
H-001	17.06.1982	m	180	90	0	0	22.07.2013	09:12	1	09:17	2
H-002	10.05.1987	m	177	78	0	0	22.07.2013	09:14	3	09:19	4
H-003	24.07.1990	f	168	54	0	0	23.07.2013	09:27	5	09:30	6
H-004	31.03.1964	f	155	75	0	0	23.07.2013	09:40	7	09:43	8
H-005	01.01.1983	f	163	66	0	0	23.07.2013	09:44	9	09:46	10
H-006	18.08.1981	f	152	58	0	0	23.07.2013	09:49	11	09:52	12
H-007	04.09.1990	m	179	75	0	0	23.07.2013	10:01	13	10:05	14
H-008	17.02.1987	m	183	90	0	1	24.07.2013	10:19	15	10:23	16
H-009	13.03.1991	m	185	80	0	1	24.07.2013	10:40	17	10:43	18
H-010	15.11.1991	f	160	60	1	1	24.07.2013	10:44	19	10:46	20
H-011	01.09.1992	m	173	67	1	0	28.07.2013	10:33	20	10:36	19
H-012	08.10.1982	m	172	90	0	0	28.07.2013	11:21	18	11:25	17
H-013	05.04.1982	m	176	57	0	0	28.07.2013	11:33	16	11:37	15
H-014	04.07.1981	m	179	83	0	0	28.07.2013	11:41	14	11:45	13
H-015	14.01.1979	m	162	82	0	0	28.07.2013	13:10	12	11:13	11
H-016	20.08.1982	f	153	56	0	0	28.07.2013	13:25	10	13:29	9
H-017	13.09.1986	f	167	55	0	0	29.07.2013	08:47	8	08:52	7
H-018	24.08.1992	f	181	63	0	1	29.07.2013	09:35	6	09:38	5
H-019	21.06.1990	f	169	63	1	1	29.07.2013	09:40	4	09:43	3
H-020	17.02.1978	f	158	58	0	0	29.07.2013	10:47	2	10:59	1

Table 3: The data information that belong to patients with liver diseases according to PTR-MS measurement.

Name	Date of Birth	Sex	Height (cm)	Weight (kg)	Time of ¹³ C-methacetin injection	Time of ICG Injection	Date of Tedlar Bag Collecting	Time of Collecting the 1 st Tedlar Bag	Nr. of the Bag	Time of Collecting the 2 nd Tedlar Bag	Nr. of the Bag
P-001	16.02.1956	m	173	75	15:42	-	06.08.2013	15:20	25	16:39	26
P-002	03.01.1938	m	181	103	17:29	-	06.08.2013	17:02	27	18:32	28
P-003	27.03.1956	m	175	82	12:42	12:59	07.08.2013	12:03	29	13:21	30
P-004	23.11.1942	f	163	73	14:24	-	07.08.2013	13:37	31	15:29	32
P-005	21.02.1940	m	190	106	16:47	-	07.08.2013	16:25	33	17:23	34
P-006	01.07.1941	m	180	107	14:17	14:48	08.08.2013	13:52	35	14:57	36
P-007	29.04.1945	m	178	72,5	16:56	-	09.08.2013	16:33	37	18:02	38
P-008	25.06.1935	m	161	87,5	18:50	-	09.08.2013	18:27	39	19:18	40
P-009	12.12.1958	m	176	67	20:14	-	09.08.2013	19:51	21	20:55	22
P-010	15.09.1960	f	165	63	15:21	-	12.08.2013	14:37	23	16:13	24
P-011	26.12.1953	m	182	76,5	12:51	13:10	13.08.2013	12:30	25	13:21	26
P-012	11.12.1970	m	170	70	14:05	14:53	13.08.2013	13:41	27	15:07	28
P-013	15.09.1953	m	182	78,5	16:38	-	13.08.2013	16:15	29	17:39	30
P-014	27.03.1956	m	175	85	13:02	13:15	14.08.2013	12:40	31	13:31	32
P-015	20.10.1945	m	173	99	10:41	11:05	15.08.2013	10:02	33	11:20	34
P-016	01.07.1941	m	180	107	12:55	13:00	15.08.2013	11:53	35	13:22	36
P-017	23.11.1942	f	163	67,8	16:41	-	15.08.2013	15:59	37	17:41	38
P-018	06.10.1976	m	180	97,5	16:33	-	16.08.2013	16:00	39	17:13	40
P-019	08.02.1940	m	165	84,5	18:18	-	16.08.2013	17:54	21	19:00	23
P-020	08.04.1941	m	180	103	16:08	-	21.08.2013	15:45	24	17:07	22
P-021	12.03.1949	f	164	65,5	17:58	-	21.08.2013	17:34	25	18:50	26
P-022	01.09.1941	f	168	79	19:34	-	21.08.2013	19:11	27	20:24	28
P-023	01.07.1941	m	180	107	13:17	13:36	22.08.2013	12:39	29	13:53	30
P-024	12.12.1947	m	175	106	14:39	-	22.08.2013	14:13	31	15:12	32
P-025	15.09.1953	m	182	72	16:40	-	22.08.2013	15:46	33	17:07	34
P-026	28.01.1969	m	174	64	17:56	-	22.08.2013	17:32	35	18:17	36
P-027	04.01.1986	m	180	63	15:03	-	23.08.2013	14:37	37	15:50	38
P-028	03.03.1990	f	172	56	17:00	-	23.08.2013	16:38	39	17:52	40
P-029	05.01.1945	f	170	54	10:35	10:52	26.08.2013	10:12	21	10:55	22
P-030	24.05.1972	f	165	82	12:52	-	26.08.2013	12:06	23	13:34	24
P-031	02.05.1940	f	158	66	14:23	-	26.08.2013	13:47	25	15:15	26
P-032	14.09.1933	m	178	80,5	16:18	-	26.08.2013	15:52	27	16:56	28
P-033	02.01.1960	m	183	79	08:59	09:25	27.08.2013	08:25	29	09:18	30
P-034	26.12.1953	m	182	77	13:27	13:42	27.08.2013	12:54	31	13:54	32
P-035	07.07.1946	f	169	64	15:31	16:07	27.08.2013	15:09	33	16:20	34

P-036	28.02.1946	f	170	92	18:06	-	28.08.2013	17:39	35	18:45	36
P-037	06.09.1959	m	182	114	16:06	-	29.08.2013	15:44	37	17:10	38
P-038	20.09.1944	f	165	65,5	08:58	-	02.09.2013	08:17	39	10:05	40
P-039	01.07.1941	m	180	112	14:36	14:39	02.09.2013	13:32	21	15:10	22
P-040	18.10.1982	f	169	71,2	17:36	-	02.09.2013	16:58	23	18:15	24
P-041	13.06.1948	m	176	74	09:11	-	03.09.2013	08:15	25	09:58	26
P-042	01.01.1961	f	158	99	10:54	-	03.09.2013	10:17	27	11:25	28
P-043	07.08.1955	f	168	69	12:09	-	03.09.2013	11:46	29	13:14	30
P-044	13.08.1940	f	159	79	08:27	-	05.09.2013	08:25	31	08:56	32
P-045	14.05.1951	m	170	75,5	11:34	-	05.09.2013	11:13	33	12:37	34
P-046	17.09.1945	f	156	59	13:05	-	05.09.2013	12:44	35	13:37	36
P-047	20.03.1936	f	156	77	14:21	-	05.09.2013	13:50	37	14:53	38
P-048	31.08.1956	f	170	70	12:07	-	06.09.2013	11:44	39	12:41	40
P-049	19.07.1955	f	160	82	18:31	-	10.09.2013	17:55	21	19:28	22
P-050	01.12.1942	f	156	75	08:07	-	11.09.2013	07:30	23	08:38	24
P-051	03.05.1961	m	176	65	08:27	-	12.09.2013	07:51	25	08:48	26
P-052	25.08.1934	m	172	70	11:50	-	12.09.2013	11:25	27	12:21	28
P-053	15.09.1953	m	183	75	14:31	-	12.09.2013	14:08	31	15:33	32
P-054	13.11.1967	w	169	64	08:20	-	13.09.2013	07:43	35	08:48	36
P-055	02.01.1950	m	187	95	12:55	-	13.09.2013	12:27	37	13:59	38
P-056	19.08.1955	w	163	74	09:10	-	16.09.2013	08:21	39	09:47	40
P-057	15.03.1957	m	169	68	10:38	-	16.09.2013	10:13	29	11:16	30
P-058	14.05.1951	m	170	71	13:01	-	16.09.2013	12:37	21	14:05	22
P-059	08.09.1952	f	163	68,6	15:13	-	16.09.2013	14:46	23	16:16	24

Table 4: The DOB and LiMAx values according to the type of liver disease for FANci and FLIP.

Name	DOB Value		LiMAx Value		Diagnosis
	FANci	FLIP	FANci	FLIP	
P-001	24.33	15.1	347	215	chronic function deterioration of liver transplantation
P-002	20.16	27.2	253	341	HCC recurrence: z.n. atypical liver resection
P-003	27.9	24.8	383	341	colorectal liver metastases
P-004	10.17	2.6	143	37	medicines tox. acute liver failure
P-005	28.78	27	363	340	v.a. liver metastases recurrence
P-006	30.31	28.6	372	351	colorectal liver metastases, DM insulin (14 PED)
P-007	16.52	11.2	242	164	CCC, cholangiocellular cancer
P-008	38.69	36.8	499	474	CCC, cholangiocellular cancer
P-009	32.02	29.6	484	446	primary sclerosing cholangitis
P-010	25.65	19.8	389	300	Hypothyroidism
P-011	33.79	3.8	487	55	klatskin tumor
P-012	7.02	-	103	-	liver cirrhosis
P-013	14.79	-	211	-	z.n. liver resection for colorectal liver metastases
P-014	24.94	22.5	337	304	colorectal liver metastases (1mal/Woche)
P-015	19.36	23	243	288	colorectal liver metastases
P-016	34.6	32.4	425	398	colorectal liver metastases (21 PED)
P-017	8.22	-	120	-	subakules liver failure
P-018	24.76	26.8	318	344	Pot. liver liver donation
P-019	18.77	19.6	248	259	3T/OP liver metastases resection hemicolectomy
P-020	16.42	10.6	205	133	HCC segment 6 in cirrhosis
P-021	20.87	21.8	310	324	v.a. GB cholestatic liver infiltration
P-022	20.54	20.4	283	281	a.d. Advanced hemihep. Re. In v.a. GG - Ca space requirement
P-023	41.31	40.8	508	501	colorectal liver metastases (Thomas: 1time/week) pre-op
P-024	34.36	32.4	419	395	z.n. trisectomy large CCC
P-025	26.32	23.3	390	345	liver resection
P-026	31.53	29.4	485	452	CCC hep. Recurrence
P-027	21.26	19.6	334	308	PSC LTX-Evaluation
P-028	17.45	14.7	284	239	CF liver cirrhosis
P-029	22.67	22.1	373	364	Colon Ca. Chemether. (FOLFOX)
P-030	21.29	17.6	286	236	adenoma in fatty liver
P-031	25.44	17.4	371	254	CCC
P-032	27.25	23.3	380	325	NET Tumor
P-033	26.22	26.6	373	378	FOLFOX
P-034	28.15	27.4	404	394	klatskin tumor

P-035	29.72	21.5	452	327	FOLFOX
P-036	23.52	26	303	322	HCC re LL
P-037	6.93	2.3	83	28	tox. Hep. mit ALV und HRS
P-038	18.52	26.2	367	390	HCC
P-039	10.1	9.3	121	112	10 POD (PVE) colorectal
P-040	25.26	24	365	347	Hydatid disease, Hashimoto's thyroiditis
P-041	22.48	19.1	325	276	Hep. Metastatic adenocarcinoma. (colon-rectum Approx)
P-042	37.68	38.2	456	462	v.a. G.B. ca.
P-043	6.23	3.3	91	48	LTX-evaluation in HCV cirrhosis
P-044	30.48	34.9	410	449	klatskin tumor
P-045	2.94	5.3	42	74	CASH, cardia-ca (Abdom-Thoracic, Osophag-res)
P-046	25.91	23.4	396	351	LTX-evaluation bei PBC
P-047	20.56	19.4	279	250	z.n. Ext. hemi-hep
P-048	33.97	33.6	496	487	HCC
P-049	17.25	14.1	229	187	HCV, HCC seg. IV
P-050	29.89	31.8	409	435	hydatid liver cyst
P-051	36.2	37.6	555	576	CCC bei PSC
P-052	30.15	28.6	443	420	CCC re.
P-053	19.16	17.1	279	249	subtot liver-res.
P-054	33.82	36.6	514	556	pot. LDLT donor f. adults
P-055	14.88	13.9	196	183	z.n. LTX klatskin TM
P-056	19.47	18.5	273	259	NET functionally, Hedinger syndrome (liver Met.)
P-057	16.91	14.8	250	219	chron., hep. B, liver cirrhosis, HCC suspicion
P-058	4.32	4.1	63	59	cardia-Ca, CASH
P-059	5.2	4	75	57	acute liver failure in AIH, LTX Evaluation

Table 5: The data information that belong to volunteers according to IMS measurement.

Name	Date of Birth	Sex	Height (cm)	Weight (kg)	Smoking	Alcohol	Date of Collecting the Tedlar Bag	Time of 1 st Direct Breathing	Time of the Tedlar Bag Filling	Nr. of the Bag	Time of the Tedlar Bag Measurement	Time of 2 nd Direct Breathing
H-001	17.02.1978	F	158	60	0	0	11.11.2013	11:21	11:36	1	11:37	11:51
H-002	05.05.1974	F	174	75	0	0	11.11.2013	13:10	13:23	2	13:25	13:39
H-003	17.02.1978	F	158	60	0	0	11.11.2013	14:08	14:21	3	14:23	14:36
H-004	09.10.1981	M	186	71	0	1	11.11.2013	14:53	15:07	4	15:08	15:24
H-005	17.02.1978	F	158	60	0	0	11.11.2013	15:39	15:53	5	16:09	16:23
H-006	17.10.1988	M	189	75	0	1	11.11.2013	16:38	16:52	6	16:54	17:10
H-007	17.02.1978	F	158	60	0	0	11.11.2013	17:26	17:39	7	17:40	17:55
H-008	25.12.1990	M	193	84	1	1	11.11.2013	18:34	18:48	8	18:53	19:11
H-009	17.02.1978	F	158	60	0	0	11.11.2013	19:30	19:41	9	19:44	20:00
H-010	20.03.1984	M	190	75	0	1	11.11.2013	20:41	20:54	10	20:57	21:14

Table 6: Tentative assignments of some compounds at each protonated mass (m/z).

(*): the m/z ratios with a deviation of less than 30%.

m/z	Name	References	Solubility	Stability	Property of Occurrence
1*					
2*					
3					
4*					
5					
6					
7					
8					
9*					
10*					
11*					
12*					
13					
14*					
15	Methyl group (CH ₃)	139			High
16					
17					
18	Ammonia (NH ₃) produced in the ion source	140	highly soluble in water 47% w/w (0°C) 31% w/w (25°C) 18% w/w (50°C)	stable for 3 hours at 2-4°C or 24 hours at -20°C	High
19*	Water (Hydronium/primary) ion (H ₃ . ¹⁶ O ⁺)	3			High
	H ₃ O	141			High
20*	Isotope of water (H ₃ ¹⁷ O ⁺)	3			High
	H ₃ O	141			High
21	Isotope of water (H ₃ ¹⁸ O ⁺)	3			High
	H ₃ O	141			High
22*					
23*	Isotope of water (D ₃ O ⁺)				High
24*					
25*					
26					
27*	Acetylene	3	slightly soluble in water	It is unstable in pure form and thus is usually handled as a solution	Low
	Cyanide		in water complete	it is very reactive,	High

			at 25°C, 6.9 g/100 mL at 20°C, in other solvents completely miscible in almost all organic solvents, Most organic solvents (mixtures are unstable)	forming simple salts	
28	Hydrogen cyanide	142	hydrogen cyanide ionize in blood and are very water soluble	hydrogen cyanide is a stable compound, but it polymerizes readily in the presence of basic substances	High
29*	N ₂ H ⁺ most likely produced in collision chamber. Decreases slightly for breath gas due to more water in drift tube. N ₂ H ⁺ + H ₂ O → H ₃ O ⁺ + N ₂	143			Low
	Ethanol fragment. Loss of water molecule from ethanol in the drift tube.	144			Low
	Ethene (Ethylene)		low solubility in blood	ethyne so much less stable than ethene or ethane	High
30	NO ⁺ most likely ionized via backward intake into the intermediate ion source region. It can react as a precursor ion.	143			Low
31	NO ⁺ isotope from m/z=30 is 0.4%.	3			Low
	Formaldehyde CH ₂ NH ₂	142	formaldehyde is readily soluble in water at room temperature	formaldehyde solutions are most stable between pH values of about 2 and about 4	High
	Methylene, 1-amino-, CH ₂ NH ₂	3	solubility in water (reacts)		Low
	Ethane		solubility in water is 56.8 mg L ⁻¹ , in human and rat blood it is solubility is greater than in water	the relative stability of ethane conformations as a result of single bond rotation	High
32*	O ₂ ⁺ is produced by backflow of air into the intermediate ion source region. It can ionize VOCs e.g. R + O ₂ → R ⁺ + O ₂	143			Low

	Formaldehyde	141	very soluble in water; soluble in ethanol, ether, and acetone, solubility in water is 400 g dm^{-3}	formaldehyde solutions are most stable between pH of about 2 and about 4	Low
	Methylamine		solubility in water is 1.08 kg L^{-1} (at $20 \text{ }^\circ\text{C}$), 1 g in about 1.3 mL water or about 90 mL alcohol	stable at room temperature in closed containers under normal storage and handling conditions	High
33	Methanol (main fragment)	142	solubility in H_2O at 23°C is infinite	methanol is the most stable of the alcohols	High
34	Methanol (isotope of main fragment, 1.2% of m/z 33)	142			High
35	Hydrogen sulfide	142	solubility in water is 4 g dm^{-3} (at $20 \text{ }^\circ\text{C}$), it is also soluble in alcohol, ether, glycerol, gasoline, kerosene, crude oil, and carbon disulfide	unstable toward oxygen and consequently but in water it is stable under anoxic and metal free conditions	High
	$\text{NH}_3\text{-NH}_4^+$, Ammonia Cluster	3			Low
	Hydrogen peroxide	3	solubility in water is miscible, hydrogen peroxide a high degradation capacity is present in the blood and tissues	under normal conditions hydrogen peroxide is extremely stable when properly stored	Low
36*	$\text{NH}_3\text{-H}_3\text{O}^+$	140			Low
37	Water cluster	142			High
	Water dimer $(\text{H}_2\text{O})_2\text{H}^+$	120			High
38*	Isotope of water m/z = 37, 0.2%	3			High
39*	Isotope of Isoprene (22.6% of m/z 69)	142			High
40					
41*	Propadiene	145	insoluble in water	uninhibited material may decompose violently at increased temperature and/or pressure	Low
	Propanol	146	solubility in water is miscible	propanol did show some decay,	Low

				especially at the higher temperatures and lower pH's	
	1-Propanol (37.1% of m/z 43)	142			Low
	2-Propanol (34.7% of m/z 43)	142			Low
	Isotope of Isoprene (88.7% of m/z 69)	142			High
42*	Acetonitrile	142	miscible with water, methanol, methyl acetate, acetone, ether, chloroform, and carbon tetrachloride	stable and decompose on heating	High
43	Propene (Propylene)	147	solubility in water is 0.61 g/m ³	propene can protonate to give two different carbocations, one 2° and the other 1°	High
	Esters of Acetic acid	146			Low
	Fragments of oxy-VOCs	145			Low
	Cyclopropane	145	low solubility in the blood but it is greater than in water	very reactive	High
	Propanol	145	solubility in water is miscible	propanol did show some decay, especially at the higher temperatures and lower pH's	Low
	1-Propanol (main fragment)	142			Low
	2-Propanol (main fragment)	148			Low
	Acetonitrile	141	miscible with water, methanol, methyl acetate, acetone, ether, chloroform, and carbon tetrachloride	stable and decompose on heating	Low
	Acetaldehyde (1.5% of m/z 45, possibly by reaction with parasitic ion NO ⁺)	142	extremely soluble in both water and oil and easily absorbed orally, but only minimal amount enters the circulating blood	at room temperature, acetaldehyde (CH ₃ CH=O) is more stable than vinyl alcohol (CH ₂ =CHOH) by 42.7 kJ/mol	Low
44*	Propanol	146	solubility in water	propanol did	Low

			is miscible	show some decay, especially at the higher temperatures and lower pH's	
	1-Propanol (isotope of main fragment, 3.4% of m/z 43)	3			Low
	2-Propanol (isotope of main fragment, 3.5% of m/z 43)	142			Low
	Isocyanic acid	142	solubility in water is dissolves, it is soluble in blood and if levels exceed 1 pppv then it may contribute to health problems	the simplest stable chemical compound	Low
	CH ₂ CHO	142			Low
	n-Methylmethanamine	142	solubility in water is miscible	stable under ordinary conditions	Low
	Ethanimine (Acetaldimine)	142			Low
	Ethenamine (Vinylamine)	142	soluble in water and denser than water	highly flammable	High
	Ethyleneimine	142	water solubility is miscible	highly flammable, reacts with a wide variety of materials	Low
	Nitrous oxide, N ₂ O ⁺	3	solubility in water is 1.5 g/L (15°C), soluble in alcohol, ether, sulfuric acid	stable at room temperature	Low
45*	Acetaldehyde (main fragment) (Ethanal)	142	extremely soluble in both water and oil and easily absorbed orally, but only minimal amount enters the circulating blood	at room temperature, acetaldehyde (CH ₃ CH=O) is more stable than vinyl alcohol (CH ₂ =CHOH) by 42.7 kJ/mol	High
	Carbon dioxide	142	solubility in water is 1.45 g/L at 25°C, 100 kPa, 0.06 mL CO ₂ /dLblood per mm Hg (20 times higher than O ₂ solubility)	under normal conditions it is stable	Low
	CO ₂ H ⁺ , it appears at m/z = 45 due to its very high concentration in exhaled breath and due to non-	143			Low

	equilibrium phenomena in the drift chamber.				
	Carbon monosulfide	142	solubility in water is insoluble	it is not intrinsically unstable, but it tends to polymerize	Low
	Ethylene oxide	142	solubility in water is miscible, it is readily soluble in water, ethanol, diethyl ether and many organic solvents	aqueous solutions of ethylene oxide are rather stable	Low
	Propane		solubility in water is 40mg L ⁻¹ (at 0°C)	it is very stable at normal temperature and storage conditions	High
46*	N-methylmethanamine	142	solubility in water is 3.540 kg L ⁻¹	stable, generally used as a solution in water at concentrations up to around 40%, extremely flammable in the pure form, incompatible with strong oxidizing agents	Low
	Acetone (1.4% of m/z = 59)	142	miscible in benzene, diethyl ether, methanol, chloroform, ethanol	stable at room temperature in closed containers under normal storage and handling conditions	Low
	Acetaldehyde (isotope of main fragment, 2.5% of m/z = 45)	142	extremely soluble in both water and oil and easily absorbed orally, but only minimal amount enters the circulating blood	at room temperature, acetaldehyde (CH ₃ CH=O) is more stable than vinyl alcohol (CH ₂ =CHOH) by 42.7 kJ/mol	Low
	NO ₂ ⁺	143	increased reactivity of the nitronium ion in strongly acidic solution	it is stable enough to exist in normal conditions	Low
	Isotope of CO ₂ H ⁺	143			Low
	CH ₂ CH ₂ OH	142			Low

	Formamide	142	it is miscible with water, methanol, ethanol, acetone, acetic acid, dioxane, ethylene glycol, U.S.P. glycerol and phenol, it is very slightly soluble in ether and benzene	it may be stored at room temperature and should be protected from exposure to moisture	Low
	Ethylamine	142	solubility in water is miscible	specific, stable, and easier to quantitate than the free amine	High
	Dimethylamine	3	solubility in water is 3.540 kg L ⁻¹ , very soluble in water forming a very strong alkaline solution	decompose into toxic gas when burnt	High
47*	Formic acid (CH ₃ O ₂ ⁺), H ₃ N ₂ O ⁺ and NO ₂ H ⁺ as an instrument background. Potentially produced in the ion source.	143			Low
	Fragments of oxy-VOCs	145			Low
	Thioformaldehyde	142	slightly soluble in water, highly soluble in benzene	the encapsulated thioformaldehyde had a much longer life-time	Low
	Ethanol	142	miscible in water	it is stable to hydrolysis but is readily biodegradable	High
	Dimethyl ether	142	highly water-soluble, 71 g dm ⁻³ (at 20°C (68°F))	stable but is extremely flammable	Low
	Methylhydrazine	142	solubility in water is miscible	stable	Low
48*	NO ⁺ ·H ₂ O	143			Low
	Isotope of Ethanol	141			High
	o-Methylhydroxylamine	142	miscible with water, alcohol, ether and hexane	stable	Low
49	Methanethiol (Methyl mercaptan)	142	solubility in water is 2%, soluble in alcohol and ether	stable	High
50	O ₂ ⁺ H ₂ O	143			High
51	Water cluster of methanol (0.7% of m/z 33)	142			High

	1,3-Butadiyne	142		highly flammable	Low
	Difluoromethylene	142	assumed to be soluble in common organic solvents	the thermochemistry of difluoromethylene is of considerable interest in view of the apparent high stability of this radical	Low
52	Propiolonitrile	142	soluble in benzene, EtOH, acetonitrile, cyclohexane, toluene, ether, insoluble in water	have a good stability towards moisture, light, heat, air, electric fields and electromagnetic radiation	Low
	Possibly from Teflon in the PTR-MS	143			Low
53*					
54*	2-Propenenitrile	142	solubility in water is 70 g/L, soluble in water and most common organic solvents such as acetone, benzene, carbon tetrachloride, ethyl acetate, and toluene	it is used for fire resistance coating	Low
	NH ₃ ·H ₃ O ⁺ ·H ₂ O	140			Low
55*	Fragment of 3-heptanone (10.4% of m/z = 115)	142			Low
	Water trimer (H ₂ O) ₃ H ⁺	120			High
	Water cluster	142			Low
	Aldehyde fragments	146			Low
	Butadiene		solubility in water 0.735 g/100 mL, very soluble in acetone, soluble in ether, ethanol	at room temperature, 96% of butadiene exists as the s-trans conformer, which is 2.3 kcal/mole more stable than the s-cis structure.	High
56*	Propanenitrile	142	solubility in water is 11.9% (20°C)	reactivity (1.1), this degree includes materials that are normally stable, but that	Low

				may become unstable at elevated temperatures and pressures	
	Isocyano-ethane	142		thermally stable molecules	Low
	1-Azabicyclo[1.1.0]butane	142	N/A	stable for a few months or longer if stored properly (at -18°C)	Low
	Propargylamine	142	solubility in water is miscible	stable under normal conditions	Low
	Vinylimine	142			Low
	Possibly from Teflon in the PTR-MS	143			Low
57	1-Butene (Butylene)	145	solubility in water is 0.221 g/100 mL, soluble in alcohol, ether, benzene	it is stable in itself but polymerizes exothermically	High
	2-Butene	142	solubility in water is 347.58 mg/L	trans-2-butene is more stable than cis-2-butene	Low
	Propenal (Acrolein)	3	solubility in water is g/100ml at 20°C	unstable and very dependent on pH	Low
	2-Propenal (Acrolein)	142	solubility in water is g/100ml at 20°C	unstable and very dependent on pH	Low
	2-Methyl-1-propene (Isobutylene)	142	solubility in water is insoluble	stable	High
	2-Aminoacetonitrile, NCCH ₂ NH ₂	142	soluble	stable under ordinary conditions, moisture sensitive	Low
	Methylketene	142	water solubility is 1.70E+05 mg/L in 25°C		Low
	C ₂ S	142			Low
	Acrolein (Propenal)	141	solubility in water is g/100ml at 20°C	unstable and very dependent on pH	High
	Butanol	146	solubility in water is 73 g L ⁻¹ at 25°C, very soluble in acetone miscible with ethanol, ethyl ether		Low
	Cyclobutane		it is insoluble in water but is soluble in alcohol, acetone, and ether	cyclobutane is more stable than cyclopropane	High
58	Isocyanatomethane	142	solubility in water	stable, but highly	Low

			is 10% (15°C), it is soluble in water to 6–10 parts per 100 parts, but it also reacts with water	reactive, highly flammable, readily forms explosive mixtures with air, note low boiling point, low flash point	
	2-Oxopropyl, CH ₂ COCH ₃	142			Low
	Methyl azide	142	solubility in water is slightly soluble, solubility alkane, ether. soluble in most organic solvents	it is stable at ambient temperature but may explode when heated	Low
	Cyclopropylamine	142	solubility in water is miscible, soluble in ethanol	stable	Low
	2-Propen-1-amine (Allylamine)	142	miscible with water, alcohol, chloroform, ether	it is stable, but absorbs carbon dioxide from the air, incompatible with oxidizing agents	Low
	2-Methylaziridine (Propyleneimine)	142	solubility in water is miscible	unstable	Low
	1-Methylaziridine	142			Low
	2-Propanimine	142			Low
	1-Methylethenylamine	142			Low
	Azetidine	142	solubility in water is miscible	it has four-membered ether ring oxetane, although similar in structure, the stability and chemistry of these rings is known to be very different	Low
	Acrolein (isotope m/z=57)	141			Low
59	Acetone (main fragment)	142	solubility in water is miscible and miscible in benzene, diethyl ether, methanol, chloroform, ethanol	stable at room temperature in closed containers under normal storage	High
	Propanal (Propionaldehyde)	142	solubility in water is 20 g/100 mL and 540 g/L (20°C)	stable, highly flammable, incompatible with oxidizing agents,	High

				strong acids, strong bases	
	Propylene oxide	142	solubility in water is 41% (20°C)	it is stable under recommended storage conditions	Low
	Thioketene	142		thioketenes are much more reactive and less stable than the corresponding ketenes	Low
	Methoxy-ethene	142			Low
	(e)-Dimethyldiazene	142			Low
	Dimethyl-diazene	142			Low
	CH ₃ C(=NH)NH ₂	142			Low
	Butane		solubility in water is 61 mg L ⁻¹ (at 20°C), solubility in water and salt solutions at low temperatures	the staggered conformation of ethane is a more stable	High
60	Acetone (isotope of main fragment, 3.4% of m/z 59)	142			Low
	CH ₂ CH ₂ CH ₂ OH	142			Low
	N-methylformamide	142	solubility in water is miscible	DMF is favored over NMF as a solvent due to its greater stability	Low
	Acetamide	142	solubility in water is 2000 g L ⁻¹ , solubility in ethanol is 500 g L ⁻¹ , pyridine is 166.67 g L ⁻¹ , soluble in chloroform, glycerol, benzene	it is used as the solvent	Low
	1-Propylamine	3	soluble	Stable, highly flammable, note low flash point, readily forms explosive mixtures with air, incompatible with oxidising agents, strong acids, store cool	Low
	Isopropylamine	3	solubility in water is soluble	stable, extremely flammable - note low boiling point	Low

				and low flash point	
	Methylethylamine	3	water solubility is 418.0 mg/mL		Low
	Trimethylamine	142	solubility in water is miscible		High
	1-Propanamine	142			Low
	2-Propanamine	142			Low
	N-methyl-ethanamine	142			Low
61*	Acetaldehyde (3.7% of m/z = 45)	142			High
	Methoxyethane	142	soluble in water and acetone, miscible in ethyl alcohol and ethyl ether	stable, but may become unstable at elevated temperatures and pressures	Low
	Ethylenediamine	142	solubility in water is miscible	stable under ordinary conditions	Low
	Acetic acid	142	solubility in water is miscible	it is extremely stable stored at room temperature	High
	Esters of Acetic acid	146			Low
	Methyl formate	142	solubility in water is 30% (20°C)	Stable, extremely flammable, readily forms explosive mixtures with air, note low flash point and very wide explosion limits, incompatible with oxidizing agents	Low
	Propanol	145	solubility in water is miscible		High
	1-Propanol (but this fragments mostly to m/z 43 by loss of water)	142	solubility in water is miscible	1-propanol > ethanol > 2-propanol	Low
	2-Propanol (but this fragments mostly to m/z 43 by loss of water)	142	solubility in water is miscible	1-propanol > ethanol > 2-propanol	Low
	1,1-dimethylhydrazine	142	solubility in water is miscible	solution stored in dark and cold are relatively stable in absence of oxidants	Low
	Glycolaldehyde	146	H ₂ O: 0.1 g/mL, clear, colorless	high stability of glycolaldehyde	Low
	Carbonyl sulfide		soluble in water (0.80 mL/mL of	stable under normal conditions	High

			water at 13.5°C, 1 atm), very soluble in KOH, CS ₂ , soluble in alcohol, toluene		
	Dimethylsilane			stable at room temperature and atmospheric pressure	High
62*	Isotope of Acetic acid	146			Low
63*	Dimethyl sulfide	142	it is a water-insoluble flammable liquid that boils at 37 °C	stable	High
	Ethanethiol (Ethyl mercaptan)	142	solubility in water is 0.7% (20°C), soluble in most organic solvents, but only slightly soluble in water	stable under ordinary conditions	High
	Nitramide, (H ₂ N-NO ₂)	142	very soluble in water		Low
	Sulfine, CH ₂ =S=O	142			Low
	1,2-Ethanediol (Ethylene-glycol)	142	soluble in most organic solvents, soluble or miscible with water	chemically stable in air and in solution	Low
	CO ₂ H ⁺ ·H ₂ O	143			Low
	Cluster of acetaldehyde with primary Ion	3			Low
	Ethylene-glycol (1,2-Ethanediol)		soluble in most organic solvents, soluble or miscible with water	chemically stable in air and in solution	High
64*	Nitric acid	3	solubility in water is completely miscible	stable under ordinary conditions of use and storage	Low
	2-Fluoro-ethylamine	3			Low
65	2-Fluoro-ethanol	3	solubility in water is miscible	this colorless liquid is one of the simplest stable fluorinated alcohols	Low
	1,1-Difluoroethene	3	solubility in water is 0.254 g/L		Low
	Cluster of ethanol and primary Ion	3			Low
	Ethanol water	145			Low
	Ethylchloride (Chloroethane)	3	solubility in water, 0.447 g/100 mL	stable for three years after receipt	Low

			(0°C), 0.574 g/100 mL (20°C), solubility soluble in alcohol, ether, solubility in ethanol 48.3 g/100 g (21°C)	of order if stored under recommended conditions	
66					
67	Isoprene (3.8% of m/z = 69, possibly by reaction of isoprene with parasitic ion NO ⁺)	142			High
	Malononitrile	142	solubility in water is 13% (20°C), 13.3 g/100 mL (20°C)	stable under ordinary conditions	Low
	Chlorofluoromethylene	142			Low
	1,3-Cyclopentadiene	142	solubility in water is insoluble	it is slightly more stable than expected	Low
68*	Cyanoketene	142			Low
	Cyclopropanecarbonitrile	142	soluble in water	stable under normal temperatures and pressures	Low
	HNCCCO	142			Low
	Pyrrole	142	insoluble in water; soluble in alcohol, ether, and dilute acids	stable under ordinary conditions	Low
69*	Isoprene (2-Methyl-1,3-butadiene) (main fragment)	142	it has a water solubility of 642 mg/l (25°C)	unstable	High
	Cluster of methanol and water dimer	140			Low
	Cyclopentene	142	immiscible	stable	Low
	Furan	142	it is soluble in common organic solvents, including alcohol, ether, and acetone, but is slightly soluble in water	it is sensitive to heat and may turn brown upon standing	High
	2-Pentyne	142			Low
	Ethenylcyclopropane	142			Low
	3-Methyl-1-butyne	142			Low
	2-Methyl-1,3-butadiene (Isoprene)	142	it has a water solubility of 642 mg/l (25° C)	unstable	Low
	1,3-pentadiene	142	water solubility is 690 mg/L, soluble	more stable than an isolated diene	Low

			in ether, alcohol, acetone and benzene		
	3,3-Dimethyl-cyclopropene	142		it is quite stable at room temperature	Low
	1H-Pyrazole	142	solubility in water is about 1g/mL, very soluble	stable under normal temperatures and pressures	Low
	C ₃ S	142			Low
	1H-Imidazole	142	0.1 M at 20°C	stable	High
	1-Methyl-cyclobutene	142			Low
70*	Isoprene (isotope of main fragment, 5.9% of m/z = 69)	142			Low
	Acetyl cyanide (CH ₃ COCN)	142	special smell ether and can be soluble in acetonitrile, in water or alcohol decomposition		Low
	Butanenitrile	142	solubility in water is 0.033 g/100 mL, soluble in benzene, miscible in alcohol, ether, dimethylformamide		Low
	2-Methyl-propanenitrile	142			Low
	Isoxazole	142	it is scarcely soluble in water (15 g per 100 ml at 25°C)	stable under normal temperatures and pressures	Low
	Oxazole	142	it is soluble in alcohol and ether and slightly soluble in water	stable under ordinary conditions	Low
	1,2,3-Triazole-1H	142	solubility in water is very soluble	it is a surprisingly stable structure compared to other organic compounds	Low
	1,2,4-Triazole-1H	142	solubility in water is very soluble, clear to hazy	stability is sensitive, reacts with acids and oxidizing agents	Low
71	Cyclobutanone	142	it is considerably soluble in water	slightly soluble in water, soluble in most organic solvents	Low
	2-Methyl-2-propenal	142	water solubility is 5.9% (59,000	unstable and readily undergo	Low

		mg/L) at 20°C	violent chemical change	
2-Methyl-1-butene	3	soluble in ether, ethanol, and benzene, insoluble in water	stable, incompatible with oxidizing agents, extremely flammable	Low
2-Methyl-2-butene	142	solubility in water is insoluble, solubility in alcohols and ether is miscible	acts as guest and forms stable solid host-guest complexes with self-assembled benzophenone bis-urea macrocycles	Low
2,5-Dihydro-furan	142	solubility in water is slightly soluble	stable under ordinary conditions	Low
2-Butenal (Crotonaldehyde)	142	solubility in water is 18% (20°C), very soluble in ethanol, ethyl ether, acetone soluble in chloroform, miscible in benzene	it is relatively stable in pure water but undergoes hydrolysis in the presence of water with low or high pH	Low
Methyl vinyl ketone (3-buten-2-one)	142	it is soluble in water and polar organic solvents	stabilized	Low
Dimethyl-cyanamide	142	stable but which may become unstable at elevated temperatures and pressures	very soluble in water, soluble in alcohol, ether and acetone	Low
Methylaminoacetonitrile; CH ₃ NHCH ₂ CN	142	it is material is stable if stored under proper conditions.		Low
3-Aminopropionitrile; H ₂ NCH ₂ CH ₂ CN	142		easily oxidized and unstable	Low
2,3-Dihydro-furan	142			Low
Crotonaldehyde (2-Butenal)	141	solubility in water is 18% (20°C), very soluble in ethanol, ethyl ether, acetone soluble in chloroform, miscible in	it is relatively stable in pure water but undergoes hydrolysis in the presence of water with low or high pH	Low

			benzene		
	3-buten-2-one Methyl vinyl ketone	149	it is soluble in water and polar organic solvents	stabilized	Low
	Methacrolein	146	6 g/100 mL (20°C)	stable	Low
	Pentene		water solubility is 0.15 g/L (20 °C)		High
	Cyclopentane		solubility in water is 0.01% at 20°C	slightly more stable	High
72*	Methoxyacetonitrile	142			Low
	2-Azetidinone	142			Low
	Acrylamide	142	solubility in water is 2.04 kg/L (25°C), 50 mg/mL at 20°C	If it is kept protected from light, it is expected to be stable	Low
	2-Methyl-2-propen-1-amine	142			Low
	Pyrrolidine	142	solubility in water is miscible		Low
	Ethenamine, (CH ₃) ₂ NCH=CH ₂	142			Low
	Ethyl azide	142	solubility in water is slightly soluble, soluble in alkane and ether	it is stable at ambient temperature but may explode when heated	Low
	N-ethyl-azetidine	142			Low
	N-thylidene-ethanamine	142			Low
	Crotonaldehyde (isotope)	141			Low
	Methacrolein (isotope)	146			Low
	73	Water tetramer (but in relatively low concentrations) (H ₂ O) ₄ H ⁺	3		
Water cluster (but in relatively low concentrations)		142			Low
Butanal		142	solubility in water is 7.6 g/100 mL (20°C), miscible with ethanol, ether, toluene, very soluble in acetone, benzene, slightly soluble in chloroform	readily oxidizes on prolonged exposure to air to form explosive peroxides	High
Isobutanal (2-Methylpropanal)		3	solubility in water is moderate, solubility in other solvents is miscible in organic solvents	stable	Low
2-Silaisobutene		142			Low
	2-Methylpropanal (Isobutanal)	142	solubility in water	stable	Low

			is moderate, solubility in other solvents is miscible in organic solvents		
	Tetrahydrofuran	142	solubility in water is miscible		Low
	2-Butanone (methyl ethyl ketone)	142	solubility in water is 27.5 g/100 mL	normally stable	High
	Ethoxy-ethene	142	water solubility is 7.8 g/L (25°C)	stable	Low
	2-Methoxy-1-propene	142	solubility in water is slightly soluble in (20°C)	stable under normal temperatures and pressures	Low
	Iron monoxide	142			Low
	Methylglyoxal	146	water solubility is ≥ 10 g/100 mL at 17°C	very stable	Low
	Pentane		solubility in water is 40 mg L ⁻¹ (at 20°C)	the branched isomers are more stable	High
	Malondialdehyde		solubility in water is miscible	stable	High
	Isopentane		solubility in water is 48 mg/L (25°C)	stable under normal conditions	High
	Neopentane		solubility in water is 33.2 mg/L (25°C)	normally stable	High
74*	Thiocyanic acid methyl ester (Methyl thiocyanate)	142	solubility in water is slightly soluble, solubility in diethyl ether is miscible	this material is stable if stored under proper conditions	Low
	Isothiocyanato-methane	142	soluble in ethanol, ethyl ether, slightly soluble in water	stable under normal temperatures and pressures	Low
	N,N-dimethylformamide	142	solubility in water is miscible	stable under ordinary conditions	Low
	N-methyl-acetamide	142	solubility in water is stable	stable, combustible, incompatible with strong oxidizing agents	Low
	2-Methyl-1-propanamine	142	water solubility is 1000 mg/mL at 25°C		Low
	1-Butylamine	3	solubility in water is miscible	stable in closed containers at room temperature under normal	High

				storage	
	2-Methyl-2-propanamine	3			Low
	Diethylamine	3	solubility in water is miscible		Low
	N,N-dimethylethanamine	142	soluble in water, 3.45×10^5 mg/L at 25°C	stable	Low
	1-Butanamine	142	solubility in water is miscible	stable in closed containers at room temperature under normal storage	Low
	2-Butanamine	142	solubility in water is miscible	normally stable	Low
	N-methyl-2-propanamine	142			Low
	2-methyl-2-propanamine	142			Low
	N-ethyl-ethanamine	142			Low
	2-Butanone or methyl ethyl ketone	141	solubility in water is 27.5 g/100 mL	stable	Low
75*	1-Butanol	141	solubility in water is 73 g L^{-1} at 25°C, solubility is very soluble in acetone miscible with ethanol, ethyl ether	stable under ordinary conditions	High
	2-Butanol	142	solubility in water is 290 g/L		High
	2-Methyl-1-propanol	142	solubility in water is 8.7 mL/100 mL		Low
	Propionic acid	142	solubility in water is 8.19 g/g (-28.3°C), 34.97 g/g (-23.9°C), miscible (≥ -19.3 °C), solubility is miscible in EtOH, ether, CHCl_3	stable under recommended storage conditions	High
	Diethyl ether (Ethoxy ethane)	3	solubility in water is 69 g/L (20°C)	stable	Low
	Formic acid ethyl ester	142	soluble in C-tung, 11.8g/100ml solubility in water	instability in the water can be gradual decomposition	Low
	1,1-Dimethyl-ethanol	142	soluble in water	stable under normal temperatures and pressures	Low
	Methyl propyl ether	142	solubility in water is 30.5 g/L		Low
	Acetic acid methyl ester (Methyl	142	25% in water at	is not stable in the	Low

	acetate)		room temperature	presence of strong aqueous bases or aqueous acids	
	2-Methoxy-propane	142			Low
	Ethoxy ethane (Diethyl ether)	142	solubility in water is 69 g/L (20°C)	stable	Low
	Thietane	142			Low
	Methyl-thiirane	142			Low
	Methyl vinyl sulfide	142			Low
	1,3-Propanediamine	142	it is soluble in water and many polar organic solvents	stable	Low
	Methyl acetate (Acetic acid methyl ester)	149	25% in water at room temperature	is not stable in the presence of strong aqueous bases or aqueous acids	Low
	1-Hydroxy-2-propanone	145	solubility in water is soluble, solvent solubility is soluble in alcohol and ether	stable under normal conditions	Low
	Hydroxyacetone	146	solubility in water (g/L) is miscible	stable	Low
76*	Chloro-acetonitrile	142	insoluble	stable under normal temperatures and pressures	Low
	Nitroethane	142	solubility in water is slightly soluble (4.6 g/100 ml at 20°C)	stable 7 days at 25°C	Low
	Nitrous acid ethyl ester	142			Low
	N-hydroxy acetamide	142	highly soluble in H ₂ O (500 mg mL ⁻¹), alcohols, DMSO	stable under normal conditions	Low
	Ethanethioamide	142	water solubility is 16.3 g/100 mL (25 °C)	stability incompatible with water, mineral acids	Low
	Glycine	142	solubility in water is 24.99 g/100 mL (25 °C), is soluble in pyridine, sparingly soluble in ethanol, insoluble in ether	stable under ordinary conditions	High
	2-Methoxy-ethanamine	142			Low
	3-Amino-1-propanol	142	solubility in water	stable under	Low

			is miscible, solvent solubility is soluble in most organic solvents	ordinary conditions, hygroscopic	
	N-oxide-N,N-dimethylmethanamine	142			Low
	Hydroxyacetone (isotope)	146			Low
	Propionic acid (isotope)	146			Low
	Methyl acetate (isotope)	146			Low
77	2-Methoxy-ethanol	142	solubility in water is miscible	stable	Low
	Methyl alcohol	3	it is alcohol is completely miscible(soluble) in water because the polarity of the hydroxyl group is greater than the non-polarity of the Carbon chain	stable under normal temperatures and pressures	Low
	Propanethiol (1-Propanethiol)	146	soluble in water (1.9 g/l) at 25°C		High
	1-Propanethiol (Propanethiol)	142	soluble in water (1.9 g/l) at 25°C		Low
	1-Fluoro-2-propanone	142			Low
	2-Propanethiol	142	soluble in water	stable	Low
	Benzyne	142			Low
	(Methylthio)-ethane	142	insoluble in water, soluble in alcohols and oils		Low
	1,2-Propanediol	146	solubility in water is miscible	stable at room temperature for years 6	Low
	1,3-Propanediol	142	solubility in water is miscible	stable under normal temperatures and pressures	Low
	Thiourea	142	solubility in water is 14.2 g/100ml	hydrolytically stable	Low
	Trimethyl-phosphine	142	very soluble in aliphatic, aromatic and ethereal solvents.	stable at ambient temperature	Low
	Acetone + m/z = 19 (primary ions)	140			Low
	Aceton water	145			Low
	Carbon disulfide		solubility in water is 0.258 g/100 mL (0°C), 0.239 g/100 mL (10°C), 0.217	it is a rather stable compound	High

			g/100 mL (20°C), 0.014 g/100 mL (50°C), soluble in alcohol, ether, benzene, oil, CHCl ₃ , CCl ₄		
	Thioacetic acid		water solubility is 27 g/L (15°C) (hydrolyse)	stable	High
78	Methyl nitrate	142	soluble in water	unstable	Low
	1,5-Hexadiyn-3-yl radical	142			Low
	3-Fluoropropylamine, FCH ₂ CH ₂ CH ₂ NH ₂	142			Low
79	Benzene	142	it is fairly soluble in water	more stable than cyclohexane	High
	Fluoroacetic acid	142	solubility in water is soluble	stable	Low
	Dimethyl sulfoxide	142	solubility in water is miscible, solubility in diethyl ether is very soluble	stable in neutral or alkaline conditions	High
	Acetic acid water	145			Low
	Propanol (isotope)	146			Low
	2-mercaptoethanol		miscible in water in all proportions, and miscible in alcohol, ether and benzene	stable under ordinary conditions	High
80*	Pyridine	142	solubility in water is miscible	more stable than benzene	High
	Benzene (isotope)	141			Low
81	2-Chloroethanol	142	solubility in water is miscible	normally stable	Low
	1,4-Cyclohexadiene	142	soluble in common organic solvents (i.e., diethyl ether, THF, toluene)	stable	Low
	1,3-Cyclohexadiene	142	solubility in water is none	1,3- cyclohexadiene is about 8.5 kJ/mol more stable than 1,4- Cyclohexadiene	Low
	Pyrazine	142	solubility in water is soluble	stable	High
	1-Methyl-3-methylenecyclobutene	142			Low
	1,3-Diazine (Pyrimidine)	142	soluble	stable	High
	Pyridazine	142			High

	Cluster of acetaldehyde and water Dimer	3			Low
	Monoterpene fragment	145	soluble	stable	Low
82	NCC(CH ₃)CO	142			Low
	1,3,5-Triazine	142			Low
	CH ₃ NCCCO	142			Low
	2,2-Difluoro-ethylamine	142			Low
	Ethanol, 2,2-difluoro-CF ₂ HCH ₂ OH	142			Low
83	Cyclohexene	142	solubility in water is insoluble, miscible with organic solvents	stable	Low
	1-Methyl-cyclopentene	142			Low
	Phosphorous-acid-, H ₃ PO ₃	142			Low
	Methylene-cyclopentane	142			Low
	2,3-Dimethyl-1,3-butadiene	142	soluble in chloroform, insoluble in water	stable if stored under proper conditions	High
	3-Methyl-furan	142			Low
	1-Hexyne	3	in water at 25°C was reported to be 360 g(1)/106 g	stable under normal temperatures and pressures	Low
	2-Methyl-1,3-pentadiene	142			Low
	2-Methyl-furan	3	solubility in water is 3000 mg/L (20°C), solubility in ethanol is soluble		Low
	(1-Methylethenyl)-cyclopropane	142			Low
	1,3,3-Trimethylcyclopropene	142			Low
	3(5)-Methylpyrazole	142			Low
	4-Methylpyrazole	142	soluble in water	stable under storage conditions of up to about 55°C	High
	1-Methylpyrazole	142			Low
	4-Methylimidazole	142	very soluble in water and alcohol	stable under ordinary conditions	Low
	1-Methyl-1H-imidazole	142	solubility in water is very soluble	stable at room temperature in closed containers under normal storage and handling conditions	Low
	2-Methyl-1H-imidazole	142			Low

	Cluster of ethanol and water dimer	140			Low
	1,2-Dimethylcyclobutene	142			Low
	3-Methyl-1,3-pentadiene $\text{CH}_3\text{CH}=\text{C}(\text{CH}_3)\text{CH}=\text{CH}_2$	142			Low
	1-Ethenyl-1-methyl-cyclopropane dichloromethylene	142			Low
	1,5-Hexadiene	145	in water at 25°C was reported to be 169 g(1)/10 ⁻⁶ g(2)		Low
84*	Pentanenitrile	142	water solubility is 0.1-0.5 g/100 mL at 22.5°C	stable	Low
	2,2-Dimethyl-propanenitrile	142			Low
	tert-Butyl isocyanide	142			Low
	4-NH ₂ -pyrazole	142			Low
	3(5)-Aminopyrazole	142			Low
	N,N-dimethyl-2-propyn-1-amine	142			Low
85	2-Methyl-2-pentene	142	insoluble in water, soluble in ethanol, ethyl ether	stable	Low
	1-Hexene	3	solubility in water is insoluble	stable	High
	2,3-Dimethyl-2-butene	142	not soluble in water, soluble in ethanol, ethyl ether, acetone and chloroform etc.	stable under normal temperatures and pressures	Low
	Thiophene	142	solubility in water is insoluble	stable under ordinary conditions	Low
	Methylcyclopentene	3	water solubility is 117.68 mg/L		Low
	2-Pentenal	142	solubility in water is 45 g/L, soluble in ethanol, diethyl ether, carbon tetrachloride, chloroform		Low
	3-Methyl-3-buten-2-one	142	soluble in water (4.7%), ethanol, acetone, and ether		Low
	2-Methyl-2-butenal	142			Low
	1-Cyclopropyl-ethanone	142	solubility in water is 185 g/L	stable under ordinary conditions	Low
	3-Methyl-2-butenal	142	solubility in water, g/100ml at 20°C		Low
	3-Penten-2-one	142	water solubility is slight	stable	Low

	3,4-Dihydro-2H-pyran	142	solubility in water is soluble	stable under normal temperatures and pressures.	Low
	4-Methyl-2,3-dihydrofuran	142			Low
	(Dimethylamino)-acetonitrile	142			Low
	2,3-Dihydro-5-methyl-furan	142			Low
	CH ₃ CH=C(CH ₃)C ₂ H ₅	142			Low
	Cyclopentanone	142	solubility in water is slightly soluble	stable	Low
	1,4,5,6-Tetrahydropyrimidine	142			Low
	Ethyl vinyl ketone	149			Low
	Cyclohexane		solubility in water is immiscible, soluble in ether, alcohol, acetone miscible with olive oil	stable	High
86*	Methacrylamide	142	solubility in water is 202 g/L (20°C)	stable	Low
	2-Butenamide	142			Low
	Thiazole	142	solubility in water is sparingly soluble	stable under ordinary conditions	Low
	Piperidine	142	solubility in water is miscible	stable under ordinary conditions	Low
	N,N-dimethylallyl amine	142	soluble	stable	Low
	(CH ₃) ₂ C=NC ₂ H ₅	142			Low
	1-Methyl-pyrrolidine	142	water solubility is fully miscible	stable under normal temperatures and pressures	Low
	CH ₃ CH=CHN(CH ₃) ₂	142			Low
	Carbonocyanic acid methyl ester; CH ₃ COOCN	142			Low
	2-Methyl-2H-azetidin-2-one	142			Low
	N-(2-propylidene)ethanamine	142			Low
87	Pentanal	142	solubility in water is very slightly soluble	stable at room temperature in closed containers under normal storage and handling conditions	Low
	2,3-Butanedione	142	water solubility is 200 g/L (20°C)	stable	Low
	2-Pentanone	145	less dense than water and soluble	stable	High

		in water		
Acetic acid ethenyl ester	142	slightly soluble in water	polymerizes in light	Low
2-Methyl-2-propenoic acid	142	solubility in water is 9% (25°C)	may be stabilized by the addition of MEHQ (Hydroquinone methyl ether)	Low
Crotonic acid	142	soluble in water and less dense than water	normally stable, even under fire exposure conditions	Low
Tetrahydro-2H-pyran	142			Low
Cyclopropanecarboxylic acid	142	soluble in water	stable under normal temperatures and pressures	Low
2-Propenoic acid methyl ester	142	solubility in water is slightly soluble (52 g/l)	the stability depends upon dissolved oxygen and MEHQ inhibitor	Low
Isocrotonic acid	142			Low
$C_2H_5OCH_2CH=CH_2$	142			Low
3-Methyl-2-butanone	142	water solubility is 6 g/L (20 °C)	stable under normal temperatures and pressures	Low
3-Methyl-2-buten-1-ol	149	water solubility is 170 g/L (20 °C)		Low
3-Pentanone	142	solubility in water is 50 g/L (20°C)	stable	Low
2-penten-1-ol	149			Low
γ -Butyrolactone	142	solubility in water is miscible, soluble in CCl_4 , methanol, ethanol, acetone, benzene, ethyl ether	stable under ordinary conditions	Low
Tetrahydro-2-methylfuran	142	solubility in water is 15 g/100 mL (25°C)	stable	Low
4-Fluoropyrazole	142			Low
Ethyl-1-propenyl ether, $C_2H_5OCH=CHCH_3$	142			Low
trans- $CH_3CH=CH-OC_2H_5$	142			Low
Allyl ethyl ether	3	solubility in water is insoluble		Low
Piperazine	142	readily soluble in	stable against	Low

			water, methanol and ethanol; poorly soluble in diethyl ether, benzene and heptane	oxidative and thermal degradation	
	Tetramethylhydrazine	3	soluble in water or alcohol	stable	Low
	1,4-butanediamine	3	soluble in water (40 mg/ml at 20°C), ether, and alcohol	normally stable, even under fire conditions	Low
	Acetaldehyde, dimethylhydrazone (CH ₃) ₂ N-CH=N-CH ₃	142			Low
	2,3-Dihydro-1,4-dioxin	142			Low
	c-C(CH ₃)(C ₂ H ₅)NHNH	142			Low
	N,N'-Dimethylethylenediamine, CH ₃ NHCH ₂ CH ₂ NHCH ₃	142	solubility in Water is insoluble	it is stable if stored under proper conditions	Low
	Hexane		solubility in water is 9.5 mg L ⁻¹	stable	High
88*	(Methylthio)-acetonitrile, CH ₃ SCH ₂ CN	142		stable under normal temperatures and pressures	Low
	1,4-Dioxyl radical	142			Low
	N-C ₃ H ₇ NHCHO	142			Low
	N-ethyl-acetamide	142			Low
	N,N-dimethyl-acetamide from tedlar sampling bags	143	solubility in water is miscible	stable under ordinary conditions	Low
	N-methyl-propanamide	142	solubility in water is very soluble	stable under normal temperatures and pressures	Low
	1-Pentylamine	142	solubility in water is miscible	stable if stored as per the conditions specified under storage of below 30°C	Low
	Morpholine	142	soluble in water, methanol, ethanol, ethyl acetate, acetone, benzene, chloroform. Practically insol in toluene, xylene, petr ether, ether, carbon	stable	Low

			tetrachloride.		
	Neopentylamine	142	soluble in ethyl ether, slightly soluble in water	stable under recommended storage conditions	Low
	2-Propanamine, (C ₂ H ₅)(i-C ₃ H ₇)NH	142	solubility in water is miscible		Low
	N,N-Dimethyl-1-propanamine, (CH ₃) ₂ (n-C ₃ H ₇)N	142			Low
	N-ethyl-N-methyl-ethanamine	142			Low
	N,N-dimethylacetamide	3	solubility in water is miscible	stable under ordinary conditions	Low
	2-Methyl-2-butanamine	142			Low
	N,N-dimethyl-2-propanamine	142			Low
	Dimethylacetamide, DMAC		solubility in water is miscible	stable up to its atmospheric boiling point	Low
89*	1-pentanol	3	water solubility is 22 g/L (22°C)	stable	Low
	2-methyl-2-butanol	3	solubility in water is 120 g.dm ⁻³	normally stable	Low
	1,3-Dioxane	142	water solubility is miscible		Low
	1,4-Dioxane	142	slightly denser than water and soluble in water	stable	Low
	Formic acid propyl ester	142			Low
	Formic acid 1-methylethyl ester	142			Low
	Ethylene carbonate	142	soluble in water, alcohol, ether, and benzene	stable	Low
	1-Methoxy-butane	142	less dense than water and slightly soluble in water	oxidizes readily in air to form unstable peroxides that may explode spontaneously	Low
	Propanoic acid methyl ester	142	solubility in water is 72 g/L (20°C)		Low
	Ethyl acetate	142	water solubility is 80 g/L (20°C)	stable	Low
	Butyl methyl ether	3	solubility in water is 26 g/L (20°C)	stable, but may form explosive peroxides in contact with air	Low
	2-Ethoxy-propane	3			Low
	Tetrahydrothiophene	142	water solubility is immiscible	stability highly flammable	Low
	CH ₂ =C(CH ₃)–SCH ₃	142			Low

	Tetramethylhydrazine	142	soluble in water or alcohol	stable	Low
	1,4-Butanediamine	142	soluble in water with strongly basic reaction	normally stable	Low
	2,2-Dimethyl-1-propanol	142	soluble in water (40 mg/ml at 20°C), alcohol, and ether	stable	Low
	2-Methoxy-2-methyl-propane	142	solubility in water is slightly soluble (4.5 - 5.5 g/l at 25°C)	stable under ordinary conditions	Low
	1,1-Dimethoxy-ethene	142	miscible with water, alcohol, chloroform, ether	highly flammable, may form unstable peroxides when exposed to oxygen	Low
	2-Hydroxybutanal	145	soluble in all prop. in water, alcohol, soluble in ether, very soluble in acetone	Unstable	Low
	Esters of butyric acid	146			Low
	Butyric acid		solubility in water is miscible, slightly soluble in CCl ₄ , miscible with ethanol, ether	stable	High
	Isobutyric acid		water solubility is 210 g/L (20°C)	stable under ordinary conditions	High
90*	Propanenitrile, Cl(CH ₂) ₂ CN	142	solubility in water is 11.9% (20°C)	stable	Low
	iso-Propyl nitrite	142			Low
	N-Hydroxy-N-methyl acetamide	142		stable under normal conditions	Low
	N,N-dimethyl-methanethioamide	142			Low
	4-Amino-1-butanol, NH ₂ (CH ₂) ₄ OH	142	solubility in water is very soluble	stable under normal temperatures and pressures	Low
	N-Methoxy acetamide	142			Low
	Esters of butyric acid	146			Low
	Alanine		solubility in water is 167.2 g/L (25°C)	it produces a stable alkyl free radical	High
91	1-Butanethiol (Butyl mercaptan)	142	less dense than water and slightly	normally stable, even under fire	High

			soluble in water	exposure conditions	
	2-Methyl-1-propanethiol (Isobutyl Mercaptan)	142	soluble in ethanol, ether, liquid hydrogen sulfide, and cold water, hot water	stable if stored under proper conditions	Low
	2-Butanethiol	142	solubility in water is slightly soluble		Low
	2-Methyl-2-propanethiol (tert-butyl-mercaptan)	142	solubility in water is slightly soluble	stable	High
	Ethanethioic acid S-methyl ester	142	soluble in oil and alcohol		Low
	Carbonic acid dimethyl ester	142	solubility in water, is $1.38 \times 10^{+5}$ mg/L at 25°C, miscible with alcohol and ether	stable in the presence of water	Low
	CH ₃ C(=S)OCH ₃	142			Low
	Diethyl sulfide	142	solubility in water is insoluble, in ethanol is fully miscible, in diethyl ether is fully miscible	stable	Low
	1,2-Dimethoxyethane	142	solubility in water is miscible	stable	Low
	1,4-Butanediol	142	solubility in water is miscible, in ethanol is soluble	stable	Low
	Water pentamer, (H ₂ O) ₅ H ⁺	120			Low
	N-Methyl-N-nitro-methanamine	142			Low
	1,3-Butanediol	146	solubility in water is 1 kg dm ⁻³	stable under normal temperatures and pressures	Low
92					Low
93	Ethyl fluoroformate, FCO ₂ C ₂ H ₅	142			Low
	Toluene	142	solubility in water is 0.052% at 25°C	stable when stored under a dry, inert atmosphere and away from heat	High
	2,5-Norbornadiene	142	solubility in water is insoluble	stable under normal conditions	Low
	1,2,3-Propanetriol	142	solubility in water is slightly soluble (soluble alcohol; slightly soluble in ether, carbon	stable under ordinary conditions	Low

			disulfide; insoluble in benzene)		
	Trimethylphosphine oxide	142	solubility in water is low, in other solvents is polar organic solvents	thermally stable	Low
	3-Ethynylfuran	145			Low
94*	Aniline	142	solubility in water is 3.6 g/100 mL at 20°C	stable under normal temperatures and pressures	High
	N-2-propynyl-2-propyn-1-amine	142			Low
	3-Methylpyridine	142	solubility in water is very soluble	chemically stable	Low
	4-Methylpyridine	142	solubility in water is fully miscible	stable under recommended storage conditions	Low
	2-Methylpyridine	142	solubility in water is miscible	stable	Low
	Toluene (isotope)	141			Low
95*	1,3-Difluoro-2-propanone, CFH ₂ COCFH ₂	142			Low
	Chloroacetic acid	142	solubility in water is 85.8 g/100mL (25°C), soluble in methanol, acetone, diethyl ether, benzene, chloroform, ethanol	normally stable, even under fire conditions	Low
	3,3'-Oxybis-1-propyne	142		stable under recommended storage conditions	Low
	Dimethyl disulfide	142	solubility in water is 2.5 g/L (20°C)	stable	High
	Phenol from Tedlar sampling Bags	143	solubility in water is 8.3 g/100 mL (20°C)	stable under ordinary conditions	High
	acetone + m/z = 37 (water dimmer)	140			Low
	2-Norbornene	142	water solubility at 20°C is 134 mg/l	stable at normal temperatures and pressure even without stabilizer	Low
	3-Pyridinamine	142	solubility in water is soluble, solubility in alcohol and benzene is soluble	stable	Low
	2-Pyridinamine	142	solubility in water is >100%	Stable under ordinary	Low

			conditions	
	4-Pyridinamine	142	soluble in water (50 mg/ml), 100% ethanol, methanol (slightly), alcohol, and DMSO (100 mM)	stable under recommended storage conditions Low
	1-Oxidepyridine			Low
	Methyl sulfonyl methane (Dimethylsulfone)		solubility in water is 150 g/l	stable under ordinary conditions, hygroscopic High
96*	2,5-Dimethyl-1H-pyrrole	142		Low
	1-Oxidepyridine	142		Low
97	Fluorobenzene	142	solubility in water is low	stable under ordinary conditions Low
	Methanesulfonic acid	142	it is soluble in water, slightly soluble in benzene	stable Low
	Phosphabenzene	142		Low
	1-Methyl-cyclohexene	142		stable Low
	1,2-Dimethylcyclopentene	142		Low
	3-Heptanone (2.7% of m/z = 115).	142		Low
	7-oxabicyclo[2.2.1]hept-2-ene	142		Low
	2,5-Dimethylfuran	142	solubility in water is insoluble	chemically stable Low
	3,4-Dimethylfuran	142	solubility in water is slightly soluble (2.5 g/L) (25°C)	Low
	2,4-Dimethylfuran	142	soluble in alcohol water 956.1 mg/L at (25°C), insoluble in water	Low
	2(1H)-Pyrimidinone	142		Low
	1,3-Pentadiene, (CH ₃) ₂ C=CHC(CH ₃)=CH ₂	142	water solubility is 690 mg/L, soluble in ether, alcohol, acetone, benzene	stable Low
	trans-Dimethylamino acrylonitrile	142		Low
	3(5),4-Dimethylpyrazole	142		Low
	1,4-Dimethylpyrazole	142		Low
	1,3-Dimethylpyrazole	142		Low
	1,5-Dimethylpyrazole	142		Low
	3,5-Dimethyl-1H-pyrazole	142		Low
	1,4-Dimethylimidazole	142		Low
	1,5-Dimethylimidazole	142		Low
	1,2-Dimethyl-1H-imidazole	142		Low
	Furan-2-carboxaldehyde (Furfural)		solubility in water	stable High

			is 83 g/L		
98*	4-NO ₂ -pyrazole	142			Low
	2-Fluoropyridine	142	solubility in water is soluble	stable under normal temperatures and pressures	Low
	3-F-pyridine	142	solubility in water is soluble	stable at room temperature in closed containers under normal storage and handling conditions	Low
	4-F-pyridine	142			Low
	1-Methyl-3-aminopyrazole	142			Low
	1-Methyl-5-aminopyrazole	142			Low
	N'-cyano-N,N-dimethyl formamidine	142			Low
	N-2-propenyl-2-propen-1-amine	142			Low
99	2,4-Dimethyl-2-pentene	142			Low
	3,3'-oxybis-1-Propene (CH ₂ =CHCH ₂) ₂ O	142	solubility in water is insoluble (immiscible)	Stable	Low
	2-hexenal	145	solubility in water is almost insoluble		Low
	Trans-2-hexenal	3	insoluble in water, soluble in alcohol	stable	Low
	Trans-2-heptene	3			Low
	7-Oxabicyclo[2.2.1]heptane	142			Low
	Cyclohexanone	142	water solubility is 150 g/L (10 °C)	stable	Low
	Cyclohexene oxide	142	solubility in water is insoluble (soluble in alcohol, ether and acetone)	stable under normal conditions	Low
	2-Methyl-thiophene	142	solubility in water is slightly soluble	stable under normal temperatures and pressures	Low
	Cis-3-hexenal	3	soluble in alcohol	unstable and tends to rearrange to the more stable trans-2-hexenal	Low
	3-Methyl-3-penten-2-one	142		stable	Low
	4-Methyl-3-Penten-2-one	142	less dense than water and slightly soluble in water	normally stable, but that may become unstable at elevated temperatures and	Low

				pressures	
	(CH ₃) ₂ NCOCN	142			Low
	4,4-Dimethyl-2-imidazoline	142			Low
	(CH ₃) ₂ N-CH=N-(2-propenyl)	142			Low
	Methylcyclohexane	3	solubility in water is insoluble	stable	Low
	3-Hexen-2-one(E)	142	soluble in alcohol water, 8974 mg/L at 25°C, insoluble in water		Low
	Heptene		solubility in water is 0.0003% at 25°C	stable	High
	Cyclo-heptane		solubility in water is immiscible, solubility in ethanol is miscible	stable	High
100	Trifluoro(nitroso)methane	142		stable under normal conditions	Low
	Carbonocyanidic acid, NCCOOC ₂ H ₅	142			Low
	2,2,2-Trifluoroethylamine	142	soluble in water (highly)	stable under recommended storage conditions	Low
	N-Methyl-2-pyrrolidone	3	it is completely soluble with water at all temperatures and is soluble with most organic solvents	stable	Low
	2-Methylthiazole	142			Low
	Cyclohexanamine	142	solubility in water is miscible, very soluble in ethanol, oil miscible in ethers, acetone, esters, alcohol, ketones	stable under normal temperature conditions and recommended use	Low
	1-Methyl-piperidine	142	soluble in water, alcohol, and ether	stable under ordinary conditions	Low
	1-Methyl-2-pyrrolidinone	142	water solubility is ≥ 10 g/100 mL at 20°C	stable, but decomposes upon exposure to light	Low
	(CH ₃) ₂ NC(CH ₃)=CHCH ₃	142			Low
	3-Ethoxy pentanenitrile	142			Low
	N,N-dimethyl-2-propenamide	142			Low
	N-butylidene-ethanamine	142			Low
	N,N-2-trimethyl-1-propen-1-amine	142			Low
	Allyl isothiocyanate		sparingly soluble in		High

			water, very soluble in benzene, ethyl ether and ethanol, miscible with most organic solvents		
101 *	CF ₃ OCH ₃	142			Low
	Cyclobutane carboxylic acid	142	solubility in water is very soluble	stable at room temperature in closed containers under normal storage and handling conditions	Low
	3-Methyl-2-butenic acid	142	soluble in water, and methanol		Low
	2-Methyl-2-butenic acid	142			Low
	2-Propenoic acid	142			Low
	Eta-pentenoic acid trans-alpha	142			Low
	2-methyl-methyl ester	142			Low
	Oxepane	142	water solubility is 2680 mg/L in 25°C		Low
	Ethenyltrimethyl-silane	142	this material is lighter than water and insoluble in water	stable under normal temperatures and pressures	Low
	3,3-Dimethyl-2-butanone	142	solubility in water is soluble	stable under normal temperatures and pressures, volatile in steam	Low
	Hexone (Methyl isobutyl ketone)	150	solubility in water is 1.91 g/100 mL (20°C)	stable	High
	2-Hexanone (Methyl butyl ketone)	150	solubility in water is 1.4% (14 g/L)	stable under ordinary conditions	High
	3-Hexanone	142	solubility in water is 14.7 g/L	stable, but may form peroxides on prolonged storage	Low
	Cyclopropanecarboxylic acid methyl ester	142	solubility in water is moderate	stable under ordinary conditions	Low
	2,2-Dimethyltetrahydrofuran	142			Low
	Acetylacetone	142	solubility in water is 16 g/100 mL	stable under ordinary conditions	Low
2-Aminothiazole	142	solubility in water is soluble	stable under normal temperatures and	Low	

				pressures	
	(CH ₃) ₂ N-CH=N-C ₂ H ₅	142			Low
	(CH ₃) ₂ N-C(CH ₃)=NCH ₃	142			Low
	2-Butenoic acid methyl	142			Low
	1,2-Dimethyl-pyrazolidine	142			Low
	3-hexeb-1-ol	149			Low
	Hexanal	149	solubility in water is 4.8 g/L (20°C)	stable	Low
	Heptane		solubility in water is 0.0003% at 25°C		High
102	1-Hexanamine	142	solubility in water is 12 g/L (20°C), soluble in Methanol, dichloromethane, acetone, ethanol		Low
	N-propyl-1-propanamine	142	solubility in water is soluble, and soluble in ethanol, benzene , ethyl acetate	stable under ordinaty conditions	Low
	N,N-dimethyl isobutylamine	142		stable under recommended storage conditions	Low
	N,N-dimethyl-1-butanamine	142			Low
	N-(1-methylethyl)-2-propanamine	142	very soluble in acetone, benzene, ether, and ethanol, in water, 1.1×10 ⁵ mg/l at 25°C	normally stable, even under fire exposure conditions	Low
	(sec-C ₄ H ₉)(CH ₃) ₂ N	142			Low
	N,N-2-trimethyl-2-propanamine	142			Low
	Triethylamine	142	water solubility is 133 g/L (20°C)	stable	Low
	S-methyl thioacrylate				High
103	Formic acid butyl ester	142	water solubility is slowly decomposes	stable under ordinary conditions	Low
	1-Methoxy-2,2-dimethyl-propane	142			Low
	Phenylacetylene	142	water solubility is insoluble	stable	Low
	Methyl butyrate	3	less dense than water and slightly soluble in water	stable	Low
	Acetic acid 1-methylethyl ester	142	less dense than water and slightly soluble in water	stable under normal laboratory conditions	Low
	2-Methyl-propanoic acid methyl ester	142			Low

	n-Propyl acetate	142	solubility in water is 18.9 g/L	normally stable, even under fire exposure conditions	Low
	Dipropyl ether	3	solubility in water is 3 g/L (20°C)		Low
	di-n-Propyl ether	142	less dense than water and slightly soluble in water	normally stable, but that may become unstable at elevated temperatures and pressures and materials	Low
	Tetrahydro-2H-thiopyran	142			Low
	Diisopropyl ether	142	solubility in water is 2 g/L at 20°C	stable	Low
	2-Ethoxy-2-methyl-propane	142	solubility in water is 1.2 g/100 g	stable under normal conditions	Low
	4-Cl-pyrazole	142			Low
	cis-1,2-Cyclopentanediol	142		stable	Low
	2-Imidazolidinethione	142	soluble in ethanol; slightly soluble in dimethyl sulfoxide; insoluble in ethyl ether, benzene, chloroform	stable	Low
	(CH ₃) ₂ N-CH=N-OCH ₃	142			Low
	N,N-N',N'-tetramethylmethanediamine	142			Low
	1,5-Diaminopentane	142	solubility in water is very soluble	stable under normal temperatures and pressures	Low
	N,N-dimethyl-1,3-propanediamine	142	solubility in water is soluble	stable under ordinary conditions	Low
	Butanoic acid methyl ester	142			Low
	Ketone acetate				Low
	Isovaleric acid		solubility in water is (25 g/l), (Soluble in alcohol, chloroform and ether)	stable under ordinary conditions	High
	Acetoacetic acid		soluble in water, alcohol, and ether	stable	High
104	Benzonitrile	142	solubility in water is <0.5 g/100 ml (22 °C)	stable	High
	t-Butyl nitrite, (CH ₃) ₃ CONO	142	solubility in water is slightly soluble	stable under normal	Low

				temperatures and pressures	
	Isocyano-benzene	142			Low
	(CH ₃) ₂ NCOOCH ₃	142			Low
	N-Methylurethane, CH ₃ NHCOOC ₂ H ₅	142	very soluble in water, soluble in alcohol	stable if stored under proper conditions	Low
	Dimethyl thioacetamide	142			Low
	N-(2-aminoethyl)-1,2-Ethanediamine	142			Low
105	2,2-Dimethyl-1-propanethiol	142			Low
	Styrene	142	solubility in water is 0.03% (20°C)	stable	High
	C ₂ H ₅ OCOCH ₃	142			Low
	Thioacetic acid o-ethyl ester	142			Low
	o-Xylylene	142		stable	Low
	2-Pyridinecarbonitrile	142	solubility in water is partly miscible	stable	Low
	3-Pyridinecarbonitrile	142	soluble in water, alcohol, benzene, ether, hot petrol ether	stable under normal temperature and pressure	Low
	4-Pyridinecarbonitrile	142	solubility in water is 40 g/l	stable under ordinary conditions	Low
	1,3-Dimethoxypropane	142			Low
	3,6-bis(Methylene)-1,4-Cyclohexadiene	142			Low
	N,N' dimethyl-thiourea	142	solubility in water is slightly soluble	stable under ordinary conditions, hygroscopic	Low
	Hydroxybutyric acid				High
106	C ₆ H ₅ CH=NH	142			Low
*	4-Ethenyl-pyridine	142	soluble in water, soluble in dilute acids, alcohol, hydrocarbons, esters, ketones.	reactive, inhibitor prevents polymerization	Low
	2,3-Cyclobutenopyridine	142			Low
	3,4-Cyclobutenopyridine	142			Low
	Diethanolamine	142	miscible with water, methanol, acetone, ethanol, chloroform and glycerine	stable at usual use temperatures	Low
	Possibly from Teflon in the PTR-MS	143			Low
	Serine		solubility in water		High

			is soluble		
	Cyanogen bromide	142	solubility in water is reacts	stable under recommended storage conditions	Low
107	Ethylbenzene	142	solubility in water is 0.015 g/100 mL (20°C)	stable	High
	Xylenes	150	solubility in water at 25°C is 106 mg/L, miscible with alcohol and ether	normally stable even under fire exposure conditions	High
	m-Xylene	3	solubility in water at 25°C is 161 mg/L, miscible with alcohol, ether, and other solvents	normally stable even under fire exposure conditions	Low
	o-Xylene	3	solubility in water at 25°C is 178 mg/L, Miscible with alcohol and ether	normally stable even under fire exposure conditions	Low
	p-Xylene	142	solubility in water at 25°C is 162 mg/L, soluble in alcohol, ether, and other organic solvents	normally stable even under fire exposure conditions	Low
	1,2-Dimethyl-benzene (Xylene)	142		stable	Low
	1,3-Dimethyl-benzene (m-Xylene)	142			Low
	Benzaldehyde	142	solubility in water is 0.3 g/100 mL (20°C), soluble in liquid ammonia	stable	High
	Methyl dithioacetate	142			Low
	HOCH ₂ CH(OH)CH ₂ CH ₂ OH	142			Low
	Tropone, 2,4,6-Cycloheptatrien-1-one	142			Low
	4-Methylene-2,5-cyclohexadiene-1-one	142			Low
108	CICON(CH ₃) ₂	142			Low
	Nitroso-benzene	142	solubility in water is low, soluble in organic solvents	stable	Low
	2-Me-phenoxy	142			Low
	3-Me-phenoxy	142			Low
	4-Me-phenoxy	142			Low
	2-OH-benzyl	142			Low
	3-OH-benzyl	142			Low

4-OH-benzyl	142			Low
2-Methyl-benzenamine (O-toluidine)	142	solubility in water is 1.5 g/100 mL (25°C)		Low
3-Methyl-benzenamine	142	soluble alcohol, ether acid and slightly soluble in water		Low
Benzylamine	142	solubility in water is miscible, miscible in ethanol, diethyl ether, very soluble in acetone, soluble in benzene, chloroform	stable	Low
O-toluidine (2-Methyl-benzenamine)	3	solubility in water is 1.5 g/100 mL (25°C)		Low
p-Toluidine	142	water solubility is 1.1 g/100 mL	stable	Low
4-Pyridinecarboxaldehyde	142	water solubility is 20 g/L (20°C)		Low
N-methyl-aniline	142	solubility in water is insoluble	stability combustible	Low
(iso-C ₅ H ₁₁) ₃ N	142			Low
2,5-Dimethyl-pyridine	142			Low
2,3-Dimethyl-pyridine	142	solubility in water is 95 g/L	stable under normal temperatures and pressures	Low
3-Ethylpyridine, 3-(C ₂ H ₅)-pyridine	142	solubility in water is soluble	stable under normal temperatures and pressures	Low
2,4-Dimethyl-pyridine	142			Low
4-Ethylpyridine, 4-(C ₂ H ₅)-pyridine	142	solubility in water is slightly soluble	stable under normal temperatures and pressures	Low
2-Ethylpyridine, 2-(C ₂ H ₅)-pyridine	142	solubility in water is 30 g/L	stable under normal temperatures and pressures	Low
3,5-Dimethyl-pyridine	142	solubility in water is 33 g/L (20°C)	stable under normal temperatures and pressures	Low
2,6-Dimethyl-pyridine	142	solubility in water is 400 g/L	stable under normal temperatures and	Low

				pressures	
	o-Xylene (isotope)	141			Low
109	Carbonochloridic acid ethyl ester	142			Low
	Benzyl alcohol	142	solubility in water is 1g/25ml water at 17°C	stable under ordinary conditions of use and storage	Low
	p-Benzoquinone	142	solubility in water is slightly soluble, soluble in petroleum ether; soluble in acetone; very soluble in ethanol, benzene, diethyl ether	stable, but light sensitive	Low
	Bicyclo[2.2.1]hept-2-en-7-one	142			Low
	Methoxy-benzene	142	solubility is insoluble	stable	Low
	2-Methyl-bicyclo[2.2.1]hept-2-ene	142			Low
	Bicyclo[2.2.1]hept-2-en-5-one	142			Low
	2-Methylenebicyclo[2.2.1]-heptanes	142			Low
	1,2-Benzenediamine	142	soluble in water, ethyl ether, benzene, chloroform; very soluble in ethanol	normally stable, even under fire exposure conditions	Low
	1,4-Benzenediamine	142	solubility in water, g/100ml at 25°C	oxidizes on exposure to air	Low
	1,3-Benzenediamine	142	soluble in water, 2.38×10^5 mg/l at 20°C	unstable in air	Low
	1,1'-Ethenylidenebis-cyclopropane	142			Low
	Water hexamer (H ₂ O) ₆ H ⁺	120			Low
	Bis-(methylthio)methane		solubility in water is immiscible	stable at room temperature in closed containers under normal storage and handling conditions	High
	3-mercaptopropane-1,2-diol		soluble in water is slightly soluble	stable under recommended transport or storage conditions	High
110	Cyclohexanecarbonitrile	142		stable under normal conditions	Low
	3-Fluorobenzyl radical	142			Low
	3-Amino-phenol	142	freely soluble in	normally stable,	Low

			amyl alcohol and hot water, soluble in 40 parts cold water, very slightly soluble in petroleum ether	even under fire conditions	
	2-Amino-phenol	142	soluble in water	normally stable, even under fire conditions	Low
	1-Methyl-2(1H)-pyridinone	142	solubility in water is very soluble	stable at room temperature in closed containers under normal storage and handling conditions	Low
	2-Methoxy-pyridine	142	solubility in water is slightly soluble	stable under normal temperatures and pressures	Low
	1-Oxide 3-methyl-pyridine	142	water solubility is soluble	stable under normal temperatures and pressures	Low
	3-Methoxy-pyridine	142			Low
	4-Methoxy-pyridine	142			Low
	1-Azabicyclo[2.2.2]oct-2-ene	142			Low
	Dimethyl selenide		solubility in water is 24.4 mg/g water	stable	High
111 *	1-Fluoro-4-methyl-benzene	142			Low
	1-Fluoro-2-methyl-benzene	142			Low
	1-Fluoro-3-methyl-benzene	142	solubility in water is insoluble		Low
	Norbornan-7-one	142			Low
	2-Norbornanone	142	soluble in methanol, insoluble in water	stable if stored under proper conditions	Low
	$(\text{CH}_3)_2\text{C}=\text{C}(\text{CH}_3)\text{C}(\text{CH}_3)=\text{CH}_2$	142			Low
	1-Carbonitrile-piperidine	142			Low
	Dicyclopropyl-methanone	142	solubility in water is soluble	stable under normal temperatures and pressures	Low
	Phosphonic acid dimethyl ester	142			Low
	4-Cyanopiperidine	142	soluble in chloroform	stable under normal conditions	Low
	3,4,5-Trimethylpyrazole	142			Low
1,3,5-Trimethylpyrazole	142	solubility in water is soluble		Low	

	(CH ₃) ₂ N-CH=N-(2-propynyl)	142			Low
	Thiophenol		solubility in water is 0.08% in water at 25°C, soluble in most organic solvents; aqueous base	stable	High
112	3-Fluoro-benzenamine	142			Low
	p-Fluoroaniline	142	solubility in water is soluble	stable under normal conditions	Low
	exo-2-Aminonorbornane	142		stable under normal conditions	Low
	endo-2-Aminonorbornane	142			Low
	(CH ₃) ₂ N-CH=N-CH ₂ CN	142			Low
	4-Amino-2(1H)-pyrimidinone	142	solubility in water is soluble	stable	Low
	Histamine	142	solubility in water is easily soluble in cold water, hot water, Solubility in other solvents is easily soluble in methanol. Very slightly soluble in diethyl ether, easily soluble in ethanol	stable	Low
113 *	1,1,1-Trifluoro-2-propanone	142	solubility in water is soluble	stable	Low
	Chloro-benzene	142	solubility in water is 0.5 g l ⁻¹ in water at 20°C, soluble in most organic solvents	stable	Low
	1,4-Cyclohexanedione	142	solubility in water is very soluble	stable under normal temperatures and pressures	Low
	4-Methyl-cyclohexanone	142	solubility in water is slightly soluble	stable under normal temperatures and pressures	Low
	Cyclooctane	3	solubility in water is 7.90 mg/L	stable	High
	Cycloheptanone	142	solubility in water is insoluble	stable under normal temperatures and pressures	Low
	c-Hexane-1,2-dione	142			Low
	1,3-Cyclohexanedione	142	soluble in alcohol, chloroform	stable under ordinary	Low

				conditions	
	Triethylenediamine	142	water solubility is 46 g/100 mL (26°C)	stable, but very hygroscopic	Low
	Tetrahydro-1H5H-pyrazolo	142			Low
	[12-a]pyrazole	142			Low
	(CH ₃) ₂ N-CH=N-(c-propyl)	142			Low
	1-octene	149	water solubility is insoluble	stable at normal temperatures and pressure	High
114	1,1,1-Trifluorotrimethylamine	142			Low
	3(5)-Nitropyrazole	142			Low
	CF ₃ CH ₂ NHCH ₃	142		stable under normal conditions	Low
	3,3,3-Trifluoro-propylamine	142			Low
	3-Fluoro-pyridine-1-oxide	142			Low
	3-Chloro-pyridine	142			Low
	2-Chloro-pyridine	142	solubility in water is 10-50 mg/ml	stable under normal temperatures and pressures	Low
	N,N,2-trimethyl-2-propenamide	142			Low
	4-Chloropyridine	142			Low
	1-Methyl-2-piperidinone	142			Low
	c-C ₆ H ₁₁ CH ₂ NH ₂	142			Low
	Acetylpyrrolidine	142			Low
	N,N-dimethyl-butenamide	142			Low
	(CH ₃) ₂ NC(C ₂ H ₅)=CHCH ₃	142			Low
Possibly from Teflon in the PTR-MS	143			Low	
Chlorobenzene (isotope)	141			Low	
115	3-Heptanone (main fragment)	142	solubility in water is 1% (20°C)	stable	Low
	Heptanal	149	solubility in water is slightly soluble		Low
	4-Heptanone	142	water solubility is 4.6 g/L (20°C)	stable under ordinary conditions	Low
	2,4-Dimethyl-3-pentanone	142	solubility in water is slightly soluble	stable under normal temperatures and pressures	Low
	Trifluoro-acetic acid	142	solubility in water is miscible	stable	Low
	1,4-Difluoro-benzene	142	solubility in water is slightly soluble	stable under normal temperatures and pressures	Low
	1,2-Difluoro-benzene	142	solubility in water	stable	Low

			is 1.14e+004 mg/L (25°C)		
	2,2,2-Trifluoroethyl methyl ether	142			Low
	1,3-Difluoro-benzene	142	solubility in water is slightly soluble	stable under normal temperatures and pressures	Low
	Carbonothioic dichloride	142	slow decomposition in cold, fast in hot water	stable	Low
	Cyclohexanemethanol	142	solubility in water is slightly soluble	stable under normal temperatures and pressures	Low
	Cyclopentane carboxylic acid	142	solubility in water is very soluble	stable at room temperature in closed containers under normal storage and handling conditions	Low
	1-Methoxycyclohexane	142		stable under normal conditions	Low
	CH ₃ COCH ₂ CH ₂ COCH ₃	142	soluble	stable	Low
	1,3-Dimethyl-2-imidazolidinone	142	water solubility is freely soluble	stable	Low
	Hexahydro-1,2-dimethyl- pyridazine	142			Low
	(CH ₃) ₂ N-CH=N-(n-propyl)	142			Low
	(CH ₃) ₂ N-CH=N-(1-methylethyl)	142			Low
	(CH ₃) ₂ N-C(CH ₃)=NC ₂ H ₅	142			Low
	Chlorobenzene (isotope)	141			Low
	2-heptanone	149	solubility in water is 0.4% by wt	stable under ordinary conditions	Low
	Octane		solubility in water is 0.007 mg dm ⁻³ (at 20°C)		High
	Furan-2-ylmethanethiol		solubility in water is insoluble, solubility in other solvents is slightly soluble in chloroform	stable under normal conditions	High
116	3-Heptanone (7.8% of m/z = 115)	142			Low
*	N,N-Dimethylbutyramide	142	solubility in water is very soluble (110 g/L) (25°C)	stable under normal conditions	Low

	1-Heptanamine	142			Low
	N,N-diethylacetamide	142	solubility in water is miscible	stable under ordinary conditions	Low
	c-C ₅ H ₁₀ N(2-OCH ₃)	142			Low
	(CH ₃) ₃ CCH ₂ N(CH ₃) ₂	142			Low
	N,N-Diethyl-1-propanamine	142			Low
	(t-C ₅ H ₁₁)(CH ₃) ₂ N	142			Low
	(i-C ₃ H ₇)N(C ₂ H ₅) ₂	142			Low
	N,N,N',N'-tetramethyl-methanehydrazonamide	142			Low
	Proline		solubility is 1.5g/100g ethanol 19°C		High
117 *	4-Hydroxy-4-methylpentan-2-on	142	solubility in water is miscible	stable	Low
	trans-1,3-Cyclohexanol	142			Low
	3-Methylphenylacetylene	142	solubility in water is immiscible	stable under normal conditions	Low
	2,2-Dimethyl-propanoic methyl ester acid	142	solubility in water is insoluble	stable under normal temperatures and pressures	Low
	Indene	142	solubility in water is insoluble	stable, but air and light sensitive	Low
	1-Ethynyl-4-methyl-benzene	142	nonsoluble in water, fully miscible with toluene, soluble in ethanol, acetone, dichloromethane , hexane	stable under normal temperature and pressure	Low
	2-Methyl-2-(1-methylethoxy)-Propane	142	soluble in chloroform	stable under normal conditions	Low
	cis-1,3-Cyclohexandiol	142			Low
	Tetramethyl-urea	142	miscible with water, petroleum ether, all common solvents	stable	Low
	N,N'-diethyl-N, N'-dimethylhydrazine	142			Low
	Propyltrimethylhydrazine	142			Low
	(CH ₂) ₅ PCH ₃	142			Low
	1,6-Hexanediamine	142	solubility in water is 490 g L ⁻¹	stable in air but combustible	Low
	N,N,N',N'-tetramethyl-1,2-ethanediamine	142	solubility in water is 10 mg/mL at 20°C	stable	Low
118	Benzeneacetonitrile	142	water solubility is	stable	Low

*			insoluble		
	(CH ₃) ₂ NCOOC ₂ H ₅	142			Low
	4-H ₂ -C ₆ H ₄ -CCH	142			Low
	Indole (2,3 benzopyrrole), (Ketole), (1-benzazole)	142	solubility in water is 0.19 g/100 ml (20°C), soluble in hot water	stable	High
	NH ₂ (CH ₂) ₆ OH	142			Low
	(CH ₃) ₃ SiN(CH ₃) ₂	142			Low
119	Valine		solubility in water is soluble		High
	1-Propenyl-(e)-benzene	142			Low
	Cyclopropyl-benzene	142			Low
	1-Phenylpropene	142	solubility in water is g/100ml at 25°C	stable	Low
	3-Amino-benzonitrile	142	solubility in water is slightly soluble	stable under ordinary conditions	Low
	1-Ethenyl-3-methyl-benzene	142			Low
	1-Ethenyl-2-methyl-benzene	142			Low
	1-Ethenyl-4-methyl-benzene	142			Low
	1,1'-Thiobis-propane	142	water solubility is insoluble	stable at room temperature in closed containers under normal storage and handling conditions	Low
	Methylstyrene	142			Low
	Diisopropyl sulfide	142			Low
	1H-indazole	142			Low
	CH ₃ O(CH ₂) ₄ OCH ₃	142			Low
	1H-pyrrolo[2,3-b]pyridine	142	solubility in water is very soluble	stable under normal temperatures and pressures	Low
	Imidazo[1,2-a]pyridine	142			Low
	1H-benzimidazole	142	water solubility is 2.01×10 ⁺³ mg/l at 30°C	stable	Low
Triethyl-phosphine	142	it is slightly soluble in cold water and soluble in alcohol	stable under ordinary conditions	Low	
120 *	Azido-benzene	142			Low
	2-Phenyl-2-propyl radical	142			Low
	C ₆ H ₅ (CHC ₂ H ₅) radical	142			Low
	Benzoxazole	142	solubility in water is insoluble	stable	Low
	CH ₃ OC(S)N(CH ₃) ₂	142			Low

	1-Phenyl-aziridine	142			Low
	6,7-Dihydro-5H-1-pyridine	142			Low
	6,7-Dihydro-5H-2-pyridine	142		stable under normal conditions	Low
	2,3-Dihydro-1H-indole	142			Low
	Possibly from Teflon in the PTR-MS	143			Low
	Threonine		solubility in water is (H ₂ O, g/dl) 10.6(30°C), 14.1(52°C), 19.0(61°C)	stable	High
121 *	Propyl-benzene	142	insoluble in water and less dense than water	normally stable, even under fire exposure conditions	Low
	(1-Methylethyl)-benzene	142	solubility in water is negligible, soluble in acetone, ether, ethanol	stable, but may form peroxides in storage if in contact with the air	Low
	2,6,7-Trioxa-1-phosphabicyclo[2.2.1]heptane	142			Low
	3-FC ₆ H ₄ CCH	142		stable under normal conditions	Low
	4-FC ₆ H ₄ CCH	142			Low
	1-Phenylethanone (Acetophenone)	3	solubility in water is 5.5 g/L at 25°C, 12.2 g/L at 80°C	stable	Low
	C ₂ H ₅ S(OCH ₃)CO	142			Low
	1,3,5-Trimethylbenzene	142	solubility in water is 20 mg/L	stable under normal temperatures and pressures	Low
	3-CH ₃ C ₆ H ₄ CHO	142			Low
	4-Methyl-benzaldehyde (Tolualdehyde)	142	solubility in water is slightly soluble	stable under ordinary conditions	High
	Acetophenone (1-Phenylethanone)	142	solubility in water is 5.5 g/L at 25°C, 12.2 g/L at 80°C	stable	Low
	1-Oxide 4-pyridinecarbonitrile	142	water solubility is 3.46E+05 mg/L 25°C	stable under normal conditions	Low
	1-Oxide 3-pyridinecarbonitrile	142			Low
	9H-purine	142	solubility in water is 400 g/L	stable under normal temperatures and pressures	Low

	1-(Dimethylthio)ethane	142			Low
	3-Methyl-thiopropionate	146	soluble in alcohol, water slightly, 158.7 mg/L at 25°C, insoluble in water	stable in most media	Low
	2-mercapto-pyruvate	146			Low
122 *	Benzamide	142	water solubility is 1.35 g/100 mL (20°C)	stable	Low
	3-C ₂ H ₅ C ₆ H ₄ NH ₂	142			Low
	2,6-Dimethyl-benzenamine	142	do not dissolve in water, soluble in ethanol, ether and diluted hydrochloric acid		Low
	4-Aminobenzenecarbonal	142			Low
	1-(4-pyridinyl)-ethanone	142			Low
	1-(3-pyridinyl)-ethanone	142	solubility in water is soluble in hot water	stable under ordinary conditions	Low
	n-Ethyl-benzenamine	142	insoluble in water	normally stable, even under fire exposure conditions	Low
	Benzeneethanamine	142			Low
	OP(N(CH ₃) ₂)(CH ₃) ₂	142			Low
	N,N-dimethyl-benzenamine	142	solubility in water is 1,454 mg/L at 25°C	stable under recommended storage conditions	Low
	4-(i-C ₃ H ₇)-C ₅ H ₄ N	142			Low
	2-(C ₃ H ₇)-pyridine	142			Low
	2-(i-C ₃ H ₇)-pyridine	142		stable under normal conditions	Low
	Cysteine		solubility in water is soluble, 1.5g/100g ethanol 19°C	stable	High
123	(Methoxymethyl)-benzene	142			Low
	Benzoic acid	142	slightly soluble in water, soluble in alcohol, benzene, ether	stable under normal temperatures and pressures	Low
	Carbonodithioic acid O, S-dimethyl ester	142			Low
	2-Methoxy-1,3,2-Dioxaphospholane	142			Low
	Niacinamide	142	freely soluble in water and in	stable	Low

			ethanol		
	N,N-dimethyl-2-pyridinamine	142	solubility in water is soluble	stable under normal temperatures and pressures	Low
	N,N-dimethyl-3-pyridinamine	142			Low
	N,N-dimethyl-4-pyridinamine	142	water solubility is 76 g/L (25°C), solubility methanol is 50 mg/mL	stable	Low
	Phenethyl alcohol	149	slightly soluble in water (2 mL/100 mL H ₂ O)	stable under ordinary conditions	Low
	4-ethylphenol		solubility in water is slightly soluble	stable under normal temperatures and pressures	High
124	Nitro-benzene	142	solubility in water is 0.19 g/100 ml at 20°C	stable	Low
	CF ₂ HCON(CH ₃) ₂	142			Low
	4-Methoxy-benzenamine	142			Low
	2-Methoxy-benzenamine	142			Low
	3-Methoxy-benzenamine	142	soluble alcohol, ether, benzene and acid and water-soluble	stable	Low
	2-(CH ₃ OCH ₂)-pyridine	142			Low
	3-Methylene 1-azabicyclo [2.2.2]octane	142		stable under normal conditions	Low
125	O(CH ₂ CH ₂ CN) ₂	142			Low
	3-FC ₆ H ₄ CHO	142			Low
	4-Fluorobenzaldehyde	142	solubility in water is slightly soluble	stable under ordinary conditions	Low
	5,5-Dimethyl-2-cyclohexenone	142			Low
	(Methylthio)-benzene	142	solubility in water is 506 mg/l at 25°C, soluble in most common organic solvents	stable under ordinary conditions	Low
	4-Nitropyridine	142			Low
	2,3,4,5-Tetramethylfuran	142			Low
	3(5)-t-butylpyrazole	142			Low
	Phosphorous acid trimethyl ester	142	solubility in water is good	stable under ordinary conditions	Low
	N-butylpyrazole	142			Low
	2,6-Dimethyl-4H-Pyran-4-one	142	solubility in water	stable under	Low

			is slightly soluble	normal temperatures and pressures	
	1-t-Butylimidazole	142			Low
	1-Diazabicyclo[4.3.0]non-5-ene	142			Low
	Guaiacol	149	water solubility is 17 g/L (15°C)	stable, but air and light sensitive	Low
126 *	2-Bromo-ethanol	142	water solubility is 1-5 g/100 mL at 19°C	stable, but probably light sensitive	Low
	1-Azabicyclo[2.2.2]octan-3-one	142	solubility in water is soluble	stable under normal conditions	Low
	2-(Methylthio)-pyridine	142			Low
	3-(Methylthio)-pyridine	142	solubility in water is slightly soluble (7.4 g/L) (25°C)		Low
	4-(Methylthio)-pyridine	142			Low
	(CH ₃) ₂ N-CH=N-CH ₂ CH ₂ CN	142			Low
	4-Methyl-1-azabicyclo[2.2.2]octane	142			Low
	1,4,4-(CH ₃) ₃ -1,2,3,4-Tetrahydropyridine	142			Low
	3-Methyl 1-azabicyclo[2.2.2]-octane	142			Low
	2-Methyl 1-azabicyclo[2.2.2]-octane	142			Low
	Taurine		solubility in water is (50 mg/ml)	stable	High
127	1-Chloro-4-methyl-benzene	142	practically insoluble in water, soluble in non-polar solvents such as aromatic hydrocarbons	stable under ordinary conditions	Low
	1-Chloro-2-methyl-benzene	142	practically insoluble in water, soluble in non-polar solvents such as aromatic hydrocarbons		Low
	1-Chloro-3-methyl-benzene	142	practically insoluble in water, soluble in non-polar solvents such as aromatic hydrocarbons		Low
	c-C ₆ H ₁₁ COCH ₃	142			Low
	Cyclooctanone	142	solubility in water is 15g/L (20°C),	stable under normal conditions	Low

			solubility in other solvents, soluble in alcohol, acetone and benzene		
	(c-C ₃ H ₅) ₂ CS	142			Low
	3-Amino-1-azabicyclo[2.2.2]octane	142			Low
	2-Methyl-1,2-diazabicyclo[2.2.2]octane	142			Low
	2,3-Dimethyl-2,3-diazabicyclo[2.2.1]heptane	142			Low
	(CH ₃) ₂ N-C(CH ₃)=N(c-C ₃ H ₅)	142			Low
	Nonene		poor water solubility	stable	High
	Cyclononane				High
128 *	1-Methyl-3-nitropyrazole	142			Low
	1-Methyl-5-nitropyrazole	142			Low
	m-Chloroaniline	142	solubility in water is soluble, most organic solvents, carbon tetrachloride (miscible)	stable under ordinary conditions	Low
	p-Chloroaniline	142	soluble in hot water, soluble in ether, carbon disulfide, organic solvents, alcohol	stable under ordinary conditions	Low
	1-Methyl-5-nitroimidazole	142			Low
	Dimethyl(2,2-difluoroethyl)amine	142			Low
	4,4,4-Trifluorobutylamine	142		stable under recommended transport or storage conditions	Low
	2-Cl-4-(CH ₃)-pyridine	142			Low
	2-Cl-6-(CH ₃)-pyridine	142			Low
	N,3,5-trimethylpiperidine	142			Low
	1,4,4-Trimethylpiperidine	142			Low
	N,N-dimethyl-cyclohexanamine	142	partially soluble in water, miscible with alcohol, benzene, acetone		Low
	129	CF ₃ C(O)OCH ₃	142		
2,2,2-Trifluoroethyl formate		142	solubility is soluble in organics (Et ₂ O, THF, MTBE)	stable	Low
Ethyl 2,2,2-trifluoroethyl ether		142			Low
1,4-Benzenedicarbonitrile		142	solubility in water is soluble	stable under normal temperatures and	Low

				pressures	
	1,3-Benzenedicarbonitrile	142	solubility in water is slightly soluble, soluble in benzene, ether, hot alcohol, chloroform	stable under ordinary conditions	Low
	Naphthalene	142	solubility in water is 3mg/100mL at room temperature, solubility in methanol/ethanol is 7.7g/100mL, very soluble in ether	stable	High
	Cyclohexanecarboxylic acid	142	water solubility is 0.201 g/100 mL (15°C)		Low
	C ₆ H ₁₁ CH ₂ OCH ₃	142			Low
	2,2,4-Trimethyl-3-pentanone	142		stable	Low
	Azulene	142	solubility in water is 0.02 g/l	stable	Low
	Hexahydro-1,2-dimethyl	142			Low
	1H-1,2-diazepine	142			Low
	(CH ₃) ₂ N-CH=N-(n-butyl)	142			Low
	(CH ₃) ₂ N-CH=N-(2-methylpropyl)	142			Low
	(CH ₃) ₂ N-CH=N-(1-methylpropyl)	142			Low
	(CH ₃) ₂ N-CH=N(t-C ₄ H ₉)	142			Low
	(CH ₃) ₂ N-C(CH ₃)=N(n-C ₃ H ₇)	142			Low
	(CH ₃) ₂ N-C(CH ₃)=N(i-C ₃ H ₇)	142			Low
	Nonane		solubility in water is g/100ml at 25°C: 0.00002 (very poor)	stable	High
130	3-Chloro-pyridine-1-oxide	142			Low
*	1-Octanamine	142	solubility in water is 0.2 g/l (25°C)	stable under normal conditions	Low
	Isoquinoline	142	low solubility in water but dissolve well in ethanol, acetone, diethyl ether, carbon disulfide, and other common organic solvents	stable	Low
	Quinoline	142	solubility in water is slightly soluble, soluble in alcohol, ether, and carbon disulfide	stable	Low
	2-Methyl-N-(2-methylpropyl)-1-	142	solubility in water	stable under	Low

	Propanamine		is 5 G/L (20°C)	normal conditions		
	n-Butyl-1-butanamine	142			Low	
	N-(1-methylpropyl)-2-butanamine	142	solubility in water is slightly soluble (7 g/l), miscible with common organic solvents	stable under ordinary conditions	Low	
	(t-C ₄ H ₉) ₂ NH	142			Low	
	(i-C ₃ H ₇) ₂ (C ₂ H ₅)N	142			Low	
	Octylamine		water solubility is 0.2 g/L (25°C)	stable	High	
131 *	c-C ₆ H ₁₁ CH ₂ SH	142			Low	
	n-Butyl ether	142			Low	
	5-(CH ₃) ₂ -C ₆ H ₃ -CCH ₃	142			Low	
	Heptamethylenesulfide	142			Low	
	c-C ₆ H ₁₁ SCH ₃	142			Low	
	di-sec-butyl ether	142			Low	
	di-tert-butyl ether	142			stable	Low
	Quinoxaline	142	water solubility is soluble	stable	Low	
	CH ₃ C(OCH ₃)=CHCOOCH ₃	142			Low	
	CH ₂ =(CH ₃)OSi(CH ₃) ₃	142			Low	
	Cinnoline	142		stable	Low	
	tert-Butyl trimethylhydrazine	142			Low	
	Butyltrimethylhydrazine	142			Low	
	1,7-Diaminoheptane	142	water solubility is soluble	stable	Low	
	(CH ₃) ₂ N-CH=N-(2-methoxyethyl)	142			Low	
	N,N, N', N'-tetramethyl-1, 3-propanediamine	142	solubility in water is very soluble	stable under normal temperatures and pressures	Low	
	1-Octanol		solubility in water is 0.460 g/liter	stable	High	
132	4-Formyl-benzonitrile	142	solubility in water is insoluble, solubility in other solvents is soluble in acetone, methylene chloride	stable under normal conditions	Low	
	CH ₃ CONHCH ₂ COOCH ₃	142			Low	
	N,N-di-2-propynyl-2-propyn-1-amine	142		stable under normal conditions	Low	
	Dimethyl(trimethylsilylmethyl)amine	142			Low	
	NH ₂ (CH ₂) ₃ NH(CH ₂) ₃ NH ₂	142			Low	
Skatole		insoluble in water, soluble in alcohol and benzene	stable, but light-sensistive	High		

133	1,2,3-Trifluorobenzene	142	soluble in most organic solvents	stable	Low
	1,2,4-Trifluorobenzene	142	solubility in water is insoluble	stable at room temperature in closed containers under normal storage and handling conditions	Low
	1,3,5-Trifluorobenzene	142	solubility in water is insoluble	stable at room temperature in closed containers under normal storage and handling conditions	Low
	(C ₂ H ₅) ₃ SiOH	142			Low
	1-Cyclopropyl-3-methyl-benzene	142		stable under normal conditions	Low
	1-Cyclopropyl-2-methyl-benzene	142			Low
	1-Cyclopropyl-4-methyl-benzene	142			Low
	1-Methyl-2-(1-methylethenyl)-Benzene	142			Low
	2-Methylbenzofuran	142	solubility in water (g/L) is partly miscible	stable	Low
	1-Methyl-3-(1-methylethenyl) benzene	142		stable under normal conditions	Low
	3-CH ₃ C ₆ H ₄ C(CH ₃)=CH ₂	142			Low
	4-CH ₃ C ₆ H ₄ C(CH ₃)CH ₂	142			Low
	4-CH ₃ O-C ₆ H ₄ -CCH	142			Low
	1-Methylindazole	142			Low
	CH ₃ O(CH ₂) ₅ OCH ₃	142			Low
	2-Methyl-2H-indazole	142			Low
	Tetramethyl-thiourea	142	water solubility is 5,400 mg/l, soluble in water and alcohol	stable	Low
	1-Methylbenzimidazole	142	solubility is soluble in methanol		Low
	(n-C ₃ H ₇) ₂ (CH ₃)P	142			Low
	5-Methylimidazo(1,2-a)pyridine	142			Low
	2-Methylimidazo(1,2-a)pyridine	142			Low
	7-Methylimidazo(1,2-a)pyridine	142		stable under normal conditions	Low
	Ornithine		solubility in water is soluble, soluble in ethanol	stable	High
Cinnamaldehyde		solubility in water	stable under	High	

			is insoluble	normal temperatures and pressures	
134	2-Methyl-2H-benzotriazole	142			Low
	Aspartic acid	142	solubility in water is 4.5 g/L	stable under ordinary conditions	Low
	4-H ₂ NC ₆ H ₄ C(CH ₃)=CH ₂	142			Low
	1-Methylbenzotriazole	142	soluble in benzene and petroleum ether		Low
	N-phenylazetidine	142		stable for a few months	Low
	5,6,7,8-Tetrahydro-quinoline	142	slightly soluble in water, soluble alcohol, ether, carbon disulfide and readily in many organic solvents	stable under ordinary conditions	Low
	5,6,7,8-Tetrahydro-isoquinoline	142		stable if stored under proper conditions	Low
	Oxindole		solubility in water is insoluble	stable under normal temperatures and pressures	High
135 *	Butyl-benzene	142	water solubility is insoluble	stable	Low
	Methyltrioxaphosphabicycloheptane	142			Low
	Benzyl methyl ketone	142	water solubility is insoluble	stable	Low
	1,2,3,5-tetramethyl-benzene	142			Low
	((CH ₃) ₂ SiH) ₂ O	142			Low
	1-Phenyl-1-propanone	142		stable	Low
	1-(3-Methylphenyl)-ethanone	142			Low
	2,6,7-Trioxa-1-phosphabicyclo[2.2.2]octane	142			Low
	1-(4-Methylphenyl)-ethanone	142	solubility in water is slightly soluble		Low
	1,1'-Oxybis(2-methoxyethane)	142	solubility in water is 0.4 g/L, solubility in other solvents is miscible with alcohol, ether, hydrocarbon	stable under normal conditions	Low
	(C ₂ H ₅) ₃ PO	142			Low
6-Methyl-1H-purine	142			Low	

	p-cymene	149	solubility in water is 23.4 mg/L		Low
	Durene				High
136 *	4-Methyl-benzamide	142			Low
	m-Toluamide	142			Low
	4'-Amino-acetophenone	142	solubility in water is soluble in hot water	stable under ordinary conditions	Low
	N-ethyl-N-methylaniline	142			Low
	N,N,3-trimethyl-benzenamine	142		stable under normal temperature and pressure conditions	Low
	Adenine	142	solubility in water is 0.103 g/100 mL, negligible in ethanol	stable	Low
	N,N,4-trimethyl-benzenamine	142			Low
	N,N,2-trimethyl-benzenamine	142		stable under normal temperature and pressure conditions	Low
	4-(1,1-Dimethylethyl)-pyridine	142			Low
	2-(t-C ₄ H ₉)-pyridine	142			Low
	N,N,dimethylbenzenemethanamine	142	solubility in water is 8 g/L (20°C), solubility in other solvents is soluble in alcohol, acetone, ether and toluene, reacts with organic and inorganic acids	stable under normal conditions	Low
	2,6-(C ₂ H ₅) ₂ -pyridine	142			Low
	Homocysteine		solubility in water is soluble		High
137	Isoprene (1.6% of m/z 69)	142			Low
	3-ClC ₆ H ₄ CCH	142			Low
	3-Methylbenzoic acid	142	solubility in water is very soluble	stable under normal temperatures and pressures	Low
	1-Chloro-4-ethynyl-benzene	142		stable under normal conditions	Low
	4-Methyl-benzoic acid	142	solubility in water is slightly soluble	stable under ordinary conditions	Low
	2-Methyl-benzoic acid	142	soluble	stable under	Low

			normal temperatures and pressures	
3-FC ₆ H ₄ C(CH ₃)=CH ₂	142			Low
3-Methoxy-benzaldehyde	142	practically insoluble in water, soluble in ethanol and ether		Low
Benzoic acid methyl ester	142	water solubility is 157 mg/l at 30°C, miscible with alcohol, ether, methanol	stable, even under fire exposure conditions	Low
4-FC ₆ H ₄ C(CH ₃)=CH ₂	142			Low
1-(3-hydroxyphenyl)-ethanone	142	solubility in water is slightly soluble	stable under normal temperatures and pressures	Low
CH ₂ =C(CH ₃)-SeCH ₃	142			Low
4-Methoxy-benzaldehyde	142	practically insoluble in water, soluble in ethanol and ether		Low
4'-Hydroxy-acetophenone	142	solubility in water is Soluble (soluble alcohol and ether)	stable under ordinary conditions	Low
3-NH ₂ -C ₆ H ₄ CONH ₂	142			Low
1,5,5-Trimethyl-3-Methylenecyclohexene	142			Low
Hypoxanthine	142	soluble in water (30 mg/mL)		Low
2-Methoxy-1,3,2-Dioxaphosphorinane	142			Low
4-Amino-benzamide	142		stable under ordinary conditions	Low
2-Cyano1-azabicyclo[2.2.2]-octane	142			Low
1-Azabicyclo[2.2.2]octane-4-carbonitrile	142		stable under recommended storage conditions	Low
3-Cyano1-azabicyclo[2.2.2]-octane	142			Low
n,n-Dimethyl-1,4-benzenediamine	142		stable	Low
α-Pinene	141	solubility in water is 2.49 mg/L (25°C)		High
β-Pinene		solubility in water is insoluble	stable	High
γ-Pinene				High
Monoterpene	145	organic solvents,	stable	Low

			insoluble in water		
	Limonene		solubility in water is insoluble, miscible in alcohol, benzene, chloroform, ether, CS ₂	stable	High
138	1-Methyl-4-nitrobenzene	142	soluble in water, 442 mg/L at 30°C, soluble in alcohol, benzene, ether, chloroform, acetone	normally stable, but that may become unstable at elevated temperatures and pressures	Low
	p-Aminobenzoic acid	142	slight soluble in water, insoluble in chloroform, petroleum ether, benzene, soluble in ethyl acetate, acetic acid, ether,	stable under ordinary conditions	Low
	3-Aminobenzoic acid	142	solubility in water is 5.9 g/L (15°C)	stable under ordinary conditions	Low
	Anthranilic acid	142	water solubility is 5.7 g/L (25 °C)	stable	Low
	1-(3-Pyridinyl-1-oxide)ethanone	142			Low
	Pyridine-4-carboxylic acid methyl ester	142			Low
	Methyl nicotinate	142	very soluble in water, in chloroform and in ethanol (96%), freely soluble in ether	stable under ordinary conditions	Low
	N,N-di-2-propenyl-2-propen-1-amine	142	water solubility is 0.25 g/l	stable under ordinary conditions	Low
	α-Pinene (isotope)	141			Low
139	3-ClC ₆ H ₄ CH=CH ₂	142			Low
*	1-(3-Fluorophenyl)-ethanone	142	solubilities is slightly soluble	stable at room temperature in closed containers under normal storage and handling conditions	Low
	1-(4-Fluorophenyl)-ethanone	142	solubility in water is slightly soluble	stable under normal temperatures and pressures	Low

	p-Nitroaniline	142	solubility in water is 0.8 g/L	stable at room temperature in closed containers under normal storage and handling conditions	Low
	3,5,5-Trimethyl-2-cyclohexen-1-One	142	solubility in water is soluble	stable under ordinary conditions	Low
	1-Methyl-5-t-butylpyrazole	142			Low
	1-Methyl-3-t-butylpyrazole	142			Low
	3(5)-Methyl-5(3)-t-butylpyrazole	142		stable under normal conditions	Low
	3,5-Diethyl-4-methylpyrazole	142			Low
	Dimethylphenylphosphine	142	solubility in water is insoluble	stable under normal conditions	Low
	1,5-Diazabicyclo[4.4.0]dec-6-ene (DBD)	142			Low
	Homosalate	149	water solubility is <0.1 g/100 mL at 26°C	photostable as an emulsion and in various solvents	Low
140 *	p-Fluorobenzamide	142	water solubility is 1.41E+04 mg/L at 25°C	stable under normal temperatures and pressures	Low
	3-Fluoro-benzamide	142			Low
	3-CH ₃ SC ₆ H ₄ NH ₂	142			Low
	N,N-Dimethyl-4-fluoroaniline	142			Low
	5,5-Dimethyl-3-amino	142			Low
	2-Cyclohexenone	142	miscible in alcohol, acetone, benzene and water	stable	Low
	1-(2-Methyl-1-propenyl)-piperidine	142			Low
	1-Cyclopentylpyrrolidine	142			Low
	Lanthanum	142			Low
	N, N-dimethylhistamine	142		stable	Low
	1,5,7-Triazabicyclo[4.4.0]dec-5-ene	142	solubility in water (g/L) is partly miscible	stable	Low
141 *	Decene				High
	Cyclodecane		solubility in water is insoluble	stable	High
142					Low
143 *	3-hexenyl acetate	149	solubility in water is insoluble, soluble in alcohol	stable under normal conditions	Low
	Nonanal	149	solubility in water is insoluble	stable	Low

	Decane		less dense than water and insoluble in water	normally stable, even under fire exposure conditions, and that do not react with water	High
144					Low
145 *					Low
146 *					Low
147	1,2-Dichlorobenzene	141	water solubility is 0.13 g/L (20°C)	stable	Low
	Glutamine		solubility in water is soluble		High
	Diallyl disulfide		soluble in alcohol, chloroform, ether, and carbon tetrachloride, insoluble in water		High
148	1,2-Dichlorobenzene	141	solubility in water is 0.01%	stable	Low
	Glutamic acid		solubility in water is 7.5 g/L (20°C), 0.00035g/100g ethanol (25°C)		High
149	1,2-Dichlorobenzene	141			Low
150	1,2-Dichlorobenzene	141			Low
	Methionine		solubility in water is soluble		High
	2-mercaptoindole			stable	High
151	1,2-Dichlorobenzene	141			High
	Thymol		solubility in water is insoluble	stable	Low
	Ethyl benzoate	149	water solubility is insoluble	stable	Low
	1,2,4,5-Hexanetetrol	145			Low
152					Low
153	Methyl salicylate	149	solubility in water is soluble slightly in water, alcohol	stable under normal conditions of use and storage	Low
154					Low
155 *	Eucalyptol		water solubility is 3500 mg/L at (21°C)	stable	Low
	Epimeric pair			stable	High
	Biphenyl		solubility in water is 4.45 mg/L	stable	High
156					

157	Menthol		solubility in water is slightly soluble		
	Decanal	149	water solubility is insoluble	stable	
	4-hydroxynonenal		soluble in ethanol to 100 mM and in DMSO to 100 mM	stable	High
158 *					
159 *					
160	Sulfur mustard		solubility in water is negligible, soluble in ether, benzene, lipids, alcohol	stable	High
161 *					
162 *	Carnitine		very soluble in water, 800 g·l ⁻¹ (20°C)	stable at room temperature and should be stored away from light to avoid any chemical degradation	High
163 *	Allicin		soluble in chloroform, water (slightly), alcohol, ether, and benzene	unstable	High
164					
165 *					
166					
167					
168					
169 *	Selenocysteine		water solubility is 325.0 mg/mL		High
170 *					
171	Grapefruit mercaptan		insoluble in water, soluble in most organic solvents	stable under recommended storage conditions	High
172					
173	Decanoic acid		solubility in water is 0.015 g/100 mL (20°C), soluble in alcohol, ether, CHCl ₃ , C ₆ H ₆ , CS ₂ , acetone		High

	Sulfanilamide		solubility in water is 7.5 g/L at 25°C	stable under normal temperatures and pressures	High
174					
175	Arginine		solubility in water is 14.87 g/100 mL (20°C), slightly soluble in ethanol insoluble in ethyl ether		High
176					
177					
178					
179	Anthracene		solubility in water is insoluble, soluble in alcohols, benzene, Hydronaphthalene, carbon disulfide, chloroform, and other organic solvents	stable under ordinary conditions	High
180					
181	1,2,4-Trichlorobenzene	141	solubility in water is 30 mg/L	stable under normal temperatures and pressures	Low
182 *	1,2,4-Trichlorobenzene	141			Low
183 *	1,2,4-Trichlorobenzene	141			Low
	Dimercaptosuccinic acid		water-soluble		High
	Benzophenone		water solubility is insoluble	stable under ordinary conditions	High
184 *	1,2,4-Trichlorobenzene	141			Low
185 *	Dibenzothiophene		solubility in water is insoluble, solubility in other solvents in benzene and related		High
	Tridecane		solubility in water is 0.0047 mg/l, very soluble in ethyl alcohol, ethyl ether, soluble in carbon tetrachloride		High
	Isoflurane		water solubility is	stable	High

			13.5 mM at (25°C)		
186					
187 *					
188					
189					
190	Dimethyldiselenide			stable	High
191					
192					
193 *					
194					
195 *					
196 *					
197 *					
198 *					
199	Tetradecane		water solubility is 2.2×10^{-3} mg/L at 25°C, soluble in ether, acetone, soluble in alcohol	normally stable, even under fire exposure conditions, and that do not react with water	High
200					

Table 7: The Organosulfur compounds.

Organosulfur Compounds	Sulfoxides	Chemical compounds that contain a sulfinyl functional group attached to two carbon atoms.	alliin
			DMSO
	Sulfones	Chemical compounds that contain a sulfonyl functional group attached to two carbon atoms.	dimethyl sulfone.
			Sulfolane
	Sulfimides	Chemical compounds that contain a sulfur to nitrogen double bond.	methylphenylsulfoximine
			S,S-diphenylsulfilimine
	Disulfides	Chemical compounds that contain a disulfide bond.	diphenyl disulfide
			C ₆ H ₅ S-SC ₆ H ₅
	Thioethers	Functional group in organosulfur chemistry with the connectivity C-S-C.	dimethylsulfide
			methionine
	Thioesters	Chemical compounds that contain a functional group C-S-CO-C. They are the product of esterification between a carboxylic acid and a thiol.	acetyl-CoA
			malonyl-CoA,
	Thioacetals	Sulfur analogue of acetals. They are prepared by reacting a thiol with an aldehyde like acetals:	
	Thioketones	Organosulfur compounds that are related to conventional ketones, thioketones have the formula R ₂ C=S, which is reflected by the prefix "thio-" in the name of the functional group.	Thiobenzophenone
	Thioaldehydes	Functional group in organic chemistry that is similar to analdehyde, RC(O)H, in which a sulfur (S) atom replaces the oxygen (O) atom of the aldehyde (R represents an alkyl or aryl group).	Thioformaldehyde
H ₂ C=S			
Thiosulfinates	Functional group that consist of the linkage R-S(O)-S-R (R are organic substituents).	Allicin	
		S-benzyl phenylmethanethiosulfinate	
Thioamides	Functional group with the general structure R-CS-NR'R, where R, R', and R are organic groups.	Thioacetamide	
Thiocarboxylic acids	Organosulfur compounds with the general formula RC(O)SH. They are related to carboxylic acids by replacement of one oxygen centre by sulfur.		
S-Nitrosothiols	Organic compounds or functional groups containing a nitroso group	S-Nitrosoglutathione	
		S-Nitroso-N-	

		attached to the sulfur atom of a thiol	acetylpenicillamine
	Thiols	Organosulfur compounds that contain a carbon-bonded sulfhydryl ($-C-SH$ or $R-SH$) group (where R represents an alkane, alkene, or other carbon-containing group of atoms).	Methanethiol
			Ethanethiol

Part 2: 5.7.1. Linear Time Dependence

In studying the changes in VOCs behaviour within the time, some of them show a linear behaviour. This linear time dependence occurs in different variants, as follows:

5.7.1.1. Constant Linear Time Dependence

Metabolites such as hydrogen sulfide ($m/z=35$), propene ($m/z=43$) and allyl isothiocyanate ($m/z=100$) show a constant linear time dependence, as illustrated in Figure 5.10 for the isotope of isoprene ($m/z=67$). The fitting curve gives us an indication that these types of VOCs do not interact with each other, there is no correlation with other analytes, so their concentrations stay nearly the same or there is some interactions that shows a decreasing and an increasing (fluctuation) around the average value.

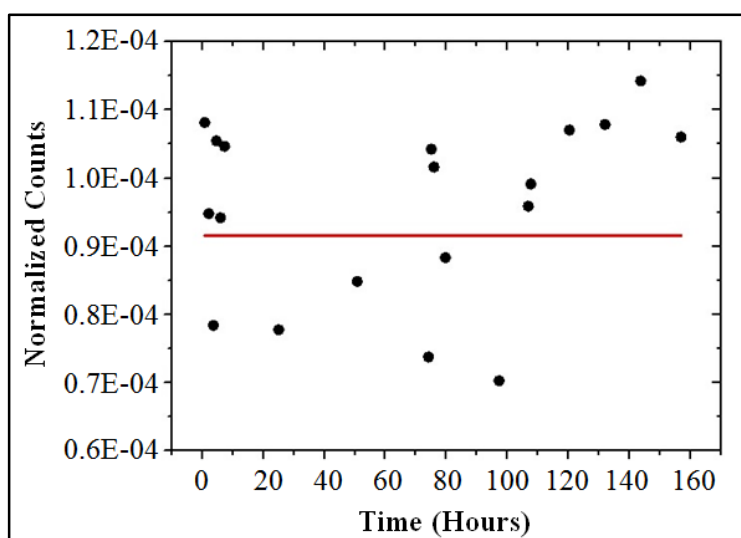


Figure 5.10: The isotope of isoprene ($m/z=67$) shows a constant linear time dependence.

5.7.1.2. Increasing Linear Time Dependence

Metabolites such as ethane ($m/z=31$), carbon disulfide ($m/z=77$) and hexene ($m/z=85$) show an increasing linear time dependence, as illustrated in Figure 5.11 for the formaldehyde

($m/z=57$). The fitting curve gives us an indication that these types of VOCs increase due to their constant relation with other metabolites that make them to increase linearly in time.

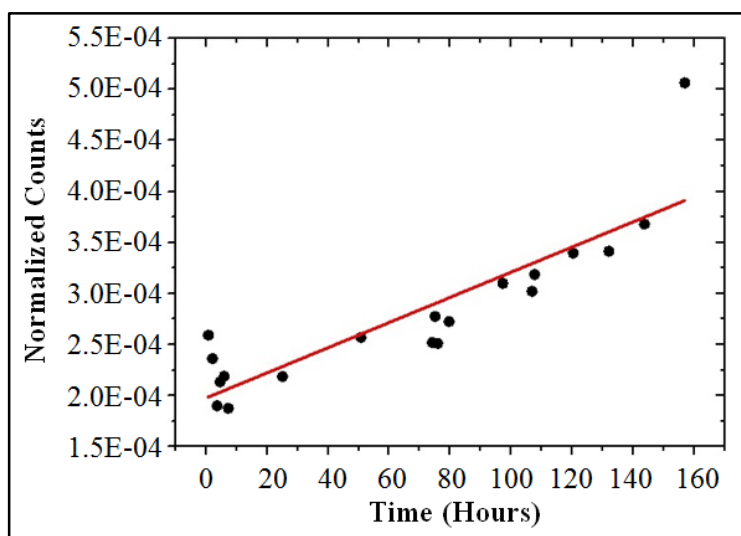


Figure 5.11: The formaldehyde ($m/z=57$) shows an increasing linear time dependence.

5.7.1.3. Decreasing Linear Time Dependence

Metabolites such as water ($m/z=50$), benzonitrile ($m/z=104$) and decanoic acid ($m/z=173$) show a decreasing linear time dependence, as illustrated in Figure 5.12 for the isotope of methanol ($m/z=34$). The fitting curve gives us an indication that these types of VOCs decrease due to their constant relation with other metabolites that make them to decrease linearly in time.

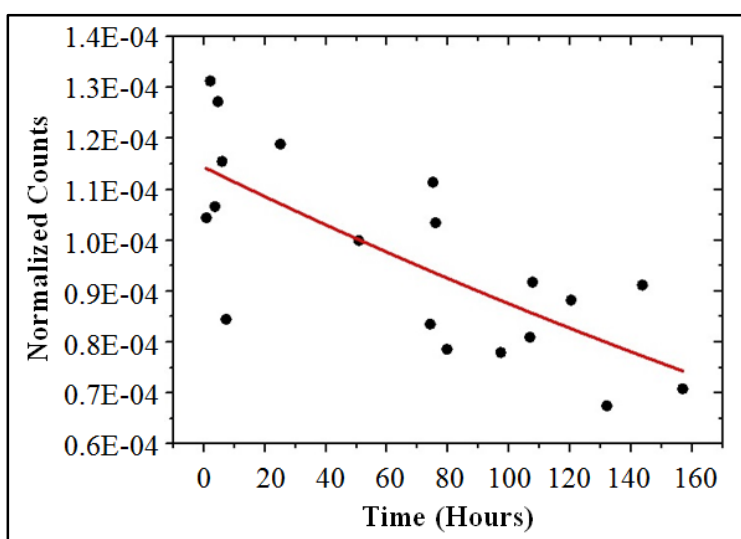


Figure 5.12: The isotope of methanol ($m/z=34$) shows a decreasing linear time dependence.

5.7.2. Nonlinear Time Dependence

Beside the linear time dependence of some VOCs, other VOCs show a non-linear behaviour. This non-linear time dependence occurs in different variants, as follows:

5.7.2.1. Rising Kinetics

Metabolites such as heptene ($m/z=99$) shows a rising kinetics, as illustrated in Figure 5.13 for the pentane ($m/z=71$). The fitting curve gives us an indication that these types of VOCs increase due to their relation with other metabolites that make them to increase in time.

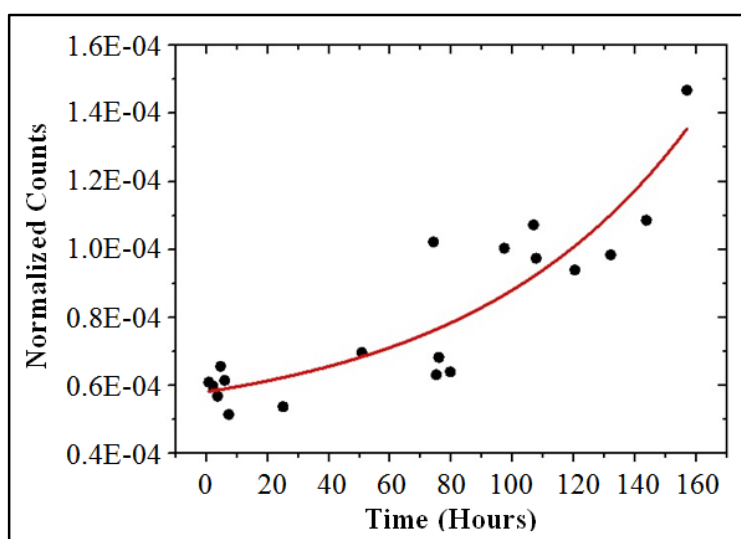


Figure 5.13: The pentane ($m/z=71$) shows a rising kinetics.

5.7.2.2. Decaying Kinetics

Metabolites such as acetone ($m/z=59$), trimethylamine ($m/z=60$) and isovaleric acid ($m/z=103$) show a decaying kinetice, as illustrated in Figure 5.14 for the methanol ($m/z=33$). The fitting curve gives us an indication that these types of VOCs decrease due to their relation with other metabolites that make them to decrease in time.

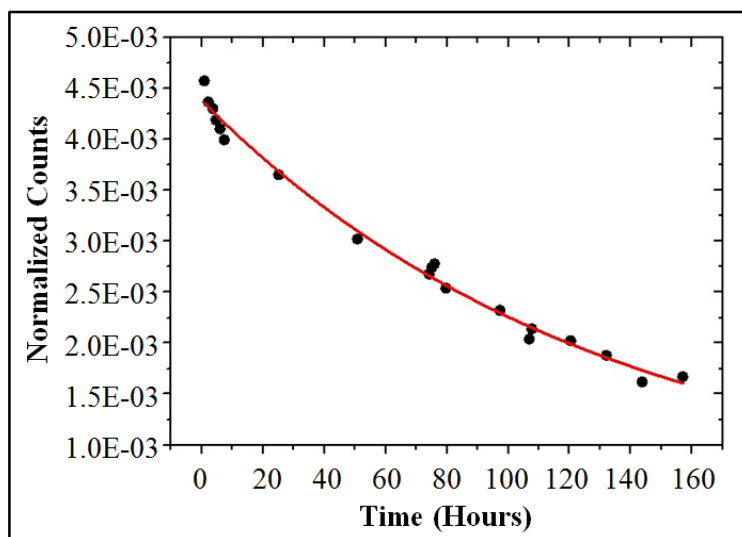


Figure 5.14: The methanol ($m/z=33$) shows a decaying kinetics.

Part 3: 5.8.2. Other VOCs Biomarkers

5.8.2.1. Methyl group-CH₃

As shown in figure 5.63, there is an increase in the methyl group-CH₃ (m/z=15) counts in vegans group compared to others, this increase may be due to the intake of B12 fortified food products and/or B12 supplements.

B12 is found naturally in animal products, so vegans suffer from B12 deficiency because they do not eat foods that come from animal, for that they must take B12 fortified food products and/or take B12 supplements to prevent this deficiency.

A (methyl group-CH₃) is transferred from methylcobalamin (B12) or trimethylglycine (TMG), this will led to the conversion of homocysteine (m/z=136) to methionine (m/z=150).

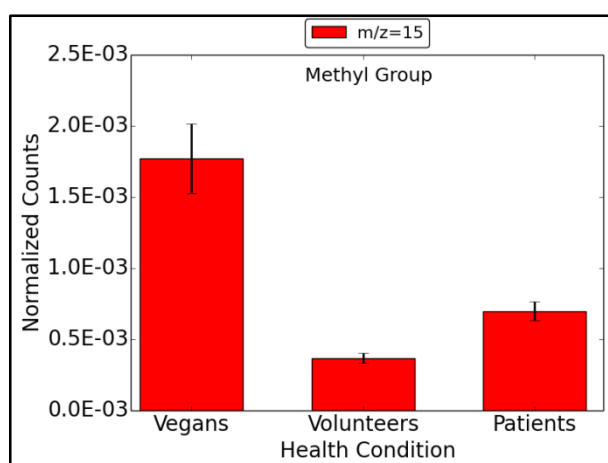


Figure 5.63: The methyl group.

5.8.2.2. The Water and Water Multimere Peak Identification

There is an increase in (H₂O) counts in volunteers group compared to others. The reason for this is not pathological, but it is due to the high humidity caused by the hot weather at the measuring time (the temperature was 30°C-35°C). The next highest counts belongs to the patients group. The samples from these two groups were collected nearly in the same month,

but at different ambient temperature. The (H_2O) counts that belongs to vegans group is less than other groups because the samples were collected later at cooler temperature.

Figure 5.64 shows the water and water multimeres such as H_3O^+ ($m/z=19$), H_2DO^+ ($m/z=20$), HD_2O^+ ($m/z=21$), D_3O^+ ($m/z=23$), $\text{H}_3\text{O}^+(\text{H}_2\text{O})$ ($m/z=37$), ($m/z=38$), $\text{O}_2^+\text{H}_2\text{O}$ ($m/z=50$) and $\text{H}_3\text{O}^+(\text{H}_2\text{O})_2$ ($m/z=55$).

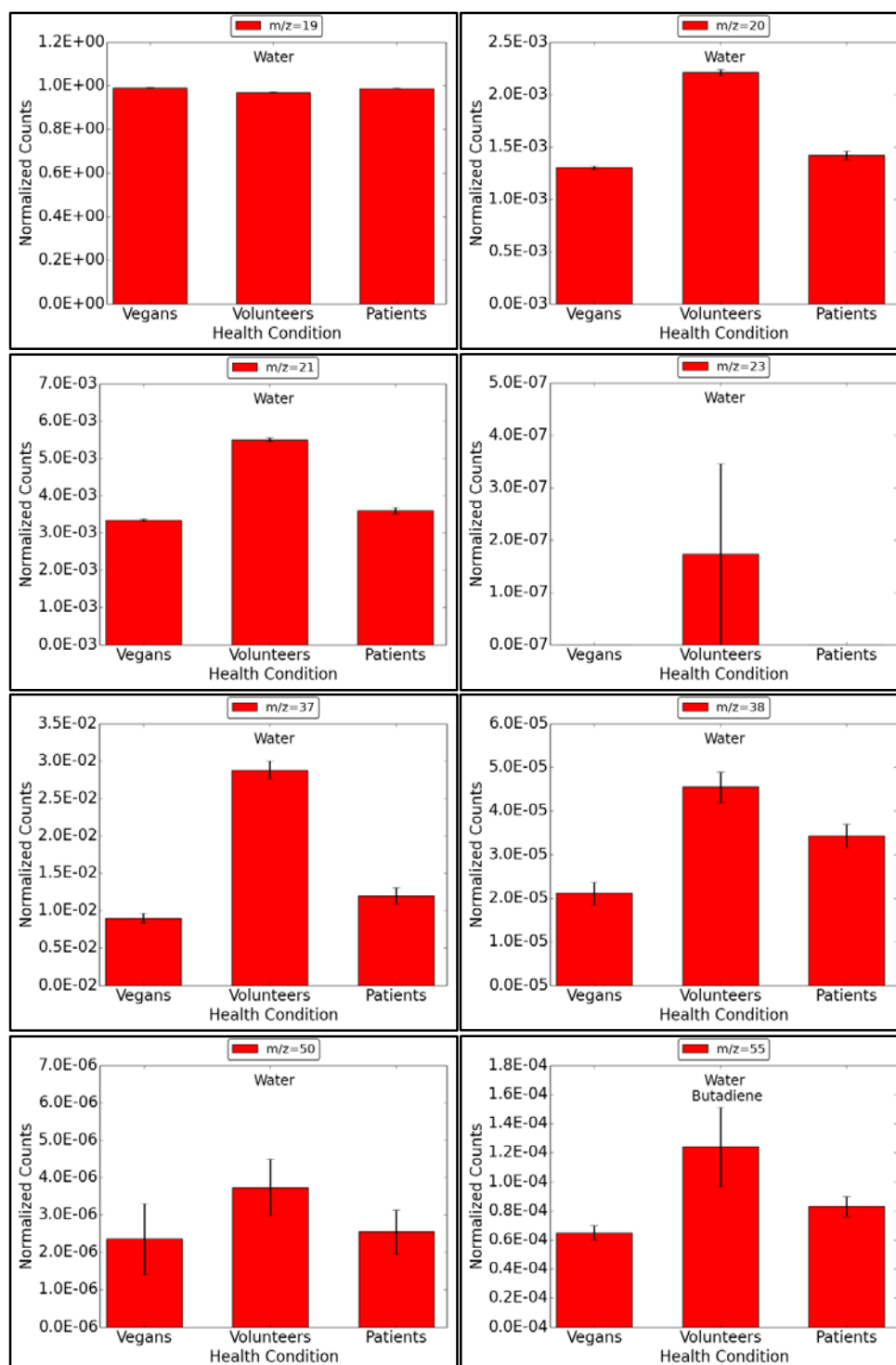


Figure 5.64: The water and water multimeres.

Part 4:

Chapter 6

Results and Discussion of IMS

The data that analyzed for breath samples using IMS are presented and discussed in this chapter.

After collecting the data from the IMS device, the data were analyzed by the VisualNow program. This program is ion mobility spectrometry program.

VisualNow was previously known as BBImAnalyse software, which was the first software designed to analyse the data from the MCC-IMS based on the thermal plot. It was developed by Bertram Bödeker during his diploma at the Leibniz Institute for Analytical Sciences (ISAS) [90]. Then B&S Analytik GmbH, Dortmund developed, improved, used and renamed this program to VisualNow, which is programmed in Java. With the VisualNow program it is possible to deal with an increased amount of measurements as analysing and comparing, in addition to applying the statistical values visualisation of the results as Box-and-Whisker-Plots.

6.1. VisualNow Window

The main VisualNow window shows two dimensional-plot displaying the whole IMS chromatogram and all technical parameters from the data file, where the height of the signal, which is the signal from the Faraday plate in the IMS device, is colour-coded in both plots, as illustrated in Figure 6.1.

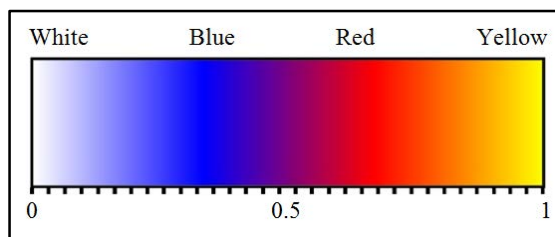


Figure 6.1: The colour-code of the heatmap visualisation [91].

The colour-code is set to map values from zero to one according to the heights or the intensities of the peaks. The white colour is zero, the blue colour is low intensity, the red colour is medium intensity and the yellow colour is one.

The term heatmap is used because the map is related to temperature. Typically, blue colour represents low value that is related to low temperature, while red and yellow colour represent high values that are related to high temperatures.

Besides the main window, there are two additional windows. The one on the right shows one single multi-capillary column spectrum at the selected ion mobility and the lower one shows single ion mobility spectrum at the selected retention time. Additionally, the parameters such as, the ion mobility (k_0), the inverse ion mobility ($1/k_0$) that is proportional to the drift time (DT) and the retention time (RT) of the data point at the current mouse position are shown in the lower-right side of the main window.

In each spectrum there is a dominant signal known as a reactant ion peak (RIP) that looks as a broad vertical line on the chromatogram and has a highest and broadest peak [83, 109]. It is considered as a dominant signal that caused by IMS radioactive ionisation source and further peaks that have the information about the sample measured substances. Due to the electrical field, the reactant ions brought into the drift region then towards the Faraday plate, where there is no analyte molecules available to form a spectrum that contains the RIP. Figure 6.2 shows the VisualNow window with RIP.

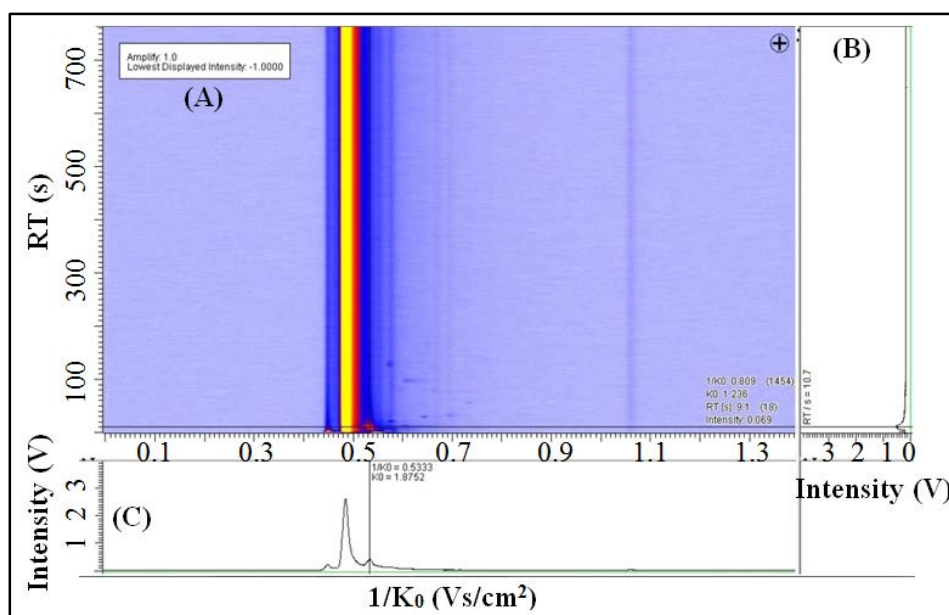


Figure 6.2: The VisualNow window showing the RIP: (A) the main window, (B) the single chromatogram at the selected ion mobility on the right side of the main window and (C) the single spectrum at the selected retention time lower the main window.

6.2. Data from MCC-IMS

The resulting data from the MCC-IMS device is stored in a file that contains many spectra sorted by the retention time. Each spectrum consists a number of ionised molecules at a specific drift time. Each spectrum is an average of many single scan. Figure 6.3 shows the MCC-IMS spectra.

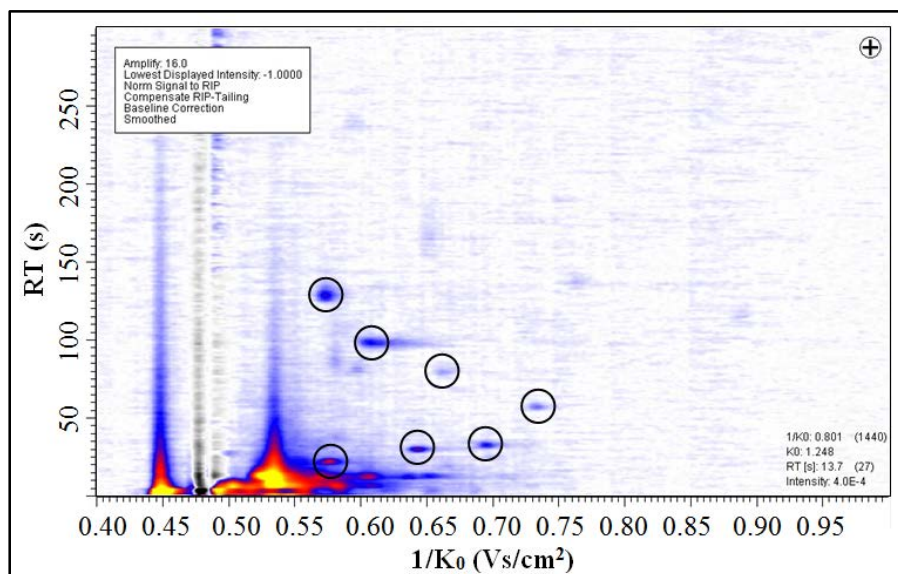


Figure 6.3: Two-dimensional MCC-IMS spectrum, the x-axis represents $1/k_0$ (Vs/cm^2) and the y-axis represents the RT (s).

One single scan requires 100 ms. To build one spectrum 10 scans are used, this leads to an acquisition speed of one spectrum per second. This is essential for signal-to-noise ratio improvement to separate the weak signals from the noise. The measurement by this device consists of 500 single spectra, each spectra has 2000 values. As a result, one million data points can be obtained and each of them has three types of parameters: i) retention time, ii) drift time and iii) intensity.

6.3. The Pre-requisites for Sample Analysis

VisualNow program can show a three-dimensional plot for the IMS chromatogram. To get a three-dimensional separation along with the ion mobility and intensity for analysis with a high resolution, it is very important to use MCC as a pre-separation unit for big and different samples. This sample analysis need to be fast, accurate and has a high resolution [77].

To show a single spectra of several peaks and examine it visually, the spectrum is selected and shown in a separate plot. The peaks that are captured by MCC-IMS can be identified and compared in three-dimensional plot in regards to the characteristics of the data.

In the three-dimensional plot, the x-axis is $1/k_0$ (Vs/cm^2), which is proportional to DT (ms) as mentioned previously, y-axis is RT (s) and z-axis is the intensity (V), as shown in Figure 6.4.

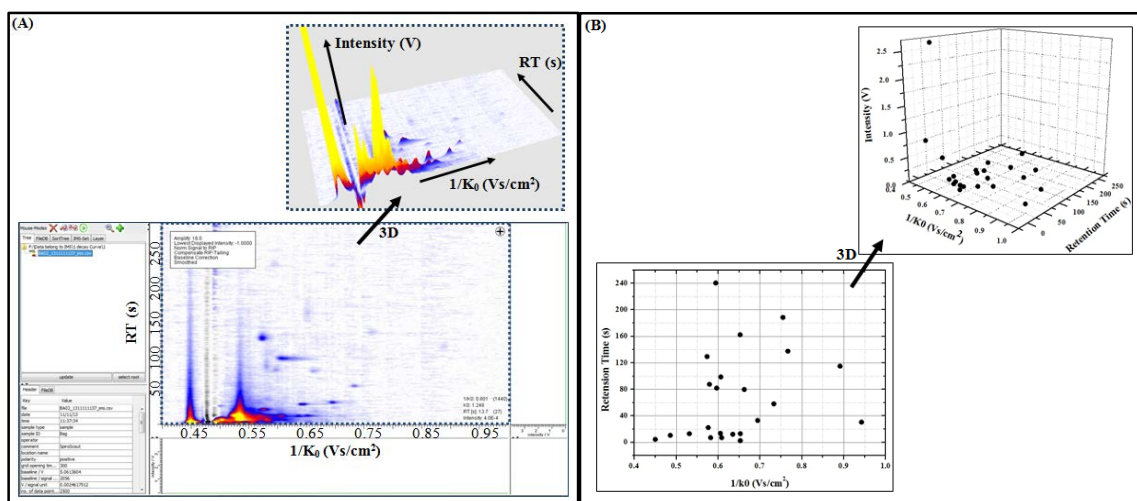


Figure 6.4: Chromatogram three-dimensional plot of MCC-IMS measurement: (A) a heatmap for the three-dimensional plot and (B) a schematic view of the three-dimensional plot.

6.4. The Comparability of the Measurements

Different factors affecting the characteristic of the drift and retention time, such as pressure, temperature and electrical field, lead to baseline shift that prevents the comparability of the measurements. Additionally, there are other affecting factors: i) baseline correction, ii) compensate RIP-tailing, iii) norm signal to RIP, iv) smoothing and v) median smoothing, as illustrated in Figure 6.5.

In the baseline correction measurement, there is no analyte peak in the values of the signal intensity, but there will be pure noise. To compare the heights of the peaks from different measurements the baseline shift should be adjusted.

In spite of the estimation of the baseline shift based on the initial measurement, the baseline correction has an effect on single RT spectrum by producing a variation around zero in the noise region for the whole spectrum, see figure 6.5.B and figure 6.6.

In the compensate RIP-tailing, there is a variation in the ion velocity because of the random reactions of the ion molecules in the drift tube, this will cause RIP-tailing, which is considered one of the major problem.

RIP-tailing is a source of distribution that appear on the right side of the RIP as a signal descent, from $1/k_0 = 0.5$ (Vs/cm²) to $1/k_0 = 0.8$ (Vs/cm²), where the baseline of a whole spectrum increases with a diminishing value by RIP leading to change the heights of the peaks parts of the drift time axis. It is difficult to separate peaks from noise with RIP-tailing and it causes problems by changing the heatmap colour-code for better visualisation of the peak.

For that, it needs to clarify the measurements of IMS by fitting the function of the detailing that represents the tailing then subtracting that from each spectrum. So by RIP detailing, the peaks in the spectra part become clearer and can hold the beneficial effects of the operations of the wavelet, see figure 6.5.C and figure 6.6.

In the norm signal to RIP, the intensity will be standardized using a correction factor in such a way that the signal height of the RIP becomes 1.0., see figure 6.5.D and figure 6.6.

In spite of that, the RIP found in every spectrum and has a great benefit for alignment of the $1/k_0$ and normalisation of the intensity, but it prevents additional analysis and visualisation of the peaks. RIP controls every measurement but it has no information about the samples analytes.

The IMS data contains a numbers of data points, which is considered as a noise that interact with data analysis. This problem remains even after introducing a pre-processing step, but by smoothing and denoising method, these problems are solved.

In the smoothing method, the high frequency components is removed regardless to their amplitude. By smoothing the wavelet, the dimensionality and a higher signal-to-noise ratio will reduce, see figure 6.5.E and figure 6.6.

In the median smoothing, it is an additional smoothing with the strong noisy data, see figure 6.5.F and figure 6.6.

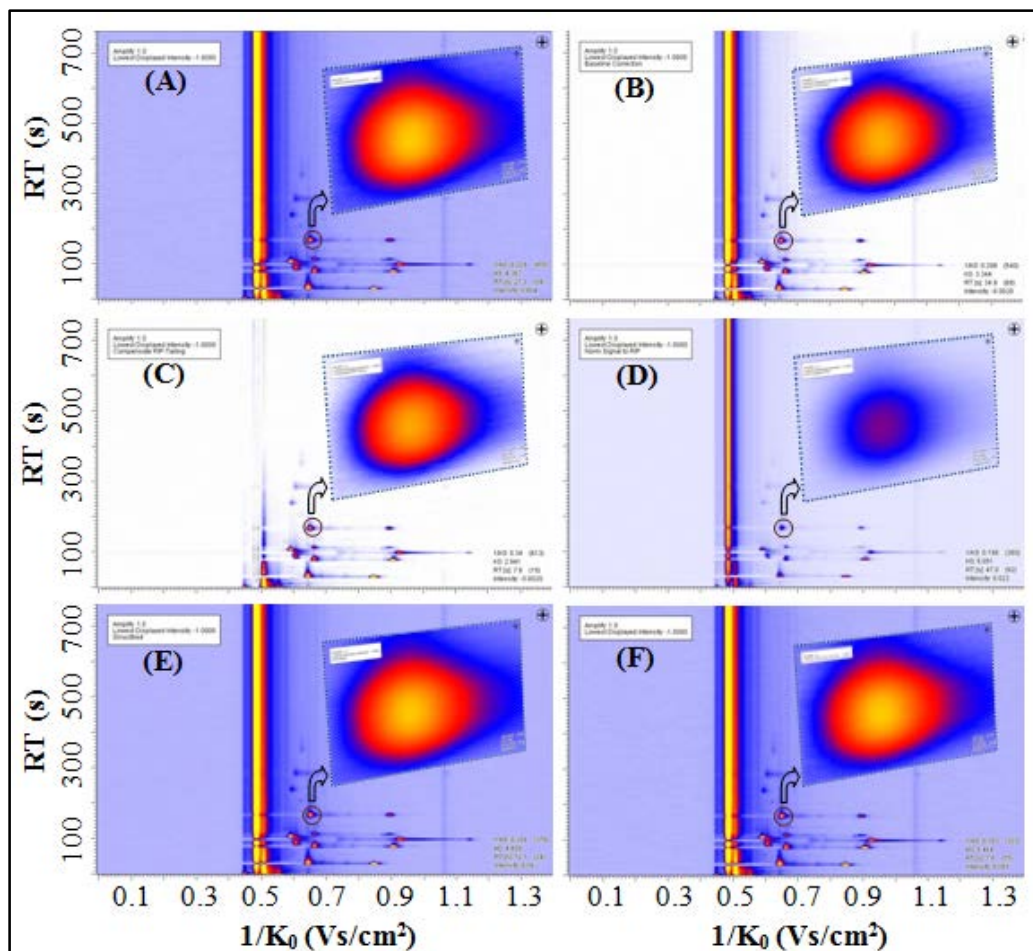


Figure 6.5: MCC-IMS chromatograms of (A) Raw, (B) Baseline Correction, (C) Compensate RIP-Tailing, (D) Norm Signal to RIP, (E) Smooth and (F) Median Smooth.

6.5. Comparisons within Spectra and Chromatograms

Comparing spectra and chromatograms of the same measurement are possible by marking the signal peaks. To compare the peaks, the positions of the peaks should be marked manually one after another in the main window.

To compare different spectra and chromatograms that belong to different measurements or different data files. These marked spectra and chromatograms should be move to another window for additional comparisons.

In the comparison of spectra, the comparison will be according to the $1/k_0$ value, which is proportional to the drift time (DT) value in the IMS, as shown is Figure 6.6.A.

In the comparison of chromatograms, the comparison will be according to the retention time (RT) value in MCC, as shown in Figure 6.6.B.

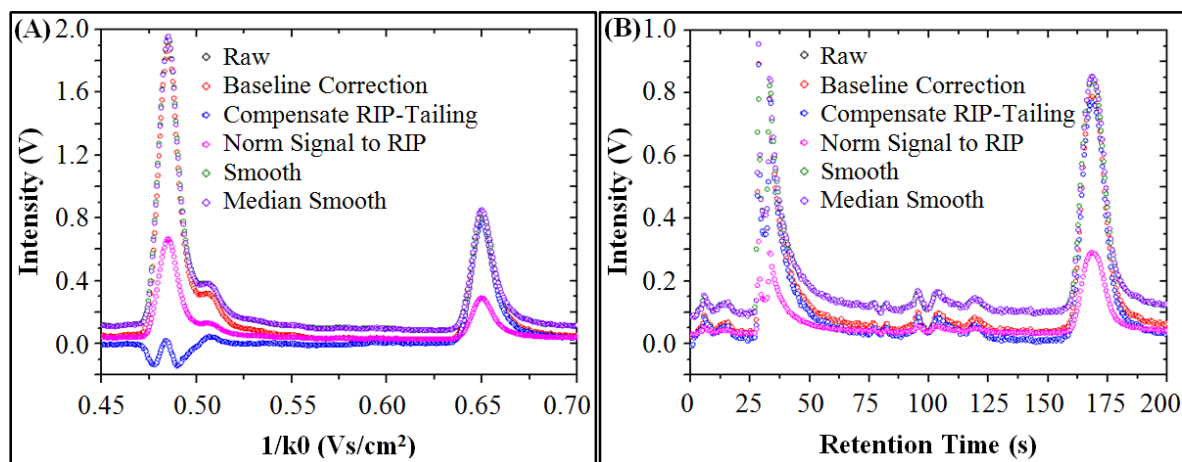


Figure 6.6: (A) the spectra and (B) the chromatogram comparisons between: raw, baseline correction, compensate RIP-Tailing, norm signal to RIP, smooth, and median smooth for the same peak.

6.6. Peak Detection and Comparison

To study the similarity and the differences of the measurements, there must be a group of peaks that are related to the same analytes. The region with the same peak characteristics is selected and compared to the same region in another measurement.

It is very important to determine the peak intensities that belong to the same analyte for the compared measurements. In the peak finding technique, the regions of the peaks will be as descriptors of the peak group, which can be identify a specific analytes. This region is characterized by the centre point, $1/k_0$ radius and RT radius.

All peak intensities can be shown in a different manner after successful peak detection and tolerance boundaries definition. The method of visualisation should support class based analysis because the purpose of many experiments depend on comparing the intensities of different classes.

For a good comparison, the detected analytes should be arranged in a list according to their peaks. $1/k_0$ and RT should also be determined.

6.7. Factors Effecting on the VOCs Intensity

There are many factors affecting the intensity or the concentration of VOCs such as, age, gender, Body Mass Index (BMI) and diet [3, 110]. The type of the consumed foods, drinks and even smoking affect the VOCs intensity [3, 111]. In this part of the study, we will discuss some of these factors.

6.7.1. Comparative Study between Different Statuses of Diet

Different statuses of diet is considered one of the factors that affect the VOCs intensity. This effect refers to the different contents or ingredients of the foods and drinks, for example, onion, mint, garlic and other types of food contents that stay in the breath for a long time as compared to others.

In our study, the comparison was done with different statuses of diet for the same person to avoid other affecting factors such as gender, age and even smoking. Figure 6.7 shows the behaviours of three different analytes, which are characterized by their $1/k_0$ and RT, affected by different diet statuses: i) before eating (fasting from the day before), ii) after eating, iii) after washing the mouth with Listerine mouthwash, iv) after washing the mouth with tap water and drinking tap water many times and v) after chewing peppermint gum.

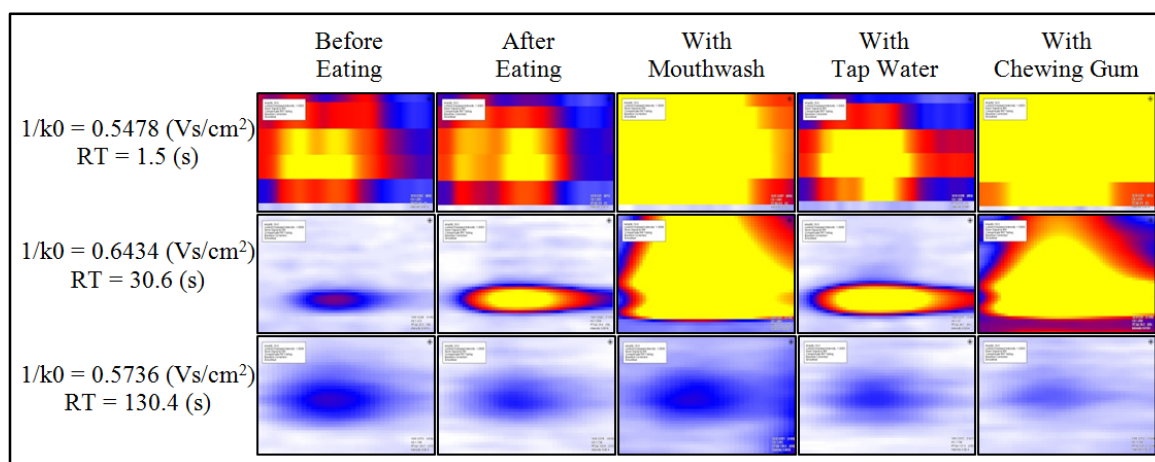


Figure 6.7: MCC-IMS heatmap showing the effect of different diet statuses on three different analytes that characterized by their $1/k_0$ and RT.

Some VOCs are decreased in their intensity and others are increased. This variability in their behaviours depends on the analyte and how it is affected by the different statuses of diet. So let us discuss each diet status separately:

i. Before Eating (Fasting From the Day Before)

During fasting or starving the carbohydrates in the body will decrease, the carbohydrates are considered the source of energy in the body. To meet its energy requirements, the body starts to metabolize the fat.

According to *Sena S.F.* [112], “Fat or long-chain fatty acids from adipose tissue are metabolized by hepatocytes via beta-oxidation to sequentially remove two-carbon units (acetyl-CoA) from the fatty acid chain. Normally, acetyl-CoA is further oxidized in the citric acid cycle but when the capacity of this cycle is exceeded, ketogenesis occurs to produce three so-called “ketone bodies”: acetone, acetoacetate (AcAc) and betahydroxybutyrate (BHB), also known as 3-hydroxybutyrate” [113, 114].

Acetone is considered a biomarker for diabetes and it is one of the most abundant VOCs in human breath and is linked to dextrose and lipolysis metabolism.

According to *Thekedar S.* [3], “many studies and publications indicate an increase of the acetone concentration in the breath samples of volunteers for different fasting duration: 12 hr.

[115, 116], 9 hr. to 16 hr. [117] and 63 hr. [118]. These studies showed that the duration of fasting, the amount and the type of food consumed in the previous night before collecting the breathing sample affect the acetone concentration”.

Some studies were showed that under fasting condition, ammonia [119], phenol and di-limonene [118] also increased compared to other statuses, but other studies were showed a decrease in ethanol [118, 119] during fasting and ammonia is independent of fasting [115].

ii. After Eating

Some of the exhaled VOCs increase after eating; this increase is due to their origin from the consumed food. This changing in the concentration depends on the type and the amount of the food.

Ethanol increases in breath sample after its oral [120, 121] or sugar [122] consumption and also increases after a protein calori meal [119] consumption. Acetaldehyde increases after consumption of ethanol [120], methanol increases after eating an apple [123], acetone increases after proan-2-ol ingestion or after garlic consumption [124], sulphide compounds increase after garlic consumption [124] and furfurylthiol increases after drinking coffee [125] and etc.

iii. After Washing the Mouth with Listerine Mouthwash

After washing the mouth with Listerine mouthwash, some VOCs were increased in the exhaled breath due to their origin depending on the ingredients of the mouthwash.

The Listerine mouthwash ingredients are aqua, alcohol, sorbitol, poloxamer 407, benzoic acid, sodium saccharin, eucalyptol, methyl salisylate, aroma, thymol, menthol, sodium benzoate, sodium fluoride, alcohol, natrium fluoride, CI 47005 and CI 42053.

Eucalyptol analyte is found normally in human breath, and by washing the mouth with the Listerine mouthwash this will lead to an increase in its concentration.

Sorbitol is a sugar alcohol with sweet taste which is metabolized slowly in human body. It can be obtained from the reduction of glucose, changing the aldehyde group to a hydroxyl group.

CI 47005 also called quinoline yellow (WS) or food yellow 13. According to *Nordic Council of Ministers* [126], “It is manufactured by sulfonating 2-(2-quinolyl) indane-1,3-dione or a mixture containing about two-thirds 2-(2-quinolyl) indane-1,3-dione and one third 2-(2-(6-methylquinolyl)) indane-1,3-dione. It consists essentially of a mixture of sodium salts of disulfonates (principally), monosulfonates and trisulfonates of 2-(2-quinolyl) indane-1,3-dione and subsidiary colouring matters together with sodium chloride and/or sodium sulphate as the principal uncoloured components, it is described as the sodium salt. While CI 42053 which is also called fast green (FCF) or food green 3, is a sea green triarylmethane food dye”.

So all the VOCs that have the same origin of the ingredients are increased, but the VOCs that have the opposite origin to the ingredients are decreased.

iv. After Washing the Mouth with Tap Water and Drinking Tap Water Many Times

VOCs are found in water, which give the water the odour and the taste. Some VOCs may be harmful to the human health such as benzene that enters the ground water in several ways: from gasoline or oil spills or even from the leakage of fuel tanks underground.

Dichloromethane (methylene chloride) is a commonly detected VOCs in water. It may be found as a trichloroethylene, which is an industrial solvent used as a septic system cleaner and/or as tetrachloroethylene (perchloroethylene) that is used in the dry-cleaning industry.

The U.S. Environmental Protection Agency (EPA) has determined a maximum contaminant level (MCL) for each chemical. When the chemicals amount are lower than MCL, the water is considered safe to drink, but when one or more VOCs is higher than the limit, the water is not safe to drink.

Therefore, before drinking water, attention must be paid to the source of the water and eliminating the VOCs sources in water if one or two chemicals are found. By knowing the VOCs that are found in water, it is easy to study the effect of drinking water on exhaled breath sample.

v. After Chewing Peppermint Gum

The ingredients of peppermint chewing gum are sorbitol (sugar alcohol with sweet taste), gum base, glycerine (humectant), mannitol (sugar alcohol with sweet taste), flavours, and aspartame (non-saccharide sweetener).

VOCs increasing or decreasing in the breath sample depending on the origin of these VOCs and chewing gum ingredients.

According to *Rösing at al.* [127], “chewing gum has an effect on the production of Volatile Sulfur Compounds (VSCs). This study was concluded that VSC production is diminished after chewing gum and that the use of chewing gums reduces temporarily the VSC production enhanced by cysteine rinses”.

Figure 6.8 shows how three different analytes, which are known by their retention time and drift time, are affected by a different diet statuses according to the MCC-retention time (**on the left**) and IMS-drift time (**on the right**).

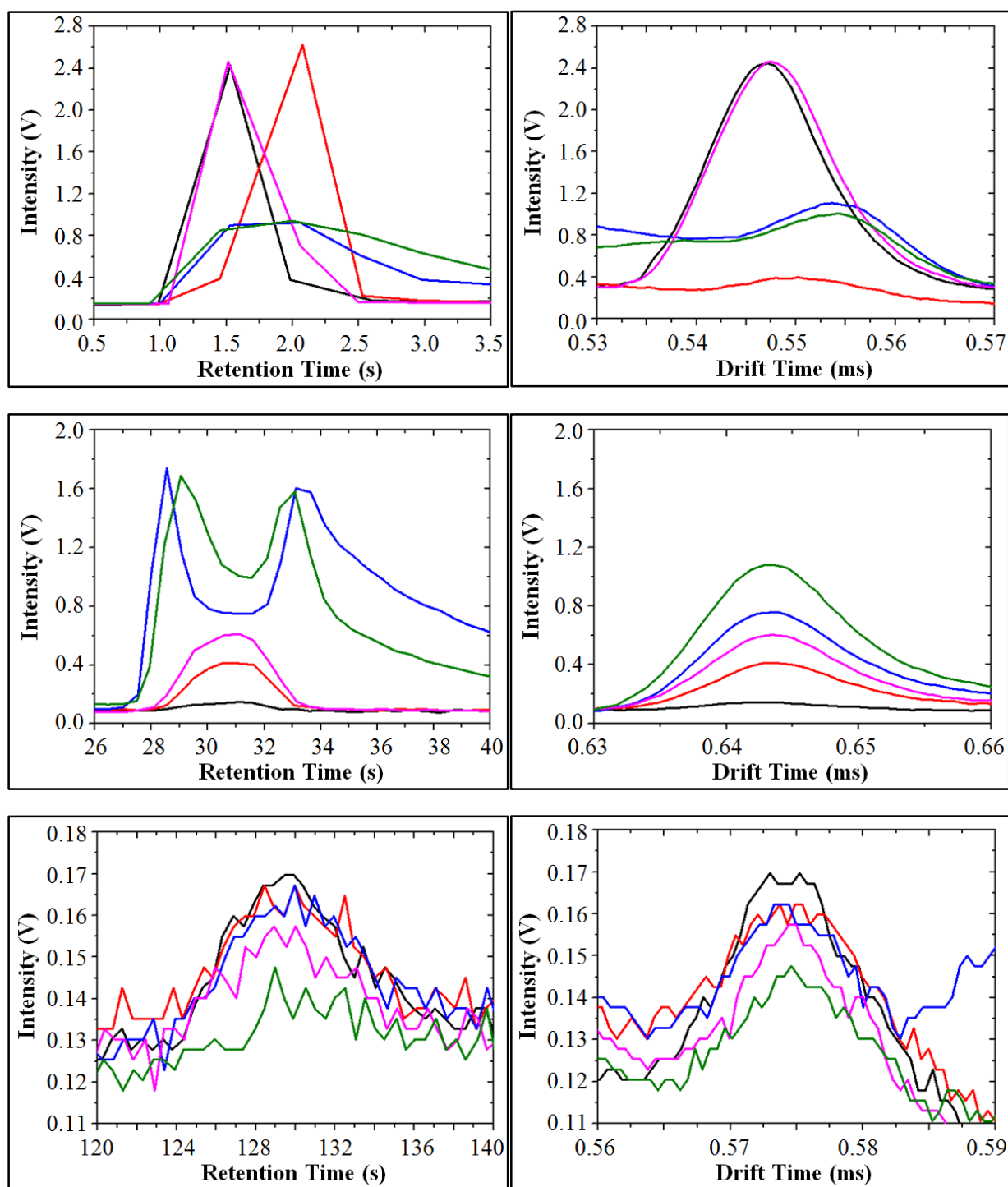


Figure 6.8: The different behaviours of three different analytes due to the different diet statuses in two parts of the device MCC (**on the left**) and IMS (**on the right**): **—** before eating, **—** after eating, **—** with mouthwash, **—** with tap water and **—** with chewing gum.

6.7.2. Comparative Study between Direct Breath and Indirect Breath

Because there are losses in the VOCs compounds that are found in Tedlar bags, this comparative study between direct breath and indirect breath from Tedlar bag is important to study the effect of Tedlar bag materials on analytes.

Figure 6.9 shows the differences in the intensities of three different analytes, which are characterized by their $1/k_0$ and RT in direct breath as compared to indirect breath.

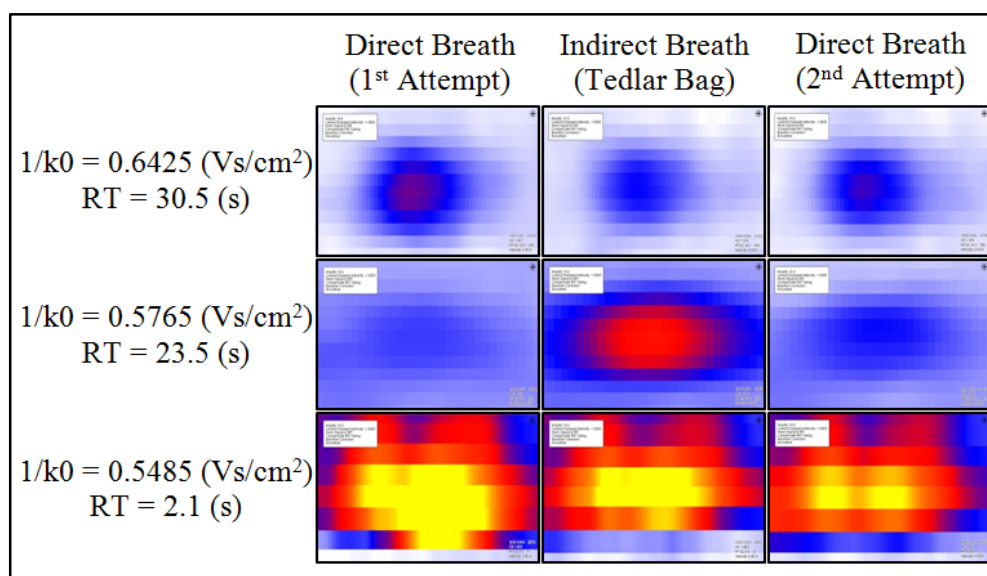


Figure 6.9: MCC/IMS heatmap showing the effect of Tedlar bag on three different analytes.

Previous studies showed that Tedlar bag produces artifacts due to its manufacturing process comparing to other types of bags, these artifacts are phenol and/or N,N-dimethylacetamide [128, 129, 130]. According to these artifacts that found in the Tedlar bag, the analysis of the chemicals are affected by increasing the concentration of the VOCs that have the same origin to these artifacts and decreasing the concentration of the VOCs that have the opposite origin to these artifacts.

Figure 6.10 illustrates how these three different analytes, which are characterized by their retention time and drift time, were affected by Tedlar bag according to the MCC-retention time (**on the left**) and IMS-drift time (**on the right**).

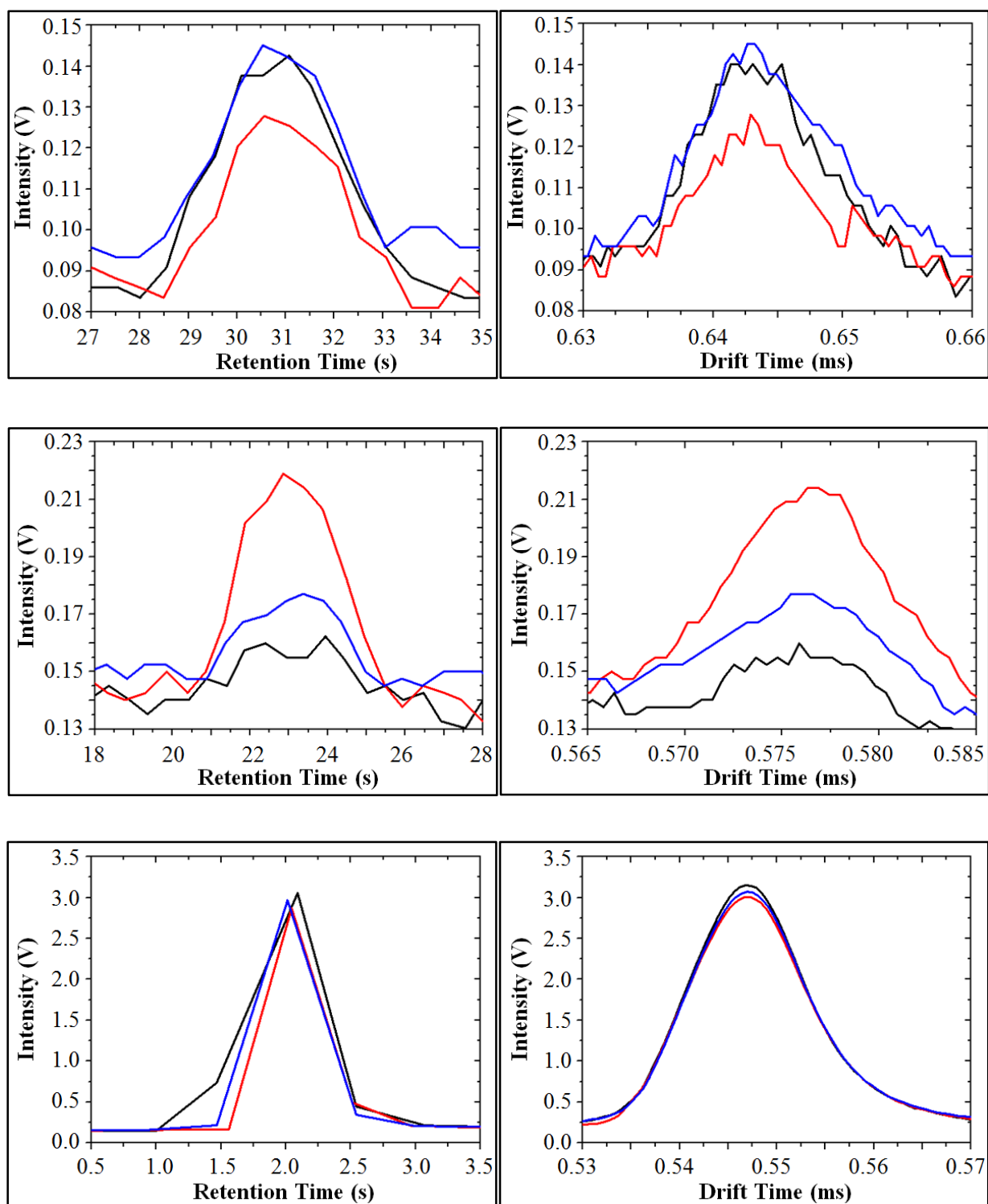


Figure 6.10: The different behaviours of three different analytes due to the way of breath in two parts of the device MCC (**on the left**) and IMS (**on the right**): — direct breath (1st attempt), — indirect breath (Tedlar bag) and — direct breath (2nd attempt).

6.7.3. Comparative Study between Smoker and non-Smoker

We studied the effect of smoking on VOCs because smoking is one of the reasons that cause lung diseases.

Figure 6.11 shows a three-dimensional of the different spectrum intensities between smoker and non-smoker. This comparison is done as: i) direct breath (1st attempt), ii) indirect breath (Tedlar bag) and iii) direct breathing (2st attempt).

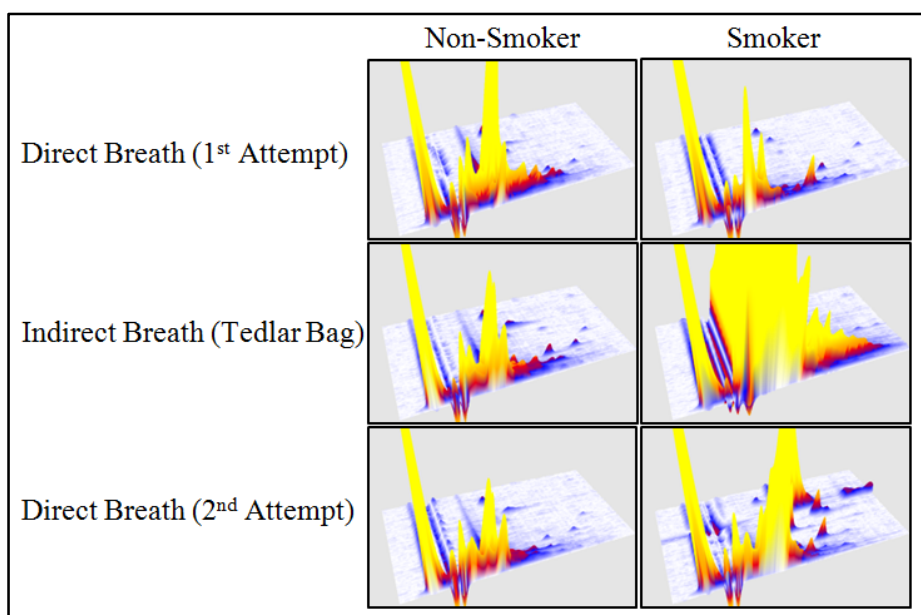


Figure 6.11: The three-dimensional view shows the effect of smoking and non-smoking on the spectra.

In direct breath (1st Attempt), the spectra of the smoker is nearly the same as the spectra of the non-smoker, because the smoker had not smoke for a while

In indirect breath (Tedlar bag), after smoking and breathing in the Tedlar bag, one can see how the spectra of the smoker changes when compared to spectra of the non-smoker. This difference between both spectra refers to two reasons: i) effect of smoking and ii) effect of Tedlar bag.

In direct breath (2nd Attempt), the intensity of both spectra decrease, but the spectra of the smoker still higher than the spectra of the non-smoker, here it refers only to one reason, the effect of smoking, phenol and/or N,N-dimethylacetamide artifacts.

Figure 6.12 shows the heat-map of the peaks and how these analytes are effected by smoking.

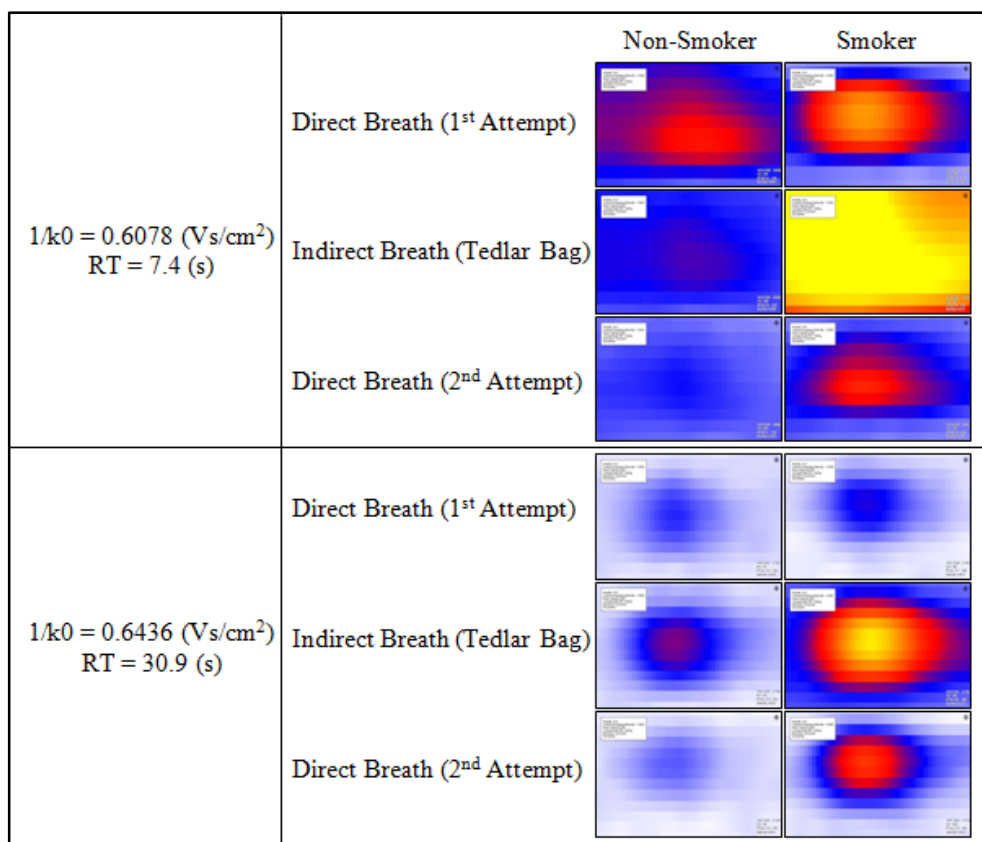


Figure 6.12: The MCC/IMS heatmap for two different analytes showing the effect of the Tedlar bag and the smoking status.

Both analytes in direct breath (1st Attempt) showed nearly the same intensity, but their intensities changed after breathing in the Tedlar bag (indirect breath) and showed different behaviours after smoking, then after direct breath (2nd Attempt), they showed a different decreases in the intensities.

The comparison between the ways of breathing into the device (direct or indirect) as well as the comparison between smoker and non-smoker are illustrated in Figure 6.13 by a Box-and-Whisker-Plot.

Box-and-Whisker-Plot is a graphical method of displaying variation in a set of data. It shows the mean and the median of the measurements as well as the ranges and the possible of the outliers. By Box-and-Whisker-Plot, it is easy to determine the peak intensity distribution in different classes and make the visualisations of a large number of peaks so clear instead of

single peak intensity. The characteristics and the benefits from Box-and-Whisker-Plot depend on the number of measurements and the aim of the analysis.

From Figure 6.13, it is obvious how the intensity of the analytes differ in both cases: i) comparing smoker with non-smoker and ii) comparing direct breath with indirect breath.

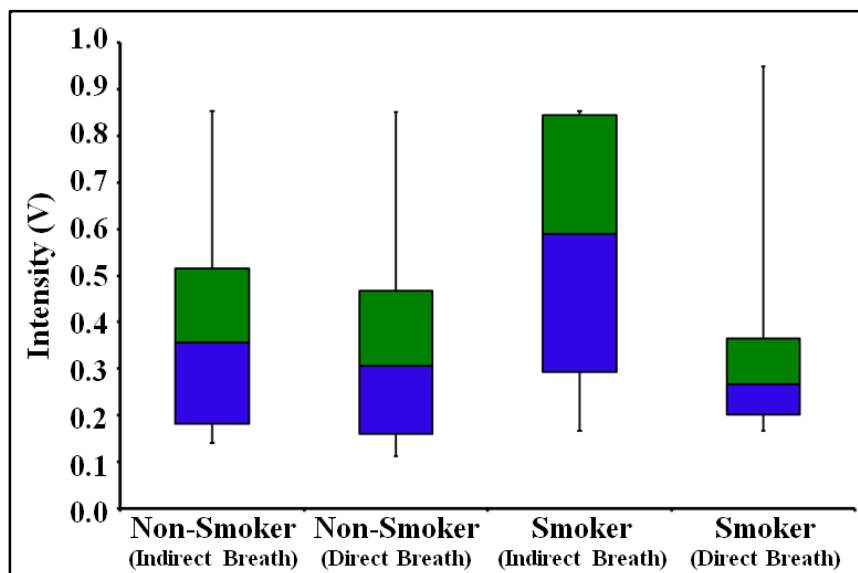


Figure 6.13: Box-and-Whisker-Plot showing the effect of the Tedlar bag and the smoking.

All VOCs that come from tobacco smoke are rapidly removed from the body by enzymatic reactions and excretion. Through smoking, two different types of VOCs are increased, acetonitrile and benzene [3, 131].

The presence of acetonitrile and other types of nitriles like acrylonitrile in breath samples are considered good markers for smoking.

After smoking, the concentrations of acetonitrile and acrylonitrile increase rapidly, then after a while the concentration of acrylonitrile decreases rapidly to the initial level, but the concentration of acetonitrile decreases very slowly and its concentration depends on the amount that had been inhaled. Thus, acetonitrile is a good marker for passive smoking [132].

Cigarette is the main source of benzene in smoker, for that benzene is a good marker for active smoking [133]. Benzene body burden in smoker is 6 to 10 times higher than in non-smoker [134].

The quantity of the detected benzene in the exhaled breath sample depends on the time of the last smoke cigarette. This study shows how the benzene concentration increases rapidly after smoking and returns back to the initial level after a while.

The cigarette smoke has a strong influence on the VOCs in exhaled breath. *Euler et al.* [135] study showed, isoprene is a predominant hydrocarbon in tobacco smoke [136] and the passive increase of this effluent in the breath of smokers might be misinterpreted as an increase in pentane. One of the anthropogenic sources of isoprene is tobacco smoke (200 to 400 μg per cigarette) [137]. The concentration of isoprene increases by a percentage of 70% after just one cigarette smoking [137, 138].

Thekedar B. [3] made a comparative study between current smokers within lung cancer patients and control smokers. In his study, he showed that the isoprene level in the lung cancer smoker patients is not significantly higher than in the control smokers. Thus, the increased level of isoprene may be due to smoking alone. On the other hand, methanol and acetone do not depend on smoking.

Due to this, if someone wants to study the VOCs that emitted from the lung cancer patients with smoking status, their VOCs must be compared to VOCs that emitted from the control persons also with smoking status to avoid the artifacts from smoking.

For this study many precautions should be taken into accounts such as the number of the years of smoking and the number of the cigarettes are smoked per day.

6.8. Influence of Tedlar Bags on VOCs concentrations

In this part of the study, ten Tedlar bags were collected from ten volunteers. After collecting the breath samples, they were analyzed for different days to study their changes over the time. The measurements were taken repeatedly over 190 hr. period (approximately one week), in order to study the variability and the stability of the VOCs in time [84].

With IMS, each sample has different numbers of peaks. After determining the intensities of the analytes that belongs to the same sample with the same $1/k_0$ (Vs/cm^2) and the same retention time (s), a list of intensities versus time was prepared.

The relation between the intensity (V) and the time (hours) were plotted and fitted with a linear exponential function using the OriginLab program:

Figure 6.14 shows the flow chart for the optimization process of the measurement done with IMS.

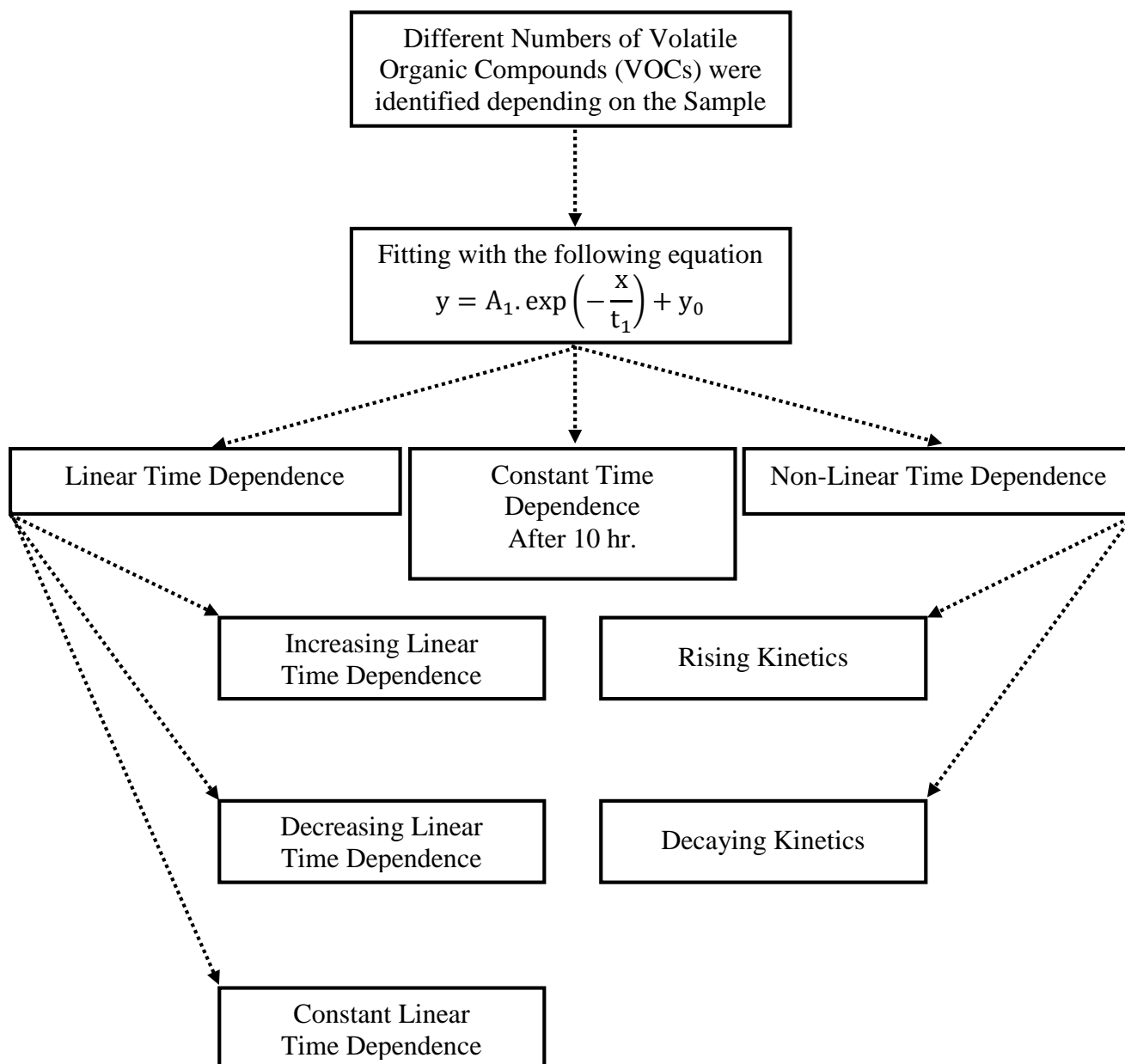


Figure 6.14: The flow chart for the optimization process of the measurement done with IMS.

6.8.1. Linear Time Dependence

In studying the changes in VOCs behaviour in time, some of them show a linear behaviour. This linear time dependence occurs in different variants, as follows:

6.8.1.1. Constant Linear Time Dependence

Some VOCs show a constant linear time dependence as illustrated in Figure 6.15. This fitting curve gives us an indication that these VOCs do not interact with each other, there is no correlation with other analytes, so their intensities stay nearly the same or there is some interaction that shows a decreasing and an increasing (fluctuation) around the average value.

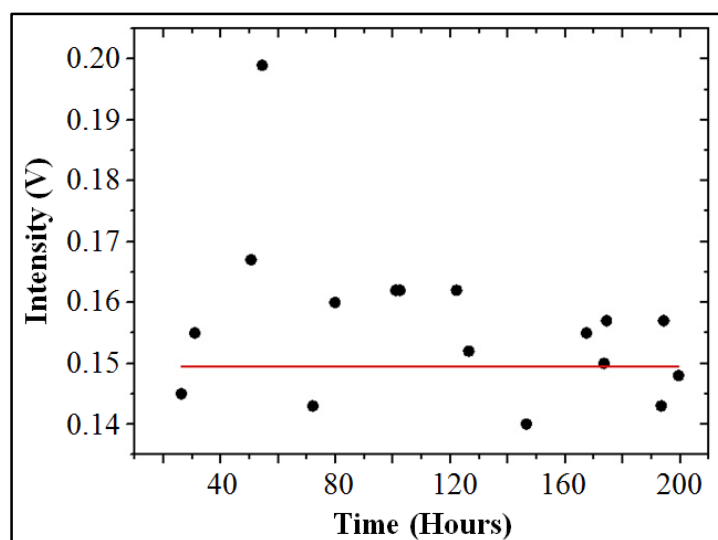


Figure 6.15: An example of analytes that shows a constant linear time dependence: Sample No. 1 (fasting volunteer) with $1/k_0=0.577$ (Vs/cm²) and $RT=22.6$ (s).

6.8.1.2. Increasing Linear Time Dependence

Some VOCs show an increasing linear time dependence as illustrated in Figure 6.16. This fitting curve gives us an indication that these VOCs increase due to their constant relation with other analytes that make them to increase linearly in time.

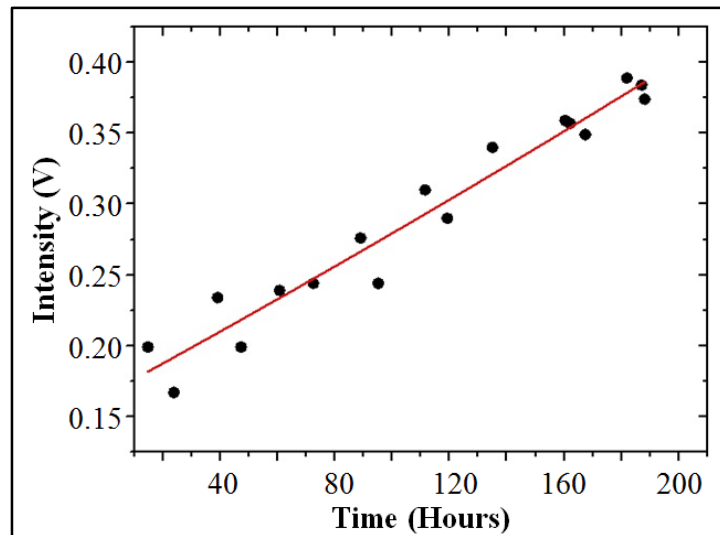


Figure 6.16: An example of analytes that shows an increasing linear time dependence: Sample No. 10 (normal volunteer) with $1/k_0=0.603$ (Vs/cm²) and $RT=8.9$ (s).

6.8.1.3. Decreasing Linear Time Dependence

Some VOCs show a decreasing linear time dependence as illustrated in figure 6.17. This fitting curve gives us an indication that these VOCs decrease due to their constant relation with other analytes that make them to decrease linearly in time.

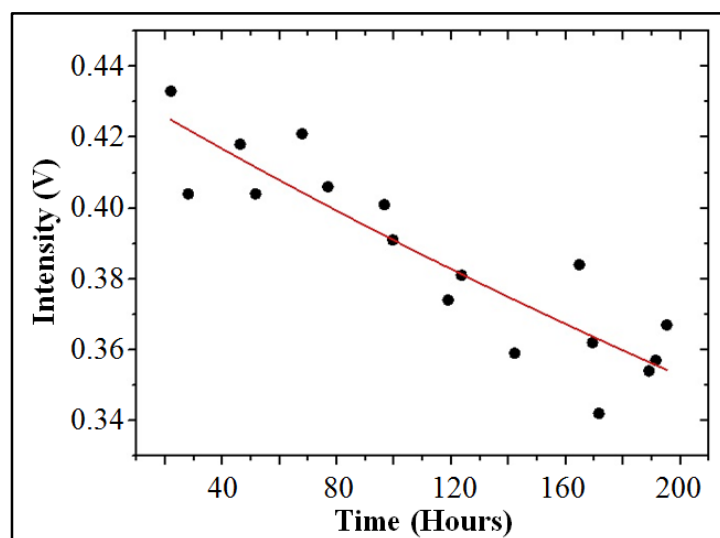


Figure 6.17: An example of analytes that shows a decreasing linear time dependence: Sample No. 4 (normal volunteer) with $1/k_0=0.535$ (Vs/cm²) and $RT=7.9$ (s).

6.8.2. Nonlinear Time Dependence

Beside the linear time dependence of some VOCs, other VOCs show non-linear time dependence. This non-linear time dependence occurs in different variants, as follows:

6.8.2.1. Rising Kinetics

Other VOCs show a rising kinetics as illustrated in Figure 6.18. This fitting curve gives us an indication that these VOCs increase due to their relation with other analytes that make them to increase in time.

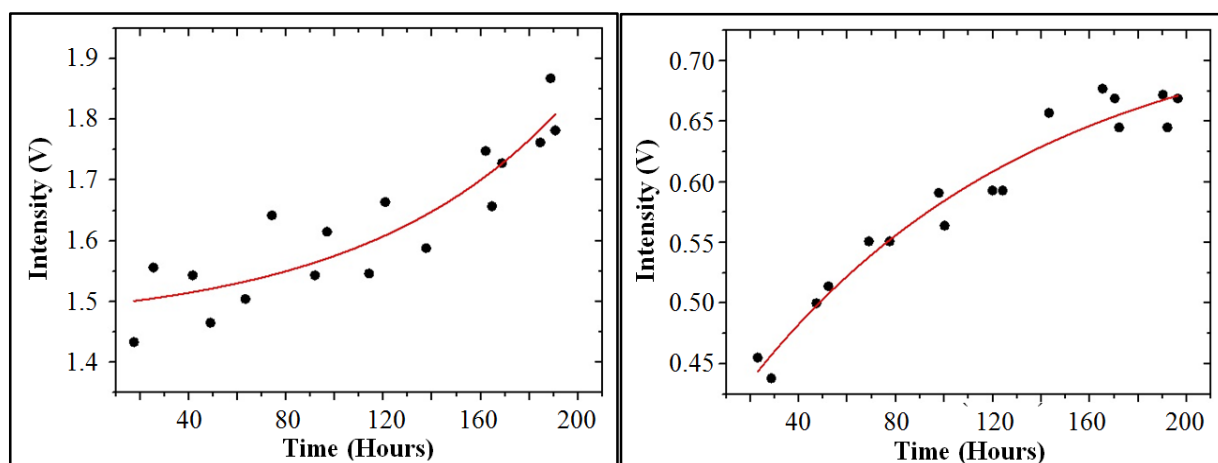


Figure 6.18: Two examples of analytes that show a rising kinetics: Sample No. 8 (smoking volunteer) with $1/k_0=0.485$ (Vs/cm^2) and $RT=42.1$ (s) (**on the left**) and Sample No. 3 (after eating) with $1/k_0=0.644$ (Vs/cm^2) and $RT=30.4$ (s) (**on the right**).

6.8.2.2. Decaying Kinetics

Other VOCs show a decaying kinetics as illustrated in figure 6.19. This fitting curve gives us an indication that these VOCs decrease due to their relation with other analytes that make them to decrease in time.

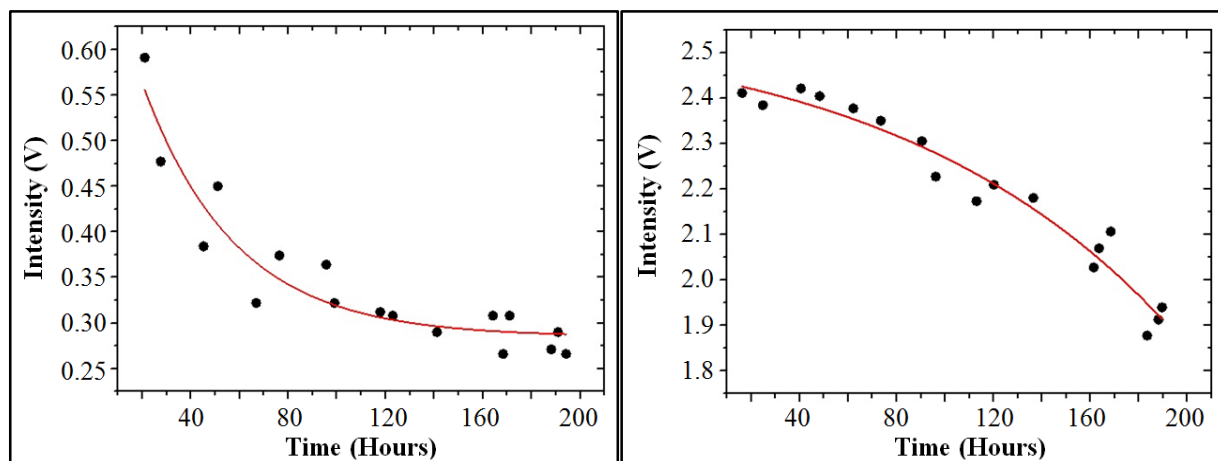


Figure 6.19: Two examples of analytes that show a decaying kinetics: Sample No. 5 (after washing the mouth with Listerine mouthwash) with $1/k_0=0.650$ (Vs/cm²) and $RT=167.5$ (s) (**on the left**) and Sample No. 9 (after chewing peppermint gum) with $1/k_0=0.450$ (Vs/cm²) and $RT=5.6$ (s) (**on the right**).

Bibliography

- [1] U. Farooq, "Plant chemistry RO pretreatment system", *NOMAC SIWEP Shuaibah Jeddah Saudi Arabia*, slide no. (57/163) 2013, <http://www.slideshare.net/umarfarooq58/plant-chemistry-pretreatment-system-presentation>.
- [2] J. Shaji and D. Jadhav, "Breath biomarker for clinical diagnosis and different analysis technique", *Research Journal of Pharmaceutical, Biological and Chemical Sciences*, INDIA, vol. 1, issue 3, pp.639-653 (2010).
- [3] B. Thekedar, "Investigations on the use of breath gas analysis with Proton Transfer Reaction Mass Spectrometry (PTR-MS) for a non-invasive method of early lung cancer detection", Technische Universität München, Fakultät für Physik, Ph.D. Diss. (2009), <https://mediatum.ub.tum.de/doc/821780/821780.pdf>.
- [4] J. de Gouw. and C. Warneke, "Measurements of volatile organic compounds in the earth's atmosphere using proton-transfer-reaction mass spectrometry", *Mass Spectrometry Reviews*, vol. 26, issue 2, pp. 223-257 (2007).
- [5] M. Alonso and J.M. Sanchez, "Analytical challenges in breath analysis and its application to exposure monitoring", *TrAC-Trends in Analytical Chemistry*, vol. 44, pp. 78-89 (2013).
- [6] M. Phillips, J. Greenberg and J. Awad, "Metabolic and environmental origins of volatile organic compounds in breath", *Journal of Clinical Pathology*, vol. 47, issue 11, pp. 1052-1053 (1994).
- [7] J. Neilsen, "Integrity of storage media for clinical applications with SIFT-MS instruments", Department of Mechanical Engineering, University of Canterbury, Master of Mechanical Engineering (2006), http://ir.canterbury.ac.nz/bitstream/10092/2579/1/thesis_fulltext.pdf.
- [8] M. Phillips, J. Herrera, S. Krishnan, M. Zain, J. Greenberg and R.N. Cataneo, "Variation in volatile organic compounds in the breath of normal humans", *Journal of Chromatography B: Biomedical Sciences and Applications*, vol. 729, issues 1-2, pp. 75-88 (1999).
- [9] W. Cao and Y. Duan, "Current status of methods and techniques for breath analysis", *Critical Reviews in Analytical Chemistry*, vol. 37, issue 1, pp. 3-13 (2007).
- [10] A. Amann, G. Poupart, S. Telser, M. Ledochowski, A. Schimid and S. Mechtcheriakov, "Applications of breath gas analysis in medicine", *International Journal of Mass Spectrometry*, vol. 239, issues 2-3, pp. 227-233 (2004).

- [11] W. Miekisch, J.K. Schubert and G.F.E. Noeldge-Schomburg, “Diagnostic potential of breath analysis-focus on volatile organic compounds”, *Clinica Chimica Acta.*, vol. 347, issues 1-2, pp. 25-39 (2004).
- [12] A.S. Modak, “Regulatory issues on breath tests and updates of recent advances on [¹³C]-breath tests”, *Journal of Breath Research*, vol. 7, no. 3, pp. 1-8, 037103 (2013).
- [13] P. Mochalski, J. King, M. Klieber, K. Unterkofler, H. Hinterhuber, M. Baumann and A. Amann, “Blood and breath levels of selected volatile organic compounds in healthy volunteers”, *Analyst.*, vol. 138, issue 7, pp. 2134-2145 (2013).
- [14] K. Badjagbo, “Potential of breath analysis: from environmental exposure assessment to medical diagnosis”, *WebmedCentral ENVIRONMENTAL MEDICINE*, Review articles, vol. 3, no. 3, pp. 1-6 (2012).
- [15] L. Pauling, A.B. Robinson, R. Teranishi and P. Cary, “Quantitative analysis of urine vapor and breath by gas-liquid partition chromatography”, *Proc. Natl. Acad. Sci. USA*, vol. 68, no. 10, pp. 2374-2376 (1971).
- [16] J. Rieder, P. Lirk, C. Ebenbichler, G. Gruber, P. Prazeller, W. Lindinger and A. Amann, “Analysis of volatile organic compounds: possible applications in metabolic disorders and cancer screening”, *Wien. Klin. Wochenschr.*, vol. 113, issues 5-6, pp. 181-185 (2001).
- [17] J. King, K. Unterkofler, G. Teschl, S. Teschl, H. Koc, H. Hinterhuber and A. Amann, “A mathematical model for breath gas analysis of volatile organic compounds with special emphasis on acetone”, *J. Math. Biol.*, vol. 63, issue 5, pp. 959-999 (2011).
- [18] T.L. Mathew, P. Pownraj, S. Abdulla and B. Pullithadathil, “Technologies for clinical diagnosis using expired human breath analysis”, Review Article, *Diagnostics*, vol. 5, no. 1, pp. 27-60 (2015).
- [19] W. Szymczak, J. Rozman, M. Fedrigo, V. Höllriegl, M. Kistler, D. Peters, C. Hoeschen, M. Klingenspor and M. Hrabe de Angelis, “Breath gas analysis in unrestrained mice: A survey of VOC screening using PTR-TOF 2000”, Applications in Medicine and Biotechnology, 6th International Conference on Proton Transfer Reaction Mass Spectrometry and its Applications, A. Hansel and J. Dunkl Contributions, Institut für Ionenphysik und Angewandte Physik, Universität Innsbruck, innsbruck university press, 1st edition, pp:40 (2013),
http://www.uibk.ac.at/iup/buch_pdfs/ptrms_2013.pdf.
- [20] C. Wang and P. Sahay, “Breath analysis using laser spectroscopic techniques: breath biomarkers, spectral fingerprints, and detection limits”, Review Article, *Sensors*, vol. 9, issue 10, pp. 8230-8262 (2009).
- [21] L. Cappellin, F. Loreto, E. Aprea, A. Romano, J.S. Pulgar, F. Gasperi and F. Biasioli, “PTR-MS in Italy: A multipurpose sensor with applications in environmental, agri-food and health science”, Review Article, *Sensors*, vol. 13, issue 9, pp. 11923-11955 (2013).

- [22] Structure of the human respiratory system,
<http://www.buzzle.com/images/diagrams/human-body/respiratory-system-diagram.jpg>.
- [23] How your lungs work?,
<http://www.nichs.org.uk/cmsfiles/article-page-images/how-yer-lungs-work.gif>.
- [24] The respiratory system,
<http://antranik.org/wp-content/uploads/2011/12/diagrammatic-view-of-capillary-alveoli-relationship.jpg>.
- [25] Breath and gas exchange,
http://leavingbio.net/Respiratory%20System/THE%20RESPIRATORY%20SYSTEM_files/image020.jpg.
- [26] J. Röpcke and M. Hannemann, “Special section on breath gas analysis”, *Journal of Breath Research*, vol. 5, no. 2, pp. 1-2, 020201 (2011).
- [27] N. Pallikarakis, N. Sphiris and P. Lefebvre, “Influence of the bicarbonate pool and on the occurrence of $^{13}\text{CO}_2$ in exhaled air”, *Eur. J. Appl. Physiol. Occup. Physiol.*, vol. 63, issue 3-4, pp. 179-183 (1991).
- [28] D.A. Schoeller, J.F. Schneider, N.W. Solomons, J.B. Watkins and P.D. Klein, “Clinical diagnosis with the stable isotope ^{13}C in CO_2 breath tests: methodology and fundamental considerations”, *J. Lab. Clin. Med.*, vol. 90, no. 3, pp. 412-421 (1977).
- [29] M.P. Saccomani, R.C. Bonadonna, E. Cavegion, R.A. DeFronzo and C. Cobelli, “Bicarbonate kinetics in humans: identification and validation of a three-compartment model”, *Am. J. Physiol.*, vol. 269, no. 1, pp. E183-E192 (1995).
- [30] C.S. Irving, M.R. Thomas, E.W. Malphus, L. Marks, W.W. Wong, T.W. Boutton and P.D. Klein, “Lysine and protein metabolism in young women. Subdivision based on the novel use of multiple stable isotopic labels”, *J. Clin. Invest.*, vol. 77, no. 4, pp. 1321-1331 (1986).
- [31] T. Raj, R. Kuriyan and A.V. Kurpad, “Bicarbonate kinetics in Indian males”, *J. Biosci.*, vol. 31, issue 2, pp. 273-280 (2006).
- [32] C.S. Irving, W.W. Wong, R.J. Shulman, E.O. Smith and P.D. Klein, “[^{13}C] bicarbonate kinetics in humans: intra- vs. interindividual variations”, *Am. J. Physiol.*, vol. 245, no. 2, pp. R190-R202 (1983).
- [33] T.J. Barstow, D.M. Cooper, S.M. Sobel, E.M. Landaw and S. Epstein, “Influence of increased metabolic rate on [^{13}C]bicarbonate washout kinetics”, *Am. J. Physiol.*, vol. 259, no. 1, pp. R163-R171 (1990).
- [34] R. Steele, “The retention of metabolic radioactive carbonate”, *Biochem. J.*, vol. 60, no. 3, pp. 447-453 (1955).

- [35] C. Cobelli, M.P. Saccomani, P. Tessari, G. Biolo, L. Luzi and D.E. Matthews, “Compartmental model of leucine kinetics in humans”, *Am. J. Physiol.*, vol. 261, no. 4, pp. E539-E550 (1991).
- [36] C.F. Poyart, A. Fréminet and E. Bursaux, “The exchange of bone CO₂ in vivo”, *Respir. Physiol.*, vol. 25, no. 1, pp. 101-107 (1975).
- [37] K. Wetzel and H. Fischer, “¹³C-Breath Tests in medical research and clinical diagnosis”, Fischer ANalysen Instrumente GmbH (FAN), Fischer ANalysen Instrumente GmbH Leipzig 4th Edition (2005),
http://www.drpiktel.com/dokumenty/13C_testy_oddechowe.pdf.
- [38] Infra Red Isotope Analyser IRIS, “¹³C-Breath Tests”, Wagner Analysen Technik (GmbH), Bremen, Germany,
http://www.imsc-bremen-2009.de/TIS/index.php/downloadable-material/doc_download/4-wagner-flyer01.
- [39] S.Y. Tan and M. Hu, “Medicine in Stamps Antoine-Laurent Lavoisier (1743-1794): Founder of Modern Chemistry”, *Singapore Medical Journal*, vol. 45, no. 7, pp. 303-304 (2004).
- [40] Regions of abdomen,
<http://www.newhealthguide.org/images/10434100/image001.jpg>.
- [41] Anatomy of the liver,
<http://www.le.ac.uk/pa/teach/va/anatomy/case5/liver1b.gif>.
- [42] basic liver biology - why things go wrong when it's infected,
<http://1.bp.blogspot.com/-9ljubdf6B3o/U6BNSXpXQpI/AAAAAAAAA9o/9O0IwHmcxy4/s1600/Liver-lobule+dnwalker.com.jpg>.
- [43] Liver “wikipedia”,
https://en.wikipedia.org/wiki/File:2423_Microscopic_Anatomy_of_Liver.jpg.
- [44] Transport of Hormones,
http://www.easynotecards.com/uploads/462/42/_5abec72a_142b10a4854__8000_00002057.PNG.
- [45] What are the different types of liver disease?,
<http://images.wisegeek.com/types-of-liver-disease.jpg>.
- [46] N. Tygstrup, “Assessment of liver function: principles and practice”, *J. Gastroenterol. Hepatol.*, vol. 5, issue 4, pp. 468-482 (1990).
- [47] L.S. Friedman, P. Martin and S.J. Munoz, “Liver function tests and the objective evaluation of the patient with liver disease”, In: Zakim D., Boyer T.D., editors, *Hepatology: A textbook of liver disease*, Philadelphia: Saunders:1134-1145 (1999).

- [48] P.J. Johnson, "Role of the standard 'liver function tests' in current clinical practice", *Ann. Clin. Biochem.*, vol. 26, Pt. 6, pp. 463-471 (1989).
- [49] D. Festi, S. Capodicasa, L. Sandri, L. Colaiocco-Ferrante, T. Staniscia, E. Vitacolonna, A. Vestito, P. Simoni, G. Mazzella, P. Portincasa, E. Roda and A. Colecchia, "Measurement of hepatic functional mass by means of ^{13}C -methacetin and ^{13}C -phenylalanine breath tests in chronic liver disease: comparison with Child-Pugh score and serum bile acid levels", *World J. Gastroenterol.*, vol. 11, no. 1, pp. 142-148 (2005).
- [50] A. Petrolati, D. Festi, G. De Berardinis, L. Colaiocco-Ferrante, D. Di Paolo, G. Tisone and M. Angelico, " ^{13}C -methacetin breath test for monitoring hepatic function in cirrhotic patients before and after liver transplantation", *Aliment. Pharmacol. Ther.*, vol. 18, no. 8, pp. 785-790 (2003).
- [51] C. Merkel, A. Gatta, M. Zoli, M. Bolognesi, P. Angeli, T. Iervese, G. Marchesini and A. Ruol, "Prognostic value of galactose elimination capacity, aminopyrine breath test, and ICG clearance in patients with cirrhosis. Comparison with the Pugh score", *Dig. Dis. Sci.*, vol.36, issue 9, pp. 1197-1203 (1991).
- [52] S.L. Baruque, M. Razquin, I. Jimenez, A. Vazquez, J.P. Gisbert and J.M. Pajares, " ^{13}C -phenylalanine and ^{13}C -methacetin breath test to evaluate functional capacity of hepatocyte in chronic liver disease", *Dig. Liver Dis.*, vol.32, issue 3, pp. 226-232 (2000).
- [53] K. Matsumoto, M. Suehiro, M. Ilo, T. Kawabe, Y. Shiratori, K. Okano and T. Sugimoto, "[^{13}C]methacetin breath test for evaluation of liver damage", *Dig. Dis. Sci.*, vol. 32, issue 4, pp. 344-348 (1987).
- [54] M. Stockmann, "Wertigkeit eines neu entwickelten Verfahrens zur Bestimmung der Leberfunktion in der Leberchirurgie (LiMAX-Test)", Habilitationsschrift, zur Erlangung der Lehrbefähigung für das Fach Chirurgie, vorgelegt dem Fakultätsrat der Medizinischen Fakultät Charité - Universitätsmedizin Berlin (2009),
http://www.diss.fu-berlin.de/diss/servlets/MCRFileNodeServlet/FUDISS_derivate_000000006911/Habil_Stockmann_20g_final_o.pdf.
- [55] A.S. Modak, "An update on ^{13}C -Breath Tests: The transition to acceptability into clinical practice", *Volatile Biomarkers: Non-Invasive Diagnosis in Physiology and Medicine*, edited by A. Amann and D. Smith, Chapter 14, pp. 245-262 (2013).
- [56] A. Kasicka-Jonderko, D. Loska, K. Jonderko, M. Kaminska and B. Blonska-Fajfrowska, "Interference of acute cigarette smoking with [^{13}C]methacetin breath test", *Isotopes Environ. Health Stud.*, vol. 47, no. 1, pp. 34-41 (2011).
- [57] P. Krumbiegel, K. Günther, H. Faust, G. Möbius, K. Hirschberg and G. Schneider, "Nuclear medicine liver function tests for pregnant women and children. 1. Breath Tests with ^{14}C -methacetin and ^{13}C -methacetin", *Eur. J. Nucl. Med.*, vol. 10, issues 3-4, pp. 129-133 (1985).

- [58] J.F. Lock, P. Taheri, S. Bauer, H.G. Holzhütter, M. Malinowski, P. Neuhaus and M. Stockmann, “Interpretation of non-invasive breath tests using (13)C-labeled substrates-- a preliminary report with (13)C-methacetin”, *Eur. J. Med. Res.*, vol. 14, no. 12, pp. 547-550 (2009).
- [59] H.G. Holzhütter, J.F. Lock, P. Taheri, S. Bulik, A. Goede and M. Stockmann, “Assessment of hepatic detoxification activity: proposal of an improved variant of the (13)C-methacetin breath test”, *PLoS One*, vol. 8, no. 8, pp. 1-10, e70780 (2013).
- [60] L.F. Prescott, “Kinetics and metabolism of paracetamol and phenacetin”, *Br. J. Clin. Pharmacol.*, vol. 10, suppl. 2, pp. 291S-298S (1980).
- [61] T. Rubin, T. von Haimberger, A. Helmke and K. Heyne, “Quantitative determination of metabolization dynamics by a real-time ¹³CO₂ breath test”, *J. Breath Res.*, vol. 5, no. 2, pp. 1-6, 027102 (2011).
- [62] Body surface area,
https://en.wikipedia.org/wiki/Body_surface_area.
- [63] M. Stockmann, J.F. Lock, M. Malinowski, S.M. Niehues, D. Seehofer and P. Neuhaus, “The LiMAx test: a new liver function test for predicting postoperative outcome in liver surgery”, *HPB (Oxford)*, vol. 12, no. 2, pp. 139-146 (2010).
- [64] C.N. Palmer, P.J. Coates, S.E. Davies, E.A. Shephard and I.R. Phillips, “Localization of cytochrome P-450 gene expression in normal and diseased human liver by in situ hybridization of wax-embedded archival material”, *Hepatology*, vol. 16, issue 3, pp. 682-687 (1992).
- [65] M. Stockmann, J.F. Lock, B. Riecke, K. Heyne, P. Martus, M. Fricke, S. Lehmann, S.M. Niehues, M. Schwabe, A. J. Lemke and P. Neuhaus, “Prediction of postoperative outcome after hepatectomy with a new bedside test for maximal liver function capacity”, *Ann. Surg.*, vol. 250, no. 1, pp. 119-125 (2009).
- [66] B. Riecke, P. Neuhaus and M. Stockmann, “Major influence of oxygen supply on ¹³CO₂:¹²CO₂ ratio measurement by nondispersive isotope-selective infrared spectroscopy”, *Helicobacter.*, vol. 10, no. 6, pp. 620-622 (2005).
- [67] T. Rubin, “Konzeption und Entwicklung eines Infrarot-Spektrometers zur Bestimmung der Konzentration von ¹³CO₂ und ¹²CO₂ im Gasuss”, Diplomarbeit, Fachbereich Physik, FU Berlin (2009).
- [68] LiMAx: the first real-time liver test,
http://www.humedics.de/index.php?article_id=14&clang=1.
- [69] B. Thekedar, W. Szymczak, V. Höllriegl, C. Hoeschen and U. Oeh, “Investigations of the variability of breath gas sampling using PTR-MS”, *J Breath Res.*, vol. 3, no. 2, pp. 1-11, 027007 (2009).
- [70] R.E. Chase, “Properties and manufacture of tedlar^(R) polyvinyl fluoride film VERL”, Ford Research Laboratory ERC Technical Report Issued, (2001).

- [71] M.M. Steeghs, S.M. Cristescu and F.J. Harren, “The suitability of Tedlar bags for breath sampling in medical diagnostic research”, *Physiol Meas.*, vol. 28, no. 1, pp. 73-84 (2007).
- [72] J. Beauchamp, J. Herbig, R. Gutmann and A. Hansel, “On the used of Tedlar^(R) bags for breath-gas sampling and analysis”, *J. Breath Res.*, vol. 2, no. 4, pp. 1-19, 046001 (2008).
- [73] Proton Ionization Molecular Mass Spectrometry,
<http://www.birmingham.ac.uk/Images/Research-and-teaching/Engineering-and-Physical-Sciences/pimms/pimms-heading.jpg>.
- [74] M.S.B. Munson and F.H. Field, “Chemical ionisation mass spectrometry. I. General introduction”, *J. Am. Chem. Soc.*, vol. 88, no. 12, pp. 2621-2630 (1966).
- [75] Detection of modified nucleosides by tandem mass spectrometry,
<http://www.pharmazie.uni-mainz.de/AK-Helm/Illustrationen/stefanie.jpg>.
- [76] M. Westhoff, P. Litterst, L. Freitag, J.I. Baumbach, “Ion Mobility Spectrometry in the diagnosis of sarcoidosis: results of a feasibility study”,
http://www.jpp.krakow.pl/journal/archive/11_07_s5/gfx/rys8001.gif.
- [77] C.B. Hariharan, “Implementation of multi-capillary column-con mobility spectrometry (MCC-IMS) for medical and biological applications”, Ph.D thesis von der Fakultät Bio- und Chemieingenieurwesen der Technischen Universität Dortmund (2012),
<https://eldorado.tu-dortmund.de/bitstream/2003/29593/1/Dissertation.pdf>.
- [78] A.K. Yocum and A.M. Chinnaiyan, “Current affairs in quantitative targeted proteomics: multiple reaction monitoring-mass spectrometry”, *Brief. Funct. Genomic. Proteomic.*, vol. 8, no. 2, pp. 145-157 (2009).
- [79] J. King, A. Kupferthaler, B. Frauscher, H. Hackner, K. Unterkofler, G. Teschl, H. Hinterhuber, A. Amann and B. Högl, “Measurement of endogenous acetone and isoprene in exhaled breath during sleep”, *Physiol Meas.*, vol. 33, no. 3, pp. 413-428 (2012).
- [80] J. King, H. Koc, K. Unterkofler, G. Teschl, S. Teschl, P. Mochalski, H. Hinterhuber and A. Amann, “Physiological modeling for analysis of exhaled breath”, in: “Volatile Biomarkers-Non-Invasive Diagnosis in Physiology and Medicine”, A. Amann and D. Smith (eds), Elsevier, pp. 27-46 (2013).
- [81] J. King, A. Kupferthaler, K. Unterkofler, H. Koc, S. Teschl, G. Teschl, W. Miekisch, J. Schubert, H. Hinterhuber and A. Amann, “Isoprene and acetone concentration profiles during exercise on an ergometer”, *J. Breath Res.*, vol. 3, no. 2, pp. 1-16, 027006 (2009).
- [82] S. Maddula, T. Rabis, U. Sommerwerck, O. Anhenn, K. Darwiche, L. Freitag, H. Teschler and J.I. Baumbach, “Correlation analysis on data sets to detect infectious agents in the airways by ion mobility spectrometry of exhaled breath”, *Int. J. Ion Mobility Spectrom.*, vol. 14, issue 4, pp. 197-206 (2011).

- [83] A. Hauschild, T. Schneider, J. Pauling, K. Rupp, M. Jang, J.I. Baumbach and J. Baumbach J., “Computational methods for metabolomic data analysis of ion mobility spectrometry data-reviewing the state of the art”, *Metabolites*, review article, vol. 2, no. 4, pp. 733-755 (2012).
- [84] C.C. Hsieh, S.H. Horng and P.N. Liao, “Stability of trace-level volatile organic compounds stored in canisters and tedlar bags”, *Aerosol and Air Quality Research*, vol. 3, no. 1, pp. 17-28 (2003).
- [85] G. Preti, H.J. Lawley, C.A. Hormann, B.J. Cowart, R.S. Feldman, L.D. Lawley and I.M. Young, “Non-oral and oral aspects of oral malodour”, In: Rosenberg M. (Ed). *Bad Breath: Research Perspectives*. Tel Aviv: Tel-Aviv University, Ramot Publishing, pp. 149-173 (1995).
- [86] S. Van den Velde, F. Nevens, P. Van hee, D. van Steenberghe and M. Quirynen, “GC-MS analysis of breath odor compounds in liver patients”, *J. Chromatogr. B Analyt. Technol. Biomed. Life Sci.*, vol. 875, issue 2, pp. 344-348 (2008).
- [87] C.S. Probert, I. Ahmed, T. Khalid, E. Johanson, S. Smith and N. Ratcliffe, “Volatile organic compounds as diagnostic biomarkers in gastrointestinal and liver diseases”, *J. Gastrointestin. Liver Dis.*, Review, vol. 18, issue 3, pp. 337-343 (2009).
- [88] A. Tangerman, M.T. Meuwese-Arends and J.B. Jansen, “Cause and composition of foetor hepaticus”, *Lancet*, vol. 343, no. 8895, pp. 483 (1994).
- [89] J. Dadamio, S. Van den Velde, W. Laleman, P. Van Hee, W. Coucke, F. Nevens and M. Quirynen, “Breath biomarkers of liver cirrhosis”, *J Chromatogr B Analyt Technol Biomed Life Sci.*, vol. 905, pp. 17-22 (2012).
- [90] H.J. Blom and A. Tangerman, “Methanethiol metabolism in whole blood”, *J. Lab. Clin. Med.*, vol. 111, no. 6, pp. 606-610 (1988).
- [91] S. Khero, M.T. Alam, M. Aurangzeb, T. Rasheed, Z. Nawaz, M.F. Jaffery and M. Masroor, “Co-relation of high serum ammonia levels with severity of hepatic encephalopathy in chronic liver disease patients”, *Rawal Medical Journal*, vol. 39, no. 2, pp. 119-123 (2014).
- [92] P. Spanel, S. Davies and D. Smith, “Breath ammonia dips after feeding independently of the protein content of the meat”, *FASEB J.*, vo. 14, pp. A490 (2000).
- [93] D. Smith, T. Wang, P. Spanel and R. Bloor, “The increase of breath ammonia induced by niacin ingestion quantified by selected ion flow tube mass spectrometry”, *Physiol. Meas.*, vol. 27, no. 6, pp. 437-444 (2006).
- [94] P. Spaněl, C. Turner, T. Wang, R. Bloor and D. Smith, “Generation of volatile compounds on mouth exposure to urea and sucrose: implications for exhaled breath analysis”, *Physiol. Meas.*, vol. 27, no. 2, pp. N7-N17 (2006).

- [95] R. Iyer, C.P. Jenkinson, J.G. Vockley, R.M. Kern, W.W. Grody and S. Cederbaum, "The human arginases and arginase deficiency", *J. Inherit Metab Dis.*, vol. 21, suppl. 1, pp. 86-100 (1998).
- [96] WHO, "Hydrogen cyanide and cyanides: human health aspects", Concise International Chemical Assessment Document 61, World Health Organization Geneva, (2004), <http://www.who.int/ipcs/publications/cicad/en/cicad61.pdf>.
- [97] M. Ansell and F.A. Lewis, "A review of cyanide concentrations found in human organs: a survey of literature concerning cyanide metabolism, 'normal', non-fatal, and fatal body cyanide levels", *J Forensic Med.*, vol. 17, no. 4, pp. 148-155 (1970).
- [98] F. Rieders, "Noxious gases and vapors. I: Carbon monoxide, cyanides, methemoglobin, and sulfhemoglobin", In: DePalma JR, ed. *Drill's pharmacology in medicine*, 4th ed. New York, NY, McGraw-Hill Book Company, pp. 1180-1205 (1971).
- [99] W. Nastainczyk, H.J. Ahr and V. Ullrich, "The reductive metabolism of halogenated alkanes by liver microsomal cytochrome P450", *Biochem. Pharmacol.*, vol. 31, issue 3, pp. 391-396 (1982).
- [100] M.A.M. Wenker, "Individual variation in biotransformation: relation to styrene kinetics and solvent-induced neur", Ph.D Thesis, AMC-UvA Faculty, the institutional repository of the University of Amsterdam (2001), <http://dare.uva.nl/document/2/15977>.
- [101] C.M. Kneepkens, G. Lepage and C.C. Roy, "The potential of the hydrocarbon breath test as a measure of lipid peroxidation", *free Radic Biol Med.*, vol. 17, issue 2, pp. 127-160 (1994).
- [102] J.M. Mathews, J.H. Raymer, A.S. Etheridge, G.R. Velez and J.R. Bucher, "Do endogenous volatile organic chemicals measured in breath reflect and maintain CYP2E1 levels in vivo?" *Toxicol. Appl. Pharmacol.*, vol. 146, no. 2, pp. 255-260 (1997).
- [103] J.D. Pritchard, "HPA compendium of chemical hazards: methanol", CRCE HQ, HPA, version 3, Health Protection Agency, Report, pp. 1-29 (2011), https://www.gov.uk/government/uploads/system/uploads/attachment_data/file/317260/Methanol.pdf.
- [104] P. Srivastava and R. Malviya, "Sources of pectin, extraction and its applications in pharmaceutical industry-An overview", *Ind. J. of natural Products and Resources*, vol. 2, no. 1, pp. 10-18 (2011).
- [105] J. Sternberg and A. Imbach, "Metabolic studies with seleniated compounds. II. Turnover studies with ⁷⁵Se-methionine in rats", *Int. J. Appl. Radiat. Isot.*, vol. 18, no. 8, pp. 557-568 (1967).
- [106] H.D. Hurt, E.E. Gary and W.J. Visek, "Growth, reproduction, and tissue concentrations of selenium in the selenium-depleted rat", *J. Nutr.*, vol. 101, no. 6, pp. 761-766 (1971).

- [107] M. Navarro-Alarcón, H. López-Ga de la Serrana, V. Pérez-Valero and M.C. López-Martinez, “Selenium concentrations in serum of individuals with liver diseases (cirrhosis or hepatitis): relationship with some nutritional and biochemical markers”, *Sci Total Environ.*, vol. 291, issue 1-3, pp. 135-141 (2002).
- [108] B. Bödeker, “Entwicklung eines Verfahrens zur Klassifikation von Ionenmobilitätsspektrometerdaten”, Diplomarbeit am Fachbereich Informatik der Universität Dortmund, Algorithm Engineering, Dortmund / Germany (2007), http://ls11-www.cs.uni-dortmund.de/_media/techreports/tr07-03.pdf.
- [109] A. Bunkowski, “MCC-IMS data analysis using automated spectra processing and explorative visualisation methods”, Zur Erlangung des akademischen Grades eines Doktors der Naturwissenschaften an der Technischen Fakultät der Universität Bielefeld vorgelegte Dissertation (2011), <http://core.ac.uk/download/pdf/15986686.pdf>.
- [110] A.M. Diskin, P. Spanel and D. Smith, “Time variation of ammonia, acetone, isoprene and ethanol in breath: a quantitative SIFT-MS study over 30 days”, *Physiol. Meas.*, vol. 24, no. 1, pp. 107-119 (2003).
- [111] J. Kwak, M. Fan, S.W. Harshman, C.E. Garrison, V.L. Dershem, J.B. Phillips, C.C. Grigsby and D.K. Ott, “Evaluation of bio-VOC sampler for analysis of volatile organic compounds in exhaled breath”, *Metabolites*, vol. 4, no. 4, pp. 879-888 (2014).
- [112] S.F. Sena, “Beta-hydroxybutyrate: New test for ketoacidosis”, Department of Pathology and Laboratory Medicine, Technically Speaking, C.S. Guidess, Editor, Danbury Hospital, A higher level of care, vol. 4, no. 8, 2 pages (2010), <http://www.danburyhospital.org/~media/Files/Publications/Technically%20Speaking/TS-Vol%204-No%208.ashx>.
- [113] L. Laffel, “Ketone bodies: a review of physiology, pathophysiology and application of monitoring to diabetes”, *Diabetes Metab Res. Rev.*, vol. 15, issue 6, pp. 412-426 (1999).
- [114] P. Tiidus, A.R. Tupling and M. Houston, “Biochemistry primer for exercise science”, 4th Edition, printed in the United States of America (2012).
- [115] C. Turner, P. Spanel and D. Smith D., “A longitudinal study of ammonia, acetone and propanol in the exhaled breath of 30 subjects using selected ion flow tube mass spectrometry, SIFT-MS”, *Physiol. Meas.*, vol. 27, no. 4, pp. 321-337 (2006).
- [116] K. Schwarz, A. Pizzini, B. Arendacká, K. Zerlauth, W. Filipiak, A. Schmid, A. Dzien, S. Neuner, M. Lechleitner, S. Scholl-Bürgi, W. Miekisch, J. Schubert, K. Unterkofler, V. Witkovský, G. Gastl and A. Amann, “Breath acetone-aspects of normal physiology related to age and gender as determined in a PTR-MS study”, *J. Breath Res.*, vol. 3, no. 2, pp. 1-9, 027003 (2009).
- [117] O.B. Crofford, R.E. Mallard, R.E. Winton, N.L. Rogers, J.C. Jackson and U. Keller, “Acetone in breath and blood”, *Trans. Am. Clin. Climatol. Assoc.*, vol. 88, pp.128-139 (1977).

- [118] M. Statheropoulos, E. Sianos, A. Agapiou, A. Georgiadou, A. Pappa, N. Tzamtzis, H. Giotaki, C. Papageorgiou and D. Kolostoumbis, "Preliminary investigation of using volatile organic compounds from human expired air, blood and urine for locating entrapped people in earthquakes", *J. Chromatogr. B Analyt. Technol. Biomed. Life Sci.*, vol. 822, issues 1-2, pp. 112-117 (2005).
- [119] D. Smith, P. Spanel and S. Davies, "Trace gases in breath of healthy volunteers when fasting and after a protein-calorie meal: a preliminary study", *J. Appl. Physiol.*, vol. 87, no. 5, pp. 1584-1588 (1999).
- [120] D. Smith, T. Wang and P. Spaněl, "On-line, simultaneous quantification of ethanol, some metabolites and water vapour in breath following the ingestion of alcohol", *Physiol. Meas.*, vol. 23, no. 3, pp. 477-489 (2002).
- [121] M.P. Hlastala, "Physiological errors associated with alcohol breath testing", *The Champion*, vol. 9, no. 6, pp. 16-19 (1985).
- [122] P. Spanel, K. Dryahina and D. Smith, "The concentration distributions of some metabolites in the exhaled breath of young adults", *J. Breath Res.*, vol. 1, no. 2, pp. 1-8, 026001 (2007).
- [123] W. Lindinger, J. Taucher, A. Jordan, A. Hansel and W. Vogel, "Endogenous production of methanol after the consumption of fruit", *Alcohol Clin. Exp. Res.*, vol 21, issue 5, pp. 939-943 (1997).
- [124] W. Lindinger, A. Hansel and A. Jordan, "Proton-transfer-reaction mass spectrometry (PTR- MS): on-line monitoring of volatile organic compounds at pptv levels", *Chem. Soc. Rev.*, vol. 27, pp. 347-354 (1998).
- [125] A. Stephan, M. Bücking and H. Steinhart, "Novel analytical tools for food flavour", *Food Res. Int.*, vol. 33, issues 3-4, pp. 199-209 (2000).
- [126] Nordic Council of Ministers Food Additives in Europe Status of safety assessments of food additives presently permitted in the EU (2000),
<http://www.feingold.org/Research/PDFstudies/FoodAdditivesEurope.pdf>.
- [127] C.K. Rösing, S.C. Gomes, D.G. Bassani and R.V. Oppermann, "Effect of chewing gums on the production of volatile sulfur compounds (VSC) in vivo", *Acta. Odontol. Latinoam.*, vol. 22, no. 1, pp. 11-14 (2009).
- [128] A. Fortune, S. Henningsen, M. Tuday, C. McGinley and M. McGinley, "Chemical and odor evaluation of various potential replacement films for sampling bags", Water Environment Federation/Air and Waste Management Association, Specialty Conference: Odors and Air Pollutants (2012),
<http://www.fivesenses.com/Documents/Library/52%20Sample%20Bag%20Material%20Performance%20Paper%20-%20WEFOdor2012.pdf>.
- [129] S.L. Trabue, J.C. Anhalt and J.A. Zahn, "Bias of Tedlar bags in the measurement of agricultural odorants", *J. Environ. Qual.*, vol. 35, no. 5, pp. 1668-1677 (2006).

- [130] A.Ph. (Ton) van Harreveld, “Odor concentration decay and stability in gas sampling bags”, *J. Air Waste Manage. Assoc.*, vol. 53, issue 1, pp. 51-60 (2003).
- [131] A. Jordan, A. Hansel, R. Holzinger and W. Lindinger, “Acetonitrile and benzene in the breath of smokers and non-smokers investigated by proton transfer reaction mass spectrometry (PTR-MS)”, *Int. J. Mass Spectrom. and Ion Proc.*, vol. 148, issues 1-2, pp. L1-L3 (1995).
- [132] L.M. Babcock and N.G. Adams, “Advances in gas phase ion chemistry”, Band 4, (University of Georgia). Elsevier Science B.V., All rights reserved: Amsterdam-Nederland, (2001).
- [133] L. Wallace, E. Pellizzari, T.D. Hartwell, R. Perritt and R. Ziegenfus, “Exposures to benzene and other volatile organic compounds from active and passive smoking”, *Arch Environ Health*, vol. 42, no. 5, pp. 272-279 (1987).
- [134] L. Wallace, “Environmental exposure to benzene: an update”, *Environmental Health Perspectives*, vol. 104, Supp. 6, pp. 1129-1136 (1996).
- [135] D.E. Euler, S.J. Davé and H. Guo, “Effect of cigarette smoking on pentane excretion in alveolar breath”, *Clin. Chem.*, vol. 42, no. 2, pp. 303-308 (1996).
- [136] S. Mendis, P.A. Sobotka and D.E. Euler, “Pentane and isoprene in expired air from humans: gas-chromatographic analysis of single breath”, *Clin Chem.*, vol 40, no. 8, pp. 1485-1488 (1994).
- [137] National Toxicology Program (NTP) (NIH), ‘Report on carcinogens’, Twelfth Edition, US Department of Health and Human Services, Public Health Service, National Toxicology Program, pp. 248 (2011),
[https://books.google.de/books?id=raW5FLj408QC&pg=PA248&lpg=PA248&dq=tobacco+smoke+\(200+to+400+%C2%B5g+per+cigarette\)+Report+on+carcinogens&source=bl&ots=5wS8Wj67RK&sig=fZj0uUjFsqx5By-5b4OUMor0Jdk&hl=de&sa=X&ved=0CCYQ6AEwAGoVChMI2oqzmYWDxwIVB89yCh0LsQsT#v=onepage&q=tobacco%20smoke%20\(200%20to%20400%20%C2%B5g%20per%20cigarette\)%20Report%20on%20carcinogens&f=false](https://books.google.de/books?id=raW5FLj408QC&pg=PA248&lpg=PA248&dq=tobacco+smoke+(200+to+400+%C2%B5g+per+cigarette)+Report+on+carcinogens&source=bl&ots=5wS8Wj67RK&sig=fZj0uUjFsqx5By-5b4OUMor0Jdk&hl=de&sa=X&ved=0CCYQ6AEwAGoVChMI2oqzmYWDxwIVB89yCh0LsQsT#v=onepage&q=tobacco%20smoke%20(200%20to%20400%20%C2%B5g%20per%20cigarette)%20Report%20on%20carcinogens&f=false)
- [138] S.T. Senthilmohan, M.J. McEwan, P.F. Wilson, D.B. Milligan and C.G. Freeman, “Real time analysis of breath volatiles using SIFT-MS in cigarette smoking”, *Redox Rep.*, vol. 6, issue 3, pp. 185-187 (2001).
- [139] R.F. Phalen and R.N. Phalen, “Introduction to air pollution science: a public health perspective”, World Headquarters, Jones & Bartlett Publishers, 331 pages, (2013),
https://books.google.de/books?id=2TGqgEY4WsMC&printsec=frontcover&hl=de&source=gbs_ge_summary_r&cad=0#v=onepage&q&f=false
- [140] P. Španěl and D. Smith, “Influence of weakly bound adduct ions on breath trace gas analysis by selected ion flow tube mass spectrometry (SIFT-MS)”, *Int J. Mass Spectrom.*, vol. 280, issue 1-3, pp. 128-135 (2009).

- [141] Ionicon Analytik, “Gas Standard”, PTRMS Viewer, Ionicon Analytik Gesellschaft m.b.H., V.3.0.0.70, 2012.
- [142] I. Kushch, K. Schwarz, L. Schwentner, B. Baumann, A. Dzien, A. Schmid, K. Unterkofler, G. Gastl, P. Spaněl, D. Smith and A. Amann, “Compounds enhanced in a mass spectrometric profile of smokers' exhaled breath versus non-smokers as determined in a pilot study using PTR-MS”, *Journal of Breath Research*, vol. 2, no. 2, pp. 1-26, 026002 (2008).
- [143] Beauchamp J., “Notes on Masses”, Innsbruck Ionimed Analytik GmbH (2007).
- [144] L. Keck, C. Hoeschen and U. Oeh, “Effects of carbon dioxide in breath gas on proton transfer reaction-mass spectrometry (PTR-MS) measurements”, *Int. J. Mass Spectrom.*, vol. 270, issue 3, pp. 156-165 (2008).
- [145] I. Kohl, J. Herbig, J. Dunkl, A. Hansel, M. Daniaux and M. Hubalek, “Smokers breath as seen by Proton-Transfer-Reaction Time-of-Flight Mass Spectrometry (PTR-TOF-MS)”, *Volatile Biomarkers Non-Invasive Diagnosis in Physiology and Medicine*, edited by Amann A. and Smith D., pp. 89-116 (2013).
- [146] S. Halbritter, M. Fedrigo, V. Höllriegl, W. Szymczak, J.M. Maier, A.G. Ziegler and M. Hummel, “Human breath gas analysis in the screening of gestational diabetes mellitus”, *Diabetes Technol. Ther.*, vol. 14, no. 10, pp. 917-925 (2012).
- [147] S. Inomata, H. Tanimoto, S. Kato, J. Suthawaree, Y. Kanaya, P. Pochanart, Y. Liu and Z. Wang, “PTR-MS measurements of non-methane volatile organic compounds during an intensive field campaign at the summit of Mount Tai, China, in June 2006”, *Atmos. Chem. Phys.*, vol. 10, pp. 7085-7099 (2010).
- [148] A. Wehinger, A. Schmid, S. Mechtcheriakov, M. Ledochowski, C. Grabmer, G.A. Gastl and A. Amann, “Lung cancer detection by proton transfer reaction mass-spectrometric analysis of human breath gas”, *Int. J. Mass Spectrom.*, vol. 265, issue 1, pp. 49-59 (2007).
- [149] K.J. Jardine, W.M. Henderson, T.E. Huxman and L. Abrell, “Dynamic solution injection: a new method for preparing pptv-ppbv standard atmospheres of volatile organic compounds”, *Atmos. Meas. Tech.*, vol. 3, pp. 1569-1576 (2010).
- [150] M. Graus, M. Müller and A. Hansel, “High resolution PTR-TOF: quantification and formula confirmation of VOC in real time”, *J. Am. Soc. Mass Spectrom.*, vol. 21, issue 6, pp. 1037-1044 (2010).

Acknowledgement

In the beginning, I would like to thank God, **ALLAH**, for having made everything possible by giving me strength and health to do this work.

I would like to thank the German Academic Exchange Service (**DAAD**) and the Ministry of Higher Education and Scientific Research (**MoHESR**) of the Republic of Iraq for this opportunity to take a Ph.D degree in Germany and for their financial support.

I would like to express my sincere thanks and appreciation to my supervisor **Prof. Dr. Karsten Heyne** who let me work in his group at the **Free University Berlin** under his supervision and also for his encouragement and assistance in finishing this research.

I also owe a huge thank you to **Prof. Dr. Ulrike Alexiev** for being my second supervisor and for **PD Dr. Christian Frischkorn** for his help in refining my article.

I would like to thank A.G Heyne especially **Dr. Valeri Kozich**, I am greatly indebted him for his continued advice and support and **Mr. Theodore Haimberger** for refining my thesis.

I would like to record my deep gratitude to **Mrs. Angelika Pasanec** and **Mrs. Gudrun May-Nasseri** for their help during this period.

Furthermore, I would like to thank the workgroup of General Visceral and Transplantation Surgery Department, Charité-University Hospital Berlin Campus Virchow Klinikum for their help in collecting the samples from the patients.

I would like to thank all the volunteers in this study for their cooperation and time, especially my friends and my neighbours. Special thanks to my friend from Iraq, **Ruba Al-Obaidi**, a real best friend and to another friend from Tunis, **Souad Khemiri**, a real true friend.

I convey my thanks and gratitude to my neighbour from Egypt **Mohammed Amin** for his continuous help and to **Daniel Tolksdorf (AG. Aziz)** for solving some problems with Python program.

I would like to thank **Prof. Dr. Zuhair Al-Shaikh** for reading my thesis and **Dr. Sabah Dahboosh** for his help.

I've been very fortunate to know **Mrs. Suhaila Salihi** and her family in Berlin, they treated me as one of their family during this period, so I want to say thank you for them and I am very grateful to her for giving me the opportunity to give a lecture in Saudi-Arabic School (König Fahad Akademie) in Berlin.

I am very much thankful to **Miss. Shatha**, **Mrs. Maysoon**, **Dr. Amal**, **Mrs. Kawther**, **Miss. Dhilal**, and **Mr. Thulfiqar**, because of them I am here in Germany and I do not forget the staff of Dentistry College, Al-Mustansiriya University, especially the Basic Science Department in Iraq-Baghdad.

Last but not least, I would like to extend my deepest gratitude to my family: to my father (**Adel**) who gave me courage and support, to my mother (**Nadia**) who gave me kindness and love, to my sisters (**Maha**, **Ola** and **Doaa**) the lily and fragrance of the family, especially **Ola** for helping me to analyze my data with Python, and to my sister's (**Maha**) husband (**Ahmed**) and their beloved children (**Rania** and **Abdullah**). They are really standing behind me, praying to me and supporting me in every step. To them, I dedicate this work a result of their efforts.

Curriculum Vitae

For reasons of data protection,
the curriculum vitae is not included in the online version.

Erklärung der Selbstständigkeit

Hiermit versichere ich, die vorliegende Arbeit selbstständig verfasst und keine andere als die angegebenen Quellen und Hilfsmittel benutzt sowie die Zitate deutlich kenntlich gemacht zu haben. Die Arbeit weder in einem früheren Promotionsverfahren angenommen noch als ungenügend beurteilt worden.

Ort, Datum

Suha Adel Al-Ani